

Novel chemical, microbiological and physical approaches in food safety control, volume II

Edited by

Marco Iammarino, Sara Panseri, Gulhan Unlu,
Speranza Barbara, Antonio Bevilacqua and Rosalia Zianni

Published in

Frontiers in Nutrition



FRONTIERS EBOOK COPYRIGHT STATEMENT

The copyright in the text of individual articles in this ebook is the property of their respective authors or their respective institutions or funders. The copyright in graphics and images within each article may be subject to copyright of other parties. In both cases this is subject to a license granted to Frontiers.

The compilation of articles constituting this ebook is the property of Frontiers.

Each article within this ebook, and the ebook itself, are published under the most recent version of the Creative Commons CC-BY licence. The version current at the date of publication of this ebook is CC-BY 4.0. If the CC-BY licence is updated, the licence granted by Frontiers is automatically updated to the new version.

When exercising any right under the CC-BY licence, Frontiers must be attributed as the original publisher of the article or ebook, as applicable.

Authors have the responsibility of ensuring that any graphics or other materials which are the property of others may be included in the CC-BY licence, but this should be checked before relying on the CC-BY licence to reproduce those materials. Any copyright notices relating to those materials must be complied with.

Copyright and source acknowledgement notices may not be removed and must be displayed in any copy, derivative work or partial copy which includes the elements in question.

All copyright, and all rights therein, are protected by national and international copyright laws. The above represents a summary only. For further information please read Frontiers' Conditions for Website Use and Copyright Statement, and the applicable CC-BY licence.

ISSN 1664-8714
ISBN 978-2-8325-5701-3
DOI 10.3389/978-2-8325-5701-3

About Frontiers

Frontiers is more than just an open access publisher of scholarly articles: it is a pioneering approach to the world of academia, radically improving the way scholarly research is managed. The grand vision of Frontiers is a world where all people have an equal opportunity to seek, share and generate knowledge. Frontiers provides immediate and permanent online open access to all its publications, but this alone is not enough to realize our grand goals.

Frontiers journal series

The Frontiers journal series is a multi-tier and interdisciplinary set of open-access, online journals, promising a paradigm shift from the current review, selection and dissemination processes in academic publishing. All Frontiers journals are driven by researchers for researchers; therefore, they constitute a service to the scholarly community. At the same time, the *Frontiers journal series* operates on a revolutionary invention, the tiered publishing system, initially addressing specific communities of scholars, and gradually climbing up to broader public understanding, thus serving the interests of the lay society, too.

Dedication to quality

Each Frontiers article is a landmark of the highest quality, thanks to genuinely collaborative interactions between authors and review editors, who include some of the world's best academicians. Research must be certified by peers before entering a stream of knowledge that may eventually reach the public - and shape society; therefore, Frontiers only applies the most rigorous and unbiased reviews. Frontiers revolutionizes research publishing by freely delivering the most outstanding research, evaluated with no bias from both the academic and social point of view. By applying the most advanced information technologies, Frontiers is catapulting scholarly publishing into a new generation.

What are Frontiers Research Topics?

Frontiers Research Topics are very popular trademarks of the *Frontiers journals series*: they are collections of at least ten articles, all centered on a particular subject. With their unique mix of varied contributions from Original Research to Review Articles, Frontiers Research Topics unify the most influential researchers, the latest key findings and historical advances in a hot research area.

Find out more on how to host your own Frontiers Research Topic or contribute to one as an author by contacting the Frontiers editorial office: frontiersin.org/about/contact

Novel chemical, microbiological and physical approaches in food safety control, volume II

Topic editors

Marco Iammarino — Experimental Zooprophyllactic Institute of Puglia and Basilicata (IZSPB), Italy

Sara Panseri — University of Milan, Italy

Gulhan Unlu — University of Idaho, United States

Speranza Barbara — University of Foggia, Italy

Antonio Bevilacqua — University of Foggia, Italy

Rosalia Zianni — Experimental Zooprophyllactic Institute of Puglia and Basilicata (IZSPB), Italy

Citation

Iammarino, M., Panseri, S., Unlu, G., Barbara, S., Bevilacqua, A., Zianni, R., eds. (2024). *Novel chemical, microbiological and physical approaches in food safety control, volume II*. Lausanne: Frontiers Media SA. doi: 10.3389/978-2-8325-5701-3

Table of contents

- 05 Editorial: Novel chemical, microbiological and physical approaches in food safety control, volume II
Marco Iammarino, Antonio Bevilacqua, Barbara Speranza, Sara Panzeri, Gulhan Unlu and Rosalia Zianni
- 08 Antimicrobial, Antibiofilm, and Antioxidant Properties of *Boletus edulis* and *Neoboletus luridiformis* Against Multidrug-Resistant ESKAPE Pathogens
Juliana Garcia, Francisca Rodrigues, Flávia Castro, Alfredo Aires, Guilhermina Marques and Maria José Saavedra
- 21 Simultaneous determination of twelve mycotoxins in edible oil, soy sauce and bean sauce by PRiME HLB solid phase extraction combined with HPLC-Orbitrap HRMS
Donghui Luo, Jingjing Guan, Hao Dong, Jin Chen, Ming Liang, Chunxia Zhou, Yanping Xian and Xiaofei Xu
- 34 Monitoring Turkish white cheese ripening by portable FT-IR spectroscopy
Hulya Yaman, Didem P. Aykas and Luis E. Rodriguez-Saona
- 44 UPLC-ESI-MS/MS-based widely targeted metabolomics reveals differences in metabolite composition among four *Ganoderma* species
Liu Wei-Ye, Guo Hong-Bo, Yang Rui-Heng, Xu Ai-Guo, Zhao Jia-Chen, Yang Zhao-Qian, Han Wen-Jun and Yu Xiao-Dan
- 57 Effects of wollastonite and phosphate treatments on cadmium bioaccessibility in pak choi (*Brassica rapa* L. ssp. *chinensis*) grown in contaminated soils
Kexin Guo, Yuehua Zhao, Yang Zhang, Jinbo Yang, Zhiyuan Chu, Qiang Zhang, Wenwei Xiao, Bin Huang and Tianyuan Li
- 70 Role of nutraceutical against exposure to pesticide residues: power of bioactive compounds
Mabil Sajad, Shabnam Shabir, Sandeep Kumar Singh, Rima Bhardwaj, Walaa F. Alsanie, Abdulhakeem S. Alamri, Majid Alhomrani, Abdulaziz Alsharif, Emanuel Vamanu and Mahendra P. Singh
- 91 Development of a highly sensitive method based on QuEChERS and GC-MS/MS for the determination of polycyclic aromatic hydrocarbons in infant foods
Mariateresa Ingegno, Rosalia Zianni, Ines Della Rovere, Andrea Chiappinelli, Valeria Nardelli, Francesco Casamassima, Anna Calitri, Maurizio Quinto, Donatella Nardiello and Marco Iammarino
- 105 The development and nutritional quality of *Lyophyllum decastes* affected by monochromatic or mixed light provided by light-emitting diode
Xiaoli Chen, Yihan Liu, Wenzhong Guo, Mingfei Wang, Jiuxiao Zhao, Xin Zhang and Wengang Zheng

- 118 **Fingerprint profiling for quality evaluation and the related biological activity analysis of polysaccharides from Liuweizhiji Gegen-Sangshen beverage**
Shulin Wei, Mingxing Li, Long Zhao, Tiangang Wang, Ke Wu, Jiayue Yang, Mingyun Tang, Yueshui Zhao, Jing Shen, Fukuan Du, Yu Chen, Shuai Deng, Zhangang Xiao, Mei Wei, Zhi Li and Xu Wu
- 133 **Valorization of fish from the Adriatic Sea: nutritional properties and shelf life prolongation of *Aphia minuta* through essential oils**
Rosaria Marino, Marzia Albenzio, Antonella della Malva, Angela Racioppo, Barbara Speranza and Antonio Bevilacqua



OPEN ACCESS

EDITED AND REVIEWED BY
Michael Rychlik,
Technical University of Munich, Germany

*CORRESPONDENCE

Marco Iammarino
✉ marco.iammarino@izspb.it;
✉ marco.iammarino@tin.it

RECEIVED 19 October 2024
ACCEPTED 24 October 2024
PUBLISHED 05 November 2024

CITATION

Iammarino M, Bevilacqua A, Speranza B,
Panseri S, Unlu G and Zianni R (2024) Editorial:
Novel chemical, microbiological and physical
approaches in food safety control, volume II.
Front. Nutr. 11:1513864.
doi: 10.3389/fnut.2024.1513864

COPYRIGHT

© 2024 Iammarino, Bevilacqua, Speranza,
Panseri, Unlu and Zianni. This is an
open-access article distributed under the
terms of the [Creative Commons Attribution
License \(CC BY\)](#). The use, distribution or
reproduction in other forums is permitted,
provided the original author(s) and the
copyright owner(s) are credited and that the
original publication in this journal is cited, in
accordance with accepted academic practice.
No use, distribution or reproduction is
permitted which does not comply with these
terms.

Editorial: Novel chemical, microbiological and physical approaches in food safety control, volume II

Marco Iammarino^{1*}, Antonio Bevilacqua², Barbara Speranza²,
Sara Panseri³, Gulhan Unlu⁴ and Rosalia Zianni¹

¹Chemistry Department, Istituto Zooprofilattico Sperimentale della Puglia e della Basilicata, Foggia, Italy, ²Department of Agriculture, Food, Natural Resources and Engineering, University of Foggia, Foggia, Italy, ³Department of Veterinary Medicine and Animal Sciences, University of Milan, Milan, Italy, ⁴Department of Animal, Veterinary and Food Sciences, University of Idaho, Moscow, ID, United States

KEYWORDS

chemical analysis, food safety, microbiological analysis, novel approaches, physical analysis

Editorial on the Research Topic

Novel chemical, microbiological and physical approaches in food safety control, volume II

The possible simultaneous presence of microbiological and chemical contaminants in the same food, also known as “cocktail effect” is an emerging topic in food safety. Given the presence of such cocktail of contaminants, high amounts of data are needed in order to develop any kind of evaluation, taking into account all possible interactions among different contaminants that can be hypothesized. Taking into account that the range of food which can be contaminated is very wide, and the need of comprehensive datasets for elaborating a significant statistical analysis, new effective analytical approaches are needed. These approaches can embrace new analytical procedures for chemical/physical determinations and new microbiological protocols characterized by high throughput, low cost and “Greenness” (1).

Most applications developed in the last years apply gas and liquid chromatography coupled to mass spectrometry for the quantification of a lot of food contaminants, detectable in the same run, using a single sample preparation procedure. Many approaches have been optimized for the determination of most significant concerns in food safety such as the presence of environmental contaminants, pesticides and veterinary drugs, etc. Moreover, the recent advances based on metabolomics, dark matter, protein fingerprint in microbiology, etc., open new frontiers in food analysis and food safety investigations.

Another new target of such novel methods is the “Green” aspects in terms of environmentally friendly processes to achieve a suitable sustainability (2).

As it regards microbiological approaches, a significant challenge in food safety is represented by the development of new and more effective methods for isolating and detecting most important foodborne pathogens, such as human noroviruses, O157:H7 and non-O157 STEC, etc. (3, 4).

This Research Topic was conceived in order to showcase the recent advances in food safety with respect to new chemical, microbiological and physical approaches for the determination and quantification of both chemical and microbiological risk factors that may contaminate food.

A brief overview of all articles collected in this Research Topic is reported below.

The original article proposed by Garcia et al. applied disk diffusion and microdilution methods for evaluating the antimicrobial and antibiofilm properties of *Boletus edulis* and *Neoboletus luridiformis* aqueous and methanolic extracts against ESKAPE isolates from clinical wound infections. High-performance liquid chromatography coupled to diode array detector was also used for phytochemical characterization based on the determination of total phenols, orthodiphenols and antioxidant activity. Finally, 3-(4, 5-dimethylthiazolyl-2)-2, 5-diphenyltetrazolium bromide (MTT) assay was performed to study the human foreskin fibroblasts-1 (HFF-1) cell viability. The authors concluded that the extracts of *B. edulis* and *N. luridiformis* exert antimicrobial and antibiofilm properties against multidrug-resistant bacteria with different efficacy rates. This effect can be explained by the relationship between the phenolic content/antioxidant activity and antimicrobial activity, especially due to the significant levels of protocatechuic acid, homogentisic acid, pyrogallol, gallic acid, p-catechin, and dihydroxybenzoic acid detected in the extract.

Luo et al. described a solid phase extraction coupled to high-performance liquid chromatography-tandem Orbitrap high resolution mass spectrometry (HPLC-Orbitrap HRMS) method for simple, sensitive, and rapid determination of 12 mycotoxins (ochratoxin A, ochratoxin B, aflatoxin B1, aflatoxin B2, aflatoxin G1, aflatoxin G2, HT-2 toxin, sterigmatocystin, diacetoxysciroenol, penicillic acid, mycophenolic acid, and citreoviridin) in edible oil, soy sauce, and bean sauce. This analytical method was characterized by low limits of detection and quantification, in the range 0.12–1.2 µg/L and 0.40–4.0 µg/L, respectively, recovery percentages in the range 78.3–115.6%, and relative standard deviations (RSDs) in the range 0.9–9.7%. The authors applied this method for the analysis of 24 samples of edible oil, soy sauce and bean sauce, verifying the presence of AFB1, AFB2, sterigmatocystin and mycophenolic acid in a concentration range from 1.0 to 22.1 µg/kg.

In the article by Yaman et al. three extraction solvents (water, methanol, and ethanol) were used to obtain soluble fractions of Turkish white cheese samples produced in a pilot plant scale. Then, reference methods, including gas and liquid chromatography, were used to detect and quantify amino acids, fatty acids and organic acids. FT-IR spectra were also collected and correlated with chromatographic data using pattern recognition analysis to develop regression and classification predictive models. The authors concluded that all models showed a good fit for predicting the target compounds during cheese ripening and that a simple methanolic extraction coupled to spectra obtained by a portable FT-IR device provides a fast, simple, and cost-effective technique to monitor the ripening of Turkish white cheese.

Wei-Ye et al. conducted a widely targeted metabolomics analysis of four commonly used edible and medicinal *Ganoderma* species based on ultra performance liquid chromatography-electrospray ionization-tandem mass spectrometry. The authors identified 575–764 significant differential metabolites among the species, most of which exhibited large fold differences. In particular, amino acids and derivatives, as well as terpenes, nucleotides and derivatives, alkaloids, and lipids resulted as the most advantageous

metabolites of *Ganoderma lingzhi*. The authors also highlighted that the most significant metabolites in the four *Ganoderma* species may regulate and participate in signaling pathways associated with diverse cancers, Alzheimer's disease, and diabetes.

Guo et al. selected Pak choi (*Brassica rapa* L. ssp. *chinensis*) as a representative leafy vegetable to be tested in pots to reveal the effects of silicate-phosphate amendments on soil Cd chemical fractions, total plant Cd levels, and plant bioaccessibility. The authors used three heavy metal-immobilizing agents, namely wollastonite, potassium tripolyphosphate and sodium hexametaphosphate (SHMP). Using an *in vitro* digestion method combined with transmission electron microscopy, the authors reported that silicate and phosphorus agents were found to reduce the bioaccessibility of Cd in pak choi by up to 66.13%. The findings of this study contribute to the development of methods for safer cultivation of commonly consumed leafy vegetables and for soil remediation.

Marino et al. conducted a study on the nutritional and microbiological characteristics of *Aphia minuta*, a pelagic species harvested from the Golfo di Manfredonia in the Adriatic Sea (Italy). They assessed its chemical composition and profiles across different seasons, noting higher protein content in spring. Fatty acids analysis showed seasonal variations, with increased n-3 polyunsaturated fatty acids in spring and summer. Essential amino acids like leucine and lysine were most abundant in spring and summer, underlining nutritional value of this species. The research also examined the microbiological quality and shelf life of *Aphia minuta*, testing essential oils against bacteria and their effects in various packaging environments. Combining citrus extract with vacuum packaging notably reduced microbial counts within a week. The study offers valuable information to exploit the nutritional benefits and market potential of *Aphia minuta*.

The review prepared by Sajad et al. describes the vital role that pesticides play in modern agriculture by safeguarding crops from pests and diseases, despite concerns about their negative impact on human health and the environment. Pesticide residues in food and water sources pose significant health risks, potentially leading to cancer, endocrine disruptions, and neurotoxicity with prolonged exposure. To address these issues, researchers and health experts are seeking alternative strategies to counteract the harmful effects of pesticide residues. Nutraceuticals and bioactive compounds derived from whole foods like fruits, vegetables, herbs, and spices, are being explored for their potential to mitigate pesticide residue toxicity. These substances, comprising minerals, vitamins, antioxidants, and polyphenols, offer diverse biological actions that could aid in detoxification and recovery from pesticide exposure. The review aims to investigate the efficacy of nutraceutical interventions as a promising approach to combat the detrimental effects of pesticide residues.

The study presented by Chen et al. is focused on the photo-sensitivity of *Lyophyllum decastes*, an edible fungus, during mushroom emergence and its responses to various light qualities. *Lyophyllum decastes* was grown under different light conditions including white light, red light, blue light, mixed red and blue light, and a combination of far-red and blue light. Results indicated that red light led to negative effects on mycelium growth and primordial formation, while the combination of red and blue light significantly increased fruiting body characteristics. Blue light

decreased stipe length and fruiting body weight. Blue and far-red light treatments deepened color in mushroom pileus and up-regulated blue photoreceptor genes. Fruiting bodies exposed to mixed red and blue light showed increased protein and polysaccharide content. The study offers insights for optimizing light conditions to enhance the quality of *Lyophyllum decastes* in industrial production.

Wei et al. investigated the Liuweizhiji Gegen-Sangshen (LGS), a very popular beverage in China for alleviating alcohol-related disorders and preventing alcoholic liver disease, in order to establish a comprehensive quality control methodology. Composed of six herbal components, LGS is polysaccharide-rich, yet the quality and activity of LGS-derived polysaccharides remained unexplored. Indeed, this study aimed to establish a quality control method for assessing LGS polysaccharides (LGSP) and investigate their antioxidant, anti-inflammatory, and prebiotic effects. LGSP was extracted and analyzed for molecular weight distribution, monosaccharide content, and structure applying various techniques such as high-performance size exclusion chromatography (HPSEC), 1-phenyl-3-methyl-5-pyrazolone-HPLC (PMP-HPLC), Fourier transform infrared spectroscopy (FT-IR) as well as nuclear magnetic resonance spectroscopy (NMR) techniques. Results revealed LGSP molecular weight distribution peaks, monosaccharide composition and structural characteristics. LGSP exhibited antioxidant properties, reduced pro-inflammatory factors, and enhanced the growth of beneficial probiotics. These findings contribute to understanding LGSP's structure-activity relationship, quality evaluation, and potential for developing healthy products.

Ingegno et al. developed and validated a highly sensitive analytical method based on gas chromatography–tandem mass spectrometry (GC–MS/MS) for the determination of polycyclic aromatic hydrocarbons (PAHs) in various baby foods. This study details the first setup of PAHs extraction and clean up through different QuEChERS-based methods and extraction solvents, considering factors like efficiency and recovery. The GC–MS/MS method was optimized, ensuring excellent linearity, sensitivity, and accuracy with detection limits ranging from 0.019 to 0.036 µg/kg. Recovery rates ranged from 73.1 to 110.7%, meeting European Commission guidelines. A survey on commercial infant food products of different types, based on meat, fish, legumes, and vegetables, confirmed PAH levels below quantification limits. The developed GC–MS/MS method offers a sensitive and reliable

approach for PAH detection in baby foods, supporting in regulatory efforts for ensuring product safety and quality through regular monitoring.

Author contributions

MI: Writing – original draft, Writing – review & editing, Supervision, Visualization. AB: Supervision, Visualization, Writing – review & editing. BS: Supervision, Visualization, Writing – review & editing. SP: Supervision, Visualization, Writing – review & editing. GU: Supervision, Visualization, Writing – review & editing. RZ: Writing – original draft, Writing – review & editing, Supervision, Visualization.

Acknowledgments

We express our gratitude to the Frontiers in Nutrition Editorial Office for the opportunity to propose and publish the second volume of this Research Topic. We also acknowledge all of the authors for their excellent contributions and the reviewers for their availability and the time spent on evaluating and improving the articles.

Conflict of interest

The authors declare that the research was conducted in the absence of any commercial or financial relationships that could be construed as a potential conflict of interest.

The author(s) declared that they were an editorial board member of Frontiers, at the time of submission. This had no impact on the peer review process and the final decision.

Publisher's note

All claims expressed in this article are solely those of the authors and do not necessarily represent those of their affiliated organizations, or those of the publisher, the editors and the reviewers. Any product that may be evaluated in this article, or claim that may be made by its manufacturer, is not guaranteed or endorsed by the publisher.

References

1. Gałuszka A, Migaszewski ZM, Namieśnik J. The 12 principles of green analytical chemistry and the SIGNIFICANCE mnemonic of green analytical practices. *TrAC Trends Anal Chem.* (2013) 50:78–84. doi: 10.1016/j.trac.2013.04.010
2. Vakh C, Tobiszewski M. Greenness assessment of analytical methods used for antibiotic residues determination in food samples. *TrAC Trends Anal Chem.* (2023) 166:117162. doi: 10.1016/j.trac.2023.117162
3. Iammarino M, Panseri S, Unlu G, Marchesani G, Bevilacqua A. Editorial: Novel chemical, microbiological and physical approaches in food safety control. *Front Nutr.* (2022) 9:1060480. doi: 10.3389/fnut.2022.1060480
4. Iammarino M, Palermo C, Tomasevic I. Advanced analysis techniques of food contaminants and risk assessment - Editorial. *Appl Sci.* (2022) 12:4863. doi: 10.3390/app12104863



Antimicrobial, Antibiofilm, and Antioxidant Properties of *Boletus edulis* and *Neoboletus luridiformis* Against Multidrug-Resistant ESKAPE Pathogens

Juliana Garcia^{1,2*}, Francisca Rodrigues³, Flávia Castro¹, Alfredo Aires¹,
Guilhermina Marques¹ and Maria José Saavedra^{1,4*}

¹ CITAB – Centro de Investigação e Tecnologias Agroambientais e Biológicas, Universidade de Trás-os-Montes e Alto Douro, Vila Real, Portugal, ² Laboratório Colaborativo AquaValor Centro de Valorização e Transferência de Tecnologia da Água – Associação, Chaves, Portugal, ³ REQUIMTE/LAQV – Polytechnic of Porto – School of Engineering, Porto, Portugal, ⁴ CECAV, Veterinary and Animal Science Research Center, Universidade de Trás-os-Montes e Alto Douro, Vila Real, Portugal

OPEN ACCESS

Edited by:

Sandrina A. Heleno,
Polytechnic Institute of Bragança
(IPB), Portugal

Reviewed by:

Claudio Ferrante,
University of Studies G. d'Annunzio
Chieti and Pescara, Italy
Ángel Serrano-Aroca,
Catholic University of Valencia San
Vicente Mártir, Spain

*Correspondence:

Juliana Garcia
juliana.garcia@aquavalor.pt
Maria José Saavedra
saavedra@utad.pt

Specialty section:

This article was submitted to
Food Chemistry,
a section of the journal
Frontiers in Nutrition

Received: 09 September 2021

Accepted: 22 November 2021

Published: 24 February 2022

Citation:

Garcia J, Rodrigues F, Castro F,
Aires A, Marques G and Saavedra MJ
(2022) Antimicrobial, Antibiofilm, and
Antioxidant Properties of *Boletus edulis*
and *Neoboletus luridiformis*
Against Multidrug-Resistant ESKAPE
Pathogens. *Front. Nutr.* 8:773346.
doi: 10.3389/fnut.2021.773346

Multidrug-resistant ESKAPE pathogens (*Enterococcus faecium*, *Staphylococcus aureus*, *Klebsiella pneumoniae*, *Acinetobacter baumannii*, *Pseudomonas aeruginosa*, and *Enterobacter species*) has become the most recurrent global cause of skin and soft-tissue infections, belonging to the WHO priority pathogens list. Successful therapy remains challenging and entails the assessment of novel and successful antibiotics. In this study, mushrooms are considered a valuable and unique source of natural antimicrobial compounds. Therefore, this study aimed to evaluate the antimicrobial and antibiofilm properties of *Boletus edulis* (*B. edulis*) and *Neoboletus luridiformis* (*N. luridiformis*) aqueous and methanolic extracts against ESKAPE isolates from clinical wound infections. Disk diffusion and microdilution methods were used to assess the antimicrobial activity. Phytochemical characterization was achieved by analysis of total phenols, orthodiphenols content, and antioxidant activity as well as by high-performance liquid chromatography-diode array detector (HPLC-DAD). Human foreskin fibroblasts-1 (HFF-1) cell viability was performed by the MTT assay. Aqueous and methanolic extracts of *B. edulis* and *N. luridiformis* showed antimicrobial and antibiofilm properties against multidrug-resistant bacteria, although with different efficacy rates. The results showed that there is a convincing relation between the content of phenolic compounds, antioxidant activity, and antimicrobial activity suggesting that the presence of phenolic compounds may explain the biological effects. HPLC analysis revealed high levels of protocatechuic acid, homogentisic acid, pyrogallol, gallic acid, p-catechin, and dihydroxybenzoic acid in the aqueous extract of *B. edulis*, explaining the highest antimicrobial and antibiofilm properties. Importantly, the mushrooms extracts were non-cytotoxic at all the tested concentrations. Overall, the tested mushrooms extracts are good candidates to further explore its use in the prevention of wound infection, particularly by multidrug-resistant pathogens.

Keywords: antibiotic resistance, wound infection, ESKAPE bacteria, wild mushroom, antibiofilm

INTRODUCTION

Nowadays, the increase in multidrug-resistant (MDR) bacteria represents an important worldwide public health problem that inspires the search for new strategies to overcome this multifarious phenomenon (1). Several studies have showed that infections by MDR strains are one of the major causes of morbidity and mortality worldwide (2, 3). MDR bacteria are increasingly involved in infections associated with a variety of cutaneous wound types including burns, combat-related, surgical, and chronic wounds. Wounds are often characterized by a complex and potentially pathogenic microflora that presents a serious risk for both the wound infection and cross-contamination (4). The efficacy of antibiotics is influenced by several factors, namely, the wound microorganisms, their antibiotic-resistance profile, and the presence of bacteria-derived biofilm, which significantly enhances their tolerance to antibiotics (4). The most notorious MDR bacteria was identified as “ESKAPE,” which includes *Enterococcus faecium*, *Staphylococcus aureus*, *Klebsiella pneumoniae*, *Acinetobacter baumannii*, *Pseudomonas aeruginosa*, and *Enterobacter* species that are among the most prevalent bacteria in cutaneous infections (5). These ESKAPE pathogens have revived the attention on mushroom extracts as promising agents with antibacterial and antibiofilm activities. In fact, mushroom species contains several bioactive compounds, namely phenolic acids, terpenoids, flavonoids, tannins, alkaloids, and polysaccharides that could be used as novel and effective antibiotics (6, 7). On that basis, this study aims to chemically characterize different extracts of *Boletus edulis* (*B. edulis*) and *Neoboletus luridiformis* (*N. luridiformis*) as well as to evaluate its antioxidant properties. Moreover, the cytotoxicity, antimicrobial action, and ability to inhibit biofilm formation against clinical MDR isolates of ESKAPE pathogens were performed.

MATERIALS AND METHODS

Chemicals and Drugs

Methanol of analytical grade purity was from Lab-Scan (Lisbon, Portugal). The culture media Brain Heart Infusion Agar (BHIA), Mueller Hinton Broth (MHB), Mueller Hinton Agar (MHA), and all the antibiotics were obtained from Oxoid (Hampshire, UK). The saline solution was prepared with NaCl from Merck (Darmstadt, Germany). The dye resazurin and crystal violet were purchased from Sigma-Aldrich (St Louis, Mosby, USA). All the organic solvents were HPLC grade. Ultrapure water from purified system (Isopad Isomantle, Gemini BV, Pr Beatrixlaan 301, 7312 DG Apeldoorn, Netherlands) was used. External standards caffeic acid, catechin, chlorogenic acid, ferulic acid, gallic acid, (-)-epicatechin, naringin, p-hydroxybenzoic acid, quercitrin, and rutin were purchased from Extrasynthese (Lyon Nord, Genay Cedex, France). Dulbecco's Modified Eagle Medium (DMEM), fetal bovine serum (FBS), non-essential amino acids, penicillin, streptomycin, and trypsin-EDTA were obtained from Invitrogen Corporation (Life Technologies, SA, Madrid, Spain).

Mushrooms Material

Boletus edulis and *Neoboletus luridiformis* mushrooms were collected in a mixed stand at Sabugal, Guarda, located at the Center of Portugal. The morphological identification of the wild macrofungi was made till species according to macro- and microscopic characteristics (8). Representative voucher specimens were deposited at the mycological herbarium of Universidade de Trás-os-Montes e Alto Douro. After taxonomic identification, the mushrooms were immediately stored at -20°C , freeze dried (Dura Dry TM μP , -41°C and 500 mTorr), and grounded to a fine powder. The samples were kept in the dark in hermetically sealed plastic bags up to analysis.

Mushrooms Extracts

Mushrooms extracts were obtained by two different extraction methods according to our previous study (6): (1) Exhaustive aqueous extracts: 5 g of dried mushrooms material was added to 150 ml of distilled water. The mixture was agitated at room temperature (orbital shaker, 1 h, 150 rpm) and centrifuged. The supernatant was filtered (Whatman no. 4 filter paper) and 100 ml of distilled water was added to the pellet. The whole procedure was repeated 4 times. The total extracted was stored at -20°C before lyophilization to obtain the final extract; (2) Exhaustive methanolic extracts: 5 g of dried mushrooms material was added to 150 ml of 80% methanol solution (methanol/distilled water v/v). The mixture was agitated at room temperature (orbital shaker, 1 h, 150 rpm) and centrifuged. The supernatant was filtered and 100 ml of the previous solution was added to the pellet. The whole procedure was repeated four times. The total extracted volume was concentrated in a vacuum rotary evaporator at 38°C to remove methanol and stored at -20°C before lyophilization to obtain the final extract.

Microorganisms and Culture Media

The microorganisms used were clinical isolates from patients hospitalized in various departments of Hospital Center of Trás-os-Montes and Alto Douro (CHTMAD)—these are located in the cities of Lamego, Peso da Régua, Chaves, and Vila Real, a Portuguese north province of Trás-os-Montes and Alto Douro. Ethical approval for this study was granted by the Ethics Committee of Hospital Vila Real (CHTMAD), according to a research collaboration protocol established in 2004. These strains belong to MJH and MJMC collections and are stored at -70°C in aliquots of BHI medium with 15% (v/v) glycerol in the Medical Microbiology Laboratory at Department of Veterinary Sciences — Antimicrobials, Biocides and Biofilms Unit at University of Trás-os-Montes and Alto Douro (UTAD). Several Gram-positive and Gram-negative bacteria isolated from wound exudates were used to screen the antimicrobial activity of the mushroom extracts. All the strains were identified by morphological and biochemical tests (morphological identification of colonies, Gram staining, conventional biochemical identification methods, and MicroScan WalkAway identification panels), followed by Kirby-Bauer antibiotic sensitivity assays, using different antibiotics. *Escherichia coli* (*E. coli*) (CETC 434) and *Staphylococcus aureus* (*S. aureus*) (CETC 976) strains were

obtained from Spanish Type Culture Collection (CETC). Ethics approval for this study was granted by the Ethics Committee of Hospital Vila Real.

Antimicrobial Activity

Briefly, bacterial suspension with the turbidity adjusted to 0.5 McFarland standard units, were spread with a sterile cotton swab onto Petri dishes (90 mm of diameter) containing 4 mm of Mueller-Hinton agar. Six-millimeter diameter sterile paper discs were dispensed on the seeded agar plates and imprinted with 12 μL of 1000 $\mu\text{g}\cdot\text{mL}^{-1}$ extracts solution (in Dimethyl Sulfoxide (DMSO) 10%). Incubation for 24 h at 37°C, followed by diameter measurement (mm) of the clear inhibitory zones around the discs imprinted with the extracts. In all experiments, a negative control (12 μL DMSO) and a positive control [standard commercial antibiotic gentamicin (10 μg)] were included.

The antimicrobial activity was classified according to the following scheme: noneffective (–): inhibition halo = 0; moderate efficacy (+): 0 < inhibition halo < antibiotic inhibition halo; good efficacy (++) : antibiotic inhibition halo < inhibition halo < 2x inhibition halo; strong efficacy (+++) : inhibition halo > 2x antibiotic inhibition halo (6). Minimum inhibitory concentration (MIC, lowest concentration of mushroom extract able to inhibit bacterial growth) was evaluated by a resazurin microdilution assay (6). Bacteria tested were picked from overnight cultures in Brain Heart Infusion. A small portion of bacteria was transferred into a bottle with 50 mL of Mueller Hinton Broth (MHB), capped and placed in an incubator overnight at 37°C. After 16 h of incubation, bacterial suspension was adjusted to an optical density of 0.5 measured at OD_{500 nm}. The resazurin solution (3.4 $\text{mg}\cdot\text{mL}^{-1}$) was prepared in sterile distilled water. A 96-wells sterilized microplate was used and a volume of 100 μL of MHB was used in each well, together with 200 μL of extract solution, or positive control. From the first well (belonging to the first horizontal line) 100 μL was taken and added to the next well and then this step was repeated to each of the following wells in the vertical line, allowing a serial fold dilution of decreasing concentration (range of 1000 $\mu\text{g}\cdot\text{mL}^{-1}$ to 7.81 $\mu\text{g}\cdot\text{mL}^{-1}$). In addition, 20 μL of bacterial suspension and 20 μL of resazurin solution was added to each well. Microplates were incubated at 37°C for 18–24 h. All tests were performed in triplicate and MIC was then assessed visually by the color change of resazurin in each well (blue to pink in the presence of bacteria growth). For the determination of minimum bactericidal concentration (MBC, the lowest concentration of mushroom extract at which bacterial growth by at least 99.0%), the content from each well without changes in color was plated on Mueller-Hinton Agar and incubated at 37°C for 24 h. The lowest concentration that yielded no growth after this subculturing was taken as the MBC.

Bacterial Adhesion/Biofilm Formation and Exposure to Extracts

The microtiter biofilm assay was used to assess the ability of the mushrooms extracts to control adhered cells of *S. aureus* CECT 976 and *E. coli* CECT 434 biofilms. Briefly, 96-well polystyrene microtiter plates were filled with 200 μL of bacterial suspension at OD_{620 nm} of 0.04 ± 0.02 and incubated for 24 h (biofilm

formation) at 37°C and 150 rpm. After the incubation period, the content of each well was aspirated and washed once with 200 μL of saline solution 0.85% (w/v). Then, 180 μL of fresh medium (MH broth) and 20 μL of extracts solution (to a final concentration at MIC, 5 \times MIC, and 10 \times MIC) were applied on biofilms. Concentrations \geq MIC were used considering that biofilm-associated cells are usually 10–1,000-fold more resistant than in the planktonic state. Controls wells containing 10% (v/v) dimethyl sulfoxide (DMSO) were included. After 24 h of exposure at 37°C and 150 rpm, the effects of extracts were analyzed in terms of biomass and metabolic activity.

Biomass Quantification

After the treatment of biofilms with the different extracts, the content of each well of the microtiter plates was removed and the wells were washed with 250 μL of saline solution 0.85% (w/v) to remove non-adherent and weakly adherent bacteria. The remaining attached bacteria were fixed with 250 μL of 96% (v/v) ethanol and after 15 min, the microtiter plates were emptied. Then, 200 μL of 1% crystal violet (Merck, Portugal) were added to each well and allowed to stain for 5 min at room temperature. Afterward, the excess of crystal violet was gently withdrawn and 200 μL of 33% (v/v) glacial acetic acid (Fisher Scientific, UK) was added to solubilize the dye. Finally, the biomass was quantified by measuring the OD at 570 nm using a microplate reader. The results were presented as the biomass reduction (%) in relation to biofilms non-exposed to extracts (Equation 1).

$$\%BR = (OD_c - OD_w)/OD_c \times 100 \quad (1)$$

where %BR is the percentage of biomass reduction, OD_c is the OD_{570 nm} value of control wells, and OD_w is the OD_{570 nm} value for the extract-treated wells.

Metabolic Activity Quantification

After the treatment of pre-established biofilms with mushroom extracts, the content of each well was removed and the wells were washed with 250 μL of saline solution 0.85% (w/v) to remove non-adherent and weakly adherent bacteria. For the staining procedure, 190 μL of fresh MH broth and 10 μL of resazurin solution at 400 μM were added to each well. Then, the microtiter plates were incubated for 20 min in the dark at room temperature. Metabolic activity was quantified by measuring the fluorescence at 570 and 590 nm, using a microtiter plate reader. The results were presented as metabolic inactivation (%) in relation to biofilms non-exposed to mushroom extracts (Equation 2).

$$\%MI = (Fluoc - Fluow)/Fluoc \times 100 \quad (2)$$

where %MI is the percentage of metabolic inactivation, Fluoc represents the fluorescence intensity of biofilms not exposed to extracts, and Fluow represents the fluorescence intensity value for biofilms exposed to extracts.

Phytochemical Analysis

Phytochemical characterization of mushroom extracts was achieved by analysis of total phenols, orthodiphenols content, and antioxidant activity as well as by high-performance liquid chromatography-diode array detector (HPLC-DAD).

Determination of Total Phenolic Compounds

The total phenolic compounds in the extracts were determined by the Folin–Ciocalteu method as previously described (9). Briefly, 10 μl of mushroom extracts at a concentration of 1 mg ml^{-1} or gallic acid standards (0.01–1.0 mg ml^{-1} in methanol) were mixed with 185 μl of distilled water in a 96-well plate followed by the addition of 25 μl of Folin–Ciocalteu reagent. After an incubation period of 5 min, sodium carbonate (75 μl of 7% sodium carbonate) was added and further incubated for 2 h in the dark and at room temperature. The absorbance was then measured at 725 nm against a blank on the BioTek Powerwave XS2 Microplate Reader (BioTek Instruments Incorporation, Winooski, Vermont, USA) at 25°C. The phenolic content was expressed as mg gallic acid equivalents (GAE) per gram of extract dry weight (mg GAE/g DW).

Orthodiphenols Content

For the analysis of the orthodiphenols content, a colorimetric method, based on a complex reaction with sodium molybdate dehydrate, was applied (9). Briefly, extract aliquots (60 μl at a concentration of 1 mg ml^{-1}) or gallic acid standards (0.01–1.0 mg ml^{-1} in methanol) were reacted for 25 min with 200 μl of a sodium molybdate dihydrate solution (5% prepared in ethanol/water, 1:1 v/v). The absorbance of the samples and standards was measured at 370 nm against a blank (ethanol/water 1:1, v/v) on a plate reader at 25°C. The results were expressed as mg of GAEs per gram of extract (mg GAE/g DW).

Determination of Antiradical and Antioxidant Capacities

To evaluate 2,2'-azinobis(3-ethylbenzothiazoline-6-sulfonic acid (ABTS) radical inhibition, 12 μl of sample or standard was placed in the microplate followed by 188 μl of ABTS + working solution. The plate was allowed to rest in the dark for 30 min at room temperature and the absorbance was read at 734 nm. The inhibition of ABTS + radicals was calculated using the following Equation (3).

$$\% \text{Inhibition} = (\text{Abs Blank} - \text{Abs samples}) / (\text{Abs Blank}) \times 100 \quad (3)$$

The antioxidant activity of the extracts was determined by interpolation of the calibration curve for Trolox, and the results were expressed in mmol Trolox per gram of DW [mmol Trolox/g DW; (9)].

To measure ferric reducing antioxidant power (FRAP), 20 μl of sample was placed in each well of the microplate followed by adding 180 μl of FRAP working solution. After incubating the reaction for 30 min at 37°C in the dark, absorbance was read at 593 nm. Trolox was used as standard and the results were expressed in mmol Trolox per gram of DW (mmol Trolox/g DW).

High-Performance Liquid Chromatography Analysis of Individual Polyphenol Compounds

The samples were submitted to HPLC-DAD in order to assess the profile and content of polyphenols, using the procedure

next described, adapted from (10). A total of 500 μl of each extract obtained previously was injected in a system with an eluent composed by water with 0.1% of trifluoroacetic acid (TFA) (solvent A) and acetonitrile with 0.1% TFA (solvent B). The elution was performed at a flow rate of solvent of 1 ml min^{-1} , with a gradient starting from 0% solvent B at 0 min, 0% solvent B at 5 min, 20% solvent B at 15 min, 50% solvent B at 30 min, 100% solvent B at 45 min, 100% solvent B at 50 min, 0% solvent B at 55 min, and 0% solvent B at 60 min. The injection volume was 10 μl of sample. Chromatograms were recorded at 254 and 280 nm for benzoic acids and flavan-3-ols, 320 nm for cinnamic acids, and 370 nm for flavonoids, with a C18 column (250, 9, 46 mm, 5 mm, ACE HPLC Columns, Advanced Chromatography Technologies Ltd, Aberdeen, Scotland, UK). Individual polyphenols were identified using peak retention time, UV spectra, and UV maximum absorbance bands and trough comparison with external commercial standards (Extrasynthese, Cedex, France). External standards were freshly prepared in 70% methanol (methanol:water) at concentration of 1.0 mg ml^{-1} and running in HPLC-DAD simultaneously to the samples. The amount of each polyphenols was calculated using the internal standard (naringin) method. The results were expressed as mg 100 g^{-1} DW and calibration curves with standards were previously prepared and injected in HPLC in order to validate the method.

Cytotoxicity Assay

Human foreskin fibroblasts-1 (HFF-1) was purchased from ATCC (ATCC Number: SCRC-1041; ATCC, Manassas, Virginia, USA). Cell line were grown in DMEM medium (Carlsbad, California, USA) fortified with L-glutamine, 10% inactivated fetal calf serum (FBS), antibiotic–antimitotic mixture (final concentration of 100 U/ml penicillin and 100 U/ml streptomycin) maintained in 5% CO_2 incubator (Cell Culture® CO_2 Incubator, ESCO GB Ltd., UK). At 90–95% confluence, cells were trypsinized and plated in microtiter dishes. The viable cells were counted using trypan blue dye (Gibco) in hemocytometer. Cell viability was assessed using the (3-(4,5-dimethylthiazol-2-yl)-5-(3-carboxymethoxyphenyl)-2-(4-sulfophenyl)-2H-tetrazolium (MTT purchased from Promega, Madison, Wisconsin, USA) conversion assay. Cells were cultured in 96-well microtiter plate at a density of 25×10^3 cells per ml culture medium for 24 h. Then, cells were incubated with 1 $\mu\text{g mL}^{-1}$ to 10 mg mL^{-1} of both the extracts and its corresponding formulation for 24 h at 37°C. After the removal of samples from the wells, cells were washed in phosphate-buffered saline, followed by addition of fresh medium. The microtiter plates were then incubated in a humidified atmosphere of 5% CO_2 at 37°C for 24 h. To evaluate the number of viable cells, 100 μl of MTT solution was added into each well and incubated for 4 h at 37°C in the dark. Afterward, the medium was removed, the intracellular formazan crystals were solubilized, and extracted with 100 μl DMSO. After 15 min in continuous stirring at room temperature, the absorbance was measured at 490 nm with background subtraction at 630 nm in the Synergy HT Microplate Reader (BioTek Instruments Incorporation, Winooski, Vermont, USA; (11)).

Statistical Analysis

Data are expressed as mean \pm SD and were statistically analyzed by the one-way ANOVA, followed by the Holm-Sidak's multiple comparison test. Statistical analyses were performed using the GraphPad Prism software (San Diego, CA) for Windows (version 7) and differences were considered significant when $p < 0.05$ (95% significance).

RESULTS

Antimicrobial Activity Evaluation of Extracts

Data on screening of antimicrobial activity of the *B. edulis* and *N. luridiformis* against Gram-positive and Gram-negative bacteria are shown in **Tables 1, 2**, respectively. Aqueous extracts from both the species of mushrooms represented high activity against most of the sensitive and resistant clinical isolates, while the methanolic extract showed a lesser activity against all the isolates. Concerning to aqueous extracts, the bacterial inhibition halos from Gram-positive varied between 8 and 25 mm and between 8 and 18 mm for *B. edulis* and *N. luridiformis*, respectively (**Table 1**). Noteworthy, aqueous extract also showed high bacterial inhibition halos in *P. aeruginosa*, with values varying between 13 and 21 mm and 7 and 17 mm for *B. edulis* and *N. luridiformis*, respectively (**Table 2**). Methanolic extracts from both the species showed lower bacterial inhibition halos values for all the clinical isolates. On the other hand, aqueous and methanolic extracts of both the species of mushrooms were not effective against *K. pneumoniae*.

The MIC and MBC of extracts against Gram-positive and Gram-negative clinical isolates are given in **Tables 3, 4**, respectively. The MIC values for Gram-positive bacteria ranged between 15.63 and 62.5 $\mu\text{g}\cdot\text{ml}^{-1}$ and 62.5 and 250 $\mu\text{g}\cdot\text{ml}^{-1}$ for aqueous *B. edulis* and *N. luridiformis*, respectively. The MIC values for *P. aeruginosa* varied from 7.81 to 62.5 $\mu\text{g}\cdot\text{ml}^{-1}$ and 31.25 to 125 $\mu\text{g}\cdot\text{ml}^{-1}$ for aqueous *B. edulis* and *N. luridiformis*, respectively. Methanolic extracts from both the species showed lower MICs values for all the clinical isolates. Similar to diffusion test, aqueous and methanolic extracts of both the species were not effective against *K. pneumoniae*.

Concerning to MBC, the lowest concentration with bactericidal effect of aqueous and methanolic extracts of *B. edulis* against Methicillin-resistant *Staphylococcus aureus* (MRSA) were 250 and 500 $\mu\text{g}\cdot\text{ml}^{-1}$, respectively. For *P. aeruginosa*, the values were 125 $\mu\text{g}\cdot\text{ml}^{-1}$ for aqueous *B. edulis* extract and 500 $\mu\text{g}\cdot\text{ml}^{-1}$ for methanolic extract. With respect to *N. luridiformis*, the MBC of aqueous and methanolic extracts against MRSA was 500 $\mu\text{g}\cdot\text{ml}^{-1}$. Similar results were achieved for *P. aeruginosa* with *N. luridiformis* aqueous and methanolic extracts.

Effect of Extracts on Biofilms

The efficacy of the different extracts at MIC, 5 \times MIC, and 10 \times MIC was tested against *S. aureus* CETC 976 and *E. coli* CETC 434 for 24 h and the biofilms were characterized in terms of biomass and metabolic activity (**Figures 1, 2**, respectively). The higher biomass removal was obtained for the aqueous extract of *B. edulis* in *S. aureus* (78.0 \pm 5.02%) and in *E. coli* (94.0 \pm

8.0%) at 10 \times MIC (**Figures 1A,B**). Concerning the remaining analyzed extracts, the biofilm removal in both the bacterial species presented the following order: *N. luridiformis* aqueous > *B. edulis* methanolic > *N. luridiformis* methanolic for each concentration tested (**Figures 1, 2**). Concerning to the biofilm inactivation, the treatments with the different extracts caused the highest inactivation and presented the following order for both the biofilms (*S. aureus* and *E. coli*): *B. edulis* aqueous > *N. luridiformis* aqueous > *B. edulis* methanolic > *N. luridiformis* methanolic for each concentration tested (**Figures 1, 2**). The percentage of biofilm inactivation with the different extracts at 5 \times MIC and 10 \times MIC was higher than with MIC.

Phytochemical Profile

Total Phenolic and Orthodiphenols Contents

Figure 3 shows the total phenolic and orthodiphenols compounds in aqueous and methanolic extracts of *B. edulis* and *N. luridiformis*, respectively. The results showed that there were significant differences between aqueous (24.74 \pm 1.11 mg GAE.g⁻¹ DW) and methanolic (21.62 \pm 0.77 mg GAE.g⁻¹ DW) extracts of *B. edulis*. Similar results were observed between aqueous (7.64 \pm 0.08 mg GAE.g⁻¹ DW) and methanolic (5.64 \pm 0.56 mg GAE.g⁻¹ DW) extracts of *N. luridiformis*. Noteworthy, the amount of total phenolic compounds content in the aqueous *B. edulis* extract was significantly higher than in the aqueous extract of *N. luridiformis*. Like the total phenolic compounds, the orthodiphenols content in the aqueous extract of *B. edulis* (30.54 \pm 4.23 mg GAE.g⁻¹ DW) was significantly higher than in the aqueous extract of *N. luridiformis* (13.50 \pm 1.90 mg GAE.g⁻¹ DW). On the other hand, no significant differences ($p > 0.05$) were observed between the aqueous and methanolic extracts of *B. edulis*.

In-vitro Antioxidant Activity

According to the previous reports, mushrooms polyphenols exhibit a variety of bioactivities, especially antioxidant properties (6). Consequently, with different approaches and mechanisms, the 2 main usual antioxidant/antiradical activity assays, FRAP and ABTS, were carried out *in vitro*. The results obtained are shown in **Figure 5**. The aqueous extracts from both the species showed a higher antioxidant activity compared to the methanolic extracts. Also, a higher ABTS^{•+} radical scavenging activity was observed for the aqueous extract of *B. edulis* (0.157 \pm 0.02 mmol Trolox.g⁻¹ DW) when compared with the methanolic extract (0.128 \pm 0.02 mmol Trolox.g⁻¹ DW). Noteworthy, a significant difference ($p > 0.05$) between the aqueous extract of *B. edulis* and the aqueous extract of *N. luridiformis* (0.044 \pm 0.02 mmol Trolox.g⁻¹ DW) was observed. The reducing power of ferrous ions in the tested extracts presents similar results to the radical scavenging capacity (**Figure 4**). The FRAP capacities of the 4 extracts were in the order of *B. edulis* aqueous (0.349 \pm 0.01 mmol Trolox.g⁻¹ DW) > *B. edulis* methanolic (0.282 \pm 0.02 mmol Trolox.g⁻¹ DW) > *N. luridiformis* methanolic (0.133 \pm 0.005 mmol Trolox.g⁻¹ DW) > *N. luridiformis* aqueous (0.08 \pm 0.005 mmol Trolox.g⁻¹ DW). These results are in accordance with those obtained for the total phenolic compounds and orthodiphenols contents of methanolic and aqueous extracts.

TABLE 1 | *In vitro* Gram-positive antimicrobial activity of positive control and aqueous and methanolic extracts of *B. edulis* and *N. luridiformis* (1,000 µg.mL⁻¹), determined by the diameter of inhibition zones (mm).

	Bacterial isolates	Code	Aqueous extrac		Methanolic extrac		Control	
			<i>B. edulis</i>	<i>N. luridiformis</i>	<i>B. edulis</i>	<i>N. luridiformis</i>	CN	DMSO
Gram ⁺	MS <i>Staphylococcus aureus</i>	MJMC 018	9 ± 2.82 (+)	8 ± 0.71 (+)	7 ± 0.0 (+)	6 ± 0.0 (–)	S ²⁰ ± 1.0	6 ± 0.0
	MR <i>Staphylococcus aureus</i>	MJMC 025	12 ± 2.12 (+)	10 ± 0.71 (+)	7 ± 0.0 (+)	6 ± 0.0 (–)	S ¹⁷ ± 0.5	
	MS <i>Staphylococcus aureus</i>	MJMC 026	12 ± 0.71 (+)	10 ± 0.71 (+)	6 ± 0.0 (–)	6 ± 0.0 (–)	S ²¹ ± 0.0	
	MS <i>Staphylococcus aureus</i>	MJMC 027	10 ± 1.41 (+)	10 ± 0.71 (+)	9 ± 0.0 (+)	6 ± 0.0 (–)	S ¹⁷ ± 1.0	
	MR <i>Staphylococcus aureus</i>	MJMC 102	18 ± 0.0 (+)	11 ± 0.71 (+)	8 ± 0.71 (+)	6 ± 0.0 (–)	S ¹⁸ ± 2.0	
	MS <i>Staphylococcus aureus</i>	MJMC 109	18 ± 1.41 (+)	13 ± 1.41 (+)	10 ± 2.12 (+)	8 ± 1.41 (+)	S ²⁰ ± 0.5	
	MS <i>Staphylococcus aureus</i>	MJMC 110	10 ± 1.41 (+)	6 ± 0.0 (–)	9 ± 2.12 (+)	7 ± 2.12 (+)	S ²⁰ ± 0.5	
	MR <i>Staphylococcus aureus</i>	MJMC 111	10 ± 0.70 (+)	8 ± 0.0 (+)	8 ± 0.71 (+)	6 ± 0.0 (–)	S ¹⁶ ± 1.0	
	MR <i>Staphylococcus aureus</i>	MJMC 507	10 ± 0.0 (+)	6 ± 0.0 (–)	6 ± 0.0 (–)	6 ± 0.0 (–)	S ¹⁷ ± 2.0	
	MS <i>Staphylococcus aureus</i>	MJMC 511	15 ± 0.71 (+)	11 ± 1.41 (+)	6 ± 0.0 (–)	6 ± 0.0 (–)	S ²⁰ ± 0.5	
	MS <i>Staphylococcus aureus</i>	MJMC 534-B	18 ± 0.71 (+)	6 ± 0.0 (–)	6 ± 0.0 (–)	6 ± 0.0 (–)	S ²¹ ± 0.5	
	MR <i>Staphylococcus aureus</i>	MJMC 539	8 ± 1.41 (+)	6 ± 0.0 (–)	6 ± 0.0 (–)	6 ± 0.0 (–)	S ¹⁹ ± 1.0	
	MR <i>Staphylococcus aureus</i>	MJMC 545	9 ± 2.12 (+)	8 ± 0.71 (+)	6 ± 0.0 (–)	6 ± 0.0 (–)	S ²⁰ ± 1.0	
	MR <i>Staphylococcus aureus</i>	MJMC 552	20 ± 1.41 (++)	9 ± 0.71 (+)	11 ± 0.71 (+)	9 ± 0.71 (+)	S ¹⁸ ± 0.0	
	MR <i>Staphylococcus aureus</i>	MJMC 565-A	13 ± 1.41 (+)	8 ± 0.71 (+)	6 ± 0.0 (–)	6 ± 0.0 (–)	S ²¹ ± 2.0	
	MR <i>Staphylococcus aureus</i>	MJMC 583	25 ± 2.12 (++)	18 ± 0.71 (++)	7 ± 0.0 (+)	6 ± 0.0 (–)	S ¹⁷ ± 1.0	
	MR <i>Staphylococcus aureus</i>	MJMC 605	8 ± 0.71 (+)	13 ± 1.41 (+)	6 ± 0.0 (–)	6 ± 0.0 (–)	S ²² ± 1.0	
	MS <i>Staphylococcus aureus</i>	MJMC 606	8 ± 0.71 (+)	6 ± 0.0 (–)	6 ± 0.0 (–)	6 ± 0.0 (–)	S ¹⁸ ± 2.0	
	MR <i>Staphylococcus aureus</i>	MJMC 615	9 ± 1.41 (+)	6 ± 0.0 (–)	6 ± 0.0 (–)	6 ± 0.0 (–)	S ¹⁹ ± 1.0	
	<i>Staphylococcus aureus</i>	CETC 976	9 ± 2.82 (+)	6 ± 0.0 (–)	6 ± 0.0 (–)	6 ± 0.0 (–)	S ²⁰ ± 1.0	

CN, Gentamicin; MR, methicillin-resistant; MS, methicillin-susceptible.

TABLE 2 | *In vitro* Gram-negative antimicrobial activity of positive control and aqueous and methanolic extracts of *B. edulis* and *N. luridiformis* (1,000 µg.mL⁻¹), determined by the diameter of inhibition zones (mm).

	Bacterial isolates	Code	Aqueous extrac		Methanolic extrac		Control	
			<i>B. edulis</i>	<i>N. luridiformis</i>	<i>B. edulis</i>	<i>N. luridiformis</i>	CN	DMSO
Gram [–]	<i>Klebsiella pneumoniae</i>	MJMC 537	6 ± 0.0 (–)	6 ± 0.0 (–)	6 ± 0.0 (–)	6 ± 0.0 (–)	S ²² ± 0.5	6 ± 0.0
	<i>Klebsiella pneumoniae</i>	MJMC 542	6 ± 0.0 (–)	6 ± 0.0 (–)	6 ± 0.0 (–)	6 ± 0.0 (–)	S ²¹ ± 0.5	
	<i>Klebsiella pneumoniae</i>	MJMC 543	6 ± 0.0 (–)	6 ± 0.0 (–)	6 ± 0.0 (–)	6 ± 0.0 (–)	S ²⁰ ± 0.0	
	<i>Klebsiella pneumoniae</i>	MJMC 555	6 ± 0.0 (–)	6 ± 0.0 (–)	6 ± 0.0 (–)	6 ± 0.0 (–)	S ²³ ± 0.5	
	<i>Klebsiella pneumoniae</i>	MJMC 562-B	6 ± 0.0 (–)	6 ± 0.0 (–)	6 ± 0.0 (–)	6 ± 0.0 (–)	S ²¹ ± 0.5	
	<i>Klebsiella pneumoniae</i>	MJMC 566	6 ± 0.0 (–)	6 ± 0.0 (–)	6 ± 0.0 (–)	6 ± 0.0 (–)	S ²¹ ± 1.0	
	<i>Klebsiella pneumoniae</i>	MJMC 569	6 ± 0.0 (–)	6 ± 0.0 (–)	6 ± 0.0 (–)	6 ± 0.0 (–)	S ²⁰ ± 0.5	
	<i>Klebsiella pneumoniae</i>	MJMC 592	6 ± 0.0 (–)	6 ± 0.0 (–)	6 ± 0.0 (–)	6 ± 0.0 (–)	S ²² ± 1.0	
	<i>Klebsiella pneumoniae</i>	MJMC 597	6 ± 0.0 (–)	6 ± 0.0 (–)	6 ± 0.0 (–)	6 ± 0.0 (–)	S ²¹ ± 0.0	
	<i>Klebsiella pneumoniae</i>	MJMC 525	6 ± 0.0 (–)	6 ± 0.0 (–)	6 ± 0.0 (–)	6 ± 0.0 (–)	S ²² ± 0.5	
	<i>Acinetobacter baumannii</i>	MJMC 561	6 ± 0.0 (–)	6 ± 0.0 (–)	6 ± 0.0 (–)	6 ± 0.0 (–)	S ²⁵ ± 0.5	
	<i>Acinetobacter baumannii</i>	MJMC 526	6 ± 0.0 (–)	6 ± 0.0 (–)	6 ± 0.0 (–)	6 ± 0.0 (–)	S ²² ± 1.0	
	<i>Pseudomonas aeruginosa</i>	MJMC 540	21 ± 0.71 (+)	17 ± 0.71 (+)	13 ± 1.41 (+)	10 ± 1.41 (+)	S ²⁵ ± 0.2	
	<i>Pseudomonas aeruginosa</i>	MJMC 553	18 ± 1.41 (+)	12 ± 0.71 (+)	14 ± 2.12 (+)	12 ± 0.70 (+)	S ²² ± 0.0	
	<i>Pseudomonas aeruginosa</i>	MJMC 559	20 ± 1.41 (++)	9 ± 0.71 (+)	6 ± 0.0 (–)	6 ± 0.0 (–)	S ¹⁷ ± 0.5	
	<i>Pseudomonas aeruginosa</i>	MJMC 568-A	13 ± 1.41 (+)	8 ± 0.71 (+)	6 ± 0.0 (–)	6 ± 0.0 (–)	S ²⁵ ± 1.0	
	<i>Pseudomonas aeruginosa</i>	MJMC 598	22 ± 1.41 (+)	13 ± 1.41 (+)	13 ± 0.70 (+)	9 ± 0.70 (+)	S ²² ± 1.0	
	<i>Escherichia coli</i>	CETC 434	13 ± 1.41 (+)	7 ± 0.0 (+)	9 ± 0.70 (+)	7 ± 0.0 (+)	S ¹⁸ ± 0.5	

CN, Gentamicin.

TABLE 3 | Minimum inhibitory concentration ($\mu\text{g.mL}^{-1}$) and minimum bactericidal concentration for aqueous and methanolic extracts of *B. edulis* and *N. luridiformis*.

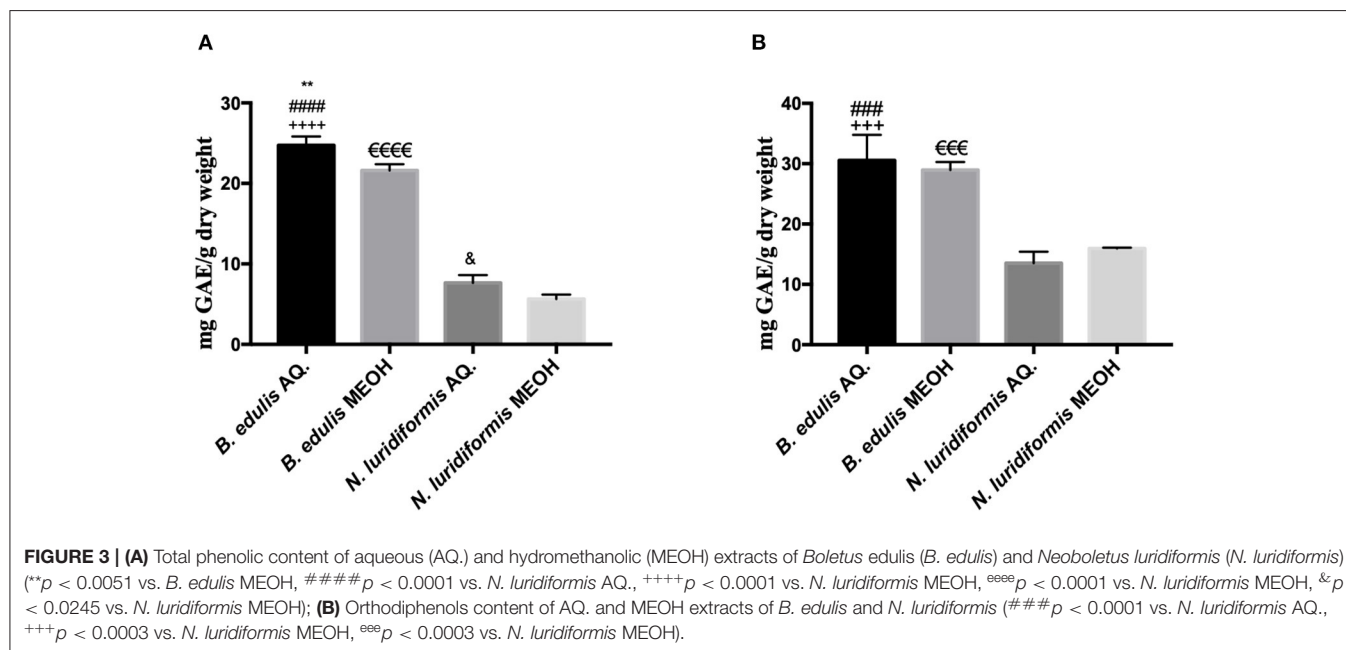
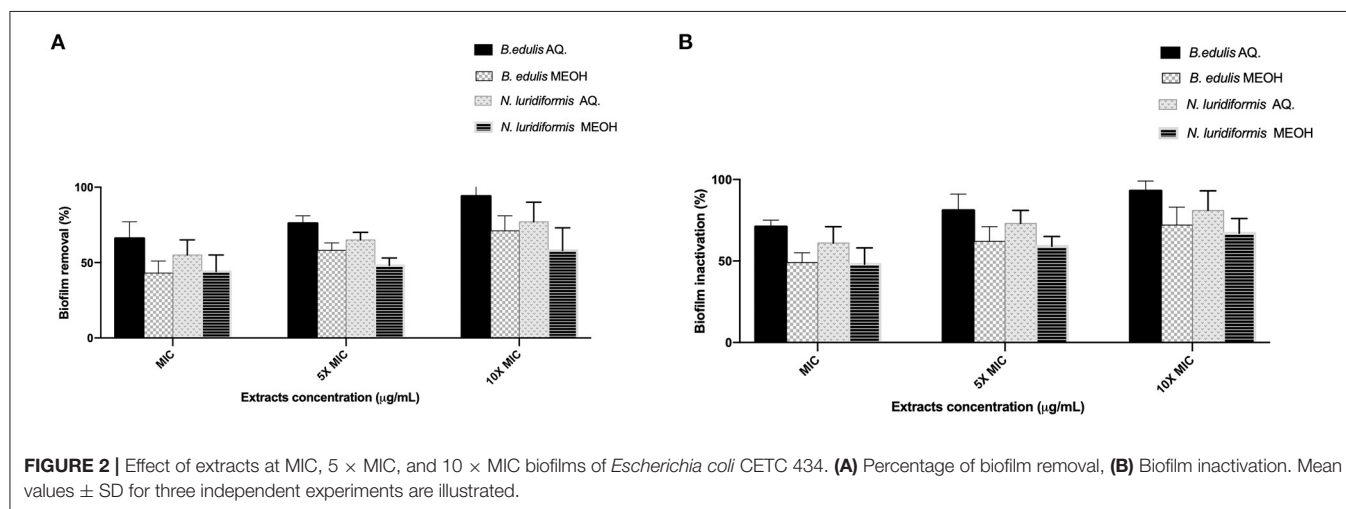
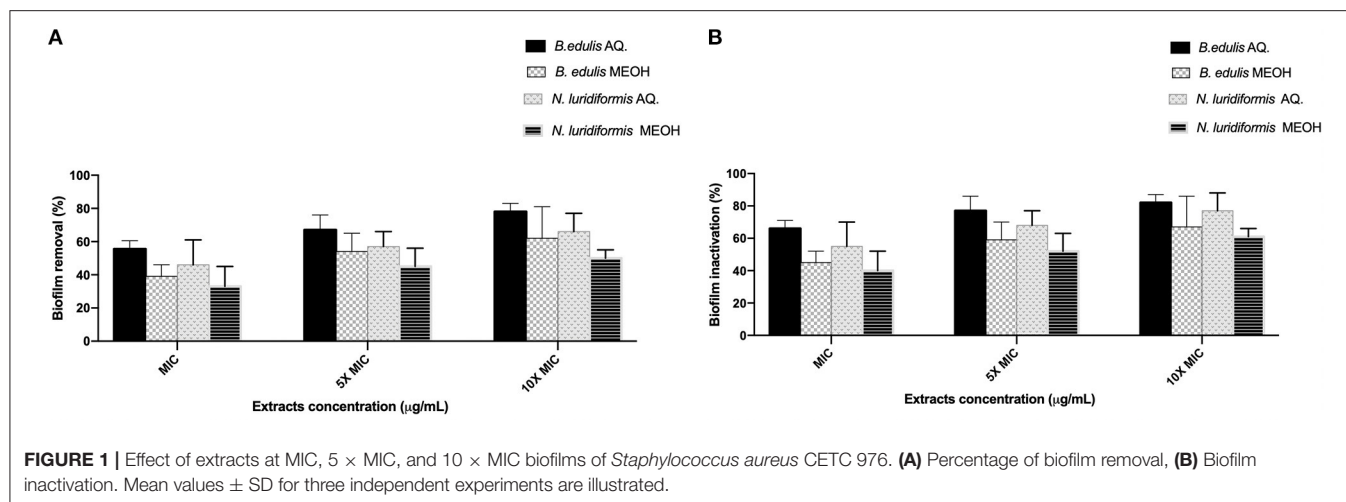
			Aqueous extract				Methanolic extracts				CN
			<i>B. edulis</i>		<i>N. luridiformis</i>		<i>B. edulis</i>		<i>N. luridiformis</i>		
			MIC	MBC	MIC	MBC	MIC	MBC	MIC	MBC	
Bacterial isolates	Code										MIC
GRAM ⁺	<i>MS Staphylococcus aureus</i>	MJMC 018	31.25	500	125	>1,000	500	1,000	1,000	>1,000	62.5
	<i>MR Staphylococcus aureus</i>	MJMC 025	62.5	1,000	125	>1,000	500	1,000	1,000	>1,000	62.5
	<i>MS Staphylococcus aureus</i>	MJMC 026	31.25	500	250	>1,000	500	1,000	1,000	>1,000	15.63
	<i>MR Staphylococcus aureus</i>	MJMC 027	31.25	500	250	>1,000	250	>1,000	500	>1,000	15.63
	<i>MR Staphylococcus aureus</i>	MJMC 102	62.5	>1,000	125	>1,000	250	>1,000	500	>1,000	15.63
	<i>MS Staphylococcus aureus</i>	MJMC 109	31.25	500	62.5	500	250	1,000	500	1,000	15.63
	<i>MS Staphylococcus aureus</i>	MJMC 110	15.63	250	62.5	500	125	500	250	1,000	7.81
	<i>MR Staphylococcus aureus</i>	MJMC 111	15.63	250	62.5	500	125	500	500	1,000	7.81
	<i>MR Staphylococcus aureus</i>	MJMC 507	62.5	500	125	>1,000	250	1,000	250	>1,000	62.5
	<i>MS Staphylococcus aureus</i>	MJMC 511	31.25	500	125	>1,000	500	1,000	1,000	>1,000	7.81
	<i>MR Staphylococcus aureus</i>	MJMC 534B	15.63	500	250	>1,000	500	>1,000	1,000	>1,000	7.81
	<i>MR Staphylococcus aureus</i>	MJMC 539	125	500	250	500	500	1,000	1,000	1,000	62.5
	<i>MR Staphylococcus aureus</i>	MJMC 545	31.25	500	62.5	>1,000	250	>1,000	500	>1,000	62.5
	<i>MR Staphylococcus aureus</i>	MJMC 552	31.25	1,000	62.5	>1,000	250	>1,000	250	>1,000	15.63
	<i>MR Staphylococcus aureus</i>	MJMC 565A	15.63	250	125	500	125	500	250	1,000	15.63
	<i>MR Staphylococcus aureus</i>	MJMC 583	62.5	500	125	1,000	125	500	500	1,000	31.25
	<i>MR Staphylococcus aureus</i>	MJMC 605	62.5	>1,000	250	>1,000	250	500	500	500	62.5
	<i>MS Staphylococcus aureus</i>	MJMC 606	125	>1,000	250	>1,000	500	500	1,000	500	31.25
	<i>MR Staphylococcus aureus</i>	MJMC 615	125	500	250	1,000	500	>1,000	1,000	>1,000	62.5
	<i>Staphylococcus aureus</i>	CETC 976	62.5	500	125	1,000	500	>1,000	1,000	>1,000	15.63

CN, Gentamicin; MR, methicillin-resistant; MS, methicillin-susceptible.

TABLE 4 | Minimum inhibitory concentration ($\mu\text{g.mL}^{-1}$) and minimum bactericidal concentration for aqueous and methanolic extracts of *B. edulis* and *N. luridiformis*.

			Aqueous extract				Methanolic extracts				CN
			<i>B. edulis</i>		<i>N. luridiformis</i>		<i>B. edulis</i>		<i>N. luridiformis</i>		
			MIC	MBC	MIC	MBC	MIC	MBC	MIC	MBC	
Bacterial isolates	Code	MIC	MBC	MIC	MBC	MIC	MBC	MIC	MBC	MIC	
GRAM	<i>Klebsiella pneumoniae</i>	MJMC 537	NI	ND	NI	ND	NI	ND	NI	ND	7.81
	<i>Klebsiella pneumoniae</i>	MJMC 542	NI	ND	NI	ND	NI	ND	NI	ND	7.81
	<i>Klebsiella pneumoniae</i>	MJMC 543	NI	ND	NI	ND	NI	ND	NI	ND	62.5
	<i>Klebsiella pneumoniae</i>	MJMC 555	NI	ND	NI	ND	NI	ND	NI	ND	62.5
	<i>Klebsiella pneumoniae</i>	MJMC 562-B	NI	ND	NI	ND	NI	ND	NI	ND	31.25
	<i>Klebsiella pneumoniae</i>	MJMC 566	NI	ND	NI	ND	NI	ND	NI	ND	31.25
	<i>Klebsiella pneumoniae</i>	MJMC 569	NI	ND	NI	ND	NI	ND	NI	ND	31.25
	<i>Klebsiella pneumoniae</i>	MJMC 592	NI	ND	NI	ND	NI	ND	NI	ND	62.5
	<i>Klebsiella pneumoniae</i>	MJMC 597	NI	ND	NI	ND	NI	ND	NI	ND	62.5
	<i>Acinetobacter baumannii</i>	MJMC 525	NI	ND	NI	ND	NI	ND	NI	ND	15.63
	<i>Acinetobacter baumannii</i>	MJMC 561	NI	ND	NI	ND	NI	ND	NI	ND	15.63
	<i>Pseudomonas aeruginosa</i>	MJMC 526	15.63	250	125	500	250	500	500	1,000	62.5
	<i>Pseudomonas aeruginosa</i>	MJMC 540	7.81	125	31.25	500	125	500	500	>1,000	31.25
	<i>Pseudomonas aeruginosa</i>	MJMC 553	31.25	500	62.5	>1,000	125	1,000	250	1,000	62.5
	<i>Pseudomonas aeruginosa</i>	MJMC 559	31.25	500	62.5	1,000	125	>1,000	250	500	31.25
	<i>Pseudomonas aeruginosa</i>	MJMC 568-A	62.5	1,000	125	>1,000	250	>1,000	500	1,000	31.25
	<i>Pseudomonas aeruginosa</i>	MJMC 598	15.63	250	125	500	250	1,000	500	>1,000	15.63
	<i>Escherichia coli</i>	CETC 434	62.5	>1,000	125	>1,000	500	1,000	1,000	>1,000	15.63

CN, Gentamicin; NI, Not inhibited; ND, Not determined.



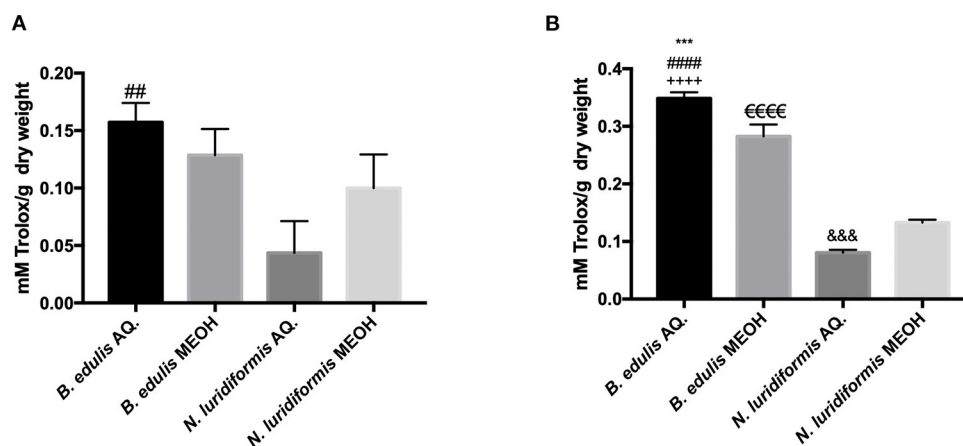


FIGURE 4 | (A) 2,2'-azino-bis(3-ethylbenzothiazoline-6-sulfonic acid (ABTS) AQ. and MEOH extracts of *B. edulis* and *N. luridiformis* ($^{##}p < 0.0001$ vs. *N. luridiformis* AQ.); **(B)** Ferric reducing antioxidant power (FRAP) AQ. and MEOH extracts of *B. edulis* and *N. luridiformis* ($^{***}p < 0.0003$ vs. *B. edulis* MEOH, $^{####}p < 0.0001$ vs. *N. luridiformis* AQ., $^{++++}p < 0.0001$ vs. *N. luridiformis* MEOH, $^{eeee}p < 0.0001$ vs. *N. luridiformis* MEOH, $^{&\&\&\&p < 0.0008$ vs. *N. luridiformis* MEOH).

TABLE 5 | Phenolic compounds identified and quantified in the aqueous and methanolic extracts of *B. edulis* and *N. luridiformis*.

Mushrooms extracts	Phenolic compounds	[.] mg. g ⁻¹ dry weight
<i>Boletus edulis</i> aqueous extract	Gallic acid	7.3 ± 1.2
	Pyrogallol	7.6 ± 0.8
	2,4-dihydroxybenzoic acid	0.5 ± 0.1
	2,5-dihydroxyphenylacetic acid (Homogentisic acid)	14.4 ± 2.7
	Protocatechuic acid	18.1 ± 1.8
	p-dihydroxybenzoic acid	1.8 ± 0.9
	Catechin	2.0 ± 1.4
<i>Boletus edulis</i> methanolic extract	Gallic acid	4.3 ± 1.1
	2,5-dihydroxyphenylacetic acid (Homogentisic acid)	6.2 ± 2.2
	Protocatechuic acid	11.5 ± 3.2
	p-dihydroxybenzoic acid	1.3 ± 0.3
	Catechin	0.9 ± 0.1
<i>Neoboletus luridiformis</i> aqueous extract	2,4-Dihydroxybenzoic acid	3.8 ± 1.7
	2,5-dihydroxyphenylacetic acid	2.4 ± 1.2
	Protocatechuic acid	19.6 ± 3.6
<i>Neoboletus luridiformis</i> methanolic extract	4-Hydroxybenzoic acid	1.9 ± 0.9
	2,4-dihydroxybenzoic acid	7.0 ± 1.5
	2,5-dihydroxyphenylacetic acid (Homogentisic acid)	2.7 ± 0.8
	Protocatechuic acid	5.8 ± 1.3
	Vanillic acid	1.4 ± 0.7

Polyphenol Composition

In this study, water and methanol extracts were used to assess polyphenol composition of the species of mushroom. The results obtained by HPLC-DAD analysis of the mushrooms extracts are given in Table 5 and *B. edulis* aqueous chromatogram can be seen in Figure 5. Differences in both the polyphenol profile and

content between water and methanol extracts were found. A total of nine different polyphenols were identified. Aqueous extract of *B. edulis* profile exhibited high content of protocatechuic acid (18.1 ± 1.8 mg 100 g⁻¹ DW) and homogentisic acid (14.4 ± 2.7 mg 100 g⁻¹ DW). Other polyphenols were gallic acid, pyrogallol, 2,4-dihydroxybenzoic acid, p-dihydroxybenzoic acid, and catechin. Protocatechuic acid (11.5 ± 3.2 mg 100 g⁻¹ DW) and homogentisic acid (6.2 ± 2.2 mg 100 g⁻¹ DW) were also the main polyphenols found in methanolic extracts of *B. edulis*, followed by gallic acid, p-dihydroxybenzoic acid, and catechin. Protocatechuic acid (19.6 ± 3.6 mg 100 g⁻¹ DW) was the main polyphenol found in the aqueous extract of *N. luridiformis*, followed by the homogentisic acid and 2,4-dihydroxybenzoic acid. The 2,4-dihydroxybenzoic acid (7.0 mg ± 1.5 100 g⁻¹ DW) was the main polyphenol identified in the methanolic extract of *N. luridiformis* followed by protocatechuic acid, homogentisic acid, 4-hydroxybenzoic acid, and vanillic acid. In general, *B. edulis* showed higher content of individual polyphenols compared to other species, which corroborates the findings of total phenolics and orthodiphenols contents. In addition, our findings, showed for all the samples the presence of important polyphenols such as protocatechuic acid, homogentisic acid, gallic acid, and 2,4-dihydroxybenzoic acid and others, often reported by literature as having important antioxidant and antimicrobial activities.

Cytotoxicity

Data of Figure 6 indicate that the cell viability of HFF-1 cell lines, after exposure to all extracts in the different concentrations, showed a cell survival rate of ~90%.

DISCUSSION

Nowadays, the incidence of human pathogens resistant to numerous antibiotics has been increased worldwide. More

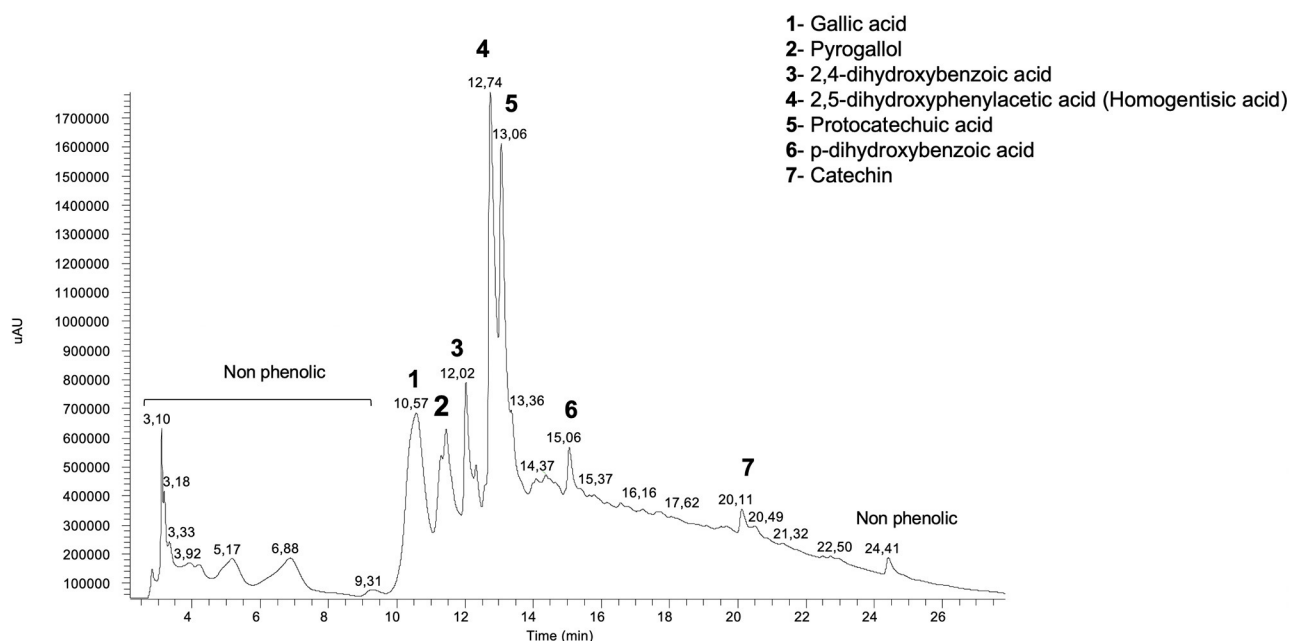


FIGURE 5 | Effect of aqueous and methanolic extracts of *B. edulis* and *N. luridiformis* on viability of human foreskin fibroblasts-1 (HFF-1). Cell viability following incubation with indicated concentrations of crude extract for 24 h was determined using the MTT assay. Cell viability is expressed as a percentage of untreated cells. Results shown in the graphs are mean \pm SD obtained from triplicate experiments.

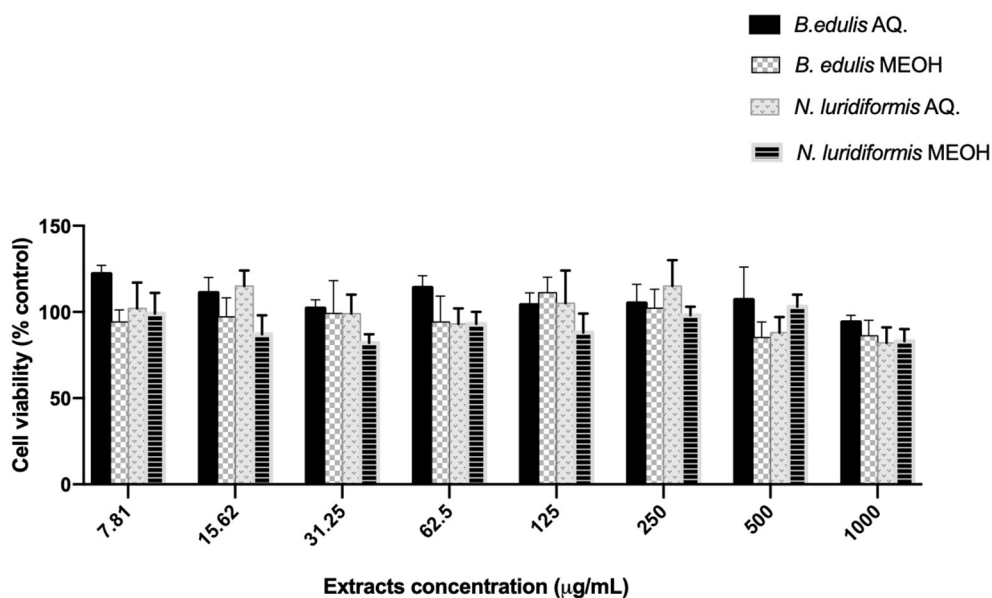


FIGURE 6 | Effect of aqueous and methanolic extracts of *Boletus edulis* and *Neoboletus luridiformis* on viability of Human foreskin fibroblasts (HFF-1). Cell viability following incubation with indicated concentrations of crude extract for 24 h was determined using the MTT assay. Cell viability is expressed as a percentage of untreated cells. Results shown in the graphs are mean \pm SD obtained from triplicate experiments.

importantly, the efficacy absence of the conventional antibiotics has generated serious problems on the treatment of infectious diseases (12). Therefore, urge to find new alternative therapies to fighting or decrease cases of infectious diseases was associated

with MDR pathogens. Due to the recognized safe status of natural products, the industry interest in antimicrobials derived from nature has boosted (13). Indeed, an outstanding amount of antimicrobial has been obtained from natural sources

including mushrooms (7). Mushrooms have been used since 1,000 of years in traditional medicine for several diseases and presently continue to play an important role in the discovery of new molecules (14). Mushrooms contain a multiplicity of bioactive compounds with chemical and structural variation that make them versatile in terms of biological activities including antimicrobial action (6). In this sense, this study provides new information with respect to the antimicrobial and antibiofilm activities, chemical composition, and characterization of 2 mushrooms species, *B. edulis* and *N. luridiformis*. To the best of our knowledge, this study provides the first report on the phenolic composition of *N. luridiformis* as well as antimicrobial activity. Moreover, this is a pioneer study with respect to *B. edulis* and *N. luridiformis* antibiofilm properties and constitutes an important step toward to combat the emergent biofilms activities that differ substantially from free-living bacterial cells (9).

The antimicrobial activity evaluation revealed that aqueous and methanolic extracts of both the species of mushrooms were effective against Gram-positive bacteria [methicillin-susceptible *Staphylococcus aureus* (MSSA) and MRSA] and Gram-negative bacteria (*P. aeruginosa* and *E. coli*). Noteworthy, the aqueous extracts from *B. edulis* presented the highest antimicrobial activity that was obtained against to MRSA MJMC 583 and *P. aeruginosa* carbapenem-resistant MJMC 540, which are in accordance with our previous study (6). Noteworthy, as clinical wound infection ESKAPE isolates that are associated to healthcare infections, these results confirmed the overwhelming importance of mushrooms as a source of antimicrobial compounds. Corroborating our findings, a study has found out that water extracts were better than methanol extracts against bacterial and fungal pathogens (15). Similarly, water extracts of wild mushrooms showed to be more effective against *P. aeruginosa*, *E. coli*, *B. subtilis*, and *C. albicans* isolates (16), which support our results. It is worth underlining the effect of different solvents on antioxidant activity. In this study, aqueous extracts had markedly higher antioxidant capacities than the methanolic extracts. Therefore, water is a more effective solvent for the extraction of antioxidant compounds from wild mushrooms. Moreover, the antimicrobial differences between the species of mushroom and the two solvents employed (aqueous and methanol) may be due to the contents of phenolic compounds, which was higher for the aqueous extract of *B. edulis*. In fact, several authors have previously associated with the antimicrobial activity of different natural sources to phenolic compounds (17–19).

Concerning to phenolic compounds profile, there are few studies with respect to the individual phenolics in wild edible mushrooms (20). Commercial species are better known in terms of composition; however, wild mushrooms are scarcely studied and, to the best of our knowledge, the polyphenol composition of the species *N. luridiformis* has not been previously described. Data showed that 2,4-dihydroxybenzoic acid, homogentisic acid, and protocatechuic acid were the only three polyphenols common to both the aqueous and methanolic extracts. Protocatechuic acid was present in higher amounts in the aqueous extract, while high levels of 2,4-dihydroxybenzoic acid were detected in the methanolic extract. 4-hydroxybenzoic

acid and vanillic acid were only present in methanolic extracts. For *B. edulis*, the experimental data are comparable to those reported in previous studies (20, 21); however, specific and characteristic composition of each mushroom may be associated with several factors, namely, genetic, physiological, and morphological characteristics, agroclimatic conditions, and ripening stage (6). The major phenolic compounds in aqueous extract were protocatechuic acid and homogentisic acid. Besides protocatechuic acid and homogentisic acid, the aqueous extract also exhibited considerable levels of gallic acid, pyrogallol, and catechin. On the other hand, the methanolic extract showed similar phenolic composition, however, in low contents, except for 2,4-dihydroxybenzoic acid and pyrogallol, which are only present in aqueous extracts. Noteworthy, the proportion of protocatechuic acid, however, is higher than in previous studies from different geographical origins (20, 22).

Alves et al. (4) confirmed that phenolics were the most important active compounds against bacteria (23). They also identified 2,4-dihydroxybenzoic and protocatechuic acids as the main phenolic compounds with higher activity against the majority of Gram-negative and Gram-positive bacteria (23). Moreover, this study highlighted the importance of the carboxylic group in the molecular structure for antimicrobial activity. In line with this, this study showed that the aqueous extract of *B. edulis* presented protocatechuic acids as the main compound, followed by homogentisic acid, pyrogallol, and gallic acid. It should be noted that protocatechuic acid as well as homogentisic acid has carboxylic groups, which may contribute for the higher antimicrobial activity. These compounds were also present in the other extracts tested, however, in low contents, explaining the highest aqueous *B. edulis* antimicrobial activity. In addition, gallic acid has been identified as the active compound for the inhibition of *E. coli*, *Salmonella enteritidis* (24), *P. aeruginosa*, *S. aureus*, and *Listeria monocytogenes* (25). Structural activity of correlation assays revealed that the three hydroxyl groups of gallic acid were effective for antibacterial activity and all the substituents of the benzene rings were effective against *S. aureus* (24). Gallic acid was only identified in *B. edulis*; however, the aqueous extracts showed an amount almost twice higher than the methanolic extract, which may explain the better antimicrobial activity of the aqueous extract.

The different phytochemical composition as well as antioxidant activity caused different effectiveness in the Gram-negative and Gram-positive biofilms. The percentages of biomass removal and inactivation were always higher for *E. coli* than for *S. aureus* for all the extracts tested. The total biofilm removal was not achieved with any of the extracts; however, the highest reduction (94%) in biomass removal was found for *E. coli* with the aqueous extract of *B. edulis*. Greater effect of extracts on biofilms of *E. coli* than on *S. aureus* is due to morphology, which is known to be different; generally, *S. aureus* biofilms are denser than those of *E. coli* (26). To the best of our knowledge, the antibiofilm properties of *B. edulis* and *N. luridiformis* have not been reported before and, therefore, our results can be evaluated as the first report about properties of these unique and wild species. Furthermore, and more importantly, all the extracts analyzed had no cytotoxic effect on the HFF-1 cell lines, which

demonstrates their potential in the management and treatment of wound.

It should be point out that specific compounds must be evaluated for further conclusions.

Finally, the antimicrobial and antibiofilm activities obtained in *Boletus* spp. extracts, especially against ESKAPE pathogens, is a capable finding to fight the most frequent causes of bacterial wound infections in developed countries. This study also provides comparative data on the potential bioactive compounds of different wild mushrooms and different solvents to help select the best system for antimicrobial application.

DATA AVAILABILITY STATEMENT

The raw data supporting the conclusions of this article will be made available by the authors, without undue reservation.

AUTHOR CONTRIBUTIONS

MJS, GM, and JG proposed the subject and designed. JG and FC carried out the chemical and the antimicrobial experiments. FR carried out the study of cytotoxicity. AA carried out the

chemical composition of the extracts. GM provided fungal samples and funding acquisition. JG, FR, and MJS wrote the manuscript. All the authors reviewed and contributed to the manuscript.

FUNDING

This study was funded by the project I&T Companies in Co-promotion FungiTech, Norte-01-0247-FEDER-033788; National Funds by FCT—Portuguese Foundation for Science and Technology, under the project UIDB/04033/2020 (CITAB—Center for the Research and Technology of Agro-Environmental and Biological Sciences).

ACKNOWLEDGMENTS

JG wish to acknowledge the project AquaValor—Centro de Valorização e Transferência de Tecnologia da Água (NORTE-01-0246-FEDER-000053), supported by Norte Portugal Regional Operational Programme (NORTE, 2020). FR was thankful for her contract (CEECIND/01886/2020) financed by FCT/MCTES—CEEC Individual 2020 Program Contract.

REFERENCES

- Mathur P, Singh S. Multidrug resistance in bacteria: a serious patient safety challenge for India. *J Lab Physicians*. (2013) 5:5–10. doi: 10.4103/0974-2727.115898
- Levin-Reisman I, Ronin I, Gefen O, Braniss I, Shoshan N, Balaban QN. Antibiotic tolerance facilitates the evolution of resistance. *Science*. (2017) 355:826–30. doi: 10.1126/science.aaj2191
- Medina E, Pieper HD. Tackling threats and future problems of multidrug-resistant bacteria. *Curr Top Microbiol Immunol*. (2016) 398:3–33. doi: 10.1007/82_2016_492
- Bowler PG, Welsby S, Towers V, Booth R, Hogarth A, Rowlands V, et al. Multidrug-resistant organisms, wounds and topical antimicrobial protection. *Int Wound J*. (2012) 9:387–96. doi: 10.1111/j.1742-481X.2012.00991.x
- Alam MM, Islam MN, Hossain Hawlader MD, Ahmed S, Wahab A, Islam M, et al. Prevalence of multidrug resistance bacterial isolates from infected wound patients in Dhaka, Bangladesh: a cross-sectional study. *Int J Surg*. (2021) 28:56–62. doi: 10.1016/j.ijsso.2020.12.010
- Garcia J, Afonso A, Fernandes C, Nunes FM, Marques G, Saavedra JM. Comparative antioxidant and antimicrobial properties of *Lentinula edodes* Donko and *Koshin* varieties against priority multidrug-resistant pathogens. *S Afr J Chem Eng*. (2021) 35:98–106. doi: 10.1016/j.sajce.2020.09.008
- Alves MJ, Ferreira IC, Dias J, Teixeira V, Martins A, Pintado M. A review on antimicrobial activity of mushroom (Basidiomycetes) extracts and isolated compounds. *Planta Med*. (2012) 78:1707–18. doi: 10.1055/s-0032-1315370
- Moser M, Kibby G. *Keys to Agarics and Boleti: Polyporales, Boletales, Agaricales, Russulales*. London: Roger Phillips (1983). p. 535.
- Flemming H-C, Wingender J, Szewzyk U, Steinberg P, Rice SA, Kjelleberg S. Biofilms: an emergent form of bacterial life. *Nat Rev Microbiol*. (2016) 14:563–75. doi: 10.1038/nrmicro.2016.94
- Aires A, Carvalho R. Kiwi fruit residues from industry processing: study for a maximum phenolic recovery yield. *J Food Sci Technol*. (2020) 57:4265–76. doi: 10.1007/s13197-020-04466-7
- Rodrigues F, Palmeira-de-Oliveira A, das Neves J, Sarmento B, Amaral MH, Oliveira MB. *Medicago* spp. extracts as promising ingredients for skin care products. *Ind Crops Prod*. (2013) 49:634–44. doi: 10.1016/j.indcrop.2013.06.015
- Morris S, Cerreo E. Trends, epidemiology, and management of multidrug resistant gram-negative bacterial infections in the hospitalized setting. *Antibiotics*. (2020) 9:196. doi: 10.3390/antibiotics9040196
- Gupta PD, Birdi JT. Development of botanicals to combat antibiotic resistance. *J Ayurveda Integr Med*. (2017) 8:266–75. doi: 10.1016/j.jaim.2017.05.004
- Ganeshpurkar A, Rai G, Jain PA. Medicinal mushrooms: towards a new horizon. *Pharmacogn Rev*. (2010) 4:127–35. doi: 10.4103/0973-7847.70904
- Gebreyohannes G, Moges F, Sahile S, Raja N. Isolation and characterization of potential antibiotic producing actinomycetes from water and sediments of Lake Tana, Ethiopia. *Asian Pac J Trop Biomed*. (2013) 3:426–35. doi: 10.1016/S2221-1691(13)60092-1
- Pinu FR, Villas-Boas SG, Aggio R. Analysis of intracellular metabolites from microorganisms: quenching and extraction protocols. *Metabolites*. (2017) 7:53. doi: 10.3390/metabo7040053
- Alves MJ, Ferreira IC, Martins A, Pintado M. Antimicrobial activity of wild mushroom extracts against clinical isolates resistant to different antibiotics. *J Appl Microbiol*. (2012) 113:466–75. doi: 10.1111/j.1365-2672.2012.05347.x
- Barros L, Venturini BA, Baptista P, Estevinho LM, Ferreira CI. Chemical composition and biological properties of portuguese wild mushrooms: a comprehensive study. *J Agric Food Chem*. (2008) 56:3856–62. doi: 10.1021/jf8003114
- Bouarab-Chibane L, Forquet V, Lantéri P, Clément Y, Léonard-Akkari L, Oulahl N, et al. Antibacterial properties of polyphenols: characterization and QSAR (quantitative structure–activity relationship) models. *Front Microbiol*. (2019) 10:829. doi: 10.3389/fmicb.2019.00829
- Palacios I, Lozano M, Moro C, D'Arrigo M, Rostagno MA, Martínez JA, et al. Antioxidant properties of phenolic compounds occurring in edible mushrooms. *Food Chem*. (2011) 128:674–8. doi: 10.1016/j.foodchem.2011.03.085
- Balik M, Sulowska-Ziaja KJ, Ziaja M, Muszyńska B. Phenolic acids—occurrence and significance in the world of higher fungi. *Med Int Rev*. (2020) 29:72–81.
- Yahia EM, Gutiérrez-Orozco F, Moreno-Pérez AM. Identification of phenolic compounds by liquid chromatography-mass spectrometry in seventeen species of wild mushrooms in Central Mexico and determination of their antioxidant activity and bioactive compounds. *Food Chem*. (2017) 226:14–22. doi: 10.1016/j.foodchem.2017.01.044

23. Alves MJ, Ferreira I, Froufe CFR, Abreu HJC, Martins RMVA, Pintado M. Antimicrobial activity of phenolic compounds identified in wild mushrooms, SAR analysis and docking studies. *J Appl Microbiol.* (2013) 115:346–57. doi: 10.1111/jam.12196
24. Tesaki S, Tanabe S, Moriyama M, Fukushi E, Kawabata J, Watanabe M. Isolation and identification of an antibacterial compound from grape and its application to foods. *Bull Chem Soc Jpn.* (1999) 73:125–8. doi: 10.1271/nogeikagaku1924.73.125
25. Borges A, Ferreira C, Saavedra MJ, Simões M. Antibacterial activity and mode of action of ferulic and gallic acids against pathogenic bacteria. *Microb Drug Resist.* (2013) 19:256–65. doi: 10.1089/mdr.2012.0244
26. Lopez-Romero JC, González-Ríos H, Borges A, Simões M. Antibacterial effects and mode of action of selected essential oils components against *Escherichia coli* and *Staphylococcus aureus*. *Evid Based Complement Alternat Med.* (2015) 2015:795435–795435. doi: 10.1155/2015/795435

Conflict of Interest: The authors declare that the research was conducted in the absence of any commercial or financial relationships that could be construed as a potential conflict of interest.

Publisher's Note: All claims expressed in this article are solely those of the authors and do not necessarily represent those of their affiliated organizations, or those of the publisher, the editors and the reviewers. Any product that may be evaluated in this article, or claim that may be made by its manufacturer, is not guaranteed or endorsed by the publisher.

Copyright © 2022 Garcia, Rodrigues, Castro, Aires, Marques and Saavedra. This is an open-access article distributed under the terms of the Creative Commons Attribution License (CC BY). The use, distribution or reproduction in other forums is permitted, provided the original author(s) and the copyright owner(s) are credited and that the original publication in this journal is cited, in accordance with accepted academic practice. No use, distribution or reproduction is permitted which does not comply with these terms.



OPEN ACCESS

EDITED BY

A. M. Abd El-Aty,
Cairo University, Egypt

REVIEWED BY

Thierry Dagnac,
Galician Agency for Food
Quality, Spain
Marco Iammarino,
Experimental Zooprophyllactic Institute
of Puglia and Basilicata (IZSPB), Italy

*CORRESPONDENCE

Hao Dong
donghao@zhku.edu.cn
Xiaofei Xu
xfxufe@gdgu.edu.cn

SPECIALTY SECTION

This article was submitted to
Food Chemistry,
a section of the journal
Frontiers in Nutrition

RECEIVED 23 July 2022

ACCEPTED 09 September 2022

PUBLISHED 28 September 2022

CITATION

Luo D, Guan J, Dong H, Chen J,
Liang M, Zhou C, Xian Y and Xu X
(2022) Simultaneous determination of
twelve mycotoxins in edible oil, soy
sauce and bean sauce by PRiME HLB
solid phase extraction combined with
HPLC-Orbitrap HRMS.
Front. Nutr. 9:1001671.
doi: 10.3389/fnut.2022.1001671

COPYRIGHT

© 2022 Luo, Guan, Dong, Chen, Liang,
Zhou, Xian and Xu. This is an
open-access article distributed under
the terms of the [Creative Commons
Attribution License \(CC BY\)](#). The use,
distribution or reproduction in other
forums is permitted, provided the
original author(s) and the copyright
owner(s) are credited and that the
original publication in this journal is
cited, in accordance with accepted
academic practice. No use, distribution
or reproduction is permitted which
does not comply with these terms.

Simultaneous determination of twelve mycotoxins in edible oil, soy sauce and bean sauce by PRiME HLB solid phase extraction combined with HPLC-Orbitrap HRMS

Donghui Luo^{1,2}, Jingjing Guan¹, Hao Dong^{3*}, Jin Chen¹,
Ming Liang⁴, Chunxia Zhou¹, Yanping Xian⁴ and Xiaofei Xu^{1*}

¹College of Food Science and Engineering, Guangdong Ocean University, Yangjiang, China,

²Chaozhou Branch of Chemistry and Chemical Engineering Guangdong Laboratory (Hanjiang Laboratory), Chaozhou, China, ³Key Laboratory of Green Processing and Intelligent Manufacturing of Lingnan Specialty Food, Guangdong Provincial Key Laboratory of Lingnan Specialty Food Science and Technology, College of Light Industry and Food Sciences, Ministry of Agriculture, Zhongkai University of Agriculture and Engineering, Guangzhou, China, ⁴Guangzhou Quality Supervision and Testing Institute, Guangzhou, China

A solid phase extraction-high-performance liquid chromatography-tandem Orbitrap high resolution mass spectrometry (HPLC-Orbitrap HRMS) method was established for the determination of 12 mycotoxins (ochratoxin A, ochratoxin B, aflatoxin B1, aflatoxin B2, aflatoxin G1, aflatoxin G2, HT-2 toxin, sterigmatocystin, diacetoxyscironeol, penicillic acid, mycophenolic acid, and citreoviridin) in edible oil, soy sauce, and bean sauce. Samples were extracted by 80:20 (v:v) acetonitrile-water solution, purified by PRiME HLB column, separated by aQ C18 column with mobile phase consisting of 0.5 mmol/L ammonium acetate-0.1% formic acid aqueous solution and methanol. The results showed that the limits of detection (LODs) and limits of quantification (LOQs) of 12 mycotoxins were 0.12–1.2 µg/L and 0.40–4.0 µg/L, respectively. The determination coefficients of 12 mycotoxins in the range of 0.20–100 µg/L were > 0.998. The average recoveries in soy sauce and bean sauce were 78.4–106.8%, and the relative standard deviations (RSDs) were 1.2–9.7% under three levels, including LOQ, 2 × LOQ and 10 × LOQ. The average recoveries in edible oil were 78.3–115.6%, and the precision RSD ($n = 6$) was 0.9–8.6%. A total of 24 edible oils, soy sauce and bean sauce samples were analyzed by this method. AFB1, AFB2, sterigmatocystin and mycophenolic acid were detected in several samples at concentrations ranging from 1.0 to 22.1 µg/kg. The method is simple, sensitive, and rapid and can be used for screening and quantitative analysis of mycotoxin contamination in edible oil, soy sauce, and bean sauce.

KEYWORDS

PRiME HLB, HPLC-Orbitrap HRMS, edible oil, mycotoxin, soy sauce

Introduction

Mycotoxins are toxic secondary metabolites produced by mycotoxin-producing fungi under suitable environmental conditions (1–3). Currently, there are more than 400 known mycotoxins. Edible oils such as rapeseed oil, peanut oil, corn oil, sesame oil, soy sauce and bean sauce are easily contaminated by mycotoxins because most cereals are used as raw materials in the preparation process (4, 5). It has been reported that ~25% of wheat, corn, sorghum and rice produce toxic and harmful mycotoxins due to mildew during production, processing, transportation and storage every year (6). At present, aflatoxin (AFT), ochratoxin A (OTA) and zearalenone (ZEN) have a great influence on human health, which will damage human liver function, cause cancer and teratogenicity and induce immunosuppressive diseases after exceeding a certain intake (7, 8). The World Health Organization has included mycotoxins in the key monitoring objects of the food safety system (9). In China, GB2761-2017 “National Standard for Food Safety Limits of Mycotoxins in Food” also has strict regulations on the limit indicators of some mycotoxins in food. Under natural conditions, edible oils and condiments may be contaminated by various mycotoxins. According to the current national standards, it is necessary to use several detection methods for multiple experimental analyses to determine the content of different mycotoxins (10–12). The determination methods are not only cumbersome but also inefficient. Therefore, it is urgent to establish a synchronous detection method for multiple mycotoxins.

Anastassiades et al. (13) proposed the QuEChERS (Quick, Easy, Cheap, Effective, Rugged, Safe) method, namely, dispersive solid phase extraction, but it is still insufficient to extract many toxins from complex substrates. Oasis PRiME HLB is a type of reversed-solid phase extraction (SPE) adsorbent that can simplify and accelerate the SPE process and can obtain cleaner extracts compared with other sample pretreatment methods. Compared with other SPE products, it can also remove more than 90% of endogenous phospholipids and is widely used in the detection of food organic pollutants (14). At present, colloidal gold immunochromatography, enzyme-linked immunosorbent assay (ELISA) kits, immunoaffinity column-high-performance liquid chromatography and isotope dilution liquid chromatography tandem mass spectrometry are commonly used to detect mycotoxins (3, 15, 16). Liquid chromatography-tandem mass spectrometry (LC-MS/MS) has higher selectivity and sensitivity and has gradually become the main means for the simultaneous detection of various mycotoxins (9, 17, 18). Orbitrap high-resolution mass spectrometry (Orbitrap HRMS) has higher selectivity and resolution than ordinary mass spectrometry and can effectively reduce the interference of impurities in complex matrices (19–22).

Therefore, the samples were simply extracted and purified by a PRiME HLB solid phase extraction column in this study, and the conditions of liquid chromatography and mass spectrometry were optimized. An HPLC-Orbitrap HRMS method for the determination of mycotoxins in edible oil, soy sauce, and bean sauce was established. The method has advantages such as simplicity, rapidity and high flux, which is suitable for the screening and detection of mycotoxins in edible oil, soy sauce and bean sauce and reduce food safety problems caused by mycotoxin residues.

Materials and methods

Instruments and reagents

The Thermo Q Exactive Focus High Performance Liquid Chromatography–Mass Spectrometry System includes a Dionex Ultimate 3000 Liquid Phase Pump, Autosampler, Column Oven and Orbitrap High Resolution Mass Spectrometry Section (Thermo Fisher Scientific, Massachusetts, USA). XCalibur 4.0 software (Thermo Fisher Scientific, Massachusetts, USA) was used for mass spectrometer control and data processing. A Thermo Accucore aQ C18 (2.1 × 150 mm, 2.6 μm) was used as the chromatographic column. The samples were vortexed with an MS3 basic vortex mixer (IKA GmbH, Staufen, Germany). A KQ-250DV CNC ultrasonic cleaning device (Kunshan, Jiangsu, China) was used for supersonic-assisted extraction. Ultrapure water (18.2 MΩ·cm) prepared from a Milli-Q ultrapure system (Millipore, Bedford, MA, USA) was used in the whole experiment.

Twelve mycotoxins, as shown in Table 1, were purchased from Shanghai Anpu Scientific Instruments Co., Ltd. and Adamas Reagent Company of Switzerland. These standards all have a purity of or higher than 98.0%. Acetonitrile, methanol, ammonium acetate, and formic acid were obtained from CNW Technologies GmbH (CNW, Düsseldorf, Germany). A PRiME HLB solid phase extraction column was purchased from Waters Company (60 mg/3 cc, Waters, Beverly, MA, USA).

Preparation of standard solutions: The standard reference materials of each mycotoxin were carefully measured and prepared into a 1.00 mg/L mixed standard reserve solution with acetonitrile, which was stored in a refrigerator at 4 °C. Then, an appropriate amount of standard reserve solution was transferred and prepared with acetonitrile to form a series of mixed standard curves with concentrations of 100, 50, 20, 10, 5, 2, 1, 0.5, and 0.2 μg/L.

Sample preparation

Thirteen kinds of edible oil samples and 11 soy sauce and bean sauce samples were purchased from local supermarkets

TABLE 1 The gradient elution procedure of HPLC.

Time (min)	Mobile phase
0–2.0	90%A*
2.0–3.0	90%A–80%A
3.0–5.0	80%A–74%A
5.0–7.0	74%A
7.0–10.5	74%A–40%A
10.5–13.5	40%A
13.5–14.5	40%A–5%A
14.5–17.0	5%A
17.0–18.0	5%A–90%A
18.0–20.0	90%A

*The mobile phase consists of 0.5 mmol/L ammonium acetate solution containing 0.1% formic acid (A) and methanol (B).

and online shopping malls in Guangzhou. A 2.0 g sample was weighed and placed in a 50 mL centrifuge tube, and 20 mL acetonitrile-water 80:20 (v/v) solution was added. After mixing, the sample was extracted by oscillation for 10 min and centrifuged at $500 \times g$ for 5 min at room temperature. Ten milliliters of supernatant was transferred into a 50 mL centrifuge tube, and 10 mL of n-hexane was added and vortexed for 1 min. Then, the mixture was centrifuged at $500 \times g$ for 3 min at room temperature. After that, a PRiME HLB column and HLB solid phase extraction column were adopted for purification. Finally, the purified solution was dried with nitrogen at 40°C. Then, the residual was reconstructed with 1.0 mL acetonitrile and filtered by a 0.22 μ m polytetrafluoroethylene (PTFE) syringe filter (Waters, Beverly, MA, USA).

LC-Orbitrap HRMS conditions

The mobile phase consisted of 0.5 mmol/L ammonium acetate solution containing 0.1% formic acid (A) and methanol (B). The gradient elution procedure is presented in Table 1. The injection volume was 5 μ L. The flow rate was 0.3 mL/min.

Mass spectrometry conditions

The Q Exactive Focus mass spectrometry system was equipped with a HESI ion source using positive ion mode, spray voltage 3.5 kV, and capillary and spray temperatures of 320°C and 250°C, respectively. The sheath and auxiliary gas pressures were set at 45 arb and 8 arb, respectively, and the S-lens RF voltage was 50 V. Both the spray gas and collision gas were nitrogen. Correction solutions (a solution of 2 μ g/mL caffeine, 1 μ g/mL MRFA, 0.001% Ultramark 1621

and 0.0005% n-butylamine; a solution of 2.9 μ g/mL sodium dodecyl sulfate, 5.4 μ g/mL sodium taurocholate and 0.001% Ultramark 1621) were used to correct the mass axis once every 7 days. The scanning mode was full MS/dd-MS₂ mode. The full MS first-level full scanning range was m/z 100–650, resolution was 70000, automatic gain control AGC and automatic injection time IT were set to 1.0 e^6 and 100 ms, respectively; the data-dependent AGC of dd-MS₂ was set to 1.0 e^5 , the resolution was set to 17,500, the maximum IT was set to 60 ms, the separation window was set to 2.0 m/z , the normalized collision energy (NCE) of each compound was set to 20, 40, and 60%, and the dynamic exclusion was set to 8 s.

Results and discussion

Optimization of mass spectrometry conditions

Compared with triple quadrupole mass spectrometry, Orbitrap high-resolution mass spectrometry is simpler to operate and optimize mass spectrometry conditions (20). First, 12 target standards (concentration 100 μ g/L) were scanned by full MS with a resolution of 70,000, and qualitative screening and quantitative detection were carried out according to the accurate mass number of primary parent ions of the target compounds. The quasi-molecular ion peaks of $[M + H]^+$, $[M + NH_4]^+$, and $[M + Na]^+$ may be produced in the positive ion mode, and the quasi-molecular ion peaks of $[M-H]^-$ are mainly produced in the negative ion mode. By comparing the response values of each quasi-molecular ion peak in the two modes, it was found that aflatoxin could produce molecular ions in both positive and negative ion modes, but the response value of $[M-H]^-$ was far lower than that of $[M + H]^+$; HT-2 toxin belongs to trichothecenes, and its parent ion can form $[M + H]^+$, $[M + Na]^+$ and $[M + NH_4]^+$, but the conjugate of $[M + Na]^+$ has the highest response value and sensitivity, so HT-2 toxin chooses $[M + Na]^+$ as the parent ion. Diacetoxysciroenol can form $[M + Na]^+$ and $[M + NH_4]^+$, but the response value and sensitivity of $[M + Na]^+$ are higher; the other six toxins all have $[M + H]^+$ ions in positive ion mode, so positive ion scanning mode was used for detection in this experiment. Then, full MS/dd-MS₂ mode was adopted, in which dd-MS₂ was used as the confirmation mode. When the parent ion strength reached the set threshold (1×10^6), it automatically triggered secondary mass spectrometry scanning, and the information of secondary fragment ions could be further confirmed by combining the accurate mass number and retention time of primary parent ions. The precise mass number, mass accuracy error and retention time of the 12 mycotoxins are shown in Table 2.

TABLE 2 HPLC and Orbitrap HRMS parameters of 12 mycotoxins.

Compounds (abbreviations)	Molecular formula	Ion	Rt/min	Measured <i>m/z</i>	Theoretical <i>m/z</i>	Fragment ions	Error (ppm)	NCE (%)
Ochratoxin A (OTA)	C ₂₀ H ₁₈ ClNO ₆	[M+H] ⁺	13.44	404.08789	404.08954	358.08279, 257.02112	−4.08	10
Ochratoxin B (OTB)	C ₂₀ H ₁₉ NO ₆	[M+H] ⁺	12.39	370.12781	370.12851	223.05954, 324.12219	−1.89	10
Aflatoxin B1 (AFB1)	C ₁₇ H ₁₂ O ₆	[M+H] ⁺	11.41	313.06979	313.07066	285.07471, 270.05087	−2.78	50
Aflatoxin B2 (AFB2)	C ₁₇ H ₁₄ O ₆	[M+H] ⁺	11.19	315.08524	315.08631	287.09055, 259.05942	−3.40	50
Aflatoxin G1 (AFG1)	C ₁₇ H ₁₂ O ₇	[M+H] ⁺	10.76	329.06464	329.06558	243.06461, 215.6949	−2.86	50
Aflatoxin G2 (AFG2)	C ₁₇ H ₁₄ O ₇	[M+H] ⁺	10.48	331.08035	331.08123	313.06967, 245.08006	−2.66	50
HT-2 toxin (HT-2)	C ₂₂ H ₃₂ O ₈	[M+Na] ⁺	11.74	447.19690	447.19894	149.02306, 345.12979	−4.56	40
Sterigmatocystin (ST)	C ₁₈ H ₁₂ O ₆	[M+H] ⁺	15.39	325.07004	325.07066	281.04382, 310.04620	−1.91	40
Diacetoxyscirpenol (DAS)	C ₁₉ H ₂₆ O ₇	[M+Na] ⁺	10.70	389.15549	389.15707	89.05946, 133.08578	−4.06	50
Penicillic acid (PA)	C ₈ H ₁₀ O ₄	[M+H] ⁺	4.92	171.06497	171.06518	125.05949, 72.04420	−1.23	40
Mycophenolic acid (MA)	C ₁₇ H ₂₀ O ₆	[M+H] ⁺	12.30	321.13220	321.13326	207.06477, 159.04353	−3.30	40
Citreoviridin (CIT)	C ₂₃ H ₃₀ O ₆	[M+H] ⁺	14.29	403.21017	403.21150	139.03871, 83.04883	−3.30	40

Optimization of chromatographic conditions

The type and proportion of the mobile phase not only affect the retention time and peak shape of the target compound but also affect the ionization efficiency of the target compounds, thus affecting the sensitivity (23–25). In this study, four different mobile phases, A: 0.1% formic acid water-methanol, B: 1 mmol/L ammonium acetate-0.1% formic acid water-methanol, A: 0.1% formic acid water-acetonitrile, and D: 1 mmol/L ammonium acetate-0.1% formic acid water-acetonitrile, were compared on the mass spectral responses of 12 mycotoxins. The results showed that when A was the mobile phase, all toxins had a mass spectrometry response. However, when ammonium acetate is present in the mobile phase, the ionic response of each target substance is obviously enhanced. Therefore, the effects of different concentrations of ammonium acetate (0.1, 0.5, 1, 2, and 5 mmol/L) on the response intensity of mass spectrometry were further optimized. The results showed that when the concentration of ammonium acetate increased to 0.5 mmol/L, the ionic responses of most of the target compounds were enhanced, but the concentration of ammonium acetate continued to increase, but the response values of the other eight target compounds decreased slightly except for four aflatoxins. Therefore, 0.5 mmol/L ammonium acetate-0.1% formic acid aqueous solution was finally selected as the mobile phase. The main organic phases were acetonitrile and methanol. It was found that the peak shape of some target compounds was poor when acetonitrile was used as the mobile phase, so methanol was selected as the organic phase in this study. Therefore, 0.5 mmol/L ammonium acetate-0.1% formic acid aqueous solution-methanol was used as the mobile phase. The chromatographic

and mass spectra of 12 mycotoxins after optimization are shown in Figures 1A,B.

Optimization of pretreatment

Optimization of extraction solvent

Mycotoxins were mainly extracted by methanol, acetonitrile or a mixture of these two solvents and water in different proportions (26, 27). Therefore, this study compared the extraction efficiency of 12 mycotoxins from soy sauce by six insoluble solvent systems: methanol, acetonitrile, 80% methanol-water, 80% acetonitrile-water, 80% methanol-water-0.1% FA and 80% acetonitrile-water-0.1% FA. The results are shown in Figure 2A. The extraction effect of acetonitrile on 12 mycotoxins was significantly better than that of methanol. The addition of water can significantly improve the extraction rate. Eighty percent acetonitrile-water and 80% acetonitrile-hydr-0.1% FA had little effect on the mycotoxin extraction efficiency, except for HT-2 and penicillin. However, 80% acetonitrile-water was better than 80% acetonitrile-hydr-0.1% FA in the extraction efficiency of HT-2 and penicillic acid. Hence, 80% acetonitrile-water was finally selected as the extraction solvent.

Optimization of extraction time

In this study, 80% acetonitrile-water was used as the extraction solvent, and the effects of different shaking extraction times (5, 10, 15, 20, and 30 min) on the extraction of 12 mycotoxins from condiments were compared. The results are shown in Figure 2B. With increasing extraction time, the

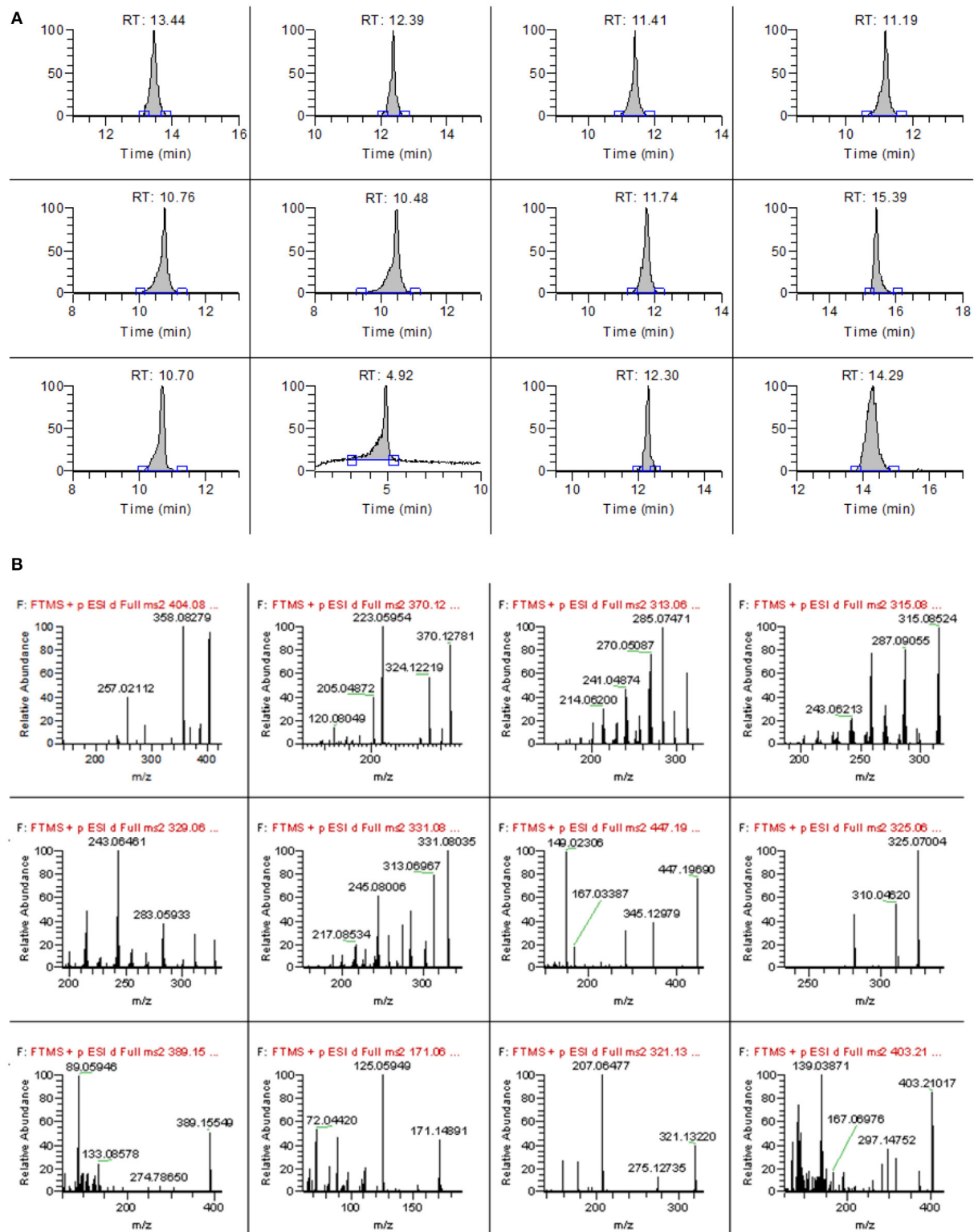


FIGURE 1
The chromatograms (A) and high-resolution mass spectrum (B) of 12 mycotoxins.

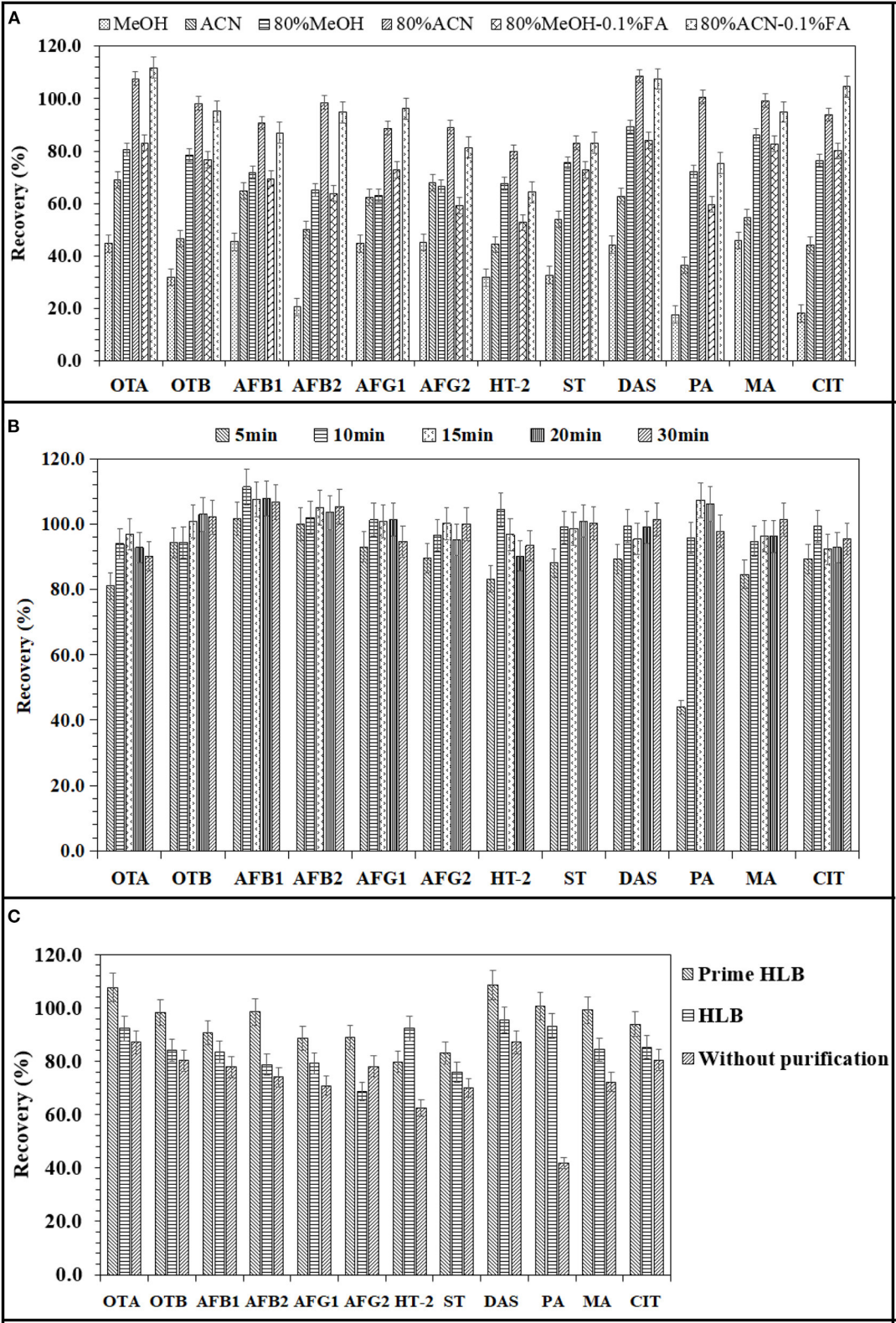


FIGURE 2
Effects of extraction solvent (A), extraction time (B), and various solid phase extraction columns (C) on the extraction recoveries of 12 mycotoxins.

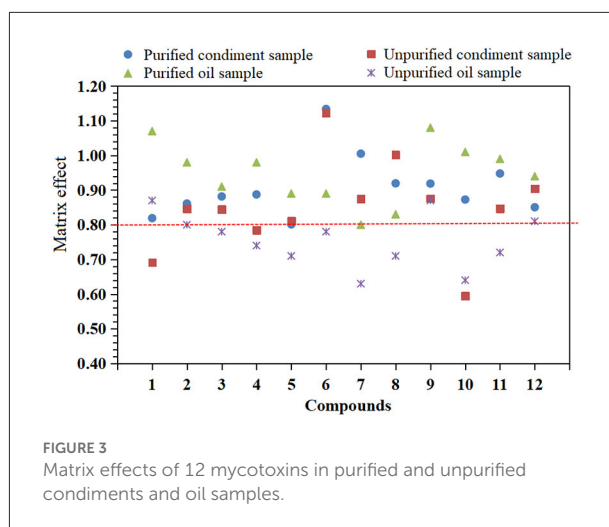
recovery rate gradually increased, and after increasing to 10 min, the recovery rate remained basically unchanged. Therefore, a 10 min shaking time was finally selected as the extraction time.

Optimization of purification conditions

The effects of two different solid phase extraction columns (HLB column and PRiME HLB column) on the recovery of mycotoxins were investigated. The HLB column was a reversed-phase solid phase extraction column, and the impurities were removed by leaching after adsorbing the target substance. Compared with other SPE products, it can remove 95% of common matrix interfering substances (such as phospholipids, fats, salts and proteins) (28). As shown in Figure 2C, the recoveries of 12 mycotoxins were improved by two purification columns. After PRiME HLB purification, the recoveries of mycotoxins ranged from 79.8 to 108.6%, and those obtained by HLB column purification ranged from 68.8 to 93.1%. Without purification, the recoveries of 12 mycotoxins ranged from 41.9 to 87.2%. Compared with the two kinds of solid phase extraction columns, the recovery rate of the impurity adsorption solid phase extraction column was better than that of the target substance adsorption solid phase extraction column except for HT-2 toxin, mainly because the HLB column did not have specific adsorption for a specific toxin, so it is easy to lose the recovery rate in the process of target substance adsorption and impurity elution. Therefore, a PRiME HLB column was selected as the purification column in this experiment.

Matrix effect

The matrix is a coextraction interfering substance other than the measured substance in the sample that often competes with the target compound for ionization, has significant interference with the analysis of the measured substance, and affects the accuracy of the determination results (29). These interferences and influences are called the matrix effect. The matrix effect is ion inhibition or ion enhancement. The existence of the matrix effect will affect the accuracy of the determination results (30, 31). The standard solution (analyte concentration is 10 µg/L) was prepared from the matrix extracts of edible oil and condiment blank samples without 12 mycotoxins. The matrix effect (ME) was evaluated by the ratio of the two with reference to the standard solution of the same concentration prepared by pure solvent, that is, the formula $ME = B/A$, where A and B represent the peak areas of analytes in pure solvent and blank sample matrix solution, respectively. If $ME < 0.8$, it indicates that the matrix has a significant inhibition on the response of analytes; if $ME > 1.2$, it indicates that the matrix will significantly enhance the response of analytes; if $0.8 \leq ME \leq 1.2$, it indicates that the matrix effect is not significant (23, 32). The experimental results are shown in Figure 3. After purification by PRiME



HLB column, the matrix effect of 12 mycotoxins in the two matrices is between 0.80 and 1.13 (see Table 2), and when it is not purified, the matrix effect is between 0.64 and 1.08. Some compounds have obvious matrix inhibition, which shows that purification by PRiME HLB column can obviously reduce the matrix effect, which is beneficial to reduce matrix interference and improve accuracy.

Method validation

Linear relationship, LOD and LOQ

In this method, pure solvent was used to dilute the standard solution step by step to the lowest concentration that could be detected by the instrument, and the samples were injected repeatedly. According to the standard deviation of the test results, the detection limit ($LOD, S/N \geq 3$) was determined by three times the signal-to-noise ratio, and the quantification limit ($LOQ, S/N \geq 10$) was determined by 10 times the signal-to-noise ratio (33, 34). Regression analysis was carried out with the peak area (y) of the exact mass-to-charge ratio of the target parent ion as the ordinate and the compound concentration (x, µg/L) as the abscissa, and the linear regression equation, linear range and detection limit of each compound were obtained, as shown in Table 3. The peak area of 12 mycotoxins showed a good linear relationship with their mass concentrations; the determination coefficient R^2 was > 0.998 , the detection limit ranged from 0.12 to 1.2 µg/L, and the quantitative limit ranged from 0.4 to 4.0 µg/L, which indicated that the method had good sensitivity. The applied regulatory levels and standards of mycotoxins vary in the different regions of the world. The current maximum levels for aflatoxins set by the European Commission (EC) are 2 µg/kg for AFB1 and 4 µg/kg for total aflatoxins in various foods. These are to be extended to cover spices with limits of 5 and 10 µg/kg for AFB1 and total aflatoxins, respectively (35).

TABLE 3 Matrix effect, linear ranges, regression equations, determination coefficients, LODs, and LOQs for 12 mycotoxins.

Compound	Matrix effect		Linear equation	R^2	Linear range (μg/L)	LOD (μg/L)	LOQ (μg/L)
	Soy sauce and bean sauce	Oils					
OTA	0.82	1.07	$y = 2.17641 \times 10^5 x - 1.57572 \times 10^5$	0.99922	2–100	1.2	4.0
OTB	0.86	0.98	$y = 5.27069 \times 10^5 x - 52541.489$	0.99969	1–100	0.6	2.0
AFB1	0.88	0.91	$y = 3.58221 \times 10^6 x - 1.30582 \times 10^6$	0.99969	0.2–100	0.12	0.4
AFB2	0.89	0.98	$y = 3.39177 \times 10^6 x - 1.11143 \times 10^6$	0.99954	0.2–100	0.12	0.4
AFG1	0.80	0.89	$y = 2.70403 \times 10^6 x - 3.11662 \times 10^6$	0.99931	0.2–100	0.12	0.4
AFG2	1.13	0.89	$y = 2.32422 \times 10^6 x - 1.26201 \times 10^6$	0.99974	0.2–100	0.12	0.4
HT-2	1.01	0.80	$y = 2.51552 \times 10^5 x - 2.35324 \times 10^5$	0.99969	2–100	1.2	4.0
ST	0.92	0.83	$y = 1.61012 \times 10^6 x - 1.23751 \times 10^6$	0.99953	0.5–100	0.3	1.0
DAS	0.92	1.08	$y = 7.06211 \times 10^5 x + 1.81285 \times 10^5$	0.99907	1–100	0.6	2.0
PA	0.87	1.01	$y = 4.55992 \times 10^5 x - 8.02080 \times 10^5$	0.99947	2–100	1.2	4.0
MA	0.95	0.99	$y = 4.97538 \times 10^5 x + 4.86495 \times 10^5$	0.99892	1–100	0.6	2.0
CIT	0.85	0.94	$y = 2.65245 \times 10^5 x - 5.99355 \times 10^5$	0.99914	2–100	1.2	4.0

TABLE 4 Recoveries and RSDs ($n = 6$) of blank samples fortified with 12 mycotoxins.

Sample	Compounds	Spiked level					
		1 LOQ		2 LOQ		10 LOQ	
		Recovery (%)	RSD (% $, n=6$)	Recovery (%)	RSD (% $, n=6$)	Recovery (%)	RSD (% $, n=6$)
Soy sauce and bean sauce	OTA	85.8	3.4	94.6	3.8	91.3	8.5
	OTB	78.4	3.3	106.2	2.3	102.4	7.6
	AFB1	95.6	1.7	97.2	6.4	89.2	3.5
	AFB2	94.8	2.6	100.5	7.6	90.6	2.9
	AFG1	80.4	6.3	95.4	3.5	86.1	1.9
	AFG2	99.0	3.9	106.8	1.3	99.5	5.4
	HT-2	82.9	7.9	89.4	2.6	80.3	4.8
	ST	82.6	1.5	104.2	9.7	100.8	8.1
	DAS	95.7	4.5	106.2	7.1	97.8	3.8
	PA	94.1	2.7	91.7	1.2	87.6	2.6
	MA	92.1	6.2	95.1	4.1	105.2	1.6
	CIT	94.8	3.2	99.3	2.9	97.3	7.9
Oils	OTA	97.0	1.3	93.3	5.1	101.3	2.2
	OTB	84.6	2.8	115.6	4.8	106.5	1.3
	AFB1	99.4	1.5	98.7	3.4	93.3	2.4
	AFB2	103.2	4.6	98.4	6.6	94.8	7.4
	AFG1	93.3	1.7	102.0	6.8	92.5	3.9
	AFG2	101.6	1.4	105.3	4.0	93.8	3.5
	HT-2	94.9	6.5	96.3	0.9	94.5	2.8
	ST	81.3	2.0	81.9	3.9	78.3	6.3
	DAS	93.9	4.1	100.4	5.1	97.6	3.9
	PA	85.5	8.6	102.1	3.1	89.8	6.1
	MA	87.4	7.7	95.3	6.6	101.8	1.2
	CIT	89.3	7.4	93.8	3.3	84.3	7.5

TABLE 5 Concentrations of mycotoxins detected in the condiments and oils.

Sample No.	Sample information	Concentrations (μg/kg)	Sample No.	Sample information	Concentrations (μg/kg)
S1	Corn oil	ND*	S13	bean sauce	AFB2 (7.3)
S2	Light soy sauce	AFB2 (12.8)	S14	Rapeseed oil	ND
S3	Sesame oil	ST (2.9) MA (7.5)	S15	Peanut oil	AFB1 (1.0) ST (2.1)
S4	Oyster sauce	ND	S16	Peanut oil	AFB1 (1.0)
S5	Light soy sauce	AFB2 (22.1)	S17	Corn oil	ND
S6	Dark soy sauce	ND	S18	Peanut oil	AFB1 (1.4)
S7	Chili sauce	ND	S19	Rapeseed oil	ND
S8	Oyster sauce	ND	S20	Peanut oil	AFB1 (0.9)
S9	Dark soy sauce	ND	S21	Sesame oil	ND
S10	Dark soy sauce	ND	S22	Zanthoxylum oil	ND
S11	Oyster sauce	AFB2 (1.8)	S23	Peanut oil	AFB1 (1.0)
S12	Sweet bean sauce	ND	S24	Peanut oil	AFB1 (4.7)

*ND, Not detectable.

Apart from aflatoxins, the maximum levels for OTA, DON, ZEN, and FBs (sum of FB1 and FB2) in various foods are also stipulated in Commission Regulation (EC) No 1881/2006 and in its amendments (36). The sensitivity parameters in this developed method are adequate to the legal limit requirements.

Recovery and precision

The blank substrate samples of edible oil and condiment without the target substance to be tested were selected for the standard addition recovery experiment. Standard solutions with three concentration levels of LOQ, 2 × LOQ, and 10 × LOQ were added, and six parallel samples were made for each standard addition concentration. The recovery rate was calculated, and the results are shown in Table 3. Table 4 shows that the average recovery rate of 12 mycotoxins in soy sauce and bean sauce is between 78.4 and 106.8%, and the precision RSD ($n = 6$) is between 1.2% and 9.7%. The average recoveries in edible oil ranged from 78.3 to 115.6%, and the precision RSD ($n = 6$) ranged from 0.9 to 8.6%.

Actual sample analysis

AFB2 was detected in 4 soy sauce and bean sauce samples (S2, S5, S11, and S13) under optimized experimental conditions with contents of 1.8–22.1 μg/kg (Table 5). AFB1 was detected in 6 edible oil samples (S15, S16, S18, S20, S23, S24) with contents ranging from 0.9 to 4.7 μg/kg. Sterigmatocystin was detected in S3 and S15 with contents of 2.9 and 2.1 μg/kg, respectively. Mycophenolic acid was detected in S3 at a concentration of 7.5 μg/kg. It could be inferred from the data that AFB2 is easily produced in soy sauce and bean sauce, and AFB1 is

easily produced in edible oil. AFBs represent a global public health issue, as they are responsible for significant adverse health issues affecting consumers worldwide. AFB1, due to its toxic, mutagenic, immunotoxic, teratogenic, and carcinogenic effects on humans and animals, is classified as a group 1 carcinogen in the International Agency for Research on Cancer (IARC) classification of carcinogenic substances (37). To avoid or minimize health concerns, the EU has also established maximum tolerable limits for AFs in chillies as 10 μg/kg for total and 5 μg/kg for AFB1 (38). Therefore, the control of AFBs, especially AFB1 and AFB2, is particularly crucial due to their high contents in soy sauce, bean sauce and edible oil. Moreover, the need for normative updates regarding legal limits for sterigmatocystin and mycophenolic acid should be considered based on their biological toxicity, as they were detected in several samples.

Comparison with other reported methods

The comparison of this established method with other reported methods for the determination of mycotoxins in oil and sauce samples is summarized in Table 6. Table 6 clearly shows that HPLC and liquid chromatography with tandem mass spectrometry (LC–MS/MS) are the most commonly used methods for the determination of mycotoxins in separate matrices (38–41, 43, 44). For the pretreatment method, the QuEChERS procedure (quick, easy, cheap, effective, rugged and safe) seems to be the most commonly used technique (9, 39, 43–46). However, all these methods listed in Table 6 are suitable for the determination of several mycotoxins in either vegetable oil samples or sauce samples. The method established in our

TABLE 6 Comparison with other methods reported in the literature*.

Mycotoxins	Matrix	Instrumental method	Pretreatment method	LODs ($\mu\text{g/L}$)	Recoveries (%)	RSDs (%)	Reference
4 mycotoxins (AOH, AME, TEN, and TeA)	tomato sauce	LC-MS/MS	QuEChERS	1.0–80	98.8–108.9	<10	(39)
5 mycotoxins (AFB1, AFB2, AFG1, AFG2, and OTA)	chili sauce	HPLC-FLD	Solvent extraction and IAC clean-up	0.05–0.1	86–93	6–15	(38)
5 mycotoxins (AFB1, AFB2, AFG1, AFG2, and OTA)	soybean paste	HPLC-FLD	Solvent extraction and IAC clean-up	0.01–0.2	/	/	(40)
6 mycotoxins (AFB1, AFB2, AFG1, AFG2, α -ZOL, and ZEA)	edible vegetable oil	UHPLC-QqQ-MS/MS	QuEChERS procedure	0.5–1.0	87.5–119.4	<20	(9)
4 mycotoxins (AFB1, AFB2, AFG1, and AFG2)	bean sauce	HPLC-UV	monolithic column based on covalent cross-linked polymer gels	0.08–0.2	76.1–113	1.1–9.6	(41)
6 mycotoxins (α -ZOL, β -ZOL, α -ZAL, β -ZAL, ZON, and ZAN)	edible vegetable oil	GC-QqQ MS	gel permeation chromatography	0.01–0.06	80.3–96.5	<11.6	(42)
9 mycotoxins (AFB1, AFB2, AFG1, AFG2, BEA, OTA, ZEA, FB1, and FB2)	vegetable oil	LC-MS/MS	QuEChERS-based procedure	0.02–14.66	70–120	<30	(43)
16 mycotoxins (α -ZAL, ZON, DON, β -ZAL, β -ZOL, α -ZOL, OTA, T-2, 3-Ac-DON, 15-Ac-DON, AFB1, AFB2, AFG1, AFG2, AFM1, and AFM2)	vegetable oil	LC-MS/MS	QuEChERS-based extraction	0.04–2.9	72.8–105.8	<7	(44)
12 mycotoxins (AFB1, AFB2, AFG1, AFG2, OTA, OTB, HT-2, ST, DAS, PA, MA, and CIT)	edible oil, soy sauce and bean sauce	HPLC-Orbitrap HRMS	PRiME HLB solid phase extraction	0.12–1.2	78.3–115.6	0.9–9.7	This work

*Abbreviations: GC-QqQ MS, Gas chromatography-triple quadrupole-mass spectrometry; HPLC-UV, high-performance liquid chromatography-ultraviolet detection; UHPLC-QqQ-MS/MS, ultrahigh-performance liquid chromatography-triple quadrupole tandem mass spectrometry; HPLC-Orbitrap HRMS, high-performance liquid chromatography-tandem Orbitrap high-resolution mass spectrometry; LC-MS/MS, liquid chromatography with tandem mass spectrometry.

AFB1, Aflatoxin B1; AFB2, aflatoxin B2; AFG1, aflatoxin G1; AFG2, aflatoxin G2; AFM1, aflatoxin M1; AFM2, aflatoxin M2; OTA, ochratoxin A; ZON, zearalenone; ZAN, zearalanone; DON, deoxynivalenol; α -ZAL, α -zearalanol; β -ZAL, β -zearalanol; β -ZOL β -zearalenol; α -ZOL, α -zearalenol; T-2, T-2 toxin; HT-2, HT-2 toxin; 3-Ac-DON, 3-acetyldeoxynivalenol; 15-Ac-DON, 15-acetyldeoxynivalenol; FB1, fumonisin B1; FB2, fumonisin B2; BEA, beauvericin; ST, sterigmatocystin; DAS, diacetoxyscirpenol; PA, penicillic acid; MA, mycophenolic acid; CIT, citreoviridin; AOH, alternariol.

work can be used for the analysis of 12 mycotoxins in not only edible oil samples but also soy sauce and bean sauce samples. The PRiME HLB solid phase extraction combined with HPLC-Orbitrap HRMS developed in the present work shows rapid extraction time as well as favorable linearity, LODs, recoveries and RSDs, which are comparable or superior in comparison with other analytical methods. In addition, this is also the first study to develop an accurate method for the determination of sterigmatocystin (ST), diacetoxyscirpenol (DAS), penicillic acid (PA), mycophenolic acid (MA), and citreoviridin (CIT) in foodstuffs.

Conclusion

Aiming at the present situation that edible oil, soy sauce and bean sauce are easily contaminated by many mycotoxins simultaneously, a new impurity adsorption purification technology was adopted, and a simultaneous determination method for rapid screening and quantitative determination of 12 mycotoxins by HPLC-Orbitrap HRMS was established. The pretreatment operation is simple and rapid. The method realizes simultaneous analysis and detection of various mycotoxins, with high stability and sensitivity, strong specificity and good reproducibility. The LODs of the 12 mycotoxins were 0.12–1.2 µg/L. The average recoveries in edible oil, soy sauce and bean sauce were 78.3–115.6% with RSDs of 0.9–9.7%. Therefore, the developed method can be used as a quantitative method for the determination of various mycotoxins in edible oils, soy sauce and bean sauce.

Data availability statement

The original contributions presented in the study are included in the article/[Supplementary material](#), further inquiries can be directed to the corresponding author/s.

Author contributions

DL prepared and wrote the manuscript. JG, JC, and ML corrected, revised, and improved the manuscript.

References

1. Wan J, Chen B, Rao J. Occurrence and preventive strategies to control mycotoxins in cereal-based food. *Comprehens Rev Food Sci Food Saf.* (2020) 19:928–53. doi: 10.1111/1541-4337.12546
2. Xu X, Xu X, Han M, Qiu S, Hou X. Development of a modified QuEChERS method based on magnetic multiwalled carbon nanotubes for the simultaneous determination of veterinary drugs, pesticides and mycotoxins in eggs by UPLC-MS/MS. *Food Chem.* (2019) 276:419–26. doi: 10.1016/j.foodchem.2018.10.051
3. Yang Y, Li G, Wu D, Liu J, Li X, Luo P, et al. Recent advances on toxicity and determination methods of mycotoxins in foodstuffs. *Trends Food Sci Technol.* (2020) 96:233–252. doi: 10.1016/j.tifs.2019.12.021
4. Abdolmaleki K, Khedri S, Alizadeh L, Javanmardi F, Oliveira CA, Khaneghah AM, et al. The mycotoxins in edible oils: an overview of prevalence, concentration, toxicity, detection and decontamination techniques. *Trends Food Sci and Technology.* (2021) 115:500–11. doi: 10.1016/j.tifs.2021.06.057

CZ and YX, modified the Tables and Figures in the manuscript. HD and XX designed the study, supervised, reviewed, and finalized the manuscript. All authors contributed to the article and approved the submitted version.

Funding

This work was financially supported by Guangdong Provincial Key R&D Programme (No. 2021B0707060001), project (No. 2020PT01) Science and Technology Project of Chaozhou Branch of Chemistry and Chemical Engineering Guangdong Laboratory (No. HJL202202B007), and Characteristic Innovation Project of Universities in Guangdong province (2022KTSCX058).

Conflict of interest

The authors declare that the research was conducted in the absence of any commercial or financial relationships that could be construed as a potential conflict of interest.

Publisher's note

All claims expressed in this article are solely those of the authors and do not necessarily represent those of their affiliated organizations, or those of the publisher, the editors and the reviewers. Any product that may be evaluated in this article, or claim that may be made by its manufacturer, is not guaranteed or endorsed by the publisher.

Supplementary material

The Supplementary Material for this article can be found online at: <https://www.frontiersin.org/articles/10.3389/fnut.2022.1001671/full#supplementary-material>

5. Arroyo-Manzanares N, Campillo N, López-García I, Hernández-Córdoba M, Viñas P. High-Resolution mass spectrometry for the determination of mycotoxins in biological samples. A review. *Microchem J.* (2021) 166:106197. doi: 10.1016/j.microc.2021.106197
6. Khodaei D, Javanmardi F, Khaneghah AM. The global overview of the occurrence of mycotoxins in cereals: a three-year survey. *Curr Opin Food Sci.* (2021) 39:36–42. doi: 10.1016/j.cofs.2020.12.012
7. Martins C, Vidal A, Boevre De, De Saeger M, Nunes S, Torres C, et al. Exposure assessment of Portuguese population to multiple mycotoxins: the human biomonitoring approach. *Int J Hygiene Environ Health.* (2019) 222:913–25. doi: 10.1016/j.ijheh.2019.06.010
8. Sarmast E, Fallah AA, Jafari T, Khaneghah AM. Occurrence and fate of mycotoxins in cereals and cereal-based products: a narrative review of systematic reviews and meta-analyses studies. *Current Opinion in Food Science.* (2021) 39:68–75. doi: 10.1016/j.cofs.2020.12.013
9. Hidalgo-Ruiz JL, Romero-González R, Martínez Vidal JL, Garrido Frenich A. A rapid method for the determination of mycotoxins in edible vegetable oils by ultra-high performance liquid chromatography-tandem mass spectrometry. *Food Chemistry.* (2019) 288:22–28. doi: 10.1016/j.foodchem.2019.03.003
10. Bessaire T, Mujahid C, Mottier P, Desmarchelier A. Multiple mycotoxins determination in food by LC-MS/MS: an international collaborative study. *Toxins.* (2019) 11:658. doi: 10.3390/toxins11110658
11. Romera D, Mateo EM, Mateo-Castro R, Gomez JV, Gimeno-Adelantado JV, Jimenez M, et al. Determination of multiple mycotoxins in feedstuffs by combined use of UPLC-MS/MS and UPLC-QTOF-MS. *Food Chem.* (2018) 267:140–8. doi: 10.1016/j.foodchem.2017.11.040
12. Turner NW, Subrahmanyam S, Piletsky SA. Analytical methods for determination of mycotoxins: a review. *Anal Chim Acta.* (2009) 632:168–80. doi: 10.1016/j.aca.2008.11.010
13. Anastassiades M, Lehota SJ, Štajnbaher D, Schenck FJ. Fast and easy multiresidue method employing acetonitrile extraction/partitioning and “dispersive solid-phase extraction” for the determination of pesticide residues in produce. *J AOAC Int.* (2003) 86:412–31. doi: 10.1093/jaoac/86.2.412
14. Facorro, R., Llopart, M., and Dagnac, T. Combined (d)SPE-QuEChERS extraction of mycotoxins in mixed feed rations and analysis by high performance liquid chromatography-high-resolution mass spectrometry. *Toxins.* (2020) 12:206. doi: 10.3390/toxins12030206
15. Pereira V, Fernandes J, Cunha S. Mycotoxins in cereals and related foodstuffs: a review on occurrence and recent methods of analysis. *Trends Food Sci Technol.* (2014) 36:96–136. doi: 10.1016/j.tifs.2014.01.005
16. Wu Z, He D, Cui B, Jin Z, Xu E, Yuan C, et al. Trimer-based aptasensor for simultaneous determination of multiple mycotoxins using SERS and fluorimetry. *Microchimica Acta.* (2020) 187:1–7. doi: 10.1007/s00604-020-04487-1
17. Dong H, Xian Y, Xiao K, Wu Y, Zhu L, He J, et al. Development and comparison of single-step solid phase extraction and QuEChERS clean-up for the analysis of 7 mycotoxins in fruits and vegetables during storage by UHPLC-MS/MS. *Food Chemistry.* (2019) 274:471–9. doi: 10.1016/j.foodchem.2018.09.035
18. Soleimany F, Jinap S, Abas F. Determination of mycotoxins in cereals by liquid chromatography tandem mass spectrometry. *Food Chem.* (2012) 130:1055–60. doi: 10.1016/j.foodchem.2011.07.131
19. Dong H, Xian Y, Li H, Wu Y, Bai W, Zeng X, et al. Analysis of heterocyclic aromatic amine profiles in Chinese traditional bacon and sausage based on ultrahigh-performance liquid chromatography-quadrupole-Orbitrap high-resolution mass spectrometry (UHPLC-Q-Orbitrap-HRMS). *Food Chem.* (2020) 310:125937. doi: 10.1016/j.foodchem.2019.125937
20. Liang M, Xian Y, Wang B, Hou X, Wang L, Guo X, et al. High throughput analysis of 21 perfluorinated compounds in drinking water, tap water, river water and plant effluent from southern China by supramolecular solvents-based microextraction coupled with HPLC-Orbitrap HRMS. *Environ Pollution.* (2020) 263:114389. doi: 10.1016/j.envpol.2020.114389
21. Xian Y, Liang M, Wu Y, Wang B, Hou X, Dong H, et al. Fluorine and nitrogen functionalized magnetic graphene as a novel adsorbent for extraction of perfluoroalkyl and polyfluoroalkyl substances from water and functional beverages followed by HPLC-Orbitrap HRMS determination. *Sci Total Environ.* (2020) 723:138103. doi: 10.1016/j.scitotenv.2020.138103
22. Xu Y, Li H, Liang J, Ma J, Yang J, Zhao X, et al. High-throughput quantification of eighteen heterocyclic aromatic amines in roasted and pan-fried meat on the basis of high performance liquid chromatography-quadrupole-orbitrap high resolution mass spectrometry. *Food Chem.* (2021) 361:130147. doi: 10.1016/j.foodchem.2021.130147
23. Dong, H., and Xiao, K. Modified QuEChERS combined with ultra high performance liquid chromatography tandem mass spectrometry to determine seven biogenic amines in Chinese traditional condiment soy sauce. *Food Chemistry.* (2017) 229:502–8. doi: 10.1016/j.foodchem.2017.02.120
24. Dong H, Xiao K, Xian Y, Wu Y, Zhu L. A novel approach for simultaneous analysis of perchlorate ($\text{ClO}[[\text{sb}]]4[[/s]]^-$) and bromate ($\text{BrO}[[\text{sb}]]3[[/s]]^-$) in fruits and vegetables using modified QuEChERS combined with ultrahigh performance liquid chromatography-tandem mass spectrometry. *Food Chemistry.* (2018) 270:196–203. doi: 10.1016/j.foodchem.2018.07.091
25. Dong, H., Zeng, X., and Bai, W. Solid phase extraction with high polarity Carb/PSA as composite fillers prior to UPLC-MS/MS to determine six bisphenols and alkylphenols in trace level hotpot seasoning. *Food Chemistry.* (2018) 258:206–13. doi: 10.1016/j.foodchem.2018.03.074
26. Campone L, Rizzo S, Piccinelli AL, Celano R, Pagano, I. Russo M, et al. Determination of mycotoxins in beer by multi heart-cutting two-dimensional liquid chromatography tandem mass spectrometry method. *Food Chem.* (2020) 318:126496. doi: 10.1016/j.foodchem.2020.126496
27. Silva AS, Brites C, Pouca AV, Barbosa J, Freitas A. UHPLC-ToF-MS method for determination of multi-mycotoxins in maize: development and validation. *Curr Res Food Sci.* (2019) 1:1–7. doi: 10.1016/j.crfs.2019.07.001
28. Hu J, Liang M, Xian Y, Chen R, Wang L, Hou X, et al. Development and validation of a multianalyte method for quantification of aflatoxins and bongkreic acid in rice and noodle products using PRiME-UHPLC-MS/MS method. *Food Chem.* (2022) 395:133598. doi: 10.1016/j.foodchem.2022.133598
29. Arce-López B, Lizarraga E, Flores-Flores M, Irigoyen Á, González-Peñas E. Development and validation of a methodology based on Captiva EMR-lipid clean-up and LC-MS/MS analysis for the simultaneous determination of mycotoxins in human plasma. *Talanta.* (2020) 206:120193. doi: 10.1016/j.talanta.2019.120193
30. Xian Y, Dong H, Wu Y, Guo X, Hou X, Wang B, et al. QuEChERS-based purification method coupled to ultrahigh performance liquid chromatography-tandem mass spectrometry (UPLC-MS/MS) to determine six quaternary ammonium compounds (QACs) in dairy products. *Food Chem.* (2016) 212:96–103. doi: 10.1016/j.foodchem.2016.05.151
31. Xian Y, Guo X, Hou X, Wang L, Wu Y, Chen, L, et al. A modified quick, easy, cheap, effective, rugged, and safe cleanup method followed by liquid chromatography-tandem mass spectrometry for the rapid analysis of perchlorate, bromate and hypophosphite in flour. *J Chromatography A.* (2017) 1526:31–8. doi: 10.1016/j.chroma.2017.10.047
32. Zeng X, Bai W, Xian Y, Dong H, Luo D. Application of QuEChERS-based purification coupled with isotope dilution gas chromatography-mass spectrometry method for the determination of N-nitrosamines in soy sauce. *Anal Methods.* (2016) 8:5248–54. doi: 10.1039/C6AY01169A
33. González-Jartín JM, Rodríguez-Cañás I, Alfonso A, Sainz MJ, Vieytes MR, Gomes A, et al. Multianalyte method for the determination of regulated, emerging and modified mycotoxins in milk: QuEChERS extraction followed by UHPLC-MS/MS analysis. *Food Chem.* (2021) 356:129647. doi: 10.1016/j.foodchem.2021.129647
34. Rodríguez-Carrasco Y, Castaldo L, Gaspari A, Graziani G, Ritieni A. Development of an UHPLC-Q-Orbitrap HRMS method for simultaneous determination of mycotoxins and isoflavones in soy-based burgers. *LWT-Food Sci Technol.* (2019) 99:34–42. doi: 10.1016/j.lwt.2018.09.046
35. Gilbert J, Anklam E. Validation of analytical methods for determining mycotoxins in foodstuffs. *TrAC Trends Anal Chem.* (2002) 21:468–86. doi: 10.1016/S0165-9936(02)00604-0
36. Eskola M, Kos G, Elliott CT, Hajšlová J, Mayar S, Krska R, et al. Worldwide contamination of food-crops with mycotoxins: Validity of the widely cited ‘FAO estimate’ of 25%. *Crit Rev Food Sci Nutr.* (2020) 60:2773–89. doi: 10.1080/10408398.2019.1658570
37. Jallow A, Xie H, Tang X, Qi Z, Li P. Worldwide aflatoxin contamination of agricultural products and foods: From occurrence to control. *Comprehens Rev Food Saf.* (2021) 20:2332–81. doi: 10.1111/1541-4337.12734
38. Iqbal SZ, Asi MR, Zuber M, Akhtar J, Jawwad Saif M. Natural occurrence of aflatoxins and ochratoxin A in commercial chilli and chilli sauce samples. *Food Control.* (2012) 30:621–5. doi: 10.1016/j.foodcont.2012.09.003
39. Berardis De, De Paola S, Montevicchi EL, Garbini G, Masino D, Antonelli F, et al. Determination of four *Alternaria alternata* mycotoxins by QuEChERS approach coupled with liquid chromatography-tandem mass spectrometry in tomato-based and fruit-based products. *Food Res Int.* (2018) 106:677–85. doi: 10.1016/j.foodres.2018.01.032
40. Jeong SE, Chung SH, Hong SY. Natural occurrence of aflatoxins and ochratoxin A in meju and soybean paste produced in South Korea. *App Biol Chem.* (2019) 62:65. doi: 10.1186/s13765-019-0472-y

41. Wei, T., Chen, Z., Li, G., and Zhang, Z. A monolithic column based on covalent cross-linked polymer gels for online extraction and analysis of trace aflatoxins in food sample. *J Chromatography A*. (2018) 1548:27–36. doi: 10.1016/j.chroma.2018.03.015
42. Qian, M., Zhang, H., Wu, L., Jin, N., Wang, J., Jiang, K., et al. (2014). (2015). Simultaneous determination of zearalenone and its derivatives in edible vegetable oil by gel permeation chromatography and gas chromatography–triple quadrupole mass spectrometry. *Food Chemistry*, 166, 23–28. doi: 10.1016/j.foodchem.2014.05.133
43. Junsai T, Poapolathep S, Sutjarit S, Giorgi M, Zhang Z, Logrieco A, et al. Determination of multiple mycotoxins and their natural occurrence in edible vegetable oils using liquid chromatography–tandem mass spectrometry. *Foods*. (2021) 10:2795. doi: 10.3390/foods10112795
44. Zhao H, Chen X, Shen C, Qu B. Determination of 16 mycotoxins in vegetable oils using a QuEChERS method combined with high-performance liquid chromatography–tandem mass spectrometry. *Food Addi Contamin: Part A*. (2017) 34:255–64. doi: 10.1080/19440049.2016.1266096
45. Payá P, Anastassiades M, Mack D, Sigalova I, Tasdelen B, Oliva J, et al. Analysis of pesticide residues using the quick easy cheap effective rugged and safe (QuEChERS) pesticide multiresidue method in combination with gas and liquid chromatography and tandem mass spectrometric detection. *Anal Bioanal Chem*. (2007) 389:1697–714. doi: 10.1007/s00216-007-1610-7
46. Hidalgo-Ruiz JL, Romero-González R, Vidal JLM, Frenich AG. A rapid method for the determination of mycotoxins in edible vegetable oils by ultra-high performance liquid chromatography–tandem mass spectrometry. *Food Chemistry*. (2019) 288:22–28.



OPEN ACCESS

EDITED BY

Alessandro Ferragina,
Teagasc Food Research Centre, Ireland

REVIEWED BY

Paolo Berzaghi,
University of Padua, Italy
Mutamed Ayyash,
United Arab Emirates University,
United Arab Emirates

*CORRESPONDENCE

Luis E. Rodriguez-Saona
✉ rodriguez-saona.1@osu.edu

SPECIALTY SECTION

This article was submitted to
Food Chemistry,
a section of the journal
Frontiers in Nutrition

RECEIVED 25 November 2022

ACCEPTED 17 January 2023

PUBLISHED 06 February 2023

CITATION

Yaman H, Aykas DP and Rodriguez-Saona LE
(2023) Monitoring Turkish white cheese
ripening by portable FT-IR spectroscopy.
Front. Nutr. 10:1107491.
doi: 10.3389/fnut.2023.1107491

COPYRIGHT

© 2023 Yaman, Aykas and Rodriguez-Saona.
This is an open-access article distributed under
the terms of the [Creative Commons Attribution
License \(CC BY\)](#). The use, distribution or
reproduction in other forums is permitted,
provided the original author(s) and the
copyright owner(s) are credited and that the
original publication in this journal is cited, in
accordance with accepted academic practice.
No use, distribution or reproduction is
permitted which does not comply with
these terms.

Monitoring Turkish white cheese ripening by portable FT-IR spectroscopy

Hulya Yaman^{1,2}, Didem P. Aykas^{1,3} and Luis E. Rodriguez-Saona^{1*}

¹Department of Food Science and Technology, The Ohio State University, Columbus, OH, United States,

²Department of Food Processing, Bolu Abant İzzet Baysal University, Bolu, Türkiye, ³Department of Food Engineering, Adnan Menderes University, Aydın, Türkiye

The biochemical metabolism during cheese ripening plays an active role in producing amino acids, organic acids, and fatty acids. Our objective was to evaluate the unique fingerprint-like infrared spectra of the soluble fractions in different solvents (water-based, methanol, and ethanol) of Turkish white cheese for rapid monitoring of cheese composition during ripening. Turkish white cheese samples were produced in a pilot plant scale using a mesophilic culture (*Lactococcus lactis* subsp. *lactis*, *Lactococcus lactis* subsp. *cremoris*), ripened for 100 days and samples were collected at 20-day intervals for analysis. Three extraction solvents (water, methanol, and ethanol) were selected to obtain soluble cheese fractions. Reference methods included gas chromatography (amino acids and fatty acid profiles), and liquid chromatography (organic acids) were used to obtain the reference results. FT-IR spectra were correlated with chromatographic data using pattern recognition analysis to develop regression and classification predictive models. All models showed a good fit ($R_{\text{Pre}} \geq 0.91$) for predicting the target compounds during cheese ripening. Individual free fatty acids were predicted better in ethanol extracts ($0.99 \geq R_{\text{Pre}} \geq 0.93$, $1.95 \geq \text{SEP} \geq 0.38$), while organic acids ($0.98 \geq R_{\text{Pre}} \geq 0.97$, $10.51 \geq \text{SEP} \geq 0.57$) and total free amino acids ($R_{\text{Pre}} = 0.99$, $\text{SEP} = 0.0037$) were predicted better by using water-based extracts. Moreover, cheese compounds extracted with methanol provided the best SIMCA classification results in discriminating the different stages of cheese ripening. By using a simple methanolic extraction and collecting spectra with a portable FT-IR device provided a fast, simple, and cost-effective technique to monitor the ripening of white cheese and predict the levels of key compounds that play an important role in the biochemical metabolism of Turkish white cheese.

KEYWORDS

cheese ripening, Turkish white cheese, FT-IR, extraction methods, organic acids, free amino acids, free fatty acids

1. Introduction

Turkish white cheese, Kashar cheese, and Tulum cheese are the most produced industrial cheeses among traditional cheese varieties in Turkey (1). These cheeses are either consumed fresh or ripened according to the traditional characteristics of the product. For example, fresh classic white cheese produced from cow's milk is taken to the market with minimum a three-week ripening, while Ezine-type white cheese can have a ripening period of up to 6 months (2). Therefore, determining the quality characteristics of the cheese is important to monitor the

degree of ripening of the cheese. The biochemical reactions and their importance for the industry have been explained in detail by many researchers (3–5). Cheese ripening involves various biochemical and microbiological changes by the metabolism of starter cultures, indigenous, clotting, adjunct enzymes, and ripening accelerating agents. The biochemical reactions that occur during cheese ripening can be classified into three main categories: (1) the catabolism of residual lactose and citrate into organic acids and other components (glycolysis); (2) the catabolism of proteins into amino acids and other amin products (proteolysis); and (3) the catabolism of the fat into fatty acids and other further lipolysis compounds (3, 4).

The degree of importance of these metabolites during the ripening period may vary according to the production method and type of cheese. While lipolysis plays a more active role in cheeses with high-fat content or ripened with mold and fatty acids formed during ripening (6–8), proteolysis is responsible for texture development, functionality, and flavor improvement through amino acids and small peptides formation (9, 10). The residual lactose is converted to organic acids and other further breakdown compounds by glycolysis depending on the used starter culture or indigenous microbiota (6, 11–14).

Monitoring the level of these molecules during ripening provides information about the development of ripening and product quality. Determination of these biochemical changes by analytic methods is time-consuming, laborious, expensive, and involves extensive chemical use also complex analysis methods with expensive equipment, especially chromatographic techniques (15). The disadvantages can be overcome using new, rapid, portable, and simple methods based on Fourier-transform infrared (FT-IR) spectroscopy. Previously, it was found a high correlation coefficient ($R > 0.90$) for the prediction of acetic, propionic, and butyric acid contents using the FT-IR spectra for Swiss cheese with a novel sample preparation method of water-soluble extractions (16). Similarly, the free amino acid content of cheddar cheese samples was determined from the water-soluble extract of cheese with a high correlation with FT-IR spectra (17, 18). Furthermore, the primary composition of Turkish white cheese through ripening were examined by three vibrational spectroscopy methods (NIR, FT-IR, and Raman), and the suitability of the analytic method has been demonstrated (19).

Our objective was to evaluate the unique fingerprint-like infrared spectra of target soluble compounds in Turkish white cheese, including amino acids (GC-MS), fatty acids (GC-FID), and organic acids (HPLC-PDA), to evaluate their influence on the metabolic profile throughout the ripening period. Solvents (water, methanol, and ethanol) with different polarities were used to extract target compounds from Turkish white cheese samples and these fractions were characterized using a metabolomics study for biomarkers to enable rapid monitoring of the cheese ripening process.

2. Materials and methods

2.1. Manufacture of Turkish white cheese

Whole cow milk (pH 6.67) was standardized (1:1 protein: fat ratios) and then pasteurized (at 65°C for 30 min) and dropped the temperature to 32°C for clotting. Mesophilic culture-specific for Turkish white cheese (*Lactococcus lactis* subsp. *lactis*, *Lactococcus lactis* subsp. *cremoris*) (Choosit MA11, Danisco, France) was added

to milk with a ratio of 0.002% and fermented until the pH reached 6.4. In addition, 0.2% CaCl₂ and rennet enzyme (CHY-MAX, Chr. Hansen, Hoersholm, Denmark) were added and rested for one and a half hours. Afterward, the clot formed was cut into 1 cm cubes, waited for 30 min for syneresis, and transferred into the cheesecloth. Subsequently, the pressure was applied as 20 kg weights for each 100 kg of cheese milk for four hours then teleme was obtained and it was cut into 7 × 7 cm cubes and waited for 12 h in 16% NaCl brine at 20°C. Cheese blocks were placed in 12% brine in an airtight Ziplock bag and stored at 4°C until further analysis. Cheese samples were ripened for 100 days and analyzed at each 20 days interval.

A batch of Turkish white cheese produced at The Ohio State University Dairy Plant was cut into 36 cubes and then divided into six groups to be used for analysis at each ripening time (1, 20, 40, 60, 80, and 100 days). The cheese production was replicated and as a total of 72 cheese blocks were manufactured in two repetitions.

2.2. Sample preparation for the FT-IR analysis

Approximately 20 g Turkish white cheese sample was blended with liquid nitrogen and ground cryogenically using a Waring Lextra 2 speed blender (East Windsor, NJ, USA) to produce a fine cheese powder.

Water-soluble extracts followed the procedure described by Subramanian et al. (18) and were prepared by mixing 0.1 g of the cheese powder with 0.5 mL of distilled water. The mixture was sonicated by an ultrasonic water bath (Fisher Scientific, Pittsburgh, PA) for 10 s to extract water-soluble components, and then 0.5 mL chloroform was added to remove the complex fats, vortexed for 30 s, and the mixture was centrifuged at 15,700 × *g* for 3 min at 25°C (Megafuge 8, Thermo Fisher Scientific, Waltham, MA, USA). Supernatants (200 µL) were mixed with 200 µL absolute ethanol to precipitate the complex proteins in the mixture and centrifuged at 15,700 × *g* for 3 min at 25°C. The supernatant was employed for further spectroscopic analysis.

Methanol and ethanol extracts were prepared by mixing 0.1 g of the cheese powder with either 1.0 mL of 100% methanol or 100% ethanol solutions. The mixtures were sonicated by using an ultrasonic water bath (Fisher Scientific, Pittsburgh, PA) for 10 s to break down the cheese clumps and improve the extraction of components and centrifuged at 15,700 × *g* for 3 min at 25°C. The supernatant was employed for further spectroscopic analysis.

2.3. FT-IR spectroscopy measurement

The FT-IR spectra of the extractions were collected using a portable FT-IR 4500a (Agilent Technologies, Santa Clara, CA, USA) equipped with a 3-bounce diamond attenuated total reflectance (ATR) accessory. The FT-IR also had Zinc Selenide (ZnSe) beam splitter, a low-powered solid-state laser, a wire-wound element infrared source, and a thermoelectrically cooled deuterated triglycine sulfate (DTGS) detector. The supernatants (10 µL) from the extracts were deposited on the ATR crystal and dried under a vacuum to generate a thin film. The infrared spectra were collected from 4,000 to 650 cm⁻¹ with a 4 cm⁻¹ resolution, and 64 scans were co-added to increase the signal-to-noise ratio. Four independent spectra were

collected from each sample to address the possible heterogeneity of the samples. The means of the four spectra per sample was used for pattern recognition analysis. Thus, a total of 72 spectra were used for model development in this study for the different extraction methods (water-soluble, methanol, and ethanol extracts) obtained from 6(ripening times) \times 6 (cheese cubes per ripening time) \times 1 (average of 4 spectra per sample) \times 2 (cheese production replications).

2.4. References analyses

2.4.1. Organic acid determination by high-performance liquid chromatography (HPLC)

The organic acid content of Turkish white cheese samples was determined by extracting the samples with chloroform and distilled water and running the sample through a Sep-Pak C18 Vac solid cartridge (Waters Corp., Milford, MA, USA). The organic acids were determined using an HPLC (1100, Agilent Technologies, Santa Clara, CA, USA), and eluted components were separated through a Prevail organic acid column with dimensions of 150 \times 4.6 mm \times 5 μ m thickness (Hichrom, Berkshire, UK). The elution of the components was carried out isocratically using pH 2.5 phosphate buffer (25 mM KH_2PO_4) as a mobile phase at a flow rate of 1.5 mL/min at room temperature. The chromatogram was automatically integrated for the organic acids at 210 nm.

2.4.2. Free amino acid determination by gas chromatography–mass spectrometry (GC-MS)

Free amino acids were extracted by dispersing 100 mg of Turkish white cheese in 1 mL of distilled water through an ultrasonic dismembrator (Fisher Scientific, Pittsburgh, PA, USA) for 10 s; then, it was centrifugated at 15,700 \times g for 3 min at room temperature. The supernatant was then derivatized using an EZ:faast amino acid analysis kit (KG0-7165, Phenomenex Inc., Torrance, CA, USA). After the derivatization, the sample was injected through a GC (7820A, Agilent Technologies, Santa Clara, CA, USA) coupled with an MS detector (5,977, Agilent Technologies, Santa Clara, CA, USA). The chromatographic separation was carried out in a ZebronTM ZB-AAA 10 m \times 0.25 mm \times 0.25 μ m capillary column (Phenomenex[®], Torrance, CA) with a 0.1 μ m film thickness. The MS acquisition was carried out in Scan mode with a range scanned set at 45–450 m/z. After identifying the ions, the quantification was achieved with selected ion monitoring (SIM). After determining the 18 individual free amino acid content in the cheese samples, the total free amino acid content was calculated by summing those 18 free amino acid contents.

2.4.3. Free fatty acid determination by gas chromatography–flame ionization detector (GC-FID)

The fat content of the cheese samples was extracted using a mixture of hexane:methanol (2:1 v/v) and methylated, as explained in Yaman et al. (19). Methylated samples were analyzed through a GC-FID (6890N, Agilent Technologies, Santa Clara, CA, USA). The separation of the fatty acids was achieved in an HP-88 capillary column (100 m \times 0.25 mm \times 0.2 μ m) (Agilent Technologies, Santa Clara, CA, USA). Fatty acids' identification was verified by comparing the sample peak retention times and percentage with reference standards (Supelco 37 Component FAME Mix, Sigma-Aldrich, St. Louis, MO, USA). The fatty acid concentrations were determined

as percent fatty acid. All the reference analyses were performed in duplicate. Short-chain fatty acid content was calculated by adding the content of fatty acids, including Butyric acid, Caproic acid, Caprylic acid, and Capric acid.

2.5. Data analysis

The changes in the target components, including individual organic acids, free amino acids, and free fatty acids during the ripening period, were evaluated by descriptive analysis and a randomized ANOVA experimental design with General Linear Model Repeated Measure analysis (SPSS Statistics software version 25.0, IBM Corp., Armonk, NY). The standard error of laboratory (SEL) was calculated according to Berzaghi et al. (20).

Infrared spectral data consist of highly rich as well as complex information (21), and multivariate data analysis was used to extract meaningful information from this complex data set. Cheese sample spectral data were analyzed with multivariate statistical analysis software (Pirouette version 4.5, Infometrix Inc., Bothell, WA, USA). The collected FT-IR spectra were imported as GRAMS (.spc) files and mean-centered, normalized, and smoothed (S-G polynomial fitting algorithm with a 35-point window) prior to the multivariate analysis. Samples with high leverage and/or studentized residual were re-analyzed or labeled as an outlier and excluded from the multivariate model. Soft independent modeling of class analogy (SIMCA) was used to classify the cheese samples according to their ripening days (day 1 to day 100). Partial least squares regression (PLSR) was employed to develop prediction models that quantify biochemical changes in the Turkish white cheese samples. In the regression model, after the outliers were excluded (if any), the remaining data set was subdivided into two groups: calibration/training and external validation. The last-mentioned group was used to unbiasedly estimate the strength of the prediction capabilities (robustness) of the generated training models in real-world situations. After removing the outliers (if any), 80% of the total data set was randomly utilized in the training model, and the remaining 20% was used in the external validation. The validation was generated with cheese samples from any ripening time that came from cheese blocks not used for the calibration set.

The FT-IR spectra of the cheese sample collected over the ripening period were grouped pursuant to the unique biochemical changes that occurred during that period. SIMCA is a supervised classification method that uses known class membership by constructing a multidimensional box for each class (ripening days: class 1: day 1, class 2: day 20. . . etc.) to generate the model to classify new samples in the future by using an F test (21). The performance of the generated SIMCA models was evaluated through class projection plots, misclassification numbers, and interclass distances (ICD). As a rule of thumb, groups with ICD higher than 3 are accepted as significantly different than each other (22).

The quantification of the specific biochemical compounds in the cheese samples over the ripening period was determined by combining the spectroscopic measurement results with the traditional reference data with chemometric regression approaches. The regression analysis tries to find the best functional relationship between the vector of measured signals (a spectrum in our case) and response (e.g., Lactic acid content) and also finds the optimal value of the parameters that will lead to the lowest error in the prediction of the responses (23). The developed PLSR model's

prediction performance was evaluated using the standard error of cross-validation (SECV), coefficient of determination (r), and outlier diagnostics.

3. Results and discussion

3.1. Changes in organic acids, fatty acids, and free amino acid concentrations during the ripening period

The starter cultures, *Lc. lactis ssp. cremoris* and *Lc. lactis ssp. lactis*, used for Turkish white cheese production, have been considered critical in developing flavor compounds because of their natural autolytic activity (24–26). Our results (Table 1) showed significant

development of organic acids, fatty acids, and free amino acids in cheese during ripening ($P < 0.05$). With respect to organic acids, we found increased levels of lactic, citric, propionic, and acetic acid throughout the ripening period ($P < 0.05$) (Table 1). Citric acid had the highest concentration in terms of the organic acids in the tested cheese samples (Table 1) and showed the most dominant changes during ripening, following a zero-order kinetics (Supplementary Figure 1A) with an average increase in the concentration of 1.40 mg/100 g per day. The high concentration of citric acid was due to the presence of native citrate in milk (~ 0.8 mmol/100 mL) (4), besides the production of citrate in the Krebs cycle utilized by lactic acid bacteria (27, 28). The increase in citrate concentration during cheese ripening has been previously reported in white cheese (7). Acetic acid was the second most important organic acid in terms of the formation rate by having

TABLE 1 Changes in certain organic acids, free fatty acids, and free amino acids in white cheese during the ripening period (Mean \pm SD).

Compound	Units	Ripening day						SEL
		1	20	40	60	80	100	
Lactic	mg/100 g cheese	13.77 \pm 0.49 ^a	14.78 \pm 0.54 ^b	15.82 \pm 0.39 ^c	17.56 \pm 0.43 ^d	19.84 \pm 0.48 ^e	24.21 \pm 0.59 ^f	0.39
Citric		132.96 \pm 3.23 ^a	164.8 \pm 6.00 ^b	184.82 \pm 8.55 ^c	205.16 \pm 9.49 ^d	231.82 \pm 10.72 ^e	282.83 \pm 13.07 ^f	3.60
Propionic		7.96 \pm 0.29 ^a	9.9 \pm 0.53 ^b	11.10 \pm 0.46 ^c	11.07 \pm 0.55 ^c	13.00 \pm 0.52 ^d	15.38 \pm 0.82 ^e	0.28
Acetic		20.16 \pm 0.94 ^a	22.38 \pm 1.04 ^b	25.28 \pm 1.18 ^c	28.25 \pm 0.95 ^d	34.46 \pm 1.15 ^e	38.45 \pm 0.93 ^f	0.87
SCFA (C ₄ – C ₁₀)		5.38 \pm 0.33 ^a	7.26 \pm 0.61 ^b	8.75 \pm 0.87 ^c	10.23 \pm 0.64 ^d	11.62 \pm 0.52 ^e	12.45 \pm 0.47 ^f	0.38
Lauric acid (C ₁₂)		5.63 \pm 0.23 ^a	7.72 \pm 0.39 ^b	6.98 \pm 0.33 ^c	7.01 \pm 0.36 ^c	7.82 \pm 0.27 ^b	8.14 \pm 0.28 ^d	0.24
Myristic acid (C ₁₄)		19.61 \pm 0.42 ^a	25.97 \pm 0.44 ^b	24.74 \pm 0.86 ^c	24.36 \pm 0.34 ^d	24.11 \pm 0.79 ^d	25.09 \pm 0.34 ^e	0.40
Palmitic acid (C ₁₆)		63.74 \pm 0.71 ^a	79.51 \pm 2.9 ^b	76.78 \pm 1.52 ^c	77.21 \pm 1.03 ^c	78.43 \pm 1.62 ^d	80.57 \pm 1.81 ^e	1.08
Stearic acid (C ₁₈)		25.6 \pm 0.27 ^a	31.55 \pm 0.51 ^b	29.96 \pm 1.04 ^c	30.28 \pm 0.56 ^c	30.82 \pm 0.71 ^d	31.97 \pm 0.62 ^e	0.35
Oleic acid (C _{18:1})		35.75 \pm 1.15 ^a	45.59 \pm 0.98 ^b	42.61 \pm 0.73 ^c	42.08 \pm 1.32 ^c	43.55 \pm 0.52 ^d	45.64 \pm 0.62 ^b	0.79
Linoleic acid (C _{18:2})		5.70 \pm 0.17 ^a	7.10 \pm 0.32 ^b	6.93 \pm 0.12 ^c	6.81 \pm 0.27 ^c	7.39 \pm 0.16 ^d	7.47 \pm 0.22 ^d	0.16
Glycine	μ g/100 g cheese	10.11 \pm 0.16 ^a	10.03 \pm 0.05 ^b	10.35 \pm 0.05 ^c	10.66 \pm 0.06 ^d	10.93 \pm 0.06 ^e	11.15 \pm 0.06 ^f	0.06
Alanine		18.55 \pm 0.09 ^a	18.69 \pm 0.09 ^b	19.24 \pm 0.1 ^c	19.78 \pm 0.11 ^d	20.28 \pm 0.12 ^e	20.68 \pm 0.10 ^f	0.07
Valine		9.5 \pm 0.05 ^a	9.64 \pm 0.05 ^b	9.9 \pm 0.05 ^c	10.16 \pm 0.06 ^d	10.41 \pm 0.06 ^e	10.61 \pm 0.05 ^f	0.03
Isoleucine		6.31 \pm 0.03 ^a	6.45 \pm 0.03 ^b	6.61 \pm 0.03 ^c	6.77 \pm 0.04 ^d	6.94 \pm 0.04 ^e	7.07 \pm 0.04 ^f	0.02
Methionine		11.57 \pm 0.06 ^a	11.89 \pm 0.06 ^b	12.16 \pm 0.06 ^c	12.44 \pm 0.07 ^d	12.74 \pm 0.07 ^e	12.97 \pm 0.07 ^f	0.04
Proline		23.24 \pm 0.12 ^a	24.04 \pm 0.12 ^b	24.54 \pm 0.13 ^c	25.07 \pm 0.14 ^d	25.65 \pm 0.15 ^e	26.12 \pm 0.13 ^f	0.08
Phenylalanine		14.47 \pm 0.07 ^a	15.06 \pm 0.07 ^b	15.35 \pm 0.08 ^c	15.65 \pm 0.09 ^d	16.01 \pm 0.09 ^e	16.3 \pm 0.08 ^f	0.05
Tyrosine		21.77 \pm 0.11 ^a	22.81 \pm 0.11 ^b	23.2 \pm 0.12 ^c	23.62 \pm 0.13 ^d	24.15 \pm 0.14 ^e	24.57 \pm 0.13 ^f	0.08
Tryptophan		43.89 \pm 0.22 ^a	46.28 \pm 0.23 ^b	46.97 \pm 0.24 ^c	47.76 \pm 0.26 ^d	48.8 \pm 0.28 ^e	49.65 \pm 0.25 ^f	0.16
Serine		73.41 \pm 0.37 ^a	73.49 \pm 0.36 ^a	75.81 \pm 0.39 ^b	78.04 \pm 0.43 ^c	80.07 \pm 0.46 ^d	81.65 \pm 0.41 ^e	0.26
Threonine		13.87 \pm 0.07 ^a	13.98 \pm 0.07 ^b	14.39 \pm 0.08 ^c	14.79 \pm 0.08 ^d	15.17 \pm 0.09 ^e	15.46 \pm 0.08 ^e	0.05
Cysteine		1.27 \pm 0.03 ^a	1.29 \pm 0.02 ^b	1.32 \pm 0.02 ^c	1.36 \pm 0.05 ^d	1.39 \pm 0.02 ^e	1.42 \pm 0.02 ^e	0.00
Lysine		41.81 \pm 0.21 ^a	42.69 \pm 0.21 ^b	43.77 \pm 0.22 ^c	44.84 \pm 0.25 ^d	45.94 \pm 0.27 ^e	46.8 \pm 0.24 ^e	0.15
Histidine		30.87 \pm 0.15 ^a	31.73 \pm 0.16 ^b	32.46 \pm 0.16 ^c	33.21 \pm 0.18 ^d	34.00 \pm 0.20 ^e	34.63 \pm 0.18 ^e	0.11
Aspartic acid		8.36 \pm 0.04 ^a	8.65 \pm 0.04 ^b	8.83 \pm 0.05 ^c	9.02 \pm 0.05 ^d	9.23 \pm 0.05 ^e	9.40 \pm 0.05 ^e	0.03
Glutamic acid		31.03 \pm 0.15 ^a	32.3 \pm 0.16 ^b	32.92 \pm 0.17 ^c	33.57 \pm 0.19 ^d	34.33 \pm 0.20 ^e	34.95 \pm 0.18 ^e	0.11
Asparagine		35.45 \pm 0.18 ^a	37.15 \pm 0.19 ^b	37.78 \pm 0.19 ^c	38.46 \pm 0.21 ^d	39.32 \pm 0.23 ^e	40.02 \pm 0.20 ^e	0.13
Glutamine		60.50 \pm 0.30 ^a	63.8 \pm 0.32 ^b	64.75 \pm 0.33 ^c	65.84 \pm 0.36 ^d	67.28 \pm 0.39 ^e	68.44 \pm 0.35 ^e	0.22
TFAA		455.98 \pm 2.36 ^a	469.97 \pm 2.33 ^b	480.36 \pm 2.46 ^c	491.04 \pm 2.70 ^d	502.65 \pm 2.91 ^e	511.89 \pm 2.58 ^f	1.66

^{a–f}Different superscript in the same line indicates significant differences ($p < 0.05$); SCFA: short chain fatty acids; TFAA: Total free amino acid; SD: standard deviation; SEL: standard error of laboratory.

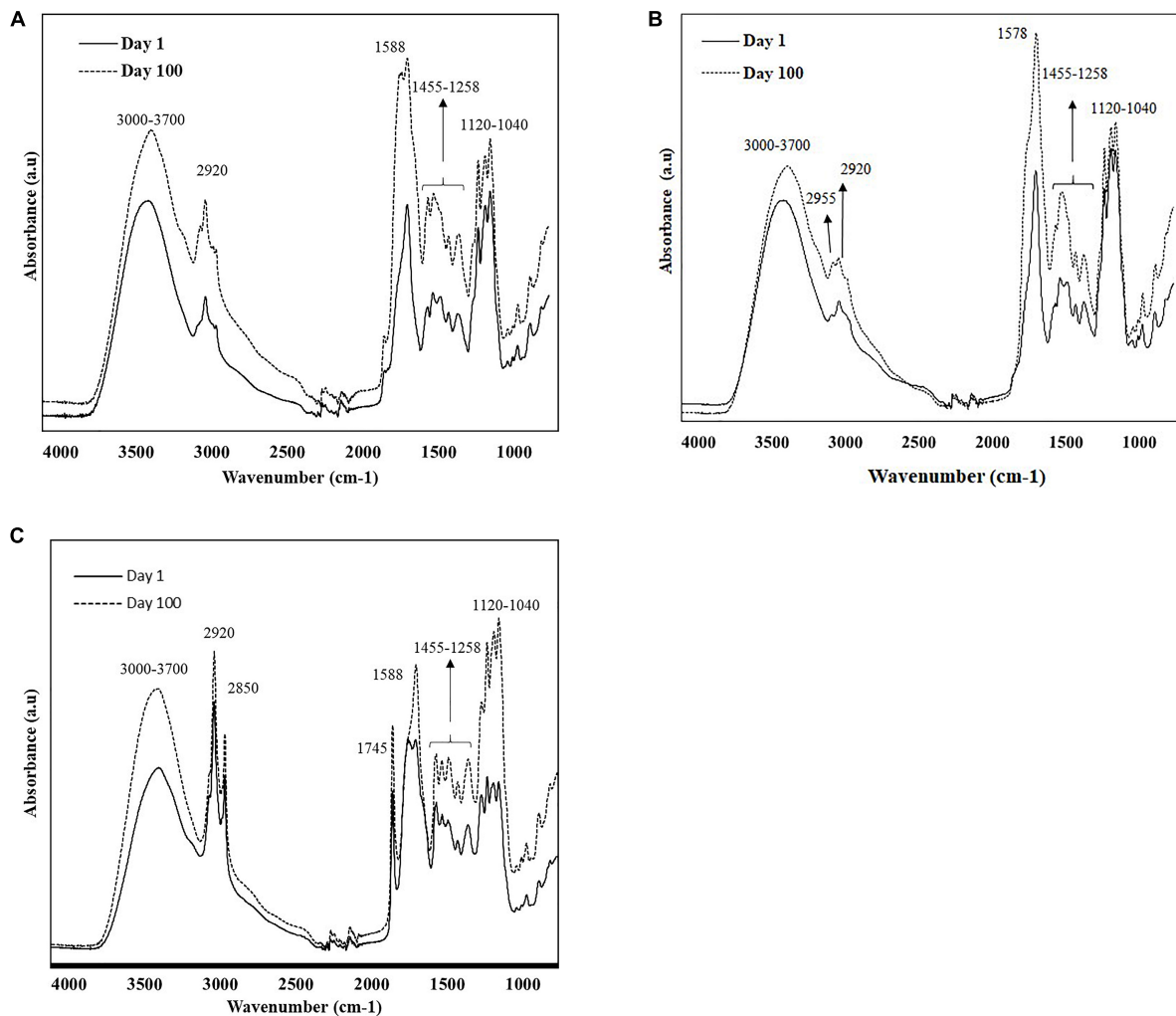


FIGURE 1

Characteristic raw spectra of soluble extracts of cheese samples (A) water; (B) methanol; and (C) ethanol on day 1 and 100, were collected using portable FT-IR (4,000–650 cm^{-1}).

a 0.19 mg/100 g increase each day. Acetic acid is generated from different pathways, including generation in the Krebs cycle (acetic acid or acetate formation from acetyl-CoA in the glycolysis step) (11), production from amino acids (glycine, alanine, glutamic acid, and leucine) (29), and lipolysis of fatty acids (4). Even though lactic acid was not predominantly present in the cheese samples, it is the precursor of the main metabolic reactions in cheese; also, it is the main component of numerous aroma compounds in the cheese (4). The limited amount of lactic acid could be due to the removal of most of the lactose (~98%) in the whey, and the residual lactose (1–2%) in the cheese curd is metabolized to lactic acid by the lactic starter in a short period of time (4). Lastly, propionic acid was the organic acid that had the lowest content in all tested cheese samples throughout the ripening and also increased at a lower rate (0.07 mg/100 g increase each day) than other organic acids with no significant change in propionic acid between days 40 and 60 (Table 1). The propionic acid increase occurs with enzymatic hydrolysis of milk fat and via *Propionibacterium* fermentation. Akalin et al. (7) reported a similar increase in organic acids, particularly lactic, propionic, butyric, and acetic acid, in Turkish white cheese when using a starter culture

that consisted of equal rates of *Lactococcus lactis* ssp. cremoris and *Lactococcus lactis* ssp. Lactis.

The free fatty acids (FFA) in cheese are produced by lipolytic processes (C_4 – $\text{C}_{18:1}$) and bacterial fermentation (C_2 – C_4). The FFA contents in the samples are presented in Table 1. Myristic, stearic, palmitic, and oleic acids contents all showed similar trends by increasing rapidly during the first 20-days of ripening, and then they all reached a plateau. On the other hand, the SCFAs accumulated linearly throughout the ripening period by showing a zero-order kinetic (Supplementary Figure 1B). Instead, the hydrolysis of lauric and linoleic acids were flat throughout the ripening (Supplementary Figure 1B). Akin and others (30) also reported similar FFA results in white cheese ripening using the same lactic acid starter bacteria. The plateau and the limited increase could be explained by the transesterification reactions between alcohol and fatty acids throughout ripening that result in fatty acid esters formation (31). Therefore, increasing FFA content through lipolysis was restricted in our samples.

Finally, the free amino acid levels of the cheese samples (Table 1) increased throughout the ripening period ($P < 0.05$) (Supplementary Figures 1C, D). Total free amino acids (TFAAs)

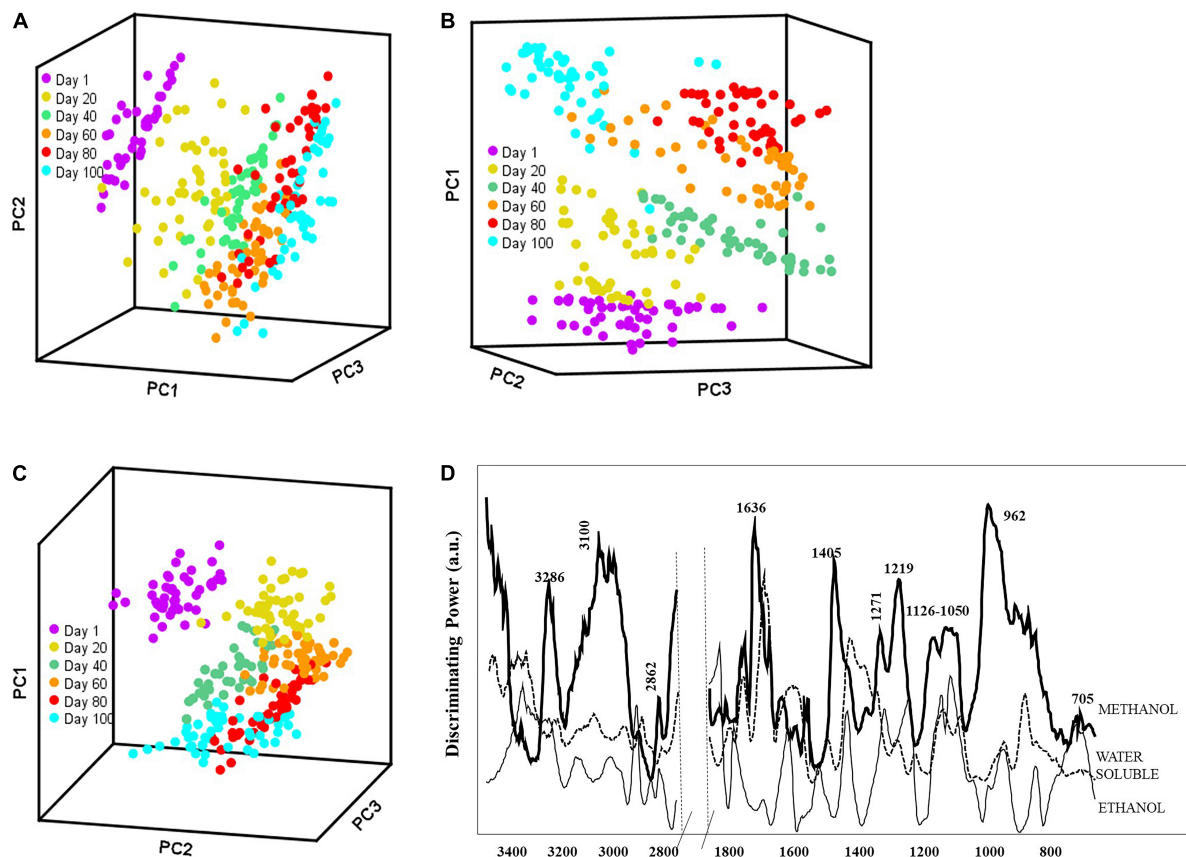


FIGURE 2

Soft independent modeling of class analogy (SIMCA) 3D projection plots for spectra collected by portable FT-IR spectrometer for soluble extracts (A) water; (B) methanol; and (C) ethanol for 100 days ripening period and (D) SIMCA discriminating plot showing the bands and regions responsible for class separation based on the corresponding FT-IR SIMCA model.

change linearly over time with a rate of production ($0.714 \mu\text{g}/100 \text{ g}$ increase per day). The leading free amino acid produced was serine ($0.091 \mu\text{g}/100 \text{ g}$), followed by glutamine ($0.074 \mu\text{g}/100 \text{ g}$), tryptophane ($0.053 \mu\text{g}/100 \text{ g}$), lysine ($0.051 \mu\text{g}/100 \text{ g}$), asparagine ($0.043 \mu\text{g}/100 \text{ g}$), histidine ($0.038 \mu\text{g}/100 \text{ g}$), and glutamic acid ($0.038 \mu\text{g}/100 \text{ g}$). The other free amino acids showed lower production rates (average of $0.017 \mu\text{g}/100 \text{ g}$ increase per day). The production of free amino acids during the ripening of Turkish white cheese was low compared to organic acids and fatty acids, likely associated with the starters' modest proteolytic characteristics.

3.2. FT-IR spectra to monitor biochemical changes during cheese ripening

Figures 1A–C show the overlaid FT-IR spectra ($4,000 - 650 \text{ cm}^{-1}$) of different extracts of cheese samples on days 1 and 100, exhibiting noticeable changes during the ripening process, primarily in the spectral range $1,800 - 900 \text{ cm}^{-1}$. The spectra collected from the different extracts showed unique patterns depending on the solubility of the cheese component in the solvents (Figures 1A–C).

The broad band at $3,700$ to $3,000 \text{ cm}^{-1}$ was associated with O-H stretching vibrations of hydroxyl groups (water); while the bands centered at $2,955$, $2,920$, and $2,850 \text{ cm}^{-1}$ were related to methylene (CH_2) asymmetrical and symmetrical stretching and methyl (CH_3) asymmetrical stretching of lipids (32–35). The distinct band at

$1,745 \text{ cm}^{-1}$ corresponds to the ester carbonyl ($-\text{C}=\text{O}$) functional group of lipids (33, 36). The prominent band at $1,578 \text{ cm}^{-1}$ and its left shoulder ($1,645 \text{ cm}^{-1}$) were attributed to the amide groups in proteins, peptides, and free amino acids (36–38). The shoulder band at $1,453 \text{ cm}^{-1}$ corresponded to methylene bending of amino side chains and the CH_3 asymmetrical deformation of amines (33, 38, 39). The band at around $1,425 \text{ cm}^{-1}$ was related to acidic amino acids (COO^- symmetrical stretching) (38), while the bands between $1,390$ and $1,429 \text{ cm}^{-1}$ can be related to the $[-\text{CH}(\text{CH}_3)]$ groups in amino acids such as alanine, valine, leucine, isoleucine, and methionine. The band at $1,315 \text{ cm}^{-1}$ was responsible for the plane bending vibration of CH bonds of amino acids (40). The band at $1,159 \text{ cm}^{-1}$ corresponded to ester linkages of fats (C-O) (41). The bands between $1,120$ and $1,040 \text{ cm}^{-1}$ were associated to C-O stretching and OH bending groups of organic acids and residual lactose (38). Cheese ripening from day 1 to day 100 showed an increase in the intensity of the infrared signal in all extracts (Figures 1A–C), evidencing the extent of proteolysis, lipolysis, and lactose metabolism during white cheese maturation.

Even though the overall spectra of the different cheese extracts (water, methanol, and ethanol) showed similar spectral characteristics, there were some remarkable distinctions due to the solvent polarity (Figures 1A–C). The region related to fats ($2,955 - 2,850 \text{ cm}^{-1}$, $1,745 \text{ cm}^{-1}$ and $1,159 \text{ cm}^{-1}$) showed higher intensities for ethanol extracts showing its ability to penetrate through the cell membrane and dissolve hydrophobic chains compared to methanol

TABLE 2 Interclass distances between various cheese extracts (a: water; b: methanol; and c: ethanol) on different ripening ages, based on SIMCA model generated by the FT-IR spectral data.

(A)						
Ripening day	1	20	40	60	80	100
1	0.0					
20	7.3 ^a	0.0				
40	14.2	3.6 ^b	0.0			
60	16.5	4.9	4.2 ^c	0.0		
80	15.8	6.3	4.3	3.2 ^d	0.0	
100	15.4	7.1	4.6	3.3	1.5 ^e	0.0
(B)						
Ripening day	1	20	40	60	80	100
1	0.0					
20	14.6 ^a	0.0				
40	24.5	9.5 ^b	0.0			
60	29.9	15.2	11.4 ^c	0.0		
80	34.5	14.8	13.2	7.7 ^d	0.0	
100	20.7	8.9	8.2	5.9	4.3 ^e	0.0
(C)						
Ripening day	1	20	40	60	80	100
1	0.0					
20	5.3 ^a	0.0				
40	8.5	6.2 ^b	0.0			
60	11.3	8.6	4.6 ^c	0.0		
80	11.0	9.8	4.7	3.4 ^d	0.0	
100	13.6	14.9	7.1	7.3	2.7 ^e	0.0

^aStage 1 (day 1 to 20), ^bStage 2 (day 20 to 40), ^cStage 3 (day 40 to 60), ^dStage 4 (day 60 to 80),

^eStage 5 (day 80 to 100).

(42). Water and methanol extracts showed more intense signal in the 1,650–1,570 cm^{-1} , attributed to protein bands, compared to ethanol extracts. The solubilities of the amino acids in water are high because they are present predominantly in zwitterionic form and their solubility decrease with the increase in the hydrophobic character of the solvents (43).

The FT-IR spectra were analyzed using pattern recognition analysis (SIMCA) to evaluate the effects of solvent extracts to classify cheese ripening stages (Figures 2A–C). The boundaries around the samples define the regions in which samples belong to a specific class fall within 95% confidence (44). The projection plots for all extraction methods showed distinct groups, with most interclass distances (ICDs) above 3, indicating that the different solvents extracted cheese metabolites that allowed to classify samples during the complex process of ripening (Tables 2A–C). In general, the greater the ICDs between two clusters, the more chemically distinct. The diagonal values of the ICDs decreased with ripening time, indicating smaller biochemical changes as cheese aging increases. Methanol extracts showed the largest ICDs between clusters indicating that its mixed polarity allowed to solubilize a wider array of metabolites compared to water and ethanol.

We evaluated the discriminating power plots in SIMCA that shows the variables with a predominant effect on the sample

grouping. Model developed with water-based extracts employed 3 factors to explain 97.8% of the variance in the data set. It is important to highlight that water extracts were further fractionated with chloroform (45), resulting in negligible amounts of neutral fat in the samples. The discriminating power (Figure 2D) for water extracts showed that the spectral regions from 1,680 to 1,510, 1,430 to 1,360, and 1,100 to 1,040 cm^{-1} were important in classifying Turkish white cheese samples based on the ripening process. The bands between 1,680 and 1,510 cm^{-1} comprise the absorbances from amide functional groups (46), and the bands between 1,430 to 1,360 cm^{-1} were related to amide III (47, 48). Furthermore, the smaller bands at 1,093 – 1,041 and 855 cm^{-1} could correlate with the organic acids in the white cheese. The changes in the amino acids and organic acids though out the ripening period (Table 1) also support these findings. Methanol extracts also employed 3 factors and explained 98.2% of the variance. The discriminating power plot revealed that bands at around 3,290 to 2,880, 1,636 to 1,611, 1,405, and 1,219 to 960 cm^{-1} were responsible for the class separations (Figure 2D). Methanol is a polar organic solvent that is effective in dissolving amino (1,650 – 1,219 cm^{-1}) and organic (1,096 – 962 cm^{-1}) acids but can also solubilize some non-polar compounds such as fatty acids (3,290 – 2,880 cm^{-1}). Finally, the discriminating power plot for ethanol extracts revealed that the clustering between classes was mainly related to the regions between 3,080 – 2,850 cm^{-1} and 1,700 – 1,685 cm^{-1} (Figure 2D), which can be corresponded to the C-H symmetric and asymmetric stretching of fatty acids and fatty acids' esters, respectively (19, 45). The band at around 1,400 cm^{-1} can be associated with acidic amino acids and the aliphatic chains of fatty acids (45). As a polar organic solvent, ethanol also had an affinity for amino and organic acids, indicated by the signal in the range of 1,230 – 835 cm^{-1} .

3.3. PLSR models for the prediction of individual organic acids, free fatty acids, and total free amino acids

Individual organic acids, free fatty acids, and free amino acids content in Turkish white cheese samples were correlated with the FT-IR spectra of the various extraction methods (including water-based solution, methanol, and ethanol) using PLSR algorithms to generate prediction models. As mentioned earlier, the sample set was divided into the calibration/training and external validation sets, and the robustness/strength of the generated calibration models was tested using the external validation set. The performance statistics of each model, as well as the range of the values and the number of samples included in each model, were given in Tables 3, 4. In order to improve the predictive capacity of each model, mathematical pre-processing procedures were employed, and the frequency regions that give low regression coefficients were excluded from each model since those regions were dominated by noisy, unreliable variables (49). The specific bands and ranges for the model generation were shown in Supplementary Table 1.

Depending on the target compound and extraction method, the cross-validation (leave-one-out) approach determined two to six LVs to generate the models (Table 3), and those LVs explained 95.36 to 99.96% of the variance in the generated calibration models. The regression models for different extraction methods showed a strong

TABLE 3 Performance statistics of the calibration models developed using FT-IR, for the prediction of free amino acids, organic acids, and free fatty acids in soluble extracts (water, methanol, and ethanol) samples during the ripening period.

Compound	Level range (mg/100g)	Water				Methanol				Ethanol			
		N ^c	F ^d	SECV ^e	R _{CV} ^f	N	F	SECV	R _{CV}	N	F	SECV	R _{CV}
Lactic acid	12.6–25.2	55	6	0.88	0.97	54	6	0.96	0.95	55	6	0.99	0.96
Citric acid	128.7–295.8	57	6	10.65	0.98	55	6	11.35	0.97	55	6	15.98	0.94
Propionic	7.41–16.3	58	4	0.71	0.95	58	4	0.72	0.95	55	4	0.71	0.95
Acetic acid	18.0–39.6	56	5	1.28	0.98	56	6	1.52	0.97	55	6	1.99	0.95
SCFA ^a	4.7–14.4	56	5	0.64	0.97	55	6	0.51	0.98	56	5	0.51	0.98
Lauric acid	4.9–9.0	55	5	0.58	0.92	55	5	0.48	0.93	55	5	0.45	0.94
Myristic acid	17.8–27.2	54	6	0.83	0.92	55	6	0.80	0.93	56	5	0.72	0.94
Palmitic acid	58.8–89.6	55	6	2.20	0.93	56	6	2.09	0.94	56	6	1.85	0.95
Stearic acid	23.8–34.8	55	5	0.93	0.91	55	6	0.82	0.93	55	6	0.79	0.93
Oleic acid	32.0–49.2	54	6	1.34	0.92	55	5	1.09	0.94	56	4	1.01	0.94
Linoleic acid	5.13–8.2	55	6	0.24	0.93	55	6	0.24	0.93	54	6	0.23	0.93
TFAA ^b	0.58–0.66	55	4	0.0029	0.99	55	4	0.0039	0.98	54	5	0.0048	0.96

^aShort chain fatty acids, ^bTotal free amino acid, ^cNumber of samples used in calibration models, ^dNumber of factors (latent variables) used to generate the models, ^eStandard error of cross validation, ^fCorrelation coefficient of cross-validation. For each model 58 sample were exist before excluding the outliers.

TABLE 4 Performance statistics of the validation models developed using FT-IR, for the prediction of free amino acids, organic acids, and free fatty acids in soluble extracts (water, methanol, and ethanol) samples during the ripening period.

Compound	Level range (mg/100g)	Water			Methanol			Ethanol		
		N ^c	SEP ^d	R _{Pre} ^e	N	SEP	R _{Pre}	N	SEP	R _{Pre}
Lactic acid	13.5–25.2	14	1.12	0.97	14	1.00	0.96	14	1.10	0.95
Citric acid	128.7–299.7	14	10.51	0.98	14	12.80	0.96	14	13.18	0.96
Propionic	7.4–16.3	14	0.57	0.97	14	0.87	0.92	14	0.64	0.96
Acetic acid	19.8–38.4	14	1.67	0.97	14	1.78	0.96	14	2.19	0.94
SCFA ^a	4.7–12.9	14	0.72	0.97	14	0.67	0.96	14	0.41	0.99
Lauric acid	4.9–9.0	14	0.63	0.92	14	0.52	0.93	14	0.38	0.95
Myristic acid	18.0–27.1	14	0.79	0.93	14	0.82	0.93	14	0.80	0.93
Palmitic acid	59.0–88.0	14	2.00	0.92	14	1.81	0.94	14	1.95	0.95
Stearic acid	23.8–34.6	14	0.92	0.92	14	0.72	0.95	14	1.07	0.94
Oleic acid	32.6–49.0	14	1.53	0.93	14	1.18	0.95	14	0.95	0.96
Linoleic acid	5.1–8.2	14	0.24	0.91	14	0.23	0.92	14	0.19	0.94
TFAA ^b	0.58–0.66	14	0.0037	0.99	14	0.0040	0.98	14	0.0057	0.95

^aShort chain fatty acids, ^bTotal free amino acid, ^cNumber of samples used in calibration models, ^dStandard error of prediction, ^eCorrelation coefficient of prediction for validation.

correlation ($0.98 \geq R_{CV} \geq 0.91$ and $0.99 \geq R_{Pre} \geq 0.91$) in predicting individual organic acids, free fatty acids, and total free amino acids (Tables 3, 4). The standard error of prediction (SEP) values ranged from 0.57 to 13.18 mg/100 g cheese for individual organic acids, 0.19 to 2.00 mg/100g cheese for SCFA and individual free fatty acids, and 0.0037 to 0.0057 mg/100 g cheese for total free amino acids; the numbers were similar to the standard error of cross-validation (SECV) for their corresponding models (Tables 3, 4) that indicates the good predictive ability of the generated calibration models. Even though all types of extraction methods provided similar prediction performances, the organic and amino acids were predicted slightly better with the water-based solution, while free fatty acids levels were predicted best in ethanol-extracted samples.

4. Conclusion

This study proposes how to improve the FT-IR prediction performance by using simple extraction methods using various solvents or mixtures to monitor soluble further ripening compounds such as free amino acids, organic acids, and fatty acids that occur with the biochemical reactions in cheese during ripening. We found that ethanol was more effective than methanol in extracting free fatty acids providing the best measurement performance for this class of compounds. However, water-based extracts were most effective in solubilizing organic acids and free amino acids. The mixed polarity of methanol provided the best classification of metabolites during ripening. Selection of extraction solvent (water,

methanol, ethanol) had a slight effect on the ability of FT-IR to monitor cheese ripening and predict several cheese components. This study could help cheese manufacturers easily monitor the rate and the products of biochemical reactions, including lipolysis, proteolysis, and glycolysis, that produce essential flavor and texture characteristics in white cheese.

Data availability statement

The raw data supporting the conclusions of this article will be made available by the authors, without undue reservation.

Author contributions

HY: methodology, validation, formal analysis, investigation, writing—original draft, and visualization. DA: methodology, validation, formal analysis, investigation, writing—original draft, and visualization. LR-S: conceptualization, validation, resources, writing—review and editing, and supervision. All authors contributed to the article and approved the submitted version.

References

1. Tarakçı Z, Bölük M, Karaağaç M. Cheese consumption habits of consumers in Ordu Province. *Ordu Üniv Bil Tek Derg.* (2015) 5:55–62.
2. Özer B, Kirmaci H, Hayaloglu A. The effects of incorporating wild-type strains of *Lactococcus lactis* into Turkish white brined cheese (Beyaz peynir) on the fatty acid and volatile content. *Int J Dairy Technol.* (2011) 64:494–501. doi: 10.1111/j.1471-0307.2011.00683.x
3. McSweeney P. Biochemistry of cheese ripening: introduction and overview. 4th ed. In: McSweeney P, Fox P, Cotter P editors. *Cheese: chemistry, physics and microbiology*. Amsterdam: Elsevier (2017). p. 379–87. doi: 10.1016/B978-0-12-417012-4.00014-4
4. Fox P, Uniacke- Lowe T, McSweeney P, O'Mahony J. Chemistry and biochemistry of cheese. In: Fox P, Uniacke- Lowe T, McSweeney P, O'Mahony J editors. *Dairy chemistry and biochemistry*. (Chap. 2), New York, NY: Springer Inc (2015). p. 499–545. doi: 10.1007/978-3-319-14892-2_12
5. Guinee T. Protein in cheese and cheese products: structure-function relationships. 4th ed. In: McSweeney P, O'Mahony J editors. *Advanced dairy chemistry - proteins: applied aspects*. New York, NY: Springer Inc (2016). p. 347–415. doi: 10.1007/978-1-4939-2800-2_14
6. McSweeney P, Sousa M. Biochemical pathways for the production of flavor compounds in cheeses during ripening: a review. *Lait.* (2000) 80:293–324. doi: 10.1051/lait:2000127
7. Akalin A, Gonc S, Akba Y. Variation in organic acids content during ripening of pickled white cheese. *J Dairy Sci.* (2002) 85:1670–6. doi: 10.3168/jds.S0022-0302(02)74239-2
8. Singh T, Drake M, Cadwallader K. The flavor of Cheddar cheese: a chemical and sensory perspective. *Comp Rev Food Sci Food Saf.* (2003) 2:166–89. doi: 10.1111/j.1541-4337.2003.tb00021.x
9. Poolman B, Kunji E, Hagting A, Juillard V, Konings W. The proteolytic pathway of *Lactococcus lactis*. *J Appl Bacteriol.* (1995) 79:65S–75.
10. Crow V, Coolbear T, Holland R, Pritchard G, Martley F. Starters as finishers: starter properties relevant to cheese ripening. *Int Dairy J.* (1993) 3:423–60. doi: 10.1016/0958-6946(93)90026-V
11. Broome M, Powel I, Limsowtin G. Starter cultures: specific properties. In: Reginski H, Fuguy J, Fox P editors. *Encyclopedia of dairy science*. London: Academic Press (2003). p. 269–75. doi: 10.1016/B0-12-227235-8/00072-9
12. Cogan T, Hill C. Cheese starter cultures. 2nd ed. In: Fox P editor. *Cheese: chemistry, physics and microbiology*. (Vol. 1), London: Chapman & Hall (1993). p. 193–255. doi: 10.1007/978-1-4615-2650-6_6
13. Fox P, Guinee T, Cogan T, McSweeney P. Biochemistry of cheese ripening. In: Fox P, Guinee T, Cogan T, McSweeney P editors. *Fundamentals of cheese science*. Gaithersburg, MD: Aspen Publishers (2000). p. 333–90.
14. McSweeney P. Biochemistry of cheese ripening. *Int J Dairy Tech.* (2004) 57:127–44. doi: 10.1111/j.1471-0307.2004.00147.x
15. McSweeney P, Fox P. Chemical methods for characterization of proteolysis in cheese during ripening. *Lait.* (1997) 77:41–76. doi: 10.1051/lait:199713
16. Koca N, Rodriguez-Saona L, Harper J, Alvarez V. Application of fourier transform infrared spectroscopy for monitoring short-chain free fatty acids in Swiss cheese. *J Dairy Sci.* (2007) 90:3596–603. doi: 10.3168/jds.2007-0063
17. Subramanian A, Harper W, Rodriguez-Saona L. Cheddar cheese classification based on flavor quality using a novel extraction method and fourier transform infrared spectroscopy. *J Dairy Sci.* (2009) 92:87–94. doi: 10.3168/jds.2008-1449
18. Subramanian A, Harper W, Rodriguez-Saona L. Rapid prediction of composition and flavor quality of cheddar cheese using ATR-FTIR spectroscopy. *J Food Sci.* (2009) 74:292–9. doi: 10.1111/j.1750-3841.2009.01111.x
19. Yaman H, Aykas D, Jiménez-Flores R, Rodriguez-Saona L. Monitoring the ripening attributes of Turkish white cheese using miniaturized vibrational spectrometers. *J Dairy Sci.* (2022) 105:40–55. doi: 10.3168/jds.2021-20313
20. Berzaghi P, Cherney J, Casler M. Prediction performance of portable near infrared reflectance instruments using preprocessed dried, ground forage samples. *Comput Electron Agric.* (2021) 182:106013. doi: 10.1016/j.compag.2021.106013
21. Beebe K, Pell RJ, Seasholtz M. *Chemometrics: a practical guide*. New York, NY: Wiley (1998).
22. Vogt N, Knutsen H. SIMCA pattern recognition classification of five infauna taxonomic groups using non-polar compounds analyzed by high resolution gas chromatography. *Mar Ecol Prog Ser.* (1985) 26:145–56. doi: 10.3354/meps026145
23. Biancolillo A, Marini F. Chemometric methods for spectroscopy-based pharmaceutical analysis. *Front Chem Sec Anal Chem.* (2018) 6:576. doi: 10.3389/fchem.2018.00576
24. Bozoudi D, Kotzamanidis C, Hatzikamari M, Tzanetakis N, Menexes G, Litopoulou-Tzanetaki E. A comparison for acid production, proteolysis, autolysis and inhibitory properties of lactic acid bacteria from fresh and mature Feta PDO Greek cheese, made at three different mountainous areas. *Int J Food Mic.* (2015) 200:87–96. doi: 10.1016/j.ijfoodmicro.2015.02.008
25. Hugenoltz J, Starrenburg M. Diacetyl production by different strains of *Lactococcus lactis* ssp. *lactis* var. *diacetylactis* and *Leuconostoc* spp. *Appl Microbiol Biotechnol.* (1992) 38:17–22. doi: 10.1007/BF00169412
26. Smit G, Smit B, Engels W. Flavour formation by lactic acid bacteria and biochemical flavour profiling of cheese products. *FEMS Microbiol Rev.* (2005) 29:591–610.
27. Niamh W, O'Neill LAJ. A role for the krebs cycle intermediate citrate in metabolic reprogramming in innate immunity and inflammation. *Front Immunol.* (2018) 9:141. doi: 10.3389/fimmu.2018.00141

Conflict of interest

The authors declare that the research was conducted in the absence of any commercial or financial relationships that could be construed as a potential conflict of interest.

Publisher's note

All claims expressed in this article are solely those of the authors and do not necessarily represent those of their affiliated organizations, or those of the publisher, the editors and the reviewers. Any product that may be evaluated in this article, or claim that may be made by its manufacturer, is not guaranteed or endorsed by the publisher.

Supplementary material

The Supplementary Material for this article can be found online at: <https://www.frontiersin.org/articles/10.3389/fnut.2023.1107491/full#supplementary-material>

28. Adda J, Gripon J, Vassal L. The chemistry of flavour and texture generation in cheese. *Food Chem.* (1982) 9:115. doi: 10.1016/0308-8146(82)90073-5
29. Ganesan B, Weimer B. Amino acid catabolism and its relationship to cheese flavor outcomes. 4th ed. In: McSweeney P, Fox P, Cotter P, Everett D editors. *Cheese chemistry, physics & microbiology*. (Chap. 19), Cambridge, MA: Elsevier (2017). p. 483–517.
30. Akin N, Aydemir S, Koçak C, Yıldız M. Changes of free fatty acid contents and sensory properties of White pickled cheese during ripening. *Food Chem.* (2003) 80:77–83. doi: 10.1016/S0308-8146(02)00242-X
31. Holland R, Liu S, Crow V, Delabre M, Lubbers M, Bennet M, et al. Esterases of lactic acid bacteria and cheese flavour: milk fat hydrolysis, alcoholysis and esterification. *Int Dairy J.* (2005) 15:711–8. doi: 10.1016/j.idairyj.2004.09.012
32. Yang H, Irudayaraj J. Characterization of semisolid fats and edible oils by Fourier transform infrared photoacoustic spectroscopy. *J Am Oil Chem Soc.* (2000) 77:291–5. doi: 10.1007/s11746-000-0048-y
33. Pax A, Ong L, Vongsivut J, Tobin M, Kentish S, Gras S. The characterisation of Mozzarella cheese microstructure using high T resolution synchrotron transmission and ATR-FTIR microspectroscopy. *Food Chem.* (2019) 291:214–22. doi: 10.1016/j.foodchem.2019.04.016
34. Gori A, Maggio R, Cerretani L, Nocetti M, Caboni M. Discrimination of grated cheeses by Fourier transform infrared spectroscopy coupled with chemometric techniques. *Int Dairy J.* (2012) 23:115–20. doi: 10.1016/j.idairyj.2011.11.005
35. Santos P, Pereira-Filho E, Rodriguez-Saona L. Application of hand-held and portable infrared spectrometers in bovine milk analysis. *J Agric Food Chem.* (2013) 61:1205–11. doi: 10.1021/jf303814g
36. Chen M, Irudayaraj J, McMahon D. Examination of full fat and reduced fat cheddar cheese during ripening by Fourier transform infrared spectroscopy. *J Dairy Sci.* (1998) 81:2791–7. doi: 10.3168/jds.S0022-0302(98)75837-0
37. Rodriguez-Saona L, Koca N, Harper W, Alvarez V. Rapid determination of swiss cheese composition by Fourier transform infrared/attenuated total reflectance spectroscopy. *J Dairy Sci.* (2006) 89:1407–12. doi: 10.3168/jds.S0022-0302(06)72209-3
38. Sakkas L, Pappas C, Moatsou G. FT-MIR analysis of water-soluble extracts during the ripening of sheep milk cheese with different phospholipid content. *Dairy.* (2021) 2:530–41. doi: 10.3390/dairy2040042
39. Alkhalf M, Mirghani M. Detection of formaldehyde in cheese using FTIR spectroscopy. *Int Food Res J.* (2017) 24:496–S500.
40. Barth A. The infrared absorption of amino acid side chains. *Prog Biophys Mol Biol.* (2000) 74:141–73. doi: 10.1016/S0079-6107(00)00021-3
41. Del Campo S, Bonnaire N, Picque D, Corrieu G. Initial studies into the characterisation of ripening stages of Emmental cheeses by mid-infrared spectroscopy. *Dairy Sci Technol.* (2009) 89:155–67. doi: 10.1051/dst/2008041
42. Patra M, Salonen E, Terama E, Vattulainen I, Faller R, Lee B, et al. Under the influence of alcohol: the effect of ethanol and methanol on lipid bilayers. *Biophys J.* (2006) 1590:1121–35. doi: 10.1529/biophysj.105.062364
43. Dey B, Lahiri S. Solubilities of amino acids in different mixed solvents. *Indian J Chem.* (1986) 25A:136–40.
44. Kvalheim O, Karstang T. SIMCA-Classification by means of disjoint cross validated principal components model. In: Breraton R editor. *Multivariate pattern recognition in chemometrics: illustrated by case studies*. Amsterdam: Elsevier (1992). p. 209–24.
45. Subramanian A, Alvarez V, Harper W, Rodriguez-Saona L. Monitoring amino acids, organic acids, and ripening changes in Cheddar cheese using Fourier-transform infrared spectroscopy. *Int Dairy J.* (2011) 21:434–40. doi: 10.1016/j.idairyj.2010.12.012
46. Chen M, Irudayaraj L. Sampling technique for cheese analysis by FTIR spectroscopy. *J Food Sci.* (1998) 63:96–9. doi: 10.1111/j.1365-2621.1998.tb15684.x
47. Barth A. Infrared spectroscopy of proteins. *Biochim Biophys Acta.* (2007) 1767:1073–101. doi: 10.1016/j.bbabi.2007.06.004
48. Schweitzer-Stenner R. Dihedral angles of tripeptides in solution determined by polarized Raman and FTIR spectroscopy. *Biophys J.* (2002) 83:523–32.
49. Scibisz I, Reich M, Bureau S, Gouble B, Causse M, Bertrand D, et al. Mid infrared spectroscopy as a tool for rapid determination of internal quality parameters in tomato. *Food Chem.* (2011) 125:1390–7. doi: 10.1016/j.foodchem.2010.10.012



OPEN ACCESS

EDITED BY

Theodoros Chatzimitakos,
University of Ioannina, Greece

REVIEWED BY

A. K. Güneş,
Selçuk University, Türkiye
Attila Kiss,
University of Debrecen, Hungary
Qi An,
Langfang Normal University, China
Mei-Ling Han,
Langfang Normal University, China
Gao-Qiang Liu,
Central South University of Forestry and
Technology, China

*CORRESPONDENCE

Yu Xiao-Dan
✉ yuxd126@126.com

[†]These authors have contributed equally to
this work

RECEIVED 09 November 2023

ACCEPTED 07 March 2024

PUBLISHED 18 March 2024

CITATION

Wei-Ye L, Hong-Bo G, Rui-Heng Y, Ai-Guo X,
Jia-Chen Z, Zhao-Qian Y, Wen-Jun H and
Xiao-Dan Y (2024) UPLC-ESI-MS/MS-based
widely targeted metabolomics reveals
differences in metabolite composition among
four *Ganoderma* species.
Front. Nutr. 11:1335538.
doi: 10.3389/fnut.2024.1335538

COPYRIGHT

© 2024 Wei-Ye, Hong-Bo, Rui-Heng, Ai-Guo,
Jia-Chen, Zhao-Qian, Wen-Jun and
Xiao-Dan. This is an open-access article
distributed under the terms of the [Creative
Commons Attribution License \(CC BY\)](#). The
use, distribution or reproduction in other
forums is permitted, provided the original
author(s) and the copyright owner(s) are
credited and that the original publication in
this journal is cited, in accordance with
accepted academic practice. No use,
distribution or reproduction is permitted
which does not comply with these terms.

UPLC-ESI-MS/MS-based widely targeted metabolomics reveals differences in metabolite composition among four *Ganoderma* species

Liu Wei-Ye^{1†}, Guo Hong-Bo^{2†}, Yang Rui-Heng³, Xu Ai-Guo⁴,
Zhao Jia-Chen¹, Yang Zhao-Qian¹, Han Wen-Jun¹ and
Yu Xiao-Dan^{1*}

¹College of Biological Science and Technology, Shenyang Agricultural University, Shenyang, China, ²College of Life Engineering, Shenyang Institute of Technology, Fushun, China, ³Institute of Edible Fungi, Shanghai Academy of Agricultural Sciences, Shanghai, China, ⁴Alpine Fungarium, Tibet Plateau Institute of Biology, Lasa, China

The Chinese name “Lingzhi” refers to *Ganoderma* genus, which are increasingly used in the food and medical industries. *Ganoderma* species are often used interchangeably since the differences in their composition are not known. To find compositional metabolite differences among *Ganoderma* species, we conducted a widely targeted metabolomics analysis of four commonly used edible and medicinal *Ganoderma* species based on ultra performance liquid chromatography-electrospray ionization-tandem mass spectrometry. Through pairwise comparisons, we identified 575–764 significant differential metabolites among the species, most of which exhibited large fold differences. We screened and analyzed the composition and functionality of the advantageous metabolites in each species. *Ganoderma lingzhi* advantageous metabolites were mostly related to amino acids and derivatives, as well as terpenes, *G. sinense* to terpenes, and *G. leucocontextum* and *G. tsugae* to nucleotides and derivatives, alkaloids, and lipids. Network pharmacological analysis showed that SRC, GAPDH, TNF, and AKT1 were the key targets of high-degree advantage metabolites among the four *Ganoderma* species. Analysis of Gene Ontology and Kyoto Encyclopedia of Genes and Genomes demonstrated that the advantage metabolites in the four *Ganoderma* species may regulate and participate in signaling pathways associated with diverse cancers, Alzheimer’s disease, and diabetes. Our findings contribute to more targeted development of *Ganoderma* products in the food and medical industries.

KEYWORDS

widely targeted metabolomics, *Ganoderma*, *Ganoderma lingzhi*, *Ganoderma sinense*, *Ganoderma leucocontextum*, *Ganoderma tsugae*

1 Introduction

“Lingzhi” is the Chinese term for a certain type of edible and medicinal fungi with a long history, generally including *Ganoderma lingzhi*, *Ganoderma sinense*, *Ganoderma tsugae*, and *Ganoderma leucocontextum* (1–3). *Ganoderma* contains a diverse range of bioactive compounds, including polysaccharides, triterpenoids, polyphenols, nucleotides, amino acids,

alkaloids, and vitamins (4–6). These active compounds exert remarkable pharmacological effects and are therefore intensively researched and widely applied in the medical field (7). The pharmacological properties of *Ganoderma* have been demonstrated in clinical trials and therapeutic applications, encompassing its anticancer, antioxidant, immunomodulatory, hypoglycemic, cardioprotective, anti-inflammatory, antiviral, and neuroprotective effects (8–11).

Ganoderma is also highly favored in the food industry (12). For thousands of years, it has been utilized as a health-promoting food supplement renowned for its properties of relaxation, mental clarity, and physical well-being (13, 14). Currently, *Ganoderma* is primarily marketed in health products and nutritional supplements, such as teas, alcoholic beverages, beverages, capsules, oral solutions (12, 14). *Ganoderma* and derived products represent a multibillion-dollar industry worldwide (15). Thus, *Ganoderma* has great potential in the food and medical industries.

However, there remain some prominent and challenging issues in the development of the *Ganoderma* industry. The most significant issue is that it is currently uncertain whether there are differences in the composition and contents of active components among different species. If so, it may be possible to develop different *Ganoderma* products based on the advantages of each species in future, which would be of great importance for the further development of *Ganoderma* for the food and medical industries. Widely targeted metabolomics tools are suitable for addressing the aforementioned issues as they offer high throughput, high sensitivity, and high qualitative accuracy, and comprehensive databases are available (16).

In this study, we collected samples of the four commonly cultivated *Ganoderma* species: *G. lingzhi*, *G. sinense*, *G. tsugae*, and *G. leucocontextum* (17). We analyzed the composition of the active components in each species and identified significantly differential metabolites using widely targeted metabolomics based on ultra performance liquid chromatography-electrospray ionization-tandem mass spectrometry (UPLC-ESI-MS/MS). The research findings are beneficial for the development of *Ganoderma* in the food and medical industries.

2 Materials and methods

2.1 Sampling and sample extraction

The abbreviations used for the fungal species in this manuscript and the production areas of the four *Ganoderma* species are presented in Table 1. The fruiting bodies of all *Ganoderma* species are harvested upon reaching maturity through artificial cultivation. The criteria for

determining *Ganoderma* fruiting body maturity are disappearance of the white growth ring of the fungus cap, cessation of expansion of the fungus cap and continuous thickening, and browning of the edge of the fungus cap (24, 25). Three replicate samples (1 g) from fungal caps were collected for each species. Using vacuum freeze-drying technology, place the biological samples in a lyophilizer (Scientz-100F), then grinding (30 Hz, 1.5 min) the samples to powder form by using a grinder (MM 400, Retsch). Next, weigh 50 mg of sample powder using an electronic balance (MS105DM) and add 1200 μ L of -20°C pre-cooled 70% methanolic aqueous internal standard extract (less than 50 mg added at the rate of 1200 μ L extractant per 50 mg sample). Vortex once every 30 min for 30 sec, for a total of 6 times. After centrifugation (rotation speed 12000 rpm, 3 min), the supernatant was aspirated, and the sample was filtered through a microporous membrane (0.22 μ m pore size) and stored in the injection vial for UPLC-MS/MS analysis.

2.2 UPLC conditions

The sample extracts were analyzed using an UPLC-ESI-MS/MS system (UPLC, ExionLCTM AD, <https://sciex.com.cn/>; MS, Applied Biosystems 6,500 Q TRAP, <https://sciex.com.cn/>). The analytical column was Agilent SB-C18 (1.8 μ m, 2.1 mm \times 100 mm), and the mobile phase comprised solvent A, pure water with 0.1% formic acid, and solvent B, acetonitrile with 0.1% formic acid. Sample measurements were performed with a gradient program comprising 95% A, 5% B, linear gradient to 5% A and 95% B within 9 min, 5% A and 95% B for 1 min, 95% A and 5.0% B within 1.1 min and kept for 2.9 min. The flow rate was 0.35 mL/min, column oven temperature was 40°C , and the injection volume was 2 μ L. The effluent was alternatively connected to an ESI-triple quadrupole (QQQ)-linear ion trap (QTRAP)-MS.

2.3 ESI-q trap-MS/MS

The ESI source operation parameters were as follows: source temperature, 500°C ; ion spray voltage (IS), 5,500 V (positive ion mode)/ $-4,500$ V (negative ion mode); ion source gas I (GSI), gas II (GSII), curtain gas were 50, 60, and 25 psi, respectively; and collision-activated dissociation, high. QQQ scans were acquired under multiple reaction monitoring (MRM), with collision gas (nitrogen) set to medium. Declustering potential (DP) and collision energy (CE) analyses for individual MRM transitions were performed, with further DP and CE optimization. A specific set of MRM transitions was monitored for each period according to the metabolites eluted within this period.

TABLE 1 Sample details of the four *Ganoderma* species.

Sample abbreviation	Species name	Production area	Host plant
Gl	<i>Ganoderma lingzhi</i>	Changbai Mountain, Jilin province, China	<i>Castanea</i> , <i>Cyclobalanopsis</i> and <i>Quercus</i> (18)
Gs	<i>Ganoderma sinense</i>		<i>Albizia mollis</i> , <i>Quercus</i> sp., <i>Dendrocalamus strictus</i> and <i>Dipterocarpus</i> sp. (19, 20)
Gt	<i>Ganoderma tsugae</i>		<i>Larix</i> sp., <i>Picea</i> sp. and <i>Tsuga</i> sp. (20–22)
Gz	<i>Ganoderma leucocontextum</i>	Linshi City, Tibet province, China	<i>Cyclobalanopsis glauca</i> (20, 23)

2.4 Qualitative and quantitative analyses of metabolites

Crucial MS parameters, such as DP, CE, retention time (RT), Q1 (precursor ion), and Q3 (product ion), were used to identify metabolites from the Metware database (Wuhan Metware Biotechnology Co., Ltd.). After identifying the compounds, we conducted a comparative analysis against the database and classified them into Class I and Class II based on their structural characteristics. Class I represents the primary classification of compounds, while Class II provides a more detailed categorization of metabolites in Class I. Metabolites were quantified using the MRM mode for mass spectrum peaks of metabolites.

2.5 Reconstruction and analysis of protein–protein interaction networks

The canonical SMILES of *Ganoderma* metabolites were retrieved from the PubChem and NPASS databases. Subsequently, protein targets for each compound were predicted using SwissTargetPrediction, with a restriction to *Homo sapiens*. The identified targets of each dominant *Ganoderma* metabolite were merged, and duplicates were eliminated. PPI networks for all targets were predicted using information provided by the STRING database, with target genes restricted to “*Homo sapiens*” genetic symbols and saved as tsv files. The tsv files were visualized in Cytoscape v3.9.1 to depict the PPI network. To identify the key targets, we conducted target screening within the PPI network of all targets. The screening criteria were as follows: key targets were determined based on a degree value greater than twice the median, and betweenness centrality, and closeness centrality values exceeding the median. The selected key targets were subsequently visualized using STRING and Cytoscape v3.9.1, leading to the construction of a PPI network for each key target of each *Ganoderma* metabolite.

2.6 Gene ontology functional annotation and Kyoto encyclopedia of genes and genomes pathway analysis

To elucidate the biological processes and signaling transduction roles of key target proteins, we employed the ClueGO tool (a Cytoscape plug-in) for GO functional annotation and KEGG pathway analysis. The analysis was performed by inputting a list of human target gene names. The pathways wherein genes were located were filtered, retaining only GO items with *p* values <0.01, while ensuring that each pathway contains more than 20 genes and has a ratio higher than 20%. The top 20 pathways were selected based on their ratio, and a bubble plot visualization was generated using the ggplot2 package in R.¹

2.7 Statistical analysis

Unsupervised principal component analysis (PCA) was performed using the statistics function prcomp in R. The data were

unit variance-scaled before unsupervised PCA. Pearson correlation coefficients between two samples were calculated using the cor function in R and the data are presented as heatmaps. In differential metabolite analysis, differential metabolites between two groups were determined based on a value importance plot (VIP) value >1 and $|\log_2 \text{fold change (FC)}| \geq 1.0$. VIP values were extracted from orthogonal projections to latent structures-discriminant analysis (OPLS-DA) results, which also contain score plots and permutation plots, generated using the R package MetaboAnalystR. The data were log-transformed and mean-centered before OPLS-DA. To avoid overfitting, a permutation test (200 permutations) was used.

3 Results and discussion

3.1 Metabolite composition of the four *Ganoderma* species

Widely targeted metabolomics analysis revealed the presence of 1,187 metabolites in the Gl, Gs, Gz, and Gt samples. All detected metabolites were categorized into 11 classes under Class I: amino acids and derivatives (387), lipids (140), alkaloids (119), organic acids (110), others (110), phenolic acids (92), terpenoids (91), nucleotides and derivatives (84), flavonoids (36), lignans and coumarins (10), and quinones (8). Polysaccharides and triterpenoids have been the focus of research on the pharmacological activities of *Ganoderma* (26, 27). The fruiting body is the most important pharmacological part of *Ganoderma*. Xie et al. (6) demonstrated that the fruiting body exhibited the highest abundance of metabolites compared to the fermentation broth, mycelium, and spores of *G. lucidum*. Additionally, most triterpenoids were exclusively detected in the fruiting body, thereby establishing the fruiting body as a more promising candidate for the development of anti-tumor and anti-AIDS drugs (6). However, the chemical composition of *Ganoderma* is remarkably complex, and efforts are underway to broaden the research scope of its pharmacological constituents (28, 29). We found that amino acids and their derivatives were the most abundant metabolites in each *Ganoderma* species, providing new insights for the development of *Ganoderma* products. Amino acids and derivatives play diverse specific physiological roles in human life activities, and derived products represent an established market globally (30–32). Our findings indicate that *Ganoderma* is suitable for developing amino acid-based health products, such as nutritional supplements and beverages. In addition, *Ganoderma* is rich in other functional components such as alkaloids and organic acids, but research on their composition and functionality is limited. Based on the detected metabolites, we analyzed the metabolite composition of each *Ganoderma* species.

3.2 Differential metabolite composition of each *Ganoderma* species

The upset Venn diagram in Figure 1 shows the numbers of metabolites in each species. We detected a total of 1,187 metabolites, including 1,117 common metabolites, in all four species, with Gt having the widest variety of metabolites (1,174), followed by Gl (1,169), Gz (1,162), and Gs (1,155). Thus, there were only minor differences in metabolite variety among the four *Ganoderma* species were.

The pie chart in Figure 2 shows the numbers of metabolites in the different categories in each *Ganoderma* species. Among all

¹ www.r-project.org

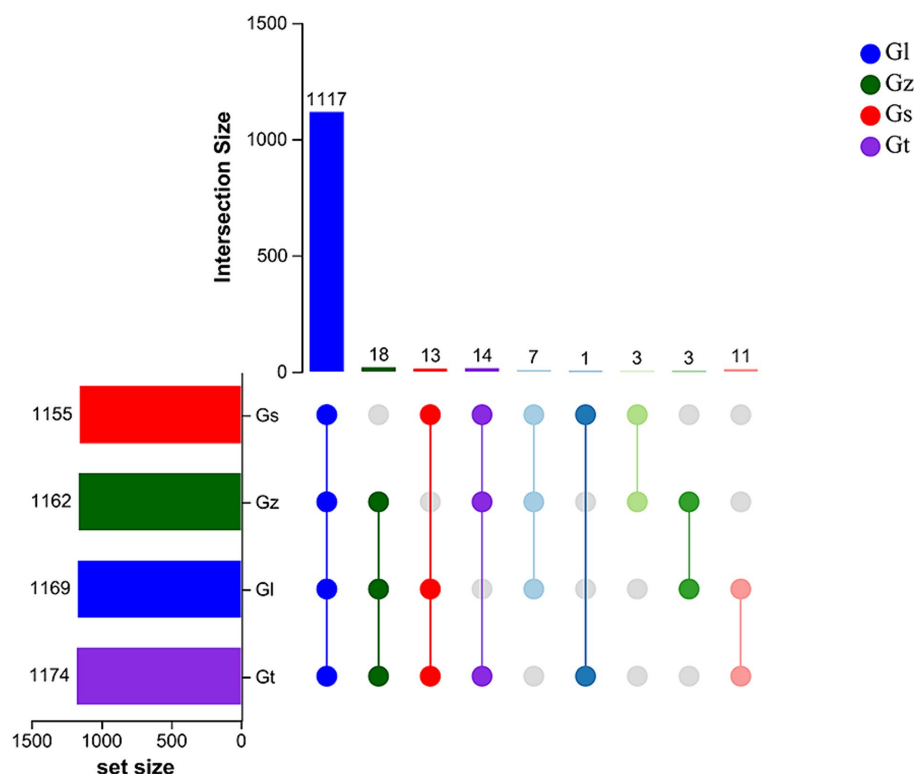


FIGURE 1
Upset Venn plots of metabolite numbers in the four *Ganoderma* species.

species, Gz was the most abundant in amino acids and derivatives, Gl in lipids, and Gt in alkaloids and terpenoids. Differences in the numbers of metabolites in other categories were relatively small (≤ 3).

The interrelationships in metabolite composition among all *Ganoderma* species were investigated using PCA (Figure 3). PC1 and PC2 contributed 35.73 and 23.46%, respectively, of the metabolic variation among all species. The central sample Qc was a mixture of equal amounts of all samples and served as a quality control. The three samples from each *Ganoderma* species clustered closely together, indicating good reproducibility of the triplicate measurements. The distance between Gz and Gs was short, whereas Gl and Gt were clustered further away from the other species. These findings indicated significant differences in metabolite composition among the different *Ganoderma* species.

3.3 Selection and analysis of advantageous metabolites in each *Ganoderma* species

3.3.1 OPLS-DA

To maximize the differentiation among groups and screen differential metabolites, an OPLS-DA model was established using multidimensional statistics (33). The results indicated that differential metabolites could be screened based on VIP values (Supplementary Figure S1).

3.3.2 Differential metabolite analysis among the four *Ganoderma* species

The volcano plots in Figure 4 show the numbers of differential metabolites (both significantly and insignificantly) in pairwise

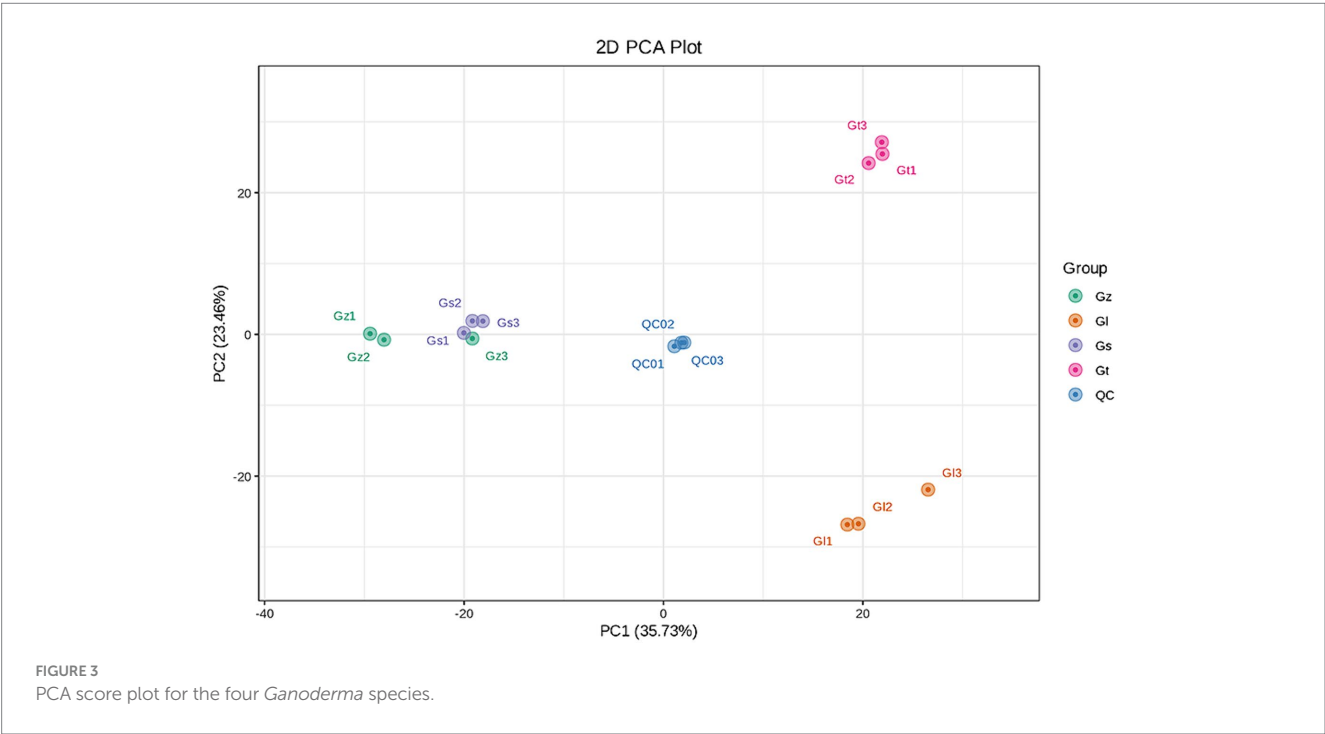
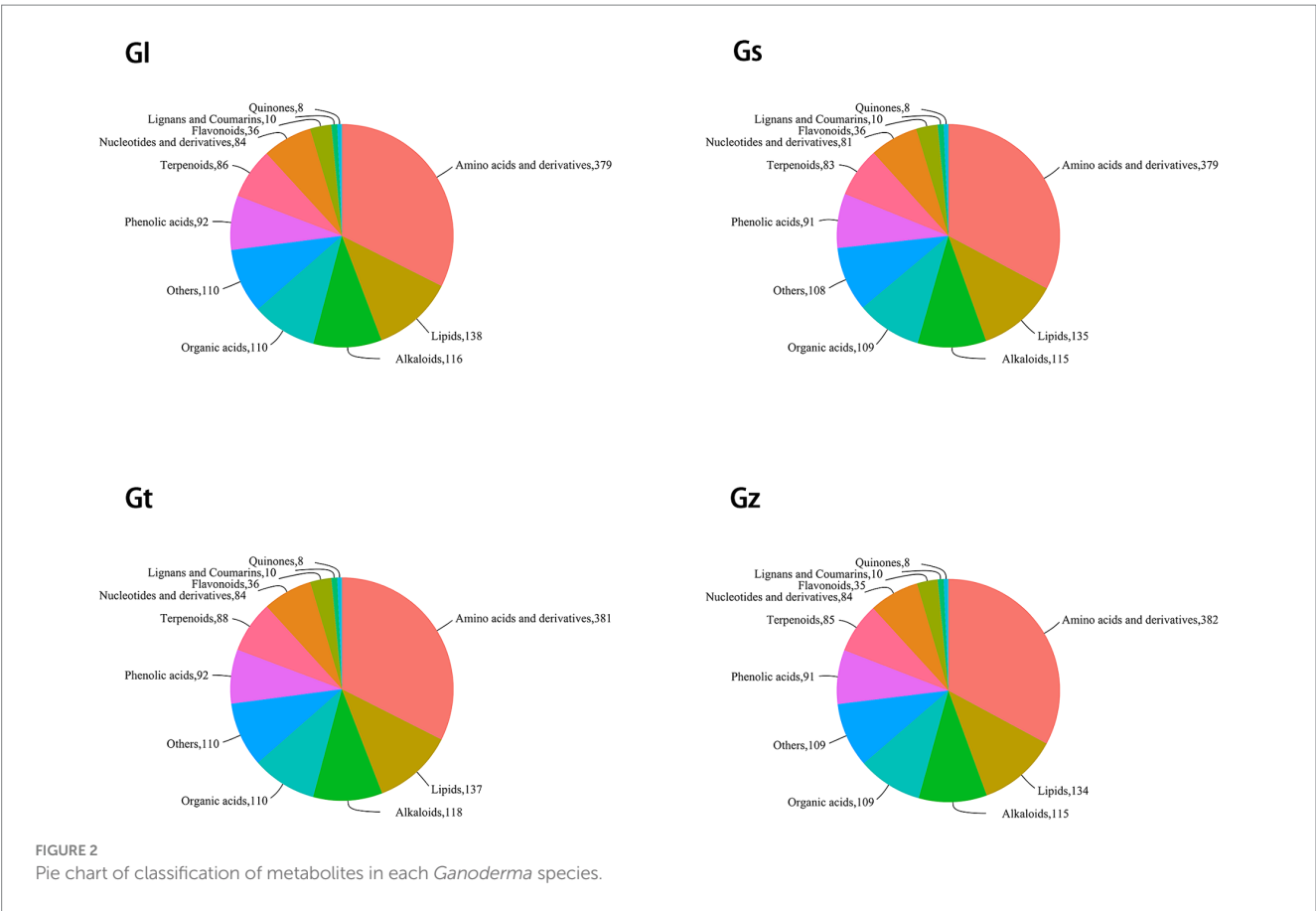
comparisons of all *Ganoderma* species. There most significantly differential metabolites (764) were found between Gs and Gt, and the least (565) between Gl and Gt (Table 2). The metabolites that were significantly more abundant in one species than in the other three were regarded advantageous metabolites and are represented in an upset Venn diagram (Figure 5). According to the numbers of advantageous metabolites, the species were ranked in the following order: Gl (179) > Gt (160) > Gz (129) > Gs (37).

3.3.3 FCs in advantageous metabolites among *Ganoderma* species

FCs represent differences in the relative abundance of metabolites. We statistically analyzed the FC of advantageous metabolites to evaluate their level of dominance (Figure 6). In general, the majority of advantageous metabolites in Gl and Gz were found in the larger FC range, whereas the majority of predominant metabolites in Gt and Gs showed smaller FCs. The advantageous metabolites with FC > 1,000 are listed in Supplementary Table S1. Most of these metabolites were unique to one species, as observed in pairwise comparisons. Some metabolites, e.g., terpenoids in Gs, exhibited a FC > 1,000-fold between two species.

3.4 Composition of advantageous metabolites of different categories among all *Ganoderma* species

Advantageous metabolites reflect the characteristics in which one *Ganoderma* species excels over the others. Therefore, we will discuss the advantageous metabolites of each species based on the



classifications of the compounds. The pie charts in [Supplementary Figures S2, S3](#) show the composition of advantageous metabolites in Classes I and II of each species.

Within Class I, the most advantageous metabolites in all species were amino acids and derivatives. According to the numbers of amino acids and derivatives among advantageous metabolites, the species

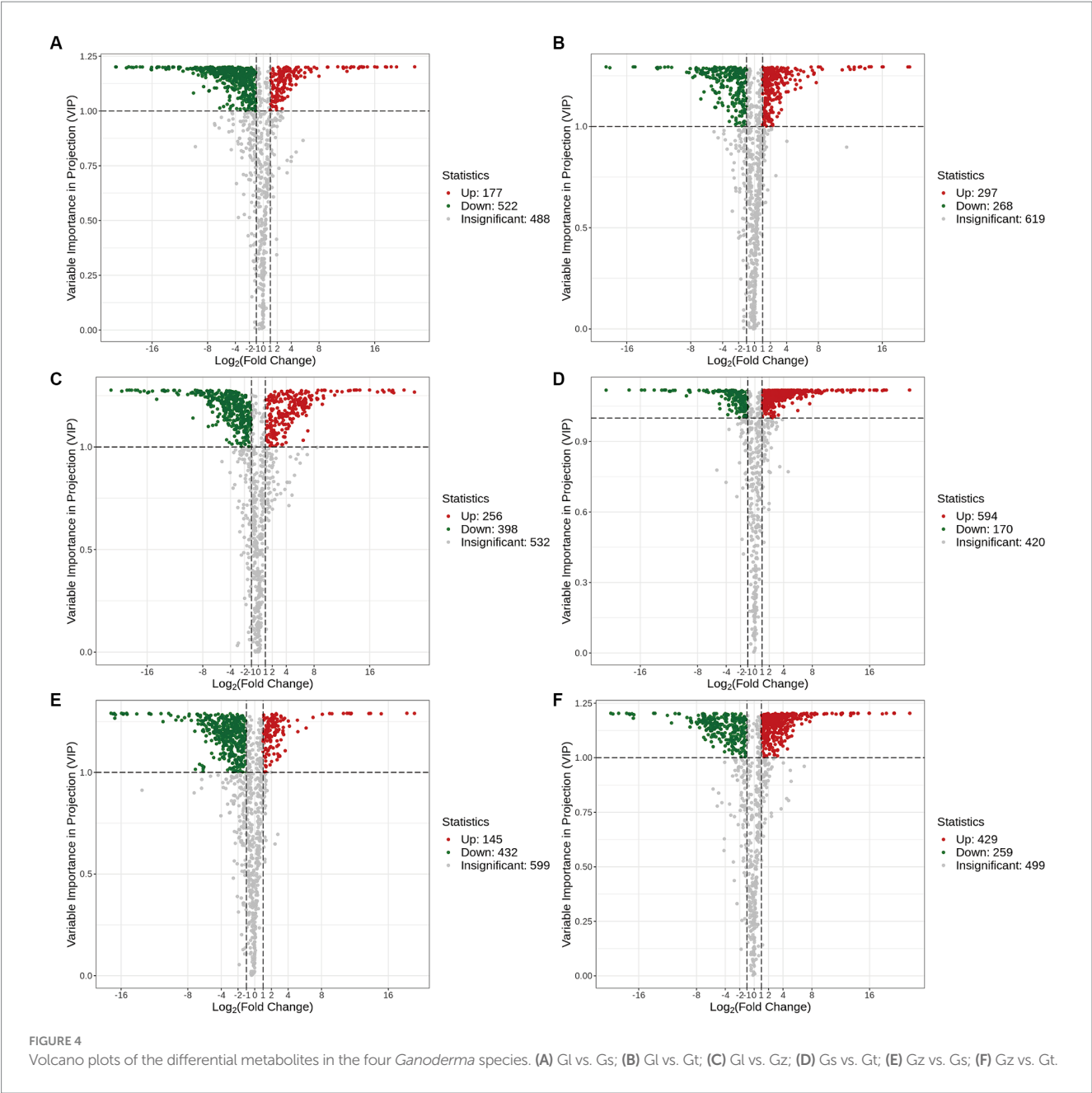


TABLE 2 Numbers of significant and non-significant differential metabolites among the four *Ganoderma* species.

Group name	Significant	Down regulated	Up regulated	Insignificant
Gl vs. Gs	699	522	177	488
Gl vs. Gt	565	268	297	619
Gl vs. Gz	654	398	256	532
Gs vs. Gt	764	170	594	420
Gz vs. Gs	577	432	145	599
Gz vs. Gt	688	259	429	499

were ranked in the following order: Gz (98) > Gl (71) > Gt (46) > Gs (15). Combining the results of Section 3.1 with these findings on dominant metabolites, it can be concluded that Gz is the most suitable among all *Ganoderma* species for developing amino acid products. Lipids were also found to be abundant in *Ganoderma*. According to

the numbers of lipids, the species were ranked as follows: Gl (35) > Gt (33) > Gs (4) > Gz (1). The major lipids in Gl were comprised lysophosphatidylethanolamine and lysophosphatidylcholine, whereas those in Gt were mainly free fatty acids. Some fatty acids are essential because they cannot be synthesized by the human body. For instance,

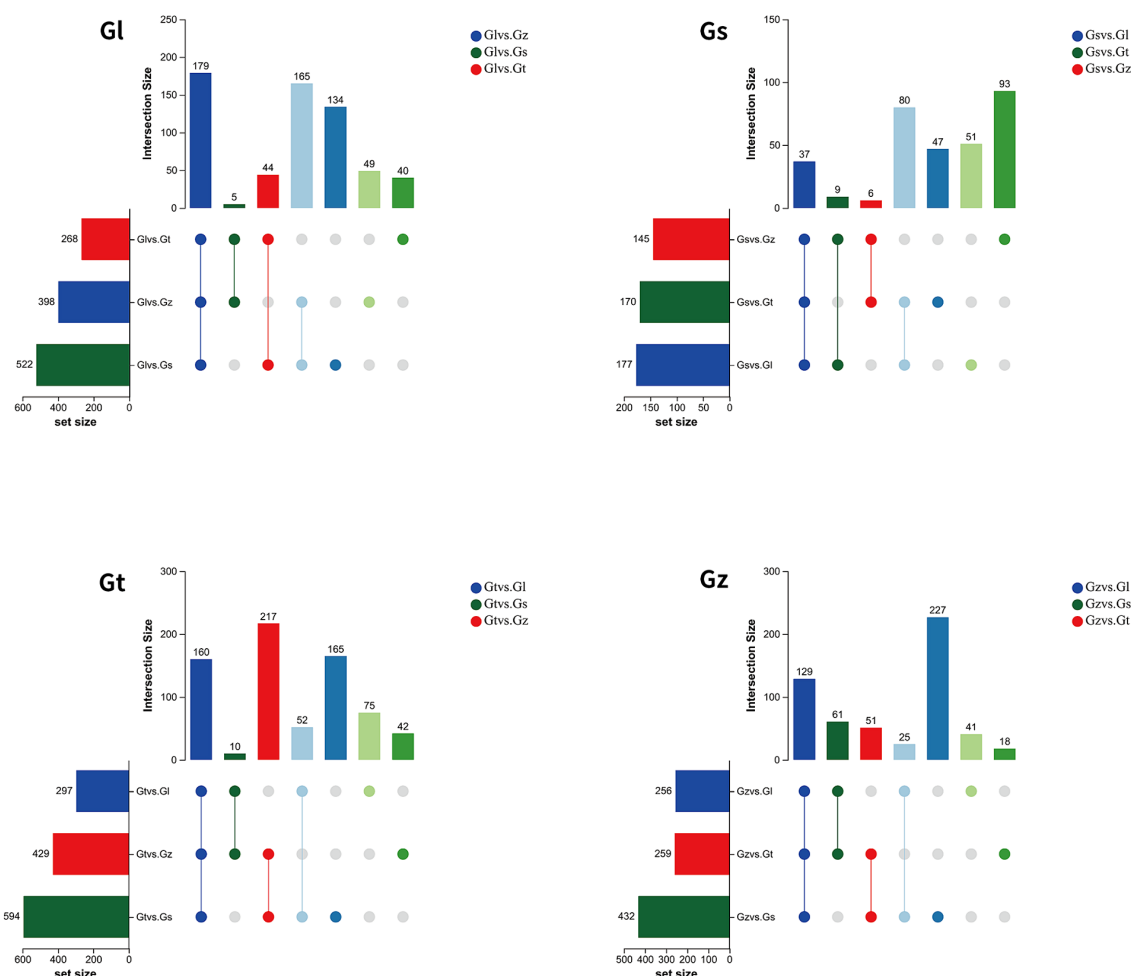


FIGURE 5
Upset Venn diagrams of metabolites specifically enriched in each of the four *Ganoderma* species.

α -linolenic acid identified in this study has antithrombotic functions and is associated with reduced mortality rates of cardiovascular diseases and cancer (34, 35).

Terpenoids are considered one of the most important chemical compounds in *Ganoderma* (26, 36). According to the numbers of terpenoids among advantageous metabolites, the species were ranked as follows: Gs (9) = Gz (9) > Gt (2) > Gl (0). The contents of many terpenoids (91 in total) were relatively similar among all *Ganoderma* species; however, Gs and Gz were more abundant in advantageous terpenoids than the other species. Nearly all terpenoids found in *Ganoderma* have been demonstrated to possess beneficial physiological activities, such as anticancer and antioxidant properties (26, 36, 37). However, when we attempted to extract a large quantity of a specific terpenoid, we were unable to determine which species contains the highest amount and allows the highest extraction efficiency. Therefore, we presented the advantageous terpenoids in [Supplementary Table S2](#) to facilitate better utilization of the terpenoids from each species.

Alkaloids are important chemical components of *Ganoderma*. Several studies have demonstrated that alkaloids in various *Ganoderma* products have remarkable health-promoting functions, including neuroprotection, renal protection, and anticancer effects

(29, 38, 39). In total, 119 different alkaloids were identified in the four *Ganoderma* species, which calls for further research and development. According to the numbers of advantageous alkaloids among advantageous metabolites, the species were ranked as follows: Gl (20) > Gt (19) > Gz (5) > Gs (2). According to the pie chart in [Supplementary Figure S2](#), Gl and Gt are more abundant in alkaloids than the other species. Compared to Gl, Gt has a wider variety of advantageous alkaloids. In addition to plumerane, which is also present in Gl, Gt contains pyridine alkaloids, pyrrole alkaloids, quinoline alkaloids, and piperidine alkaloids, which are absent in Gl. The alkaloids among the advantageous metabolites of all *Ganoderma* species are listed in [Supplementary Table S2](#). *N*-Oleylethanolamine exhibits weight-reducing and anti-atherosclerotic effects and is employed for the treatment of cardiovascular and metabolic disorders (40–42). *O*-Acetyl-L-carnitine functions in neuroprotection and the protection of brain development (43–45). Agmatine contributes to the regulation of glucose and lipid metabolism and has antidepressant, anticonvulsant, and neuroprotective effects (46, 47).

Nucleotides and derivatives are another important component of *Ganoderma* and derived health products; they exhibit pharmacological activities and health-promoting functions such as lipid-lowering effects (48–51). We identified 84 nucleotides and derivatives in the

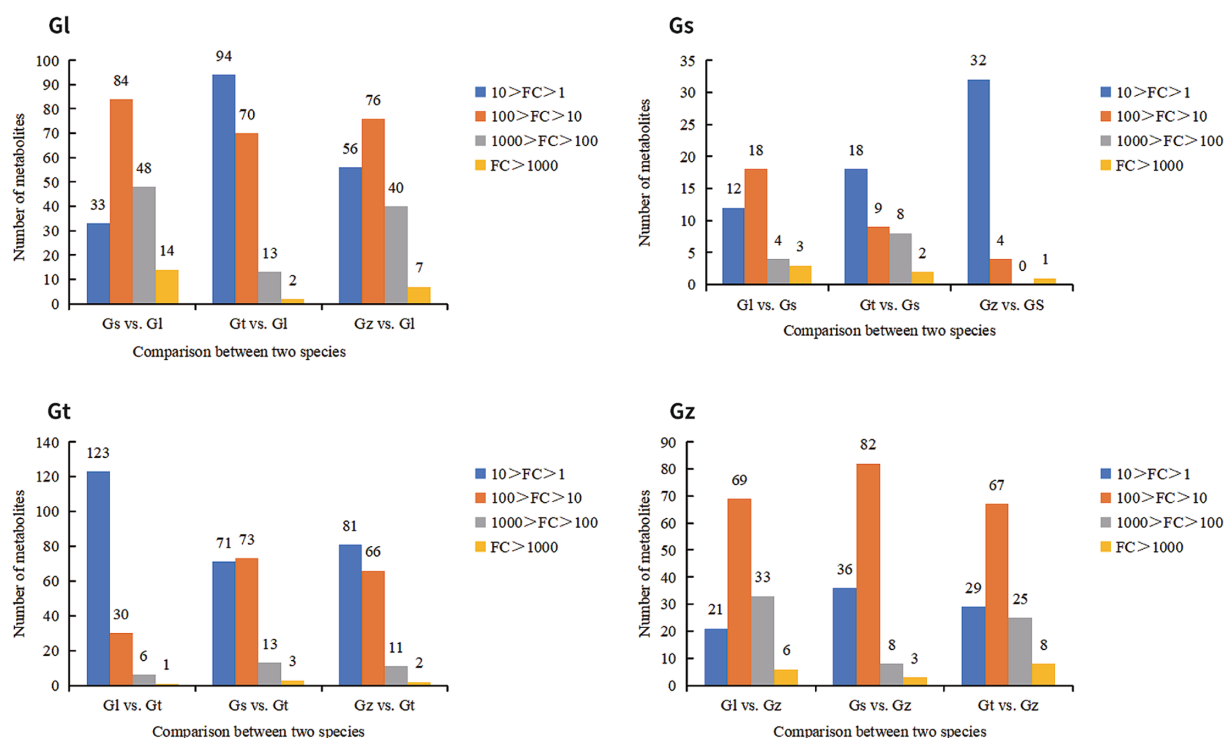


FIGURE 6
Number of advantage metabolites of each *Ganoderma* species in different FC intervals.

four *Ganoderma* species. According to the numbers of nucleotides and derivatives among advantageous metabolites, the species were ranked as follows: Gt (17) > G1 (14) > Gz (2) > Gs (0). The nucleotides and derivatives among advantageous metabolites of all *Ganoderma* species are listed in [Supplementary Table S2](#). Vidarabine exhibits potent antiviral activity and is widely used as an anti-herpesvirus agent (52). Citicoline exerts neuroprotective effects and has anticonvulsant properties (53, 54). β -Nicotinamide mononucleotide possesses anti-aging properties (55, 56). Acadesine possesses antitumor activities in several cancer types (57, 58).

Flavonoids, phenolic acids, and organic acids among advantageous metabolites of four *Ganoderma* species are listed in [Supplementary Table S2](#). Flavonoids are a research focus in *Ganoderma* studies and exhibit antioxidant and anti-inflammatory effects and cytotoxicity against cancer cells (59–62). Xanthohumol possesses antitumor activities and antiarrhythmic properties (63, 64). 2',7-Dihydroxy-3',4'-dimethoxyisoflavan possesses anti-inflammatory activity (65). The organic acid γ -aminobutyric acid improves sleep and reduces blood pressure (66–68). Shikimic acid has diverse biological activities and serves as an intermediate in the synthesis of anticancer drugs (69). The phenolic acids protocatechualdehyde, (E)-ethyl p-methoxycinnamate, and picein exhibit anticancer, anti-inflammatory, and antioxidant effects (70–73).

3.5 Network pharmacology analysis

3.5.1 PPI networks of key targets from the four *Ganoderma* species

PPI networks of key targets were constructed for advantageous metabolites of all *Ganoderma* species (Figure 7 and

[Supplementary Table S3](#)). In each PPI network, SRC, GAPDH, TNF, and AKT1 were among the top five highest-degree targets. SRC is associated with increased tumor progression, invasion, and metastasis in many cancers (74, 75). TNF plays a crucial role in cancer treatment and autoimmunity (76, 77), while AKT1 is linked to breast cancer and ovarian cancer (78, 79). Despite differences in the advantageous metabolites from the four *Ganoderma* species, their mechanisms of tumor suppression are closely related to these targets.

The third highest-degree target of TP53 was identified in Gz and Gt, but not in G1 and Gs. TP53 functions as a crucial tumor suppressor, with its mutations being frequently observed in various malignant neoplasms (80, 81). This observation implies that the tumor-suppressive mechanisms of metabolites in Gz and Gt may exhibit greater prominence in regulating TP53 than those of metabolites in G1 and Gs. Albumin (ALB) exhibited a high degree in the PPI networks of G1, Gs, and Gt. ALB is primarily synthesized by the liver in humans and serves as the predominant plasma protein (82). Extensive research has demonstrated that ALB functions as a tumor suppressor and plays a crucial role in hepatocellular carcinoma metastasis and invasion (83).

3.5.2 KEGG pathway and GO annotation analyses

GO and KEGG pathways were enriched and visualized by Cluego software (Figure 8). Among the top 20 pathways identified in the four *Ganoderma* species, several cancer-related pathways were prominently observed, including prostate cancer, non-small cell lung cancer, colorectal cancer, small cell lung cancer, pancreatic cancer, bladder cancer, and endometrial cancer. The advantageous metabolites of the four *Ganoderma* species exhibited a strong correlation with diverse cancer pathways, underscoring their potential as promising therapeutic agents. We also observed that some of the top 20 pathways

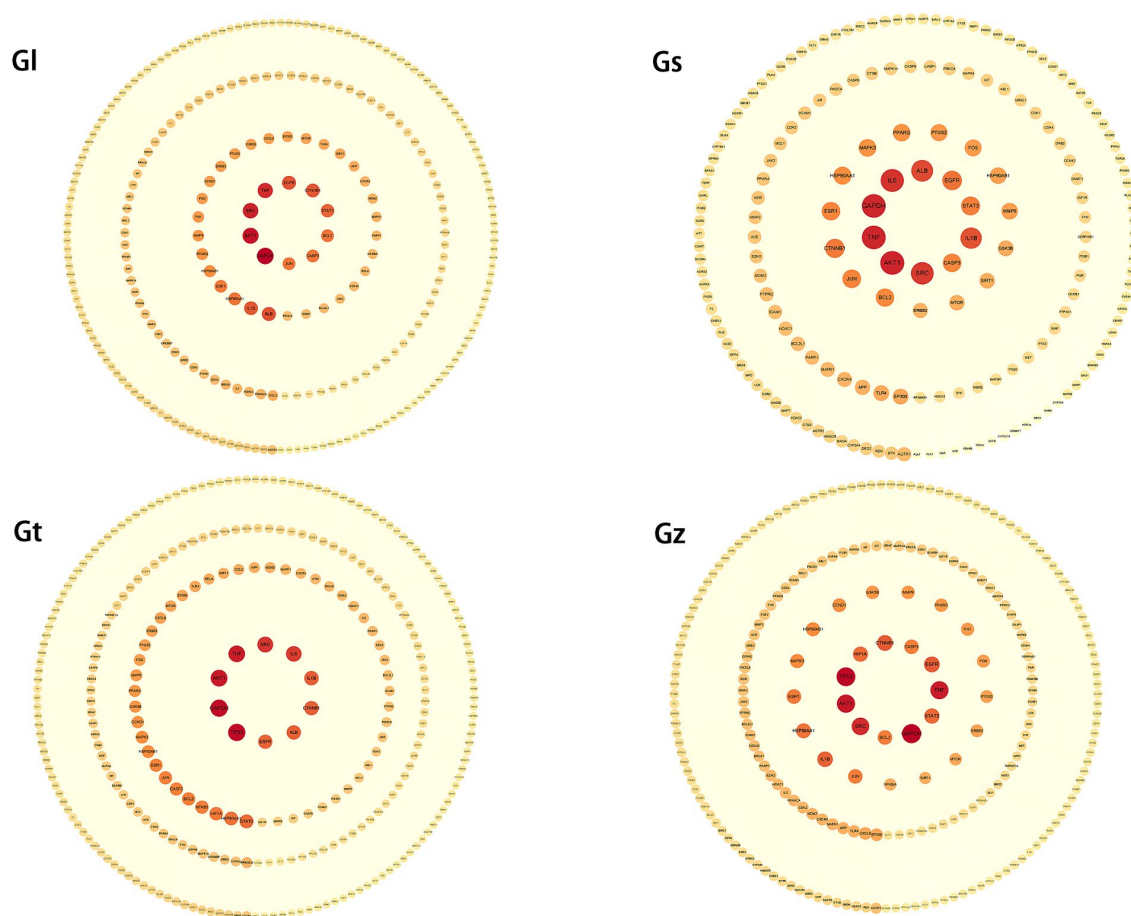


FIGURE 7

PPI networks of key targets from four *Ganoderma* species. The degree of the target increases proportionally with the darkness of the color and the size of the font.

were only found in certain species of *Ganoderma*, including cocaine addiction and B cell receptor signaling pathway in G1; TNF signaling pathway, positive regulation of smooth muscle cell proliferation, IL-17 signaling pathway, C-type lectin receptor signaling pathway, pertussis, and neuroinflammatory response in Gs; and renal cell carcinoma in Gz. The findings facilitate a more precise investigation into the therapeutic pathways of different *Ganoderma* species.

The bubble plot was utilized to compare the number and ratio of genes in the pathways (Figure 9). Prostate cancer accounted for the highest ratio in all G1 and Gt pathways, reaching more than 44%. The proteasome exhibited a high ratio in both the Gz and Gt pathways. The response to amyloid-beta in the top 20 pathways of the four *Ganoderma* species exhibited a relatively high ratio. The neurotoxicity of amyloid-beta and its strong correlation with Alzheimer's disease have been consistently demonstrated in recent studies (84, 85). Therefore, the neuroprotective effects of the four *Ganoderma* species may primarily be attributed to their modulation of the amyloid-beta pathway. Similar findings have also been corroborated in pharmacological analyses and validation studies involving *G. lucidum* (86, 87). The AGE-RAGE signaling pathway in diabetic complications had a high ratio in the four *Ganoderma* species. AGE-RAGE plays a crucial role in the development of diabetic complications, such as kidney disease and cardiovascular disease (88). Recent advancements in network pharmacological analysis and animal experiments have demonstrated that certain

natural remedies, such as *Radix Rehmanniae* and *Corni Fructus*, can effectively regulate this pathway to combat diabetic complications (89); however, limited research has been conducted on *Ganoderma*.

4 Conclusion

We conducted a widely targeted metabolomics analysis of four *Ganoderma* species commonly used in the food and medical industries. The results indicate that although there are differences in the variety of metabolites among the four *Ganoderma* species, these differences are relatively small. However, there are significant differences in the content of metabolites among the four *Ganoderma* species. The relative amounts of many metabolites in different species of *Ganoderma* vary significantly by hundreds or even thousands of times. Therefore, even if the metabolite compositions of these four species of *Ganoderma* are similar, it is imperative to determine the difference in dosage when using them interchangeably. To achieve a more targeted application of *Ganoderma* in the medical and food fields and to facilitate further development and research of each *Ganoderma* species, we identified and discussed advantageous metabolites that are significantly more abundant in one *Ganoderma* species than in the others. Among the four *Ganoderma* species, Gz is the most suitable for the development of amino acid-based products.

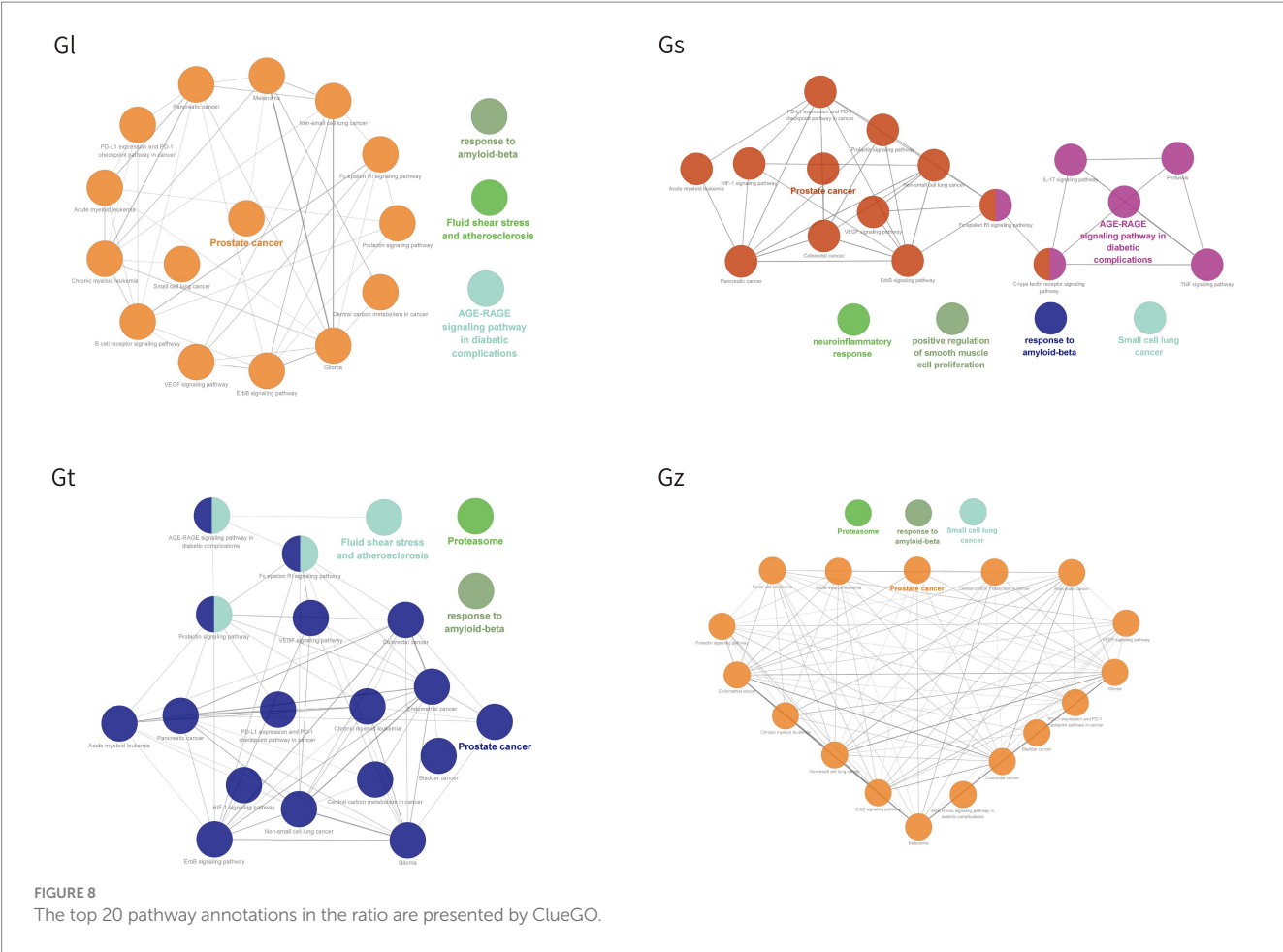


FIGURE 8 The top 20 pathway annotations in the ratio are presented by ClueGO.

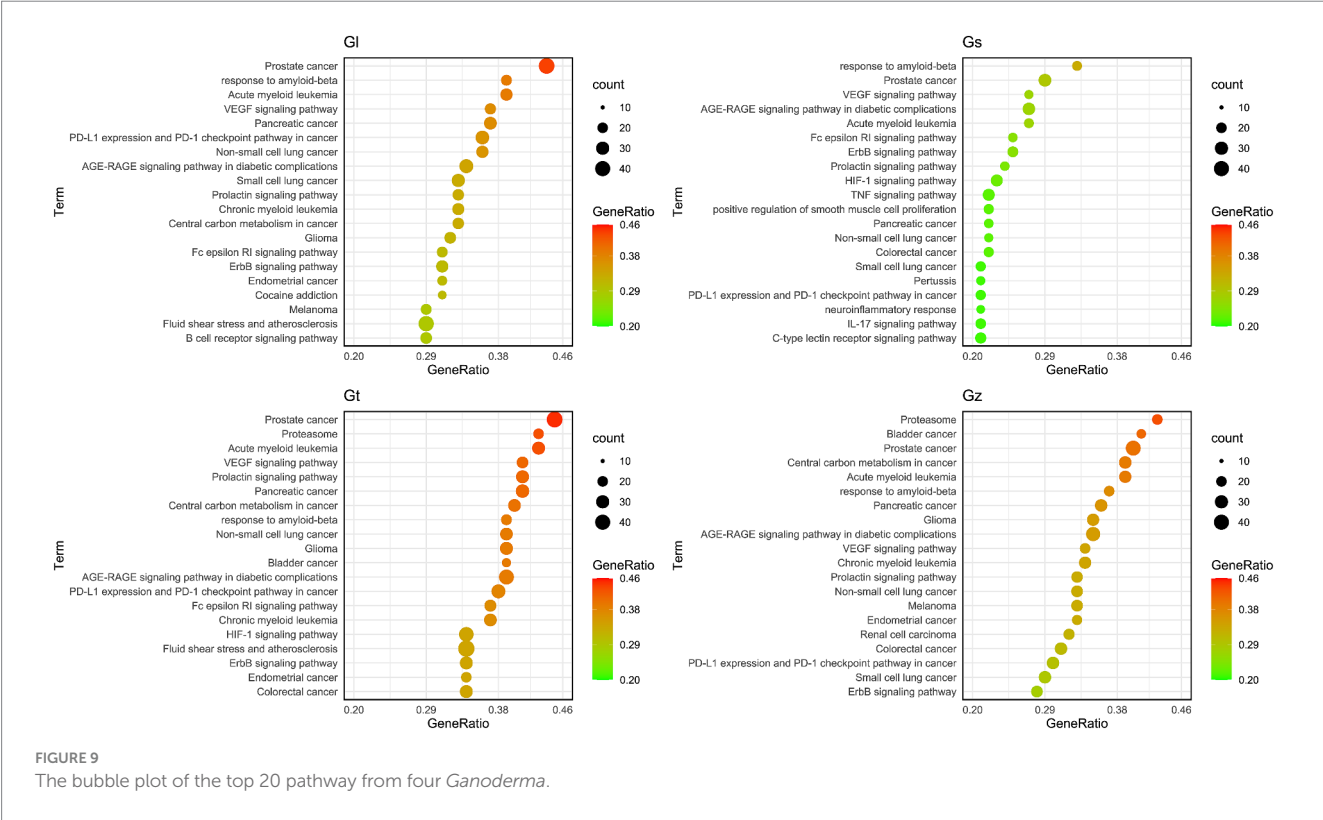


FIGURE 9 The bubble plot of the top 20 pathway from four *Ganoderma*.

Gs and Gz are richer in terpenes, whereas Gl and Gt are more abundant in nucleotides and derivatives, alkaloids, and lipids than the other species. Network pharmacological analysis showed that the top 5 targets with high degree were similar, although the compositions of dominant metabolites in the four *Ganoderma* species were different. Simultaneously, certain discrepancies were also observed. For instance, among the highly correlated targets, TP53 was exclusively present in Gz and Gt, while ALB appeared in only Gl, Gs, and Gt. These variations may reflect the specificity of different *Ganoderma* species in targeting disease-related pathways. Furthermore, KEGG and GO analyses demonstrated that the advantageous metabolites of the four *Ganoderma* species have potential regulatory effects on various pathways associated with cancer, Alzheimer's disease, and diabetes complications, among others. However, each *Ganoderma* species also displayed unique and significantly enriched pathways. The findings necessitate further comprehensive exploration and validation to facilitate the targeted utilization of diverse metabolites from *Ganoderma*. In the future, we should determine the absolute content of the advantageous metabolites of the four types of *Ganoderma* to determine their utilization value. At the same time, we should also study the thermal stability of the active ingredients in *Ganoderma* and explore the temperature range required to maintain their biological activity in daily processing.

Data availability statement

The original contributions presented in the study are included in the article/[Supplementary material](#), further inquiries can be directed to the corresponding author.

Author contributions

LW-Y: Data curation, Formal analysis, Methodology, Software, Visualization, Writing – original draft, Writing – review & editing. GH-B: Conceptualization, Investigation, Supervision, Writing – original draft, Writing – review & editing, Formal analysis, Validation. YR-H: Investigation, Writing – review & editing. XA-G: Investigation,

Writing – review & editing, Resources. ZJ-C: Visualization, Writing – original draft. YZ-Q: Writing – original draft, Resources. HW-J: Resources, Writing – original draft, Visualization. YX-D: Resources, Writing – original draft, Conceptualization, Funding acquisition, Investigation, Project administration, Supervision, Writing – review & editing.

Funding

The author(s) declare that financial support was received for the research, authorship, and/or publication of this article. This research was funded by the National Natural Science Foundation of China (No. 32370008), the Science and Technology Plan Project of Liaoning Province (2022-MS-418), Key Research and Development Plan of Tibet (XZ202201ZY0010N).

Conflict of interest

The authors declare that the research was conducted in the absence of any commercial or financial relationships that could be construed as a potential conflict of interest.

Publisher's note

All claims expressed in this article are solely those of the authors and do not necessarily represent those of their affiliated organizations, or those of the publisher, the editors and the reviewers. Any product that may be evaluated in this article, or claim that may be made by its manufacturer, is not guaranteed or endorsed by the publisher.

Supplementary material

The Supplementary material for this article can be found online at: <https://www.frontiersin.org/articles/10.3389/fnut.2024.1335538/full#supplementary-material>

References

- Cui B, Pan X, Pan F, Sun Y, Xing J, Dai Y. Species diversity and resources of *Ganoderma* in China. *Mycosystema*. (2023) 42:170–8. doi: 10.13346/j.mycosystema.220216
- Wu DT, Deng Y, Chen LX, Zhao J, Bzhelyansky A, Li SP. Evaluation on quality consistency of *Ganoderma lucidum* dietary supplements collected in the United States. *Sci Rep*. (2017) 7:7792. doi: 10.1038/s41598-017-06336-3
- Wu Q, Liu H, Shi Y, Li W, Huang J, Xue F, et al. Characteristics of the genome, transcriptome and Ganoderic acid of the medicinal fungus *Ganoderma lingzhi*. *J Fungi*. (2022) 8:1257. doi: 10.3390/jof8121257
- Ahmad MF. *Ganoderma lucidum*: persuasive biologically active constituents and their health endorsement. *Biomed Pharmacother*. (2018) 107:507–19. doi: 10.1016/j.biopha.2018.08.036
- Chaturvedi VK, Agarwal S, Gupta KK, Ramteke PW, Singh MP. Medicinal mushroom: boon for therapeutic applications. *3 Biotech*. (2018) 8:334. doi: 10.1007/s13205-018-1358-0
- Xie C, Yan S, Zhang Z, Gong W, Zhu Z, Zhou Y, et al. Mapping the metabolic signatures of fermentation broth, mycelium, fruiting body and spores powder from *Ganoderma lucidum* by untargeted metabolomics. *LWT*. (2020) 129:109494. doi: 10.1016/j.lwt.2020.109494
- Johnson BM, Doonan BP, Radwan FF, Haque A. Ganoderic acid DM: an alternative agent for the treatment of advanced prostate cancer. *Open Prostate Cancer J*. (2010) 3:78–85. doi: 10.2174/1876822901003010078
- Cör Andrejč D, Knez Ž, Knez Marevci M. Antioxidant, antibacterial, antitumor, antifungal, antiviral, anti-inflammatory, and neuro-protective activity of *Ganoderma lucidum*: an overview. *Front Pharmacol*. (2022) 13:934982. doi: 10.3389/fphar.2022.934982
- Henao SLD, Urrego SA, Cano AM, Higuera EA. Randomized clinical trial for the evaluation of immune modulation by yogurt enriched with β -glucans from Lingzhi or Reishi medicinal mushroom, *Ganoderma lucidum* (Agaricomycetes), in children from Medellin, Colombia. *Int J Med Mushrooms*. (2018) 20:705–16. doi: 10.1615/intjmedmushrooms.2018026986
- Liu Y, Lai G, Guo Y, Tang X, Shuai O, Xie Y, et al. Protective effect of *Ganoderma lucidum* spore extract in trimethylamine-N-oxide-induced cardiac dysfunction in rats. *J Food Sci*. (2021) 86:546–62. doi: 10.1111/1750-3841.15575
- Xiao C, Wu Q, Xie Y, Tan J, Ding Y, Bai L. Hypoglycemic mechanisms of *Ganoderma lucidum* polysaccharides F31 in db/db mice via RNA-seq and iTRAQ. *Food Funct*. (2018) 9:6495–507. doi: 10.1039/c8fo01656a
- Sheikha A. FEL. (2022). Nutritional profile and health benefits of *Ganoderma lucidum* Lingzhi, Reishi, or Mannentake as functional foods: current scenario and future perspectives. *Foods* 11:1030. doi: 10.3390/foods11071030
- Fu C. Development status and application prospects of derivative products of *Ganoderma lucidum*. *Edible Med Mushrooms*. (2023) 31:255–61.

14. Jian Q, Ma C, Wang A, He Z, Ma C. Analysis and reflection on food safety standards of *Ganoderma lingzhi* (pilot) products. *Edible Med Mushrooms*. (2023) 31:246–54.
15. Chang ST. *Ganoderma lucidum* – a leader of edible and medicinal mushrooms. *Int Agri Trade*. (2004) 90:22–4.
16. Gauthier L, Atanasova-Penichon V, Chéreau S, Richard-Forget F. Metabolomics to decipher the chemical defense of cereals against fusarium graminearum and Deoxynivalenol accumulation. *Int J Mol Sci*. (2015) 16:24839–72. doi: 10.3390/ijms161024839
17. Tan W, Zhou J, Zhang B, Li X, Miao R, Huang Z, et al. Investigation into the current status of *Ganoderma* cultivation and analysis of the demand for cultivation technology. *Sichuan Agric Sci Technol*. (2018) 1:11–2.
18. Cao Y, Wu S, Dai Y. Species clarification of the prize medicinal *Ganoderma* mushroom Lingzhi. *Fungal Divers*. (2012) 56:49–62. doi: 10.1007/s13225-012-0178-5
19. Hapuarachchi K, Karunarathna S, Phengsintham P, Yang H, Kakumyan P, Hyde K, et al. *Ganodermataceae* (Polyporales): diversity in greater Mekong subregion countries (China, Laos, Myanmar, Thailand and Vietnam). *Mycosphere*. (2019) 10:221–309. doi: 10.5943/mycosphere/10/1/6
20. Luangharn T, Karunarathna SC, Dutta AK, Paloi S, Promputtha I, Hyde KD, et al. *Ganoderma* (Ganodermataceae, Basidiomycota) species from the greater Mekong subregion. *J Fungi*. (2021) 7:819. doi: 10.3390/jof7100819
21. Cong V. *Ganoderma* spp. – Biology, species and culture in Vietnam and in the Czech Republic. Dissertation's thesis. Brno: Mendel University in Brno (2010).
22. Dai Y. Polypores from Hainan Province(1). *J Fungal Res*. (2004) 2:53–7.
23. Li T, Hu H, Deng W, Wu S, Wang D, Tsering T. *Ganoderma leucocontextum*, a new member of the *G. lucidum* complex from southwestern China. *Mycoscience*. (2015) 56:81–5. doi: 10.1016/j.myc.2014.03.005
24. Li G, Xu Y, Pang Q, Liang X, Li H, Hu H, et al. Substitute cultivation techniques of *Ganoderma tsugae* in greenhouse. *Protect For Sci Technol*. (2018) 4:92–93+95. doi: 10.13601/j.issn.1005-5215.2018.04.037
25. Sun H, Gao L. Planting adaptability of different *Ganoderma lucidum* strains in Lasa. *Heilongjiang Agric Sci*. (2024) 1:46–51.
26. Galappaththi MCA, Patabendige NM, Premaratne BM, Hapuarachchi KK, Tibpromma S, Dai DQ, et al. A review of *Ganoderma* triterpenoids and their bioactivities. *Biomol Ther*. (2022) 13:24. doi: 10.3390/biom13010024
27. Lu J, He R, Sun P, Zhang F, Linhardt RJ, Zhang A. Molecular mechanisms of bioactive polysaccharides from *Ganoderma lucidum* (Lingzhi), a review. *Int J Biol Macromol*. (2020) 150:765–74. doi: 10.1016/j.ijbiomac.2020.02.035
28. Liu J, Wang H, Luo Q, Qiu S, He Z, Liu Z, et al. LingZhi oligopeptides amino acid sequence analysis and anticancer potency evaluation. *RSC Adv*. (2020) 10:8377–84. doi: 10.1039/c9ra10400c
29. Luo Q, Cao WW, Cheng YX. Alkaloids, sesquiterpenoids and hybrids of terpenoid with p-hydroxycinnamic acid from *Ganoderma sinensis* and their biological evaluation. *Phytochemistry*. (2022) 203:113379. doi: 10.1016/j.phytochem.2022.113379
30. Ellery SJ, Walker DW, Dickinson H. Creatine for women: a review of the relationship between creatine and the reproductive cycle and female-specific benefits of creatine therapy. *Amino Acids*. (2016) 48:1807–17. doi: 10.1007/s00726-016-2199-y
31. Rasmussen B, Gilbert E, Turki A, Madden K, Elango R. Determination of the safety of leucine supplementation in healthy elderly men. *Amino Acids*. (2016) 48:1707–16. doi: 10.1007/s00726-016-2241-0
32. Zhou X, Dong J, Zhuang C, Chen X, Chen R, Chen W, et al. Current situation and development trend of amino acid health products. *Biotic Resourc*. (2013) 35:69–72. doi: 10.14188/j.ajsh.2013.02.014
33. Jiang N, Zhu H, Liu W, Fan C, Jin F, Xiang X. Metabolite differences of polyphenols in different Litchi cultivars (*Litchi chinensis* Sonn.), based on extensive targeted metabolomics. *Molecules*. (2021) 26:1181. doi: 10.3390/molecules26041181
34. Naghshi S, Aune D, Beyene J, Mobarak S, Asadi M, Sadeghi O. Dietary intake and biomarkers of alpha linolenic acid and risk of all cause, cardiovascular, and cancer mortality: systematic review and dose-response meta-analysis of cohort studies. *BMJ (Clinical Research Ed)*. (2021) 375:n2213. doi: 10.1136/bmj.n2213
35. Yang Q, Cao W, Zhou X, Cao W, Xie Y, Wang S. Anti-thrombotic effects of α -linolenic acid isolated from *Zanthoxylum bungeanum* maxim seeds. *BMC Complement Altern Med*. (2014) 14:348. doi: 10.1186/1472-6882-14-348
36. Wu GS, Guo JJ, Bao JL, Li XW, Chen XP, Lu JJ, et al. Anti-cancer properties of triterpenoids isolated from *Ganoderma lucidum* – a review. *Expert Opin Investig Drugs*. (2013) 22:981–92. doi: 10.1517/13543784.2013.805202
37. Yan S, Wu Z, Xin G, Xiao X, Huang M, Meng X. Progresses on synthesis and anti-tumor pharmacological a ctivity of *Ganoderma lucidum* triterpenoids. *Life Sci Res*. (2017) 21:454–7. doi: 10.16605/j.cnki.1007-7847.2017.05.015
38. Chen Y, Lan P. Total syntheses and biological evaluation of the *Ganoderma lucidum* alkaloids Lucidimines B and C. *ACS Omega*. (2018) 3:3471–81. doi: 10.1021/acsomega.8b00295
39. Wang XL, Dou M, Luo Q, Cheng LZ, Yan YM, Li RT, et al. Racemic alkaloids from the fungus *Ganoderma cochlear*. *Fitoterapia*. (2017) 116:93–8. doi: 10.1016/j.fitote.2016.11.011
40. Gai YT, Shu Q, Chen CX, Lai YL, Li WJ, Peng L, et al. Anti-atherosclerosis role of N-oleoylethanolamine in CB2. *Acta Pharm Sin*. (2014) 49:316–21.
41. Wheel AJ, Alexander SP, Randall MD. Vasorelaxation to N-oleoylethanolamine in rat isolated arteries: mechanisms of action and modulation via cyclooxygenase activity. *Br J Pharmacol*. (2010) 160:701–11. doi: 10.1111/j.1476-5381.2010.00770.x
42. Xu X, Guo H, Jing Z, Yang L, Chen C, Peng L, et al. N-Oleoylethanolamine reduces inflammatory cytokines and adhesion molecules in TNF- α -induced human umbilical vein endothelial cells by activating CB2 and PPAR- α . *J Cardiovasc Pharmacol*. (2016) 68:280–91. doi: 10.1097/FJC.0000000000000413
43. Ferreira GC, McKenna MC. L-carnitine and acetyl-L-carnitine roles and neuroprotection in developing brain. *Neurochem Res*. (2017) 42:1661–75. doi: 10.1007/s11064-017-2288-7
44. Martí-Carvajal AJ, Gluud C, Arevalo-Rodriguez I, Martí-Amarista CE. Acetyl-L-carnitine for patients with hepatic encephalopathy. *Cochrane Database Syst Rev*. (2019) 2019:CD011451. doi: 10.1002/14651858.CD011451.pub2
45. Traina G. The neurobiology of acetyl-L-carnitine. *Front Biosci*. (2016) 21:1314–29. doi: 10.2741/4459
46. Kotagale NR, Taksande BG, Inamdar NN. Neuroprotective offerings by agmatine. *Neurotoxicology*. (2019) 73:228–45. doi: 10.1016/j.neuro.2019.05.001
47. Uzbay TI. The pharmacological importance of agmatine in the brain. *Neurosci Biobehav Rev*. (2012) 36:502–19. doi: 10.1016/j.neubiorev.2011.08.006
48. Gao P. *The technology research on the extraction of Lucidum adenosine and the culture of Lucidum mycelium with tea residues*. Master's thesis. Fujian: Fujian Agriculture and Forestry University (2009).
49. Li H, Du Y, Ji H, Yang Y, Xu C, Li Q, et al. Adenosine-rich extract of *Ganoderma lucidum*: a safe and effective lipid-lowering substance. *iScience*. (2022) 25:105214. doi: 10.1016/j.isci.2022.105214
50. Wen Z, Liu L. Determination of adenosine in *Ganoderma lucidum* oral liquid by HPLC. *J North Pharmacy*. (2019) 16:1–2.
51. Xi G. Determination of uridine and adenosine content of *Ganoderma lucidum* extract by HPLC. *World Chin Med*. (2014) 44:807. doi: 10.1016/j.jpbpa.2007.03.012
52. Suita K, Fujita T, Cai W, Hidaka Y, Jin H, Prajapati R, et al. Vidarabine, an anti-herpesvirus agent, prevents catecholamine-induced arrhythmias without adverse effect on heart function in mice. *Pflugers Archiv Eur J Physiol*. (2018) 470:923–35. doi: 10.1007/s00424-018-2121-4
53. Davinelli S, Chiosi F, Di Marco R, Costagliola C, Scapagnini G. Cytoprotective effects of Citicoline and Homotaurine against glutamate and high glucose neurotoxicity in primary cultured retinal cells. *Oxidative Med Cell Longev*. (2017) 2017:2825703. doi: 10.1155/2017/2825703
54. Karpova MN, Zin'kovskii KA, Kuznetsova LV, Klishina NV. Increase of the seizure threshold in C57BL/6 mice after citicoline administration. *Bull Exp Biol Med*. (2015) 158:315–7. doi: 10.1007/s10517-015-2750-y
55. Gomes AP, Price NL, Ling AJ, Moslehi JJ, Montgomery MK, Rajman L, et al. Declining NAD(+) induces a pseudohypoxic state disrupting nuclear-mitochondrial communication during aging. *Cell*. (2013) 155:1624–38. doi: 10.1016/j.cell.2013.11.037
56. Tsubota K. The first human clinical study for NMN has started in Japan. *NPJ Aging Mechanisms Disease*. (2016) 2:16021. doi: 10.1038/npjamd.2016.21
57. Pobbati AV, Hong W. A combat with the YAP/TAZ-TEAD oncoproteins for cancer therapy. *Theranostics*. (2020) 10:3622–35. doi: 10.7150/thno.40889
58. Su CC, Hsieh KL, Liu PL, Yeh HC, Huang SP, Fang SH, et al. AICAR induces apoptosis and inhibits migration and invasion in prostate cancer cells through an AMPK/mTOR-dependent pathway. *Int J Mol Sci*. (2019) 20:1647. doi: 10.3390/ijms20071647
59. Cilerdžić J, Vukojević J, Stajić M, Stanojković T, Glamočlija J. Biological activity of *Ganoderma lucidum* basidiocarps cultivated on alternative and commercial substrate. *J Ethnopharmacol*. (2014) 155:312–9. doi: 10.1016/j.jep.2014.05.036
60. Dong F, Zhong J, Li P. Preparation and cytotoxic activity of total flavonoids extract from *Ganoderma lucidum*. *Strait Pharmaceut J*. (2022) 25:53–63. doi: 10.1615/IntJMedMushrooms.2023050232
61. Li C. Extraction and determination of ganoderic acid and total flavonoids in the wild and planted *Ganoderma lucidum*. *J Yanbian Univ*. (2013) 39:269–72. doi: 10.16379/j.cnki.issn.1004-4353.2013.04.016
62. Park MH, Kim M. Antioxidant and anti-inflammatory activity and cytotoxicity of ethanol extracts from *Rhynchosia nulubilis* cultivated with *Ganoderma lucidum* mycelium. *Prevent Nutr Food Sci*. (2018) 23:326–34. doi: 10.3746/pnf.2018.23.4.326
63. Arnaiz-Cot JJ, Cleemann L, Morad M. Xanthohumol modulates calcium signaling in rat ventricular myocytes: possible antiarrhythmic properties. *J Pharmacol Exp Ther*. (2017) 360:239–48. doi: 10.1124/jpet.116.236588
64. Chen PH, Chang CK, Shih CM, Cheng CH, Lin CW, Lee CC, et al. The miR-204-3p-targeted IGFBP2 pathway is involved in xanthohumol-induced glioma cell apoptotic death. *Neuropharmacology*. (2016) 110:362–75. doi: 10.1016/j.neuropharm.2016.07.038
65. Li W, Sun YN, Yan XT, Yang SY, Kim S, Lee YM, et al. Flavonoids from astragalus membranaceus and their inhibitory effects on LPS-stimulated pro-inflammatory cytokine production in bone marrow-derived dendritic cells. *Arch Pharm Res*. (2014) 37:186–92. doi: 10.1007/s12272-013-0174-7

66. Lin Y, Tang Q, Chu M, Gu M, Zhu J, Ghenijian O, et al. Research progress on function, production and food application of γ -aminobutyric acid. *China Condiment*. (2021) 6:173–9.
67. Yamatsu A, Yamashita Y, Pandharipande T, Maru I, Kim M. Effect of oral γ -aminobutyric acid (GABA) administration on sleep and its absorption in humans. *Food Sci Biotechnol*. (2016) 25:547–51. doi: 10.1007/s10068-016-0076-9
68. Yang S, Lu Z, Lu F, Bie X. Research Progress on microbial glutamate decarboxylase. *Food Sci*. (2005) 9:528–33.
69. Lee MY, Hung WP, Tsai SH. Improvement of shikimic acid production in *Escherichia coli* with growth phase-dependent regulation in the biosynthetic pathway from glycerol. *World J Microbiol Biotechnol*. (2017) 33:25. doi: 10.1007/s11274-016-2192-3
70. Choi J, Jiang X, Jeong JB, Lee SH. Anticancer activity of protocatechualdehyde in human breast cancer cells. *J Med Food*. (2014) 17:842–8. doi: 10.1089/jmf.2013.0159
71. Kant K, Walia M, Agnihotri VK, Pathania V, Singh B. Evaluation of antioxidant activity of *Picrorhiza kurroa* (leaves) extracts. *Indian J Pharm Sci*. (2013) 75:324–9. doi: 10.4103/0250-474X.117438
72. Li S, Yu Y, Chen J, Guo B, Yang L, Ding W. Evaluation of the antibacterial effects and mechanism of action of protocatechualdehyde against *Ralstonia solanacearum*. *Molecules*. (2016) 21:754. doi: 10.3390/molecules21060754
73. Umar MI, Asmawi MZ, Sadikun A, Atangwho IJ, Yam MF, Altaf R, et al. Bioactivity-guided isolation of ethyl-p-methoxycinnamate, an anti-inflammatory constituent, from *Kaempferia galanga* L extracts. *Molecules*. (2012) 17:8720–34. doi: 10.3390/molecules17078720
74. Raji L, Tetteh A, Amin R. Role of c-Src in carcinogenesis and drug resistance. *Cancers*. (2023) 16:32–2. doi: 10.3390/cancers16010032
75. Roskoski R. Src protein–tyrosine kinase structure and regulation. *Biochem Biophys Res Commun*. (2004) 324:1155–64. doi: 10.1016/j.bbrc.2004.09.171
76. Balkwill F. Tumour necrosis factor and cancer. *Nat Rev Cancer*. (2009) 9:361–71. doi: 10.1038/nrc2628
77. Holbrook J, Lara-Reyna S, Jarosz-Griffiths H, McDermott MF. Tumour necrosis factor signalling in health and disease. *F1000Research* 8, F1000 faculty Rev-111. *F1000Research*. (2019) 1:17023. doi: 10.12688/f1000research.17023.1
78. George B, Gui B, Raguraman R, Paul AM, Nakshatri H, Pillai MR, et al. AKT1 transcriptomic landscape in breast cancer cells. *Cells*. (2022) 11:2290. doi: 10.3390/cells11152290
79. Shi Z, Yuan H, Cao L, Lin Y. AKT1 participates in ferroptosis vulnerability by driving autophagic degradation of FTH1 in cisplatin-resistant ovarian cancer. *Biochem Cell Biol*. (2023) 101:422–31. doi: 10.1139/bcb-2022-0361
80. Olivier M, Hollstein M, Hainaut P. TP53 mutations in human cancers: origins, consequences, and clinical use. *Cold Spring Harb Perspect Biol*. (2009) 2:a001008. doi: 10.1101/cshperspect.a001008
81. Wang Z, Strasser A, Kelly GL. Should mutant TP53 be targeted for cancer therapy? *Cell Death Differentiation*. (2022) 29:911–20. doi: 10.1038/s41418-022-00962-9
82. Taguchi K, Giam Chuang VT, Maruyama T, Otagiri M. Pharmaceutical aspects of the recombinant human serum albumin dimer: structural characteristics, biological properties, and medical applications. *J Pharm Sci*. (2012) 101:3033–46. doi: 10.1002/jps.23181
83. Fu X, Yang Y, Zhang D. Molecular mechanism of albumin in suppressing invasion and metastasis of hepatocellular carcinoma. *Liver Int*. (2021) 42:696–709. doi: 10.1111/liv.15115
84. Huang Y, Liu R. The toxicity and polymorphism of β -amyloid oligomers. *Int J Mol Sci*. (2020) 21:4477. doi: 10.3390/ijms21124477
85. Itoh S, Okumura H. Promotion and inhibition of amyloid- β peptide aggregation: molecular dynamics studies. *Int J Mol Sci*. (2021) 22:1859. doi: 10.3390/ijms22041859
86. Lai CS, Yu MS, Yuen WH, So KF, Zee SY, Chang RC. Antagonizing β -amyloid peptide neurotoxicity of the anti-aging fungus *Ganoderma lucidum*. *Brain Res*. (2008) 1190:215–24. doi: 10.1016/j.brainres.2007.10.103
87. Luz DA, Pinheiro AM, Fontes-Júnior EA, Ferraz S. Neuroprotective, neurogenic, and anticholinergic evidence of *Ganoderma lucidum* cognitive effects: crucial knowledge is still lacking. *Med Res Rev*. (2023) 43:1504–36. doi: 10.1002/med.21957
88. Sanajou D, Ghorbani Haghjo A, Argani H, Aslani S. AGE-RAGE axis blockade in diabetic nephropathy: current status and future directions. *Eur J Pharmacol*. (2018) 833:158–64. doi: 10.1016/j.ejphar.2018.06.001
89. Chen J, Chen Y, Shu A, Lu J, Du Q, Yang Y, et al. *Radix Rehmanniae* and *Corni Fructus* against diabetic nephropathy via AGE-RAGE signaling pathway. *J Diabetes Res*. (2020) 2020:1–15. doi: 10.1155/2020/8358102



OPEN ACCESS

EDITED BY

Marco Iammarino,
Experimental Zooprophyllactic Institute of
Puglia and Basilicata (IZSPB), Italy

REVIEWED BY

Farzad Rassaei,
Islamic Azad University, Isfahan, Iran
Antonio Bevilacqua,
University of Foggia, Italy

*CORRESPONDENCE

Tianyuan Li
✉ tianyuan198712@163.com

RECEIVED 14 November 2023

ACCEPTED 12 March 2024

PUBLISHED 04 April 2024

CITATION

Guo K, Zhao Y, Zhang Y, Yang J, Chu Z,
Zhang Q, Xiao W, Huang B and Li T (2024)
Effects of wollastonite and phosphate
treatments on cadmium bioaccessibility in
pak choi (*Brassica rapa* L. ssp. *chinensis*)
grown in contaminated soils.
Front. Nutr. 11:1337996.
doi: 10.3389/fnut.2024.1337996

COPYRIGHT

© 2024 Guo, Zhao, Zhang, Yang, Chu, Zhang,
Xiao, Huang and Li. This is an open-access
article distributed under the terms of the
[Creative Commons Attribution License](#)
(CC BY). The use, distribution or reproduction
in other forums is permitted, provided the
original author(s) and the copyright owner(s)
are credited and that the original publication
in this journal is cited, in accordance with
accepted academic practice. No use,
distribution or reproduction is permitted
which does not comply with these terms.

Effects of wollastonite and phosphate treatments on cadmium bioaccessibility in pak choi (*Brassica rapa* L. ssp. *chinensis*) grown in contaminated soils

Kexin Guo¹, Yuehua Zhao², Yang Zhang³, Jinbo Yang²,
Zhiyuan Chu², Qiang Zhang¹, Wenwei Xiao⁴, Bin Huang⁵ and
Tianyuan Li^{1*}

¹Shandong Provincial Key Laboratory of Applied Microbiology, Ecology Institute, Qilu University of Technology (Shandong Academy of Sciences), Ji'nan, China, ²The 7th Institute of Geology & Mineral Exploration of Shandong Province, Linyi, China, ³Weifang Binhai Ecological Environment Monitoring Center, Weifang, China, ⁴Guangzhou Hexin Instrument Co., Ltd., Guangzhou, China, ⁵Zhongchuang Guoke Scientific Instrument (Shandong) Co., Ji'nan, China

Cadmium (Cd) contamination of soil can strongly impact human health through the food chain due to uptake by crop plants. Inorganic immobilizing agents such as silicates and phosphates have been shown to effectively reduce Cd transfer from the soil to cereal crops. However, the effects of such agents on total Cd and its bioaccessibility in leafy vegetables are not yet known. Pak choi (*Brassica rapa* L. ssp. *chinensis*) was here selected as a representative leafy vegetable to be tested in pots to reveal the effects of silicate–phosphate amendments on soil Cd chemical fractions, total plant Cd levels, and plant bioaccessibility. The collected Cd contaminated soil was mixed with control soil at 1:0, 1:1, 1:4, 0:1 with a view to Cd high/moderate/mild/control soil samples. Three heavy metal-immobilizing agents: wollastonite (W), potassium tripolyphosphate (KTPP), and sodium hexametaphosphate (SHMP) were added to the soil in order to get four different treatment groups, i.e., control (CK), application of wollastonite alone (W), wollastonite co-applied with KTPP (WKTPP), application of wollastonite co-applied with SHMP (WSHMP) for remediation of soils with different levels of Cd contamination. All three treatments increased the effective bio-Cd concentration in the soils with varying levels of contamination, except for W under moderate and heavy Cd contamination. The total Cd concentration in pak choi plants grown in mildly Cd-contaminated soil was elevated by 86.2% after WKTPP treatment compared to the control treatment could function as a phytoremediation aid for mildly Cd-contaminated soil. Using an *in vitro* digestion method (physiologically based extraction test) combined with transmission electron microscopy, silicate and phosphorus agents were found to reduce the bioaccessibility of Cd in pak choi by up to 66.13% with WSHMP treatment. Application of silicate alone reduced soil bio-Cd concentration through the formation of insoluble complexes and silanol groups with Cd, but the addition of phosphate may have facilitated Cd translocation into pak choi by first co-precipitating with Ca in wollastonite while simultaneously altering soil pH. Meanwhile, wollastonite and phosphate treatments may cause Cd to be firmly enclosed in the cell wall in an insoluble form, reducing its translocation to edible parts and decreasing the bioaccessibility of Cd in pak choi. This study

contributes to the mitigation of Cd bioaccessibility in pak choi by reducing soil Cd concentration through *in situ* remediation and will help us to extend the effects of wollastonite and phosphate on Cd bioaccessibility to other common vegetables. Therefore, this study thus reveals effective strategies for the remediation of soil Cd and the reduction of Cd bioaccessibility in crops based on two indicators: total Cd and Cd bioaccessibility. Our findings contribute to the development of methods for safer cultivation of commonly consumed leafy vegetables and for soil remediation.

KEYWORDS

Cd immobilization, bioaccessibility, leafy vegetables, wollastonite, cell ultrastructural

1 Introduction

Soil contamination with cadmium (Cd) has become a major environmental and public health challenge in countries such as China, Thailand, and India (1, 2). Cd readily migrates from the soil into crop plants, thus entering the food chain and posing a risk to human health. For example, Chinese cabbage plants grown in a specific region of China reportedly have maximum Cd contents of 0.09 mg/kg, exceeding the standard limit by 180% (3). Cd has also been found to exceed the standard by 53.85% in vegetables from Yunnan Province (4). Thus, effective methods are urgently needed to control Cd contamination to limit Cd transfer through the food chain.

The health risks associated with heavy metal elements in crops can be reduced through two key strategies. The first is to decrease the total concentration of heavy metals taken up by crop plants. In prior studies, immobilizing agents have proven effective in reducing heavy metal uptake from the soil (5, 6). Common heavy metal immobilizing agents include organic materials, such as compost and biochar; inorganic materials, including lime, phosphate, and silicate; and chemical chelating agents, such as ethylenediaminetetraacetic acid (EDTA) and diethylenetriaminepentaacetic acid (DTPA) (7). For example, the addition of bagasse biochar to paddy soil significantly reduced the DTPA extractable fraction of Cd and reduced the Cd content of rice plants (8). Another study found that biochar reduced Cd accumulation in pak choi (9). Similarly, straw composting resulted in a significant 69% reduction in Cd content in pak choi, as well as a reduced Cd transfer factor from soil to pak choi leaves (10). One promising inorganic immobilizing material is a calcium silicate material, wollastonite. This compound combines with heavy metals to form Si-Cd precipitates, which are less readily absorbed by plants than free Cd. Several studies have demonstrated the efficacy of wollastonite in reducing heavy metal mobility and toxicity (11–14). Phosphate is another common heavy metal immobilizing treatment for soils. The addition of phosphorus reduces the concentration of Cd (water-soluble and exchangeable) released into the soil solution in the soil, reducing the migration of its Cd to plants (15). Field experiments have demonstrated that it effectively reduces Cd concentrations in rice (16). In addition, co-application of silicate and potassium dihydrogen phosphate enhances soil adsorption of Cd, minimizing Cd uptake by altering the proportions of competing cation fractions in the soil. This has been shown to reduce Cd concentrations in amaranth and Chinese cabbage by up to 74% (17). Recently, Wang et al. (18) found that a combined application of silicate and phosphate decreases the

exchangeable Cd concentration in the soil by altering the soil pH or causing direct Cd adsorption to the surfaces of silicate minerals. Such prior studies have identified strong candidates for Cd remediation via immobilization in the soil. However, most of the current studies are on the effect of single immobilizers on Cd in vegetables or other crops, and the effect of wollastonite and phosphate on Cd in leafy vegetables, especially pak choi, is not yet known, and further studies are needed to clarify the potential mechanisms of the effect.

The second method of mitigating health risks associated with heavy metal contamination is to reduce their bioaccessibility in plants. Bioaccessibility refers to the proportion or amount of a compound in a food product that can be digested and extracted in the gastrointestinal environment. In the context of heavy metals, the total contaminant mass within a crop may not accurately reflect the mass that can be absorbed by the human body (19). Research has indicated that bioaccessibility is a more accurate reflection of human absorption and utilization of heavy metals than total heavy metal concentrations are. Thus, it is important to understand heavy metal bioaccessibility in crops. For example, Wang et al. (20) found that Cd bioaccessibility in peppermint can reach 85.8%, posing a significant health risk to humans. Similarly, Hu et al. (21) found that Cd bioaccessibility in leafy vegetables from market in Hong Kong is 71%, making it a major health risk for residents. Prior studies have indicated that Cd contamination poses a major health risk due to its generally high bioaccessibility. Strategies for minimizing bioaccessibility Cd are thus urgently needed.

In addition to preventing plant uptake of heavy metals, immobilizing agents may also impact bioaccessibility. For example, biochar can transform the exchangeable and carbonate-bound fractions of Cd into organic-bound and residual fractions. In wheat and corn, this reduces the bioaccessible Cd content by 12.7–26.0% and 13.1–20.5%, respectively (22). In celery production, a combined application of hydroxyapatite with slaked lime or hydroxyapatite with zeolite produce synergistic effects, significantly increasing soil pH and reducing Cd bioaccessibility by 54.8–79.0% (23). These types of immobilizing agents may therefore reduce heavy metal bioaccessibility in other crop plants as well. However, to date, little is known about the bioaccessibility of Cd in pak choi harvested from agricultural soils remediated by *in situ* soil immobilization of Cd and the associated risks associated with its consumption. The beneficial effects of *in situ* soil Cd immobilization in reducing Cd accumulation in other crops such as rice have been well documented (24, 25). However, its effect on the bioaccessibility of Cd in vegetables has not received sufficient attention.

Bioaccessibility content of heavy metals in agricultural products is a key indicator for assessing health risks. And chard is more likely to absorb Cd when grown on contaminated soils, leading to an increase in potential health risk (26). The addition of passivator will immobilize Cd more in the soil and reduce its migration to pak choi, meanwhile, wollastonite has non-specific immobilization and can immobilize some trace elements in the soil, and the addition of phosphorus will also change the soil nutrients. Passivator combinations of wollastonite and phosphate have been used to reduce the risk of Cd exposure in paddy and rice, however, their effect on the bioaccessibility of Cd in vegetables remains unclear. Therefore, there is a need to use a combination of wollastonite and phosphate to reduce the total amount and bioaccessibility of cadmium in the edible parts of aubergines. Prior studies of Cd bioaccessibility have primarily focused on the effects of immobilizing agents on total heavy metal concentrations in crops such as grains; research on the bioaccessibility of Cd among leafy vegetables grown in contaminated soils is extremely scarce. However, recent dietary trends have emphasized consumption of leafy green vegetables over grains, increasing the overall health risks posed by heavy metal contamination of leafy vegetables. Thus, there is a pressing need to assess Cd bioaccessibility in such plants. To address this goal, the present study had three key aims: (1) to investigate the effects of a combination of silicate and different phosphates on total Cd concentrations in the leafy green vegetable pak choi (*Brassica rapa* L. ssp. *chinensis*); (2) to assess changes in Cd chemical fractions in the soil after application of silicate and phosphates; and (3) to study the effects of a silicate–phosphate combination on Cd bioaccessibility and toxicity in pak choi. This study was designed to aid in determining appropriate strategies for controlling Cd exposure in specific populations, reducing the health risks posed by heavy metal exposure in the context of modern dietary patterns.

2 Materials and methods

2.1 Soil collection

Soil samples contaminated with Cd were collected from 0 to 20 cm topsoil of a barren land outside a chemical industrial park in Linyi City, Shandong Province, China (Supplementary Figure S1). Control soil samples were simultaneously collected ~5 km away from the industrial park. The basic properties of the experimental soil were analyzed before experimenting. Soil pH and conductivity were measured with a pH meter and a conductivity meter at a ratio of 1:2.5 soil to distilled water. Soil organic matter was measured by potassium dichromate method by oxidising soil organic carbon with excess potassium dichromate-sulphuric acid solution under heated conditions and excess potassium dichromate was titrated with ferrous sulphate standard solution. The dry matter content was obtained by drying and weighing the difference, and the basic physio-chemical properties of the collected soils were as follows (27). The pH of the Cd-contaminated soil was 7.297, with 1.94% organic matter and 97.0% dry matter content. The pH of the control soil was 7.316, with 1.99% organic matter and 97.1% dry matter content (Table 1).

TABLE 1 Physical and chemical properties of soil before and after treatment.

Properties	Values	
	Before treatment	After treatment
pH	7.29–7.32	8.15–8.65
Organic matter content (%)	1.99	1.91
Dry matter content (%)	97.0	97.6
Cation exchange capacity (CEC, cmol kg ⁻¹)	13.57	13.16
Conductivity (μs cm ⁻¹)	128.5	126.4
Texture	Brown loam	

2.2 Determination of soil Cd concentration

For each sample, 15 mL of aqua regia was transferred to a conical 100 mL flask that had been infiltrated by aqua regia vapors. An additional 6 mL of aqua regia solution was added and a glass funnel was placed at the top. Each flask was heated on an electric hot plate to maintain the aqua regia at a slight boiling state for 2 h. Then, samples were cooled to room temperature and allowed to settle. The extract was then slowly filtered through quantitative filter paper into a 50 mL volumetric flask. The glass funnel, conical flask, and residue were rinsed with a small amount of nitric acid solution at least three times, with the reinstate collected in the volumetric flask. After filtration, the inductively coupled plasma mass spectrometry (ICP-MS 1600, Hexin Mass Spectrometry, China) was used to determine Cd concentrations in the digested sample solutions.

2.3 Pot-planting experiment

The Cd-contaminated and control soils were mixed at ratios of 1:0, 1:1, 1:4, and 0:1 to yield soil samples with a range of Cd contamination levels: heavy contamination (6.28 mg/kg), moderate contamination (3.21 mg/kg), mild contamination (1.36 mg/kg), and uncontaminated soil (0.14 mg/kg). Several compounds were then tested to assess the Cd-immobilizing effects in each soil type. Wollastonite (a low cost calcium silicate mineral) was used as the main immobilizing agent of the crop and two different phosphate crops, sodium tripolyphosphate (KTPP) and sodium hexametaphosphate (SHMP), were selected to enhance the immobilizing effect of Cd based on the results of Matusik et al. and Thawornchaisit and Polprasert (28, 29). The silica fume and phosphate salt dosages were 400 mg Si kg⁻¹ soil and 0.4% P₂O₅ kg⁻¹ soil, respectively. The treatments consisted of a control check (CK), wollastonite (W), wollastonite with potassium triphosphate (WKTPP), and wollastonite with sodium hexametaphosphate (WSHMP). Each treatment was applied to each of the four soil types with differing Cd contamination levels in biological triplicate. After thoroughly mixing wollastonite and phosphate with the soil samples were incubated for 14 d soil moisture was maintained at ~70% of the field capacity. Treated soil samples were air-dried, ground, and sieved through 2 mm mesh. Each pot was filled with 0.75 kg of soil. Fertilizers were applied to all pots in the forms of urea and KCl to final concentrations of 0.2 g N and 0.15 g K per kg of soil, respectively. In the blank and W treatment groups, Na₂HPO₄ was added to a final concentration of 0.4% P₂O₅ per kg of soil.

Pak choi seeds were purchased from Sanjiang Agriculture (Zhejiang Province, China) (30) and three to four seeds were planted in each pot. After the seedlings grew four true leaves, they were thinned to one plant per pot, and all potted plants were placed in a 24 h light incubator, with the temperature maintained at 23°C and humidity at about 60%. After 45 d, the aboveground plant portions were harvested rinsed with tap water, then thoroughly washed with ultrapure water. After removing excess surface moisture, samples were weighed to determine the fresh weight. A portion of each sample was finely chopped with a ceramic knife, mixed well, and stored in a refrigerator at 4°C prior to additional analyses. The remaining portions were dried in an oven at 70°C to constant weight for further analysis.

2.4 Determination of soil Cd chemical fractions

Nowadays, methods such as BCR and Tessier are mostly used for the determination of heavy metal forms, and in this study, soil samples were analyzed using an improvement upon the Tessier sequential extraction method (31), the Tessier seven-step extraction method (32). Elements were divided into different forms: water-soluble (F1), ion exchangeable (F2), carbonate-bound (F3), humic acid-bound (F4), iron-manganese oxide-bound (F5), strong organic-bound (F6), and residual forms (F7). F1, F2, and F3 represent bioaccessible Cd (bio-Cd), which has better mobility and migration in soil and can be bioaccessible by plants, whereas F4–F7 represent inert Cd (inert-Cd), which is not easy to migrate in soil and is more stable. The specific analysis method is shown in Table 2.

2.5 Determination of Cd concentrations in pak choi

Dry samples (0.5 g) were placed in tetrafluoroethylene inner jars. After adding 5 mL of nitric acid, samples were soaked overnight, then 2–3 mL of hydrogen peroxide solution was added. After adding 2–3 mL of 30% hydrogen peroxide solution, the inner lid was covered, the stainless-steel jacket was tightened, and jars were incubated in a drying oven at 120–160°C for 4–6 h. Samples were naturally cooled to room temperature in the incubator, then opened and heated until nearly dry. The digestive solution was washed into a 25 mL volumetric flask before the inner jar and inner lid were washed with a small amount of 1% nitric acid solution three times. The rinsates were combined in a volumetric

flask and fixed to 25 mL scale with 1% nitric acid solution. Samples were mixed; at the same time, repeat the above procedure without adding samples as a blank control. The Cd contents in the digested sample solutions were then determined with an ICP-MS instrument (ICP-MS 1600, Hexi Mass Spectrometry, China). The main instrumental operating parameters for the determination of the samples are shown in Table 3. After ignition of the plasma, the ICP-MS was preheated for 30 min, and the sensitivity, oxide and double charge of the instrument were tuned with 1.0 µg/L tuning solution, and the relative standard deviation of the signal intensity of the elements contained in the tuning solution was less than or equal to 0.8% under the conditions that the sensitivity, oxide and double charge of the instrument met the requirements. The results showed that the precision RSD ranged from 0.5 to 12.3%; the recoveries of the certified standard samples ranged from 86.4 to 114.3%, and the limits of detection, precision and correctness were all in accordance with the standard determination requirements.

2.6 Determination of the Cd bioaccessibility in pak choi

Currently, PBET is used as an *in vitro* method to determine the bioaccessibility of Cd in the literature. Therefore, an improved method based on those described by experimental methods of Ruby et al. (33) and Fu et al. (34) was employed to determine the bioaccessibility of Cd in aboveground pak choi tissues using the Physiologically Based Extraction Test (PBET) method. In the simulated gastric digestion stage, 3 g of fresh sample was mixed with 30 mL of simulated gastric fluid containing 0.50 g/L sodium citrate, 0.50 g/L sodium malate, 0.42 mL/L lactic acid, 0.50 mL/L acetic acid, and 1.25 g/L gastric protease (pH adjusted to 1.50 using concentrated hydrochloric acid). The mixture was then rotated and oscillated at 4000 rpm and 37°C

TABLE 3 The major instrumental operation parameters for soil and food samples determination.

Instrumental operation parameters		Values
Radio frequency power of plasma		1,400 W
Depth of sampling		9.70 mm
Extraction voltage		−910 V
Gas flow rates	Carrier gas	0.80 L/min
	Dilution gas	0.30 L/min
	Collision gas	1.48 mL/min

TABLE 2 Tessier's seven-step sequential extraction method for Cd in soil.

Step	Fraction	Reagent(s)	Experimental conditions
I	Water-soluble	Distilled water	2.5 g soil sample reagents. Echocardiography: 30 min
II	Ionic bond	1 M magnesium chloride	Residual fraction +25 mL reagents. Echocardiography: 30 min
III	Carbonate	1 M NaAc	Residual fraction +25 mL reagents. Echocardiography: 1 h
IV	Humic acid-bound	0.1 M Na ₄ P ₂ O ₇	Residual fraction +50 mL reagents. Echocardiography: 40 min
V	Fe/Mn oxide bound	0.25 M NH ₂ OH•HCl–HCl	Residual fraction +50 mL reagents. Echocardiography: 1 h
VI	Strong organic	0.02 M HNO ₃ H ₂ O ₂ (pH 2)	Residual fraction +3 mL HNO ₃ +5 mL H ₂ O ₂ 83°C constant temperature: 1.5 h
		3.2 M NH ₄ Ac–HNO ₃	Residual fraction +2.5 mL NH ₄ Ac–HNO ₃ Set aside: 10 h Centrifugation: 20 min
VII	Residual	Ultrapure water	Residual fraction +20 mL reagents. Oscillate: 15 min

for 1 h. After centrifugation at 4000 rpm or 10 min, 5 mL of the supernatant was filtered and collected for further testing. In the simulated intestinal digestion stage, 5 mL of gastric fluid was added to the reaction solution to maintain a constant solid: liquid ratio. The pH of the digestion solution was adjusted to 7.0 with solid sodium bicarbonate (NaHCO_3). Bile salt solution was prepared by diluting 52.5 g/L porcine bile salt solution with 0.1 mol/L NaHCO_3 solution, then adding 15 mg of pancreatin. Each sample was combined with 1 mL of the bile salt solution, then the mixture was rotated and oscillated at 4000 rpm and 37°C for 4 h. After centrifugation at 4000 rpm for 10 min, the supernatant was collected and the precise volume recorded. The digestion solution of the small intestine phase was filtered through a 0.45 μm filter membrane, and the Cd content was determined by ICP-MS (ICP-MS 1600, Hexi Mass Spectrometry, China) together with the gastric digestion solution.

The bioaccessibility of cadmium was assessed during the gastric and intestinal digestion stages of cabbage samples. Equation (1) was used for calculation (35).

$$\text{BAC}(\%) = \frac{C1V1}{C2M} \times 100\% \quad (1)$$

where BAC is the percent bioaccessibility of Cd in aboveground plant tissue in the gastric or small intestinal stage; C1 is the Cd content in the reaction solution at that stage ($\mu\text{g}\cdot\text{mL}^{-1}$); V1 is the volume of the reaction solution at that stage (mL); C2 is the Cd content in the aboveground plant tissue ($\mu\text{g}\cdot\text{g}^{-1}$ DW); and M is the original mass of the sample used in the simulated digestion experiment (g).

2.7 Transmission electron microscopy

The second developed leaves were collected from pak choi plants grown for 35 d. Slices of 2 mm² in size were taken from the tops of the leaves in the subapical region (without veins or root tips). The slices were set for 12 h with 2.5% glutaraldehyde (v/v) in 0.1 M phosphate-buffered saline (PBS) at pH 7.0. After washing twice in PBS, samples were post-fixed in 1% (v/w) OsO_4 for 2 h, then washed three times with 0.1 M PBS 0.1 M for 10 min each. The samples were then dehydrated in an ethanol gradient (50, 60, 70, 80, 90, 95, and 100%) with 15–20 min between solutions before washing for 20 min in absolute acetone. Prepared samples were fixed in Spurr's resin overnight, then heated at 70°C for 9 h. Ultrathin (80 nm) sections of the samples were set up under an accelerating voltage of 60.0 kV, mounted on a copper grid, and observed under TEM (Hitachi-7800). The magnification of 5,000 and 30,000 was chosen to observe the overall cellular and subcellular changes. Images that best represented the ultrastructural cell states were selected for analysis.

2.8 Transfer factor

The TF of Cd from the soil to the edible portions of pak choi was defined as the ratio of the Cd concentration in the edible parts of the vegetable (in $\text{mg}\cdot\text{kg}^{-1}$) over the total cadmium concentration in the planting soil ($\text{mg}\cdot\text{kg}^{-1}$) (36, 37) and was calculated using Equation 2.

$$\text{TF} = C_{\text{plant}}/C_{\text{soil}} \quad (2)$$

Where C_{plant} and C_{soil} represents the Cd concentration in plants and soils on dry weight basis, respectively.

2.9 Statistical analysis

SPSS (SPSS Statistics 25) was used for statistical analysis. Data were analyzed by one-way ANOVA with Duncan's New Multiple Range Test to determine significant differences between different. Pearson's correlation test was used to establish the correlation between Cd bioavailability and total Cd in *Brassica napus* and between total pak choi Cd and total soil Cd at a significant level of $p < 0.05$ (two-tailed). Cd concentration and chemical form in soil and pak choi are given as means and standard errors, $p < 0.05$, and were analyzed by one-way ANOVA and post-hoc Tukey's honestly significant difference test because of the grouped observed variables. All of the data presented are means \pm SE of three replicates. All graphs were plotted using Origin 2022.

3 Results and discussion

3.1 Cd soil chemical fractions

We first assessed the impacts of three immobilizing treatments, W, WKTPP and WSHMP on soil properties. All three treatments increased the soil pH from 7.29–7.32 to 8.15–8.65. Furthermore, the bioaccessible Cd fractions (bio-Cd) (F1–F3) were more abundant than inert Cd fractions (inert-Cd) (F4–F8) after each treatment (Figure 1). In mildly Cd-contaminated soil, all three treatments reduced the proportion of inert-Cd; the proportion of bio-Cd in the WKTPP treatment group reached 76.8%, which was 20.48% higher than in the untreated control soil. In moderately Cd-contaminated soil, inert-Cd was reduced by WKTPP and WSHMP treatment, in which the bio-Cd proportions reached 76.7 and 78.5%, respectively. However, W treatment reduced the bio-Cd percentage from 75 to 70.9%. In highly Cd-contaminated soil, alterations in inert-Cd and bio-Cd contents were consistent with those in moderately Cd-contaminated soil, with WKTPP and WSHMP treatment increasing the bio-Cd proportions by 3.2 and 4.5%, respectively.

In general, application of W alone reduced bio-Cd levels in the tested soils, whereas combined wollastonite–phosphate applications increased bio-Cd concentrations. Soil Si has previously been shown to adsorb Cd to form silicate complexes. The resulting complexes have a limited capacity for ion exchange, limiting their solubility in soil water (38, 39). This is the reason for the decrease in bio-Cd in the soil under the W treatment alone in Figure 1.

Furthermore, the mineral form of Si has silanol (Si-OH) groups that can adsorb Cd, decreasing Cd mobility because it is kept in the stable Cd-Si-OH form (40). Unstable forms of Cd also bind to Si through oxygen bridges to create insoluble Fe-O-Si-Cd complexes (41). This is in line with the finding of Feng et al. that Si is able to transform heavy metal fractions in soil by producing Si complexes, thus reducing bioaccessible Cd (42). Phosphate alone can bind with Cd to form metal–phosphate precipitates, thus reducing bio-Cd content. However, wollastonite is Ca-based; in a simultaneous application of wollastonite with a phosphate, the phosphate will form precipitates with Ca (43), reducing binding of both compounds to soil

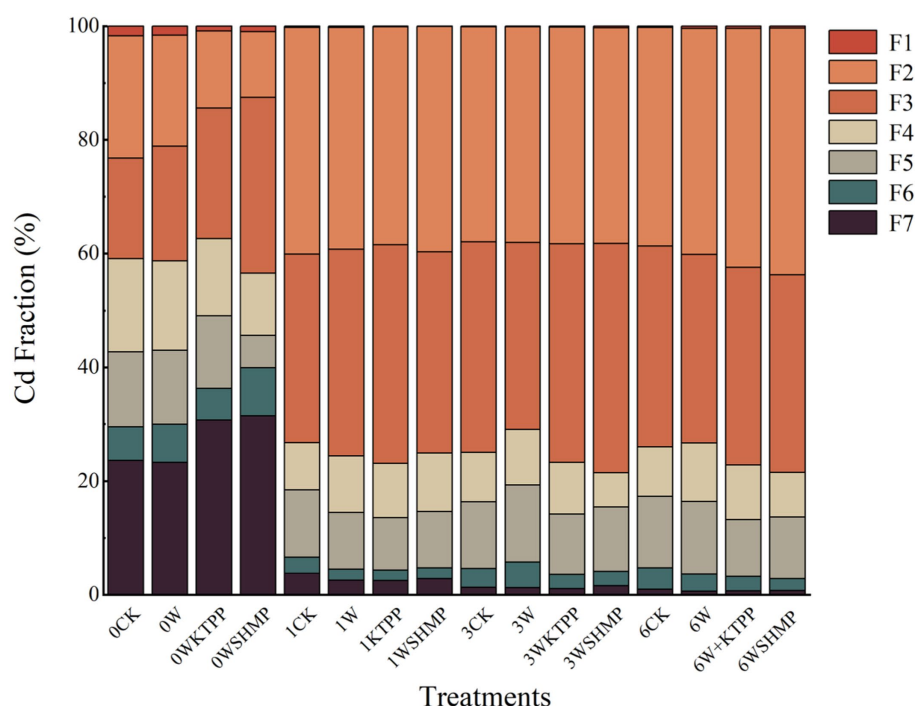


FIGURE 1

Cd chemical fractions in soils with varying degrees of Cd contamination in response to treatment with immobilizing agents. F1, water-soluble fraction; F2, ionic bond fraction; F3, carbonate fraction; F4, humic acid-bound fraction; F5, Fe/Mn oxide-bound fraction; F6, strong organic fraction; F7, residual fraction. CK, untreated control soil; W, wollastonite treatment; WKTPP, wollastonite + potassium triphosphate treatment; WSHMP, wollastonite + sodium hexametaphosphate treatment. Numbers before treatment group names indicate the soil Cd abundance: 0, control soil; 1, mild Cd contamination; 3, moderate Cd contamination; 6, high Cd contamination.

Cd and thus increasing soil bio-Cd concentrations. Furthermore, the elevated pH resulting from treatment with wollastonite and phosphate decreases the bioaccessibility of iron (Fe) and manganese (Mn). Because Cd competes for metal transporters with Fe and Mn, this treatment results in increased competitive adsorption and bioaccessibility of Cd^{2+} , promoting transportation into the soil–plant system (44, 45). Thus in Figure 1 it can be seen that the simultaneous application of wollastonite and phosphate instead led to an increase in bio-Cd concentration in the soil.

Little attention has been given in previous studies to the effects of combinations of passivators on soil Cd fractions, and this study found that Si and P in wollastonite and phosphate will combine with Cd in the soil to form precipitates and complexes to reduce the bio-Cd content. However, the addition of wollastonite and phosphate at the same time reduces the precipitation and complexation with Cd because Ca is the first to bind to P, resulting in an increase in bio-Cd content of soil in most of the treatment groups, especially in the WSHMP treatment group in moderately contaminated soil. Therefore, the simultaneous addition of immobilizing agents combination containing Si material and phosphate will instead promote the conversion of soil Cd to plant bioaccessible fractions.

3.2 Total Cd concentrations in aboveground pak choi tissues

We next assessed the effects of each treatment on Cd concentrations in aboveground pak choi tissues. In highly

Cd-contaminated soil, W treatment decreased the total aboveground Cd concentration. All other treatment group–soil combinations showed increased total aboveground Cd levels (Figure 2). For example, in moderately Cd-contaminated soil, W treatment significantly increased the total Cd in aboveground tissues to 16.61 mg/kg from 7.63 mg/kg in the control. In mildly and highly Cd-contaminated soil, Cd uptake by the plant was highest in the combined W + phosphate treatments. Specifically, WKTPP treatment increased the total aboveground pak choi Cd contents by 86.2 and 59.5% in mildly and highly Cd-contaminated soils, respectively; WSHMP treatment increased the Cd contents among plants grown in the same soils by 29.7 and 69.9%, respectively (Table 4). In mildly Cd-contaminated soils, the Cd transfer factor (TF) increased by 71.6% in the WKTPP treatment group compared to the control. In moderately and highly Cd-contaminated soils, WSHMP treatment increased the TF by 74.4 and 51.0%, respectively (Supplementary Tables S1, S3). This is generally consistent with changes in Cd fractions in the soil.

Zhou et al. (46) previously found that the addition of Si-containing materials to soil reduces the Cd content in wheat seeds by 16–30%. A combined application of sodium silicate and potassium dihydrogen phosphate has also been shown to reduce Cd concentrations in the roots, stems, and leaves of dicotyledonous plants by 52, 65, and 68%, respectively (17). However, other studies have reported that the application of Si-containing materials increases heavy metal accumulation in plants. For example, application of calcium silicate (CaSiO_3) increases Cd accumulation in maize due to the growth-promoting effects of Si (47). Similarly, in kale, potassium silicate treatment increases Cd levels in the roots; potassium phosphate

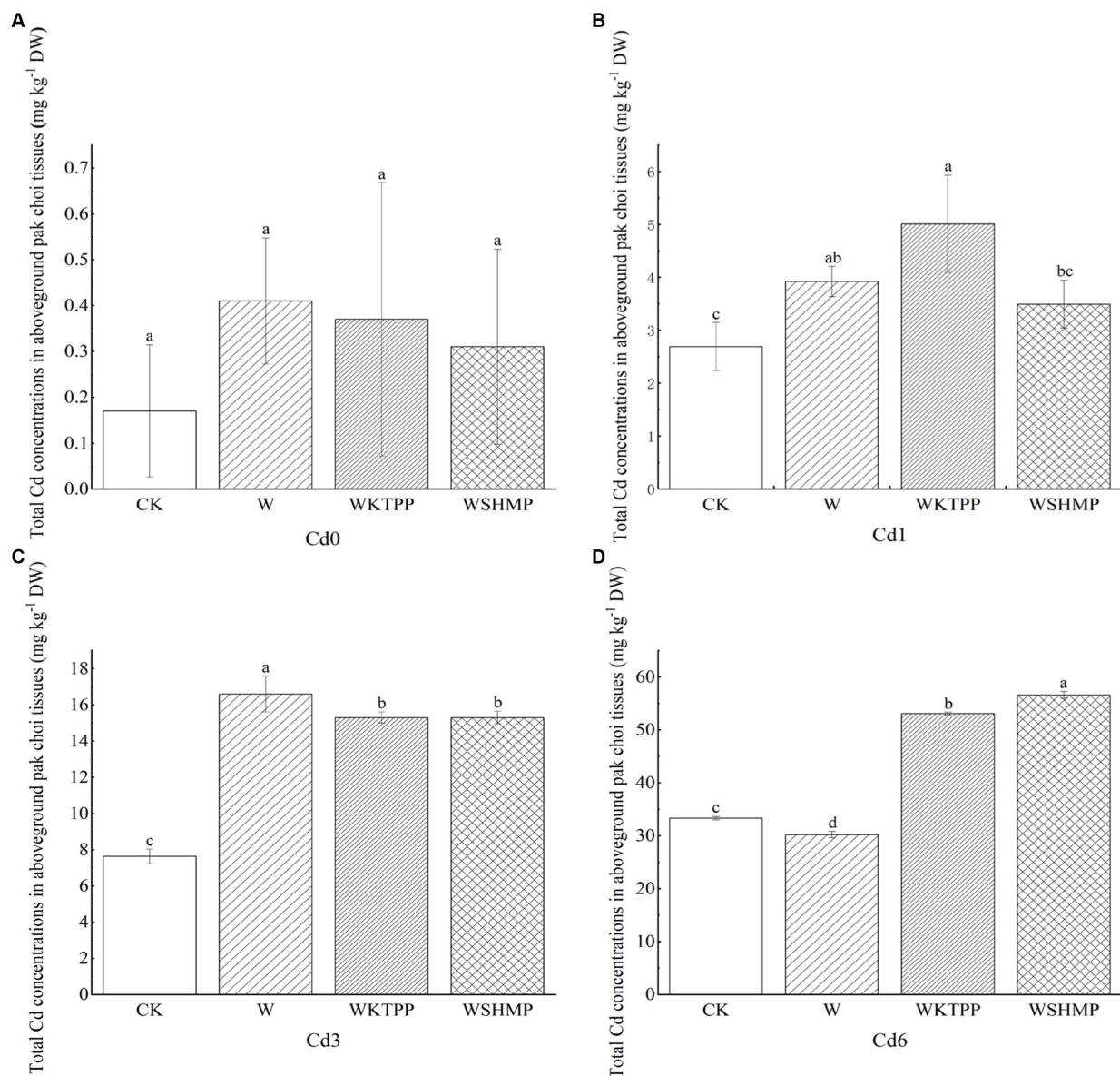


FIGURE 2

Total Cd concentrations in aboveground pak choi tissues in (A) Cd0, (B) Cd1, (C) Cd3, and (D) Cd6 soils after treatment with immobilizing agents. CK, untreated control soil; W, wollastonite treatment; WKTPP, wollastonite with potassium triphosphate treatment; WSHMP, wollastonite with sodium hexametaphosphate treatment. Numbers before treatment group names indicate the soil Cd abundance: 0, control soil; 1, mild Cd contamination; 3, moderate Cd contamination; 6, high Cd contamination. Letters above each bar indicate statistical significance groups at $p < 0.05$ (one-way analysis of variance with post-hoc Tukey's honestly significant difference test).

promotes retention of Cd in the root epidermis and endosperm of the roots and inhibits Cd transport to other tissues (17). Mao et al. (43) found that a combined W + phosphorus-containing material treatment leads to a 144% increase in Cd concentrations in brown rice compared to W treatment alone. Thus, our results were broadly consistent with those of previous studies.

Wollastonite contains Ca²⁺, which can compete with Cd²⁺ for binding sites in the roots of pak choi, thus reducing the migration of Cd to pak choi, but the addition of phosphate may disrupt this competitive adsorption and cause Ca to bind with phosphate first, so that the Cd of pak choi after the simultaneous application of wollastonite and phosphate exhibits an increase in the phenomenon shown in Figure 2. Although changes in Cd concentrations in crops

after wollastonite and phosphate application were analyzed in previous studies, Cd morphology was not included. In the present study it was found that the application of compounds containing Si may also change the soil pH, thus altering the solubility of Cd²⁺ in soil water and facilitating the migration of Cd from the soil to the pak choi plant (48). Changes in the TF of soil Cd to pak choi were consistent with changes in the soil Cd fractions; i.e., increases in the more bioaccessible fractions corresponded to higher the soil Cd mobility, suggesting that differences in Cd soil fractions heavily influenced Cd transport through the soil–pak choi system. Prior studies have indicated that the total Cd mass in *Brassica napus* is related to soil heavy metal fractions. Specifically, water-soluble heavy metals have high transport capacities and bioaccessibility, whereas those in ion-exchange state are most

TABLE 4 Effects of *in situ* soil treatment with immobilizing agents on total Cd mass and Cd bioaccessibility in pak choi.

Soil treatment group	Total Cd (mg kg ⁻¹)	Cd Bioaccessibility (%)	
		Gastric	Intestinal
0CK	0.17 ± 0.14	122.49 ± 52.72	16.03 ± 5.96
0W	0.41 ± 0.13	94.54 ± 24.43	13.78 ± 0.06
0WKTPP	0.37 ± 0.30	71.96 ± 10.06	9.73 ± 0.35
0WSHMP	0.31 ± 0.21	111.60 ± 21.99	12.71 ± 1.73
1CK	2.69 ± 0.45	100.41 ± 8.78	9.82 ± 0.84
1W	3.92 ± 0.28	57.42 ± 3.62	6.03 ± 0.85
1WKTPP	5.01 ± 0.92	49.52 ± 0.82	5.59 ± 0.36
1WSHMP	3.49 ± 0.45	92.01 ± 5.88	12.60 ± 3.10
3CK	7.63 ± 0.40	56.87 ± 21.83	8.73 ± 0.38
3W	16.62 ± 0.99	45.15 ± 5.21	5.54 ± 0.75
3WKTPP	15.31 ± 0.30	78.96 ± 6.22	10.27 ± 1.05
3WSHMP	15.25 ± 0.35	40.37 ± 14.13	5.98 ± 1.57
6CK	33.27 ± 0.33	43.13 ± 27.38	12.32 ± 2.10
6W	30.23 ± 0.61	43.30 ± 4.61	6.36 ± 0.70
6WKTPP	53.07 ± 0.27	26.07 ± 3.68	2.05 ± 0.34
6WSHMP	56.65 ± 0.65	10.35 ± 0.08	0.98 ± 0.04

CK, untreated control soil; W, wollastonite treatment; WKTPP, wollastonite with potassium triphosphate treatment; WSHMP, wollastonite with sodium hexametaphosphate treatment. Numbers before treatment group names indicate the soil Cd abundance: 0, control soil; 1, mild Cd contamination; 3, moderate Cd contamination; 6, high Cd contamination.

easily absorbed and utilized by plants. Heavy metals in the carbonate-bound state are most likely to be re-released into the aqueous phase when the soil pH is altered. The addition of wollastonite and phosphate to the soil can change stable Cd to the more mobile water-soluble, ion-exchange, or carbonate-bound states, promoting accumulation in plants (Supplementary Table S2).

Overall, as wollastonite and phosphate increase the migration of Cd from soil to *Brassica napus*, and at the same time shift soil Cd to a more migratory form, the total amount of Cd in *Brassica napus* increased in most treatment groups, in which the total amount of Cd in *Brassica napus* in mildly Cd-contaminated soils was elevated by 86.2% by the treatment of WKTPP compared to the blank control, and the treatment has the potential to become a phytoremediation. This treatment has the potential to be a phytoremediation aid for mildly Cd-polluted soil. The current study found that rice with low micronutrient content will result in poorer nutritional status of minerals such as calcium, iron and zinc in the human body, exacerbating the risk of Cd uptake and disease problems in the human body (49), suggesting that assessment of immobilization treatments should not focus on changes in Cd content alone. Consequently, subsequent studies should also focus on changes in the micronutrient content of pak choi to minimize and avoid compromising the nutritional value of pak choi.

3.3 Cd bioaccessibility in pak choi

We next analyzed the gastrointestinal bioaccessibility of Cd present in pak choi using PBET. The gastric phase bioaccessibility of Cd ranged from 10.35–122.49% (mean = 65.27%) (Figure 3), which

was significantly higher than Cd bioaccessibility in the small intestine (range = 0.98–16.03%; mean = 8.67%), suggesting that Cd uptake by plant tissues occurs mainly in the gastric digestive phase, which is in agreement with the findings of Qin et al. (50). This was likely due to the intensely low pH in the stomach (pH 1.5), which causes heavy metal release from plant tissues (51). Furthermore, proteases and other enzymes in the stomach break down proteins, releasing any protein-bound heavy metals (52, 53), and organic compounds in the stomach acid (such as sodium malate or sodium citrate) contain functional groups that may bind to heavy metals, increasing their accessibility and solubility (54). In contrast, the intestinal digestive environment is pH-neutral, with proteins that are inactivated in higher pH environments. Under high-pH conditions, soluble Cd often binds to digested products such as phytate, sulfur-containing amino acids, and glutathione, generating precipitates. Bile salts also reduce Cd solubility, decreasing Cd bioaccessibility in the small intestine (55).

We here found that wollastonite+phosphate treatments decreased Cd bioaccessibility in the gastric phase in both control soil and mildly Cd-contaminated soil. Compared to the untreated control, WKTPP treatment reduced Cd bioaccessibility in the gastric and intestinal phases by 50.53 and 6.3%, respectively; in mildly Cd-contaminated soils, WKTPP treatment significantly reduced Cd bioaccessibility in the gastric phase by 50.89%, whereas WSHMP increased Cd bioaccessibility in the intestinal phase by 2.78%. In moderately and highly Cd-contaminated soils, WSHMP treatment reduced gastric-phase Cd bioaccessibility by 16.49 and 32.78%, respectively. In highly Cd-contaminated soil, WKTPP treatment increased gastric-phase Cd bioaccessibility by 22.09% (Table 4).

In Figure 3 it can be seen that the addition of wollastonite and phosphate decreases the bioaccessibility of Cd in the gastric and small intestine almost to varying degrees. This is due to the fact that Si accumulation significantly inhibit the net cellular influx of Cd²⁺ (56), whereas phosphate treatment leads to formation of Cd-phosphate complexes. These complexes adsorb to the cell wall, thus decreasing Cd transport to portions of the plant that are consumed by humans (57). Wollastonite and phosphates can mitigate heavy metal toxicity in plants and reduce bioaccessibility to in the human body through compartmentalization and structural changes that reduce metal transfer. For example, Mao et al. (43) found that wollastonite and phosphates reduce Cd bioaccessibility in rice by 29–39% by enhancing Cd incorporation into cell walls, inhibiting its transport throughout the plant. Phosphorus-containing materials (such as hydroxyapatite) cause changes in bioaccessible heavy metal fractions by altering the pH; in chili peppers and cabbages, this leads to reductions in Cd and Pb bioaccessibility of 5.0–84.8% and 5.71–93.81%, respectively (58).

The lowest bioaccessibility of Cd by WSHMP treatment was found in the study of Mao et al. This was consistent with the results in moderate and high Cd contaminated soils, but opposite to the results in mild Cd contaminated soils, which may be related to the total amount of Cd in the soil and in the pak choi (59). In the present study, Pearson's correlation analysis showed that the total amount of Cd in pak choi was significantly negatively correlated with Cd bioaccessibility (Table 5). This suggests that high Cd concentrations in the plant were associated with a decreased capacity to release Cd from the food matrix, thus reducing Cd bioaccessibility. The addition of wollastonite and phosphate increased Si and Ca concentrations in pak choi by 50 and 10%, respectively; these increases were associated with decreased Cd bioaccessibility (Supplementary Figure S2). This is consistent with

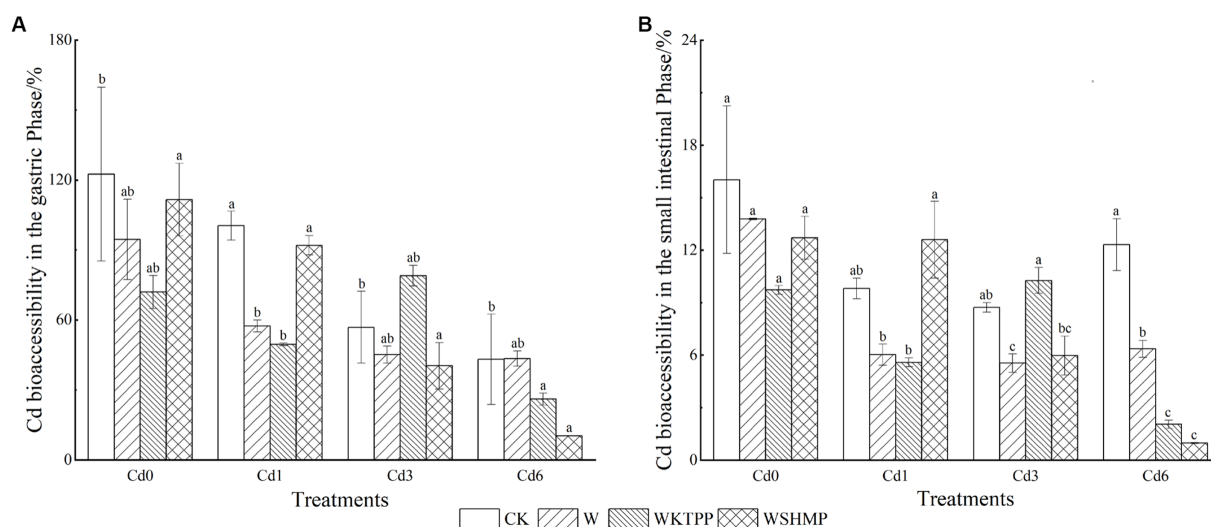


FIGURE 3

Cd bioaccessibility in pak choi grown under varying soil conditions in the (A) gastric and (B) small intestinal phases. CK, untreated control soil; W, wollastonite treatment; WKTP, wollastonite with potassium triphosphate treatment; WSHMP, wollastonite with sodium hexametaphosphate treatment. Numbers before treatment group names indicate the soil Cd abundance: 0, control soil; 1, mild Cd contamination; 3, moderate Cd contamination; 6, high Cd contamination.

TABLE 5 Correlations between Cd bioaccessibility and total Cd content in pak choi grown under varying soil conditions.

		Cd bioaccessibility from pak choi
Total Cd concentration	Pearson's correlation	−0.789**
	Significance (bilateral)	<0.001
	N	16

** Correlation is significant at the 0.01 level (2-tailed).

prior studies showing that CaCl_2 treatment significantly reduces Cd bioaccessibility in rice and vegetables (34, 35). The extent of the effect of several treatments on Cd concentration differed from the effect on Cd bioaccessibility, which indicates the importance and necessity of considering the bioaccessibility of pak choi for the rational selection of fixation treatments.

Generally, the bioaccessibility of Cd in pak choi was greater in the gastric phase than in the small intestine due to the influence of pH and other digestive fluids. Wollastonite and phosphate bind to and form complexes with Cd in the cell wall components of chard, and the bioaccessibility of Cd in pak choi is reduced in both cases, and the increase in the total amount of Cd in pak choi is a reduction in the ability of the food matrix to release Cd, which in turn further reduces its bioaccessibility.

3.4 Ultrastructural changes in pak choi due to immobilizing agent treatment

Ultrastructural changes are often overlooked in current studies on the effects of fixation treatments on Cd in vegetables, and in order to further assess the effects of the treatments on plant morphology, we analyzed the ultrastructural characteristics of plants grown in each treatment group. No structural distortions were observed in any of the

control plants (Figure 4A,F). However, the cells of leaves from plants grown in Cd-contaminated soil showed symptoms of toxicity, such as irregularly shaped cell walls and separation of cell membranes from the cell walls. Compared with plants grown in control soil, the chloroplasts of these plants were irregularly shaped; there are more osmiophilic globules increased and the granules clustered together (Figure 4B,G). Prior studies have shown that Cd exposure causes membrane lipid oxidation, significantly altering the structural features of cell membranes (60). Furthermore, cell metabolism is known to be disrupted by Cd entry into the cells, causing decreases in cell proliferation and plant biomass, which in turn increase starch granule size (61).

Here, combined applications of wollastonite and phosphate compounds also resulted in the formation of osmiophilic granules. Both these structures and the chloroplasts were of uniform size and shape, and were evenly distributed throughout the cells. These cells contained more starch granules than cells from control plants, and the cell walls and membranes were clearly defined. Impurities were isolated from the cell membranes, and the immobilizing agent treatments appeared to promote cell membrane integrity.

These ultrastructural results were consistent with earlier published findings. Heavy metals such as Cd are initially prevented from entering cells by the cell wall, which contains structural carbohydrates and proteins that act as barriers. For example, cellulose, hemicellulose, and pectin in the cell wall contain a large number of carboxyl and hydroxyl groups, which provide many binding sites for heavy metal fixation; this reduces metal solubility and decreases root-to-stem translocation (62, 63). Heavy metal contamination triggers cell wall thickening, promoting metal sequestration (64). If the heavy metal content exceeds the sequestration capacity of the cell wall, the metals are sequestered inside the cell by vesicles, which continue to protect organelles from toxicity (65).

Cd is known to interfere with chlorophyll synthase activity and to inhibit chlorophyll synthesis. Phosphate treatment of Cd-contaminated plants was here shown to cause precipitate

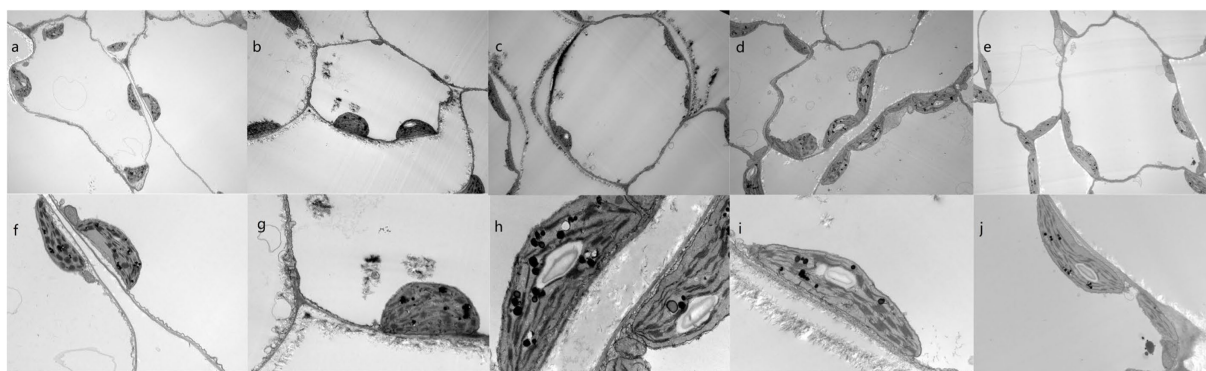


FIGURE 4

Subcellular structures of pak choi leaves from plants grown in Cd-contaminated soil with varying immobilizing treatments. (A–J) Cells of plants grown in the (A,F) blank control soil, (B,G) Cd-contaminated control soil, (C,H) Cd-contaminated soil treated with wollastonite, (D,I) Cd-contaminated soil treated with wollastonite and potassium triphosphate, and (E,J) Cd-contaminated soil treated with wollastonite and sodium hexametaphosphate. Magnification = 5,000× (A–E) and 30,000× (F–J).

formation (Figures 4D,E,I,J), which can reduce Cd-mediated prochlorophyllate oxidoreductase inhibition and decrease Cd-induced chlorophyll damage (66). Silicate addition also increases phosphate desorption from the soil and increases plant phosphate uptake, promoting chlorophyll synthesis.

Prior studies have been conducted to assess the effects of the subcellular heavy metal distribution within crops on heavy metal bioaccessibility. Chewing and digestion alone result in the release of heavy metal ions from leafy vegetable vesicles (67), although the release of heavy metal elements from cell walls requires cell wall protein and polysaccharide degradation by a variety of digestive enzymes (68). Wollastonite and phosphate treatments can thicken pak choi cell walls (69) and cause co-precipitation of Cd in the cell wall (47); thus, Cd is strongly sequestered in the cell wall in a non-soluble form. This prevents Cd-mediated damage to the cell membrane and vesicles; reduces Cd uptake; and reduces Cd release from pak choi into the body (Figures 4C,H). The incorporation of wollastonite and phosphate ameliorated the damage of Cd to the cellular structure of pak choi and maintained its integrity, while reducing the migration of Cd to the edible parts of pak choi, greatly reducing the health risks associated with its consumption.

3.5 Summary: the importance of immobilizing agents in pak choi production

Compared with traditional cereals and root crops, leafy vegetables such as pak choi are more susceptible to absorption of soil Cd. When such vegetables are consumed, Cd enters the body, which could represent a serious human health risk if the Cd has high bioaccessibility. We here sought to assess the associated risk and the effects of potential remediation strategies for soil Cd contamination. Using pak choi as a model leafy green vegetable, we here tested common immobilizing agents for soil heavy metals, including silica-containing and phosphorus-containing materials, in soils with three levels of Cd contamination. Soil Cd fractions were analyzed and pak choi cells were analyzed with transmission electron microscopy to elucidate the mechanism by which each treatment affected both the total Cd contents in pak choi and the associated bioaccessibility. These

experiments yielded several key findings. First, all three treatments led to decreases in the residual soil Cd content, except for one silica-phosphorus treatment (WSHMP) in moderately Cd-contaminated soils. Furthermore, all treatments caused increases in the soil effective-state Cd concentrations, except for W treatment in moderately Cd-contaminated soil. The second key finding was that the tested treatments had varying effects on Cd bioaccessibility in pak choi plants based on the level of soil Cd contamination. Specifically, in mildly Cd-contaminated soils, WKTPP reduced Cd bioaccessibility in pak choi, whereas WSHMP had a more pronounced reducing effect on Cd bioaccessibility in pak choi in moderately and highly Cd-contaminated soils. Transmission electron microscopy observations revealed a large number of unidentified particles in the cell walls, which were inferred to be silicate complexes and insoluble precipitates formed by Cd binding with Si and P. Overall, the treatments used in this study consistently increased the total Cd content in pak choi. For example, the WKTPP treatment increased plant Cd contents by 86.2% compared to the untreated control. This finding suggests that the WKTPP treatment could be optimized for use as a phytoremediation aid for mildly Cd-contaminated soils, especially under alkaline conditions.

4 Conclusion

Prior evaluations of heavy metal risks to human health have focused on the total amount of a given pollutant in the environment or a specific substrate, ignoring bioaccessibility. This is a serious oversight because bioaccessibility, not total contaminant mass, ultimately determines human exposure rates. Wollastonite-conjugated phosphate immobilizing combinations are also mostly used for remediation of Cd contamination in cereals such as rice, while Cd in leafy vegetables should be given more attention with the increasing consumption of vegetables in China. To address this issue, we here analyzed both total Cd and bioaccessible Cd in pak choi grown in Cd-contaminated soil treated with several immobilizing agents. We found that different types of silica-phosphorus treatments significantly reduced Cd bioaccessibility among pak choi plants grown in soil with varying levels of Cd contamination. Importantly, WKTPP treatment promoted Cd uptake by pak choi plants, leading to significant increases in the total

Cd content in the aboveground plant tissues. At the same time, we explored the mechanisms by which wollastonite and phosphate affect Cd in pak choi at the ultrastructural level, which has often been overlooked in previous studies. These treatments could therefore play important roles in controlling the human health risks associated with Cd contamination of farmland soils; they could be used to either effectively reduce Cd bioaccessibility in crops or to maximize Cd uptake by plants optimized for soil remediation. However, *in situ* soil Cd fixation sessions had different effects on the bioaccessibility of Cd in pak choi, suggesting that there is a large uncertainty in Cd health risk assessment based simply on the total amount of Cd in pak choi. This implies that there is a need to incorporate Cd bioaccessibility into health risk assessment to accurately reflect the risk of Cd exposure from pak choi consumption. This paper provides an example of an optimal fixative treatment to reduce the bioaccessibility of pak choi. However, in order to minimize the Cd exposure risk associated with pak choi consumption, further research is needed to wind up effectively reducing Cd accumulation and bioaccessibility in pak choi. We here varied the types, but not the proportions, of silica to phosphorus immobilizing agents; future studies should address the impacts of differences in silica-containing to phosphorus-containing material ratios (and of application methods) in different soil types, and also replace the use of different combinations of silica-containing and other micronutrients. Changes in nutrients such as Zn and Se and growth-friendly enzymes should also be observed to observe more growth in pak choi. The present study provides the optimal treatment combinations that can be used for soil phytoremediation and reduction of Cd bioaccessibility in different Cd-contaminated soils in pak choi, and provides a methodology for *in-situ* soil treatments to reduce the risk of heavy metal contamination in the food chain and the environment, which promotes human and ecosystem health, and provides a theoretical basis for future environmental remediation and agri-food safety production.

Data availability statement

The original contributions presented in the study are included in the article/[Supplementary material](#), further inquiries can be directed to the corresponding author.

Author contributions

KG: Conceptualization, Data curation, Methodology, Writing – original draft. YuZ: Investigation, Resources, Writing – review & editing. YaZ: Investigation, Resources, Writing – review & editing. JY:

Investigation, Resources, Writing – review & editing. ZC: Investigation, Resources, Writing – review & editing. QZ: Supervision, Writing – review & editing. WX: Resources, Writing – review & editing. BH: Resources, Writing – review & editing. TL: Conceptualization, Funding acquisition, Methodology, Project administration, Writing – review & editing.

Funding

The author(s) declare financial support was received for the research, authorship, and/or publication of this article. This work was supported by the Key research and development plan of Shandong Province (2021CXGC011201) and Youth Project of Shandong Provincial Natural Science Foundation (No: ZR2021QD115).

Acknowledgments

We thank the Shandong Provincial Science and Technology Department for financial support of this study.

Conflict of interest

WX was employed by Guangzhou Hixin Instrument Co., Ltd. BH was employed by Zhongchuang Guoke Scientific Instrument (Shandong) Co.

The remaining authors declare that the research was conducted in the absence of any commercial or financial relationships that could be construed as a potential conflict of interest.

Publisher's note

All claims expressed in this article are solely those of the authors and do not necessarily represent those of their affiliated organizations, or those of the publisher, the editors and the reviewers. Any product that may be evaluated in this article, or claim that may be made by its manufacturer, is not guaranteed or endorsed by the publisher.

Supplementary material

The Supplementary material for this article can be found online at: <https://www.frontiersin.org/articles/10.3389/fnut.2024.1337996/full#supplementary-material>

References

1. Mori M, Kotaki K, Gunji F, Kubo N, Kobayashi S, Ito T, et al. Suppression of cadmium uptake in Rice using fermented bark as A soil amendment. *Chemosphere*. (2016) 148:487–94. doi: 10.1016/j.chemosphere.2016.01.012
2. Ministry of Environmental Protection and Ministry of Land and Resources. National Soil Pollution Survey Bulletin [J]. *Resources and Habitat*. (2014) 26–27.
3. Yang L, Huang B, Hu W, Chen Y, Mao M, Yao L. The impact of greenhouse vegetable farming duration and soil types on Phytoavailability of heavy metals and their health risk in eastern China. *Chemosphere*. (2014) 103:121–30. doi: 10.1016/j.chemosphere.2013.11.047
4. Cui S, Wang Z, Li X, Wang H, Wang H, Chen W. A comprehensive assessment of heavy metal(loid) contamination in leafy vegetables grown in two mining areas in Yunnan, China—A focus on bioaccumulation of cadmium in Malabar spinach. *Environ Sci Pollut Res*. (2023) 30:14959–74. doi: 10.1007/s11356-022-23017-5
5. Sun Y, Xu Y, Xu Y, Wang L, Liang X, Li Y. Reliability and stability of immobilization remediation of cd polluted soils using Sepiolite under pot and field trials. *Environ Pollut*. (2016) 208:739–46. doi: 10.1016/j.envpol.2015.10.054
6. Guo F, Ding C, Zhou Z, Huang G, Wang X. Effects of combined amendments on crop yield and cadmium uptake in two cadmium contaminated soils under Rice-wheat rotation. *Ecotoxicol Environ Saf*. (2018) 148:303–10. doi: 10.1016/j.ecoenv.2017.10.043

7. Wang F, Zhang S, Cheng P, Zhang S, Sun Y. Effects of soil amendments on heavy metal immobilization and accumulation by maize grown in a multiple-metal-contaminated soil and their potential for safe crop production. *Toxics*. (2020) 8:102. doi: 10.3390/Toxics8040102
8. Rassaei F. Sugarcane bagasse biochar changes the sorption kinetics and Rice (*Oryza Sativa* L.) cadmium uptake in A Paddy soil. *Gesunde Pflanzen*. (2023) 75:2101–10. doi: 10.1007/s10343-023-00860-1
9. Kamran M, Malik Z, Parveen A, Zong Y, Abbasi GH, Rafiq MT, et al. Biochar alleviates cd phytotoxicity by minimizing bioavailability and oxidative stress in pak choi (*Brassica chinensis* L.) cultivated in cd-polluted soil. *J Environ Manag*. (2019) 250:109500. doi: 10.1016/j.jenvman.2019.109500
10. Li S, SUN X, Liu Y, Li S, Zhou W, Ma Q, et al. Remediation of cd-contaminated soils by GWC application, evaluated in terms of cd immobilization, enzyme activities, and Pakchoi cabbage uptake. *Environ Sci Pollut Res*. (2020) 27:9979–86. doi: 10.1007/s11356-019-07533-5
11. Cai Y, Zhang S, Cai K, Huang F, Pan B, Wang W. Cd accumulation, biomass and yield of Rice are varied with silicon application at different growth phases under high concentration cadmium-contaminated soil. *Chemosphere*. (2020) 242:125128. doi: 10.1016/j.chemosphere.2019.125128
12. Huang H, Chen H-P, Kopitke PM, Kretschmar R, Zhao FJ, Wang P. The voltaic effect as A novel mechanism controlling the remobilization of cadmium in Paddy soils during drainage. *Environ Sci Technol*. (2021) 55:1750–8. doi: 10.1021/acs.est.0c06561
13. Hussain B, Lin Q, Hamid Y, Sanaullah M, di L, Hashmi MLR, et al. Foliage application of selenium and silicon nanoparticles alleviates cd and Pb toxicity in Rice (*Oryza Sativa* L.). *Sci Total Environ*. (2020) 712:136497. doi: 10.1016/j.scitotenv.2020.136497
14. Guo L, Chen A, Li C, Wang Y, Yang D, He N, et al. Solution chemistry mechanisms of exogenous silicon influencing the speciation and bioavailability of cadmium in alkaline Paddy soil. *J Hazard Mater*. (2022) 438:129526. doi: 10.1016/j.jhazmat.2022.129526
15. Rassaei F. Effect of monocalcium phosphate on the concentration of cadmium chemical fractions in two calcareous soils in Iran. *Soil Sci Annu*. (2022) 73:1–6. doi: 10.37501/soilsa/152586
16. Xiao R, Huang Z, Li X, Chen W, Deng Y, Han C. Lime and phosphate amendment can significantly reduce uptake of Cd and Pb by field-grown rice. *Sustainability*. (2017) 9:430. doi: 10.3390/Su9030430
17. Lu H-P, Zhuang P, Li Z-A, Tai YP, Zou B, Li YW, et al. Contrasting effects of silicates on cadmium uptake by three dicotyledonous crops grown in contaminated soil. *Environ Sci Pollut Res*. (2014) 21:9921–30. doi: 10.1007/s11356-014-2947-z
18. Wang X, Zou H, Liu Q. Effects of phosphate and silicate combined application on cadmium form changes in heavy metal contaminated soil. *Sustainability*. (2023) 15:4503. doi: 10.3390/Su15054503
19. Mehta N, Cocerva T, Cipullo S, Padoan E, Dino GA, Ajmone-Marsan F, et al. Linking Oral bioaccessibility and solid phase distribution of potentially toxic elements in extractive waste and soil from an abandoned mine site: case study in Campello Monti, NW Italy. *Sci Total Environ*. (2019) 651:2799–810. doi: 10.1016/j.scitotenv.2018.10.115
20. Wang C-C, Li M-Y, Yan C-A, Tian W, Deng ZH, Wang ZX, et al. Refining health risk assessment of heavy metals in vegetables from high geochemical background areas: role of bioaccessibility and cytotoxicity. *Process Saf Environ Prot*. (2022) 159:345–53. doi: 10.1016/j.psep.2022.01.003
21. Hu J, Wu F, Wu S, Cao Z, Lin X, Wong MH. Bioaccessibility, dietary exposure and human risk assessment of heavy metals from market vegetables in Hong Kong revealed with an in vitro gastrointestinal model. *Chemosphere*. (2013) 91:455–61. doi: 10.1016/j.chemosphere.2012.11.066
22. Dun Y, Wu C, Zhou M, Tian X, Wu G. Wheat straw- and maize straw-derived biochar effects on the soil cadmium fractions and bioaccumulation in the wheat–maize rotation system. *Front Environ Sci*. (2022) 10:980893. doi: 10.3389/fenvs.2022.980893
23. Yang L, Yang Y, Yu Y, Wang Z, Tian W, Tian K, et al. Potential use of hydroxyapatite combined with hydrated lime or zeolite to promote growth and reduce cadmium transfer in the soil-celery-human system. *Environ Sci Pollut Res*. (2023) 30:12714–27. doi: 10.1007/s11356-022-23029-1
24. Li Y, Liang X, Huang Q, Xu Y, Yang F. Inhibition of cd accumulation in grains of wheat and Rice under rotation mode using composite silicate amendment. *RSC Adv*. (2019) 9:35539–48. doi: 10.1039/C9RA07137G
25. Chen H, Zhang W, Yang X, Wang P, McGrath SP, Zhao FJ. Effective methods to reduce cadmium accumulation in Rice grain. *Chemosphere*. (2018) 207:699–707. doi: 10.1016/j.chemosphere.2018.05.143
26. Wang B, Chu C, Wei H, Zhang L, Ahmad Z, Wu S, et al. Ameliorative effects of silicon fertilizer on soil bacterial community and pakchoi (*Brassica chinensis* L.) grown on soil contaminated with multiple heavy metals. *Environ Pollut*. (2020) 267:115411. doi: 10.1016/j.envpol.2020.115411
27. Lu Y, Zhu F, Chen J, Gan H, Guo Y. Chemical fractionation of heavy metals in urban soils of Guangzhou, China. *Environ Monit Assess*. (2007) 134:429–39. doi: 10.1007/s10661-007-9634-1
28. Matusik J, Bajda T, Manecki M. Immobilization of aqueous cadmium by addition of phosphates. *J Hazard Mater*. (2008) 152:1332–9. doi: 10.1016/j.jhazmat.2007.08.010
29. Thawornchaisit U, Polprasert C. Evaluation of phosphate fertilizers for the stabilization of cadmium in highly contaminated soils. *J Hazard Mater*. (2009) 165:1109–13. doi: 10.1016/j.jhazmat.2008.10.103
30. Tang L, Luo W, Tian S, He Z, Stoffella PJ, Yang X. Genotypic differences in cadmium and nitrate co-accumulation among the Chinese cabbage genotypes under field conditions. *Sci Hortic*. (2016) 201:92–100. doi: 10.1016/j.scienta.2016.01.040
31. Tessier A, Campbell PG, Bisson M. Sequential extraction procedure for the speciation of particulate trace metals. *Anal Chem*. (1979) 51:844–51. doi: 10.1021/ac50043a017
32. Ure AM, Davidson CM. *Chemical speciation in the environment*. Wiley-Blackwell: John Wiley & Sons (2008).
33. Ruby MV, Davis A, Link TE, Schoof R, Chaney RL, Freeman GB, et al. Development of an in vitro screening test to evaluate the in vivo bioaccessibility of ingested mine-waste Lead. *Environ Sci Technol*. (1993) 27:2870–7. doi: 10.1021/es00049a030
34. Fu J, Cui Y. In vitro digestion/Caco-2 cell model to estimate cadmium and Lead bioaccessibility/bioavailability in two vegetables: the influence of cooking and additives. *Food Chem Toxicol*. (2013) 59:215–21. doi: 10.1016/j.fct.2013.06.014
35. Sun S, Zhou X, Li Y, Li Y, Xia H, Li Z, et al. Use of dietary components to reduce the bioaccessibility and bioavailability of cadmium in Rice. *J Agric Food Chem*. (2020) 68:4166–75. doi: 10.1021/acs.jafc.0c01582
36. Luo C, Liu C, Wang Y, Liu X, Li F, Zhang G, et al. Heavy metal contamination in soils and vegetables near an E-waste processing site, South China. *J Hazard Mater*. (2011) 186:481–90. doi: 10.1016/j.jhazmat.2010.11.024
37. Cui Y-J, Zhu Y-G, Zhai R-H, Chen DY, Huang YZ, Qiu Y, et al. Transfer of metals from soil to vegetables in an area near A smelter in Nanning, China. *Environ Int*. (2004) 30:785–91. doi: 10.1016/j.envint.2004.01.003
38. Sui F, Wang J, Zuo J, Joseph S, Munroe P, Drosos M, et al. Effect of amendment of biochar supplemented with Si on cd mobility and Rice uptake over three Rice growing seasons in an acidic cd-tainted Paddy from central South China. *Sci Total Environ*. (2020) 709:136101. doi: 10.1016/j.scitotenv.2019.136101
39. Zeng P, Liu J, Zhou H, Wei B, Gu J, Liao Y, et al. Co-application of combined amendment (limestone and Sepiolite) and Si fertilizer reduces Rice cd uptake and transport through cd immobilization and Si–cd antagonism. *Chemosphere*. (2023) 316:137859. doi: 10.1016/j.chemosphere.2023.137859
40. Ma C, Ci K, Zhu J, Sun Z, Liu Z, Li X, et al. Impacts of exogenous mineral silicon on cadmium migration and transformation in the soil-Rice system and on soil health. *Sci Total Environ*. (2021) 759:143501. doi: 10.1016/j.scitotenv.2020.143501
41. Guan D, Wu J, Xie Y, Chen S, Chen J, Peng H. Effects of iron-based silicon salts on fractions and transformation of cadmium and arsenic in soil environment. *China Environ Sci*. (2022) 42:1803–11. doi: 10.19674/j.cnki.issn1000-6923.20220112.016
42. Feng R, Wang L, Yang J, Zhao PP, Zhu YM, Li YP, et al. Underlying mechanisms responsible for restriction of uptake and translocation of heavy metals (metalloids) by selenium via root application in plants. *J Hazard Mater*. (2021) 402:123570. doi: 10.1016/j.jhazmat.2020.123570
43. Mao P, Zhuang P, Li F, McBride MB, Ren W, Li Y, et al. Phosphate addition diminishes the efficacy of Wollastonite in decreasing cd uptake by Rice (*Oryza Sativa* L.) in Paddy soil. *Sci Total Environ*. (2019) 687:441–50. doi: 10.1016/j.scitotenv.2019.05.471
44. Sasaki A, Yamaji N, Yokosho K, Ma JF. Nramp 5 is a major transporter responsible for manganese and cadmium uptake in Rice. *Plant Cell*. (2012) 24:2155–67. doi: 10.1105/tpc.112.096925
45. Liang X, Xu Y, Xu Y, Wang P, Wang L, Sun Y, et al. Two-year stability of immobilization effect of Sepiolite on cd contaminants in Paddy soil. *Environ Sci Pollut Res*. (2016) 23:12922–31. doi: 10.1007/s11356-016-6466-y
46. Zhou J, Zhang C, Du B, Cui H, Fan X, Zhou D, et al. Soil and foliar applications of silicon and selenium effects on cadmium accumulation and plant growth by modulation of antioxidant system and cd translocation: comparison of soft vs. durum wheat varieties. *J Hazard Mater*. (2021) 402:123546. doi: 10.1016/j.jhazmat.2020.123546
47. Da Cunha KPV, Do Nascimento CWA. Silicon effects on metal tolerance and structural changes in maize (*Zea Mays* L.) grown on A cadmium and zinc enriched soil. *Water Air Soil Pollut*. (2009) 197:323–30. doi: 10.1007/s11270-008-9814-9
48. Khan I, Awan SA, Rizwan M, Ali S, Hassan MJ, Brestic M, et al. Effects of silicon on heavy metal uptake at the soil-plant interphase: a review. *Ecotoxicol Environ Saf*. (2021) 222:112510. doi: 10.1016/j.ecoenv.2021.112510
49. Zhao D, Juhasz AL, Luo J, Huang L, Luo XS, Li HB, et al. Mineral dietary supplement to decrease cadmium relative bioavailability in Rice based on A mouse bioassay. *Environ Sci Technol*. (2017) 51:12123–30. doi: 10.1021/acs.est.7b02993
50. Qin J, Niu A, Liu Y, Lin C. Arsenic in leafy vegetable plants grown on mine water-contaminated soils: uptake, human health risk and remedial effects of biochar. *J Hazard Mater*. (2021) 402:123488. doi: 10.1016/j.jhazmat.2020.123488
51. Zhuang P, Zhang C, Li Y, Zou B, Mo H, Wu K, et al. Assessment of influences of cooking on cadmium and arsenic bioaccessibility in Rice, using an in vitro physiologically-based extraction test. *Food Chem*. (2016) 213:206–14. doi: 10.1016/j.foodchem.2016.06.066

52. Goodman BE. Insights into digestion and absorption of major nutrients in humans. *Adv Physiol Educ.* (2010) 34:44–53. doi: 10.1152/advan.00094.2009
53. Sun G-X, Van De Wiele T, Alava P, Tack F, Du Laing G. Arsenic in cooked Rice: effect of chemical, enzymatic and microbial processes on bioaccessibility and speciation in the human gastrointestinal tract. *Environ Pollut.* (2012) 162:241–6. doi: 10.1016/j.envpol.2011.11.021
54. Zheng X, Zhang Z, Chen J, Liang H, Chen X, Qin Y, et al. Comparative evaluation of in vivo relative bioavailability and in vitro bioaccessibility of arsenic in leafy vegetables and its implication in human exposure assessment. *J Hazard Mater.* (2022) 423:126909. doi: 10.1016/j.jhazmat.2021.126909
55. Aziz R, Rafiq MT, Li T, Liu D, He Z, Stoffella PJ, et al. Uptake of cadmium by Rice grown on contaminated soils and its bioavailability/toxicity in human cell lines (Caco-2/HL-7702). *J Agric Food Chem.* (2015) 63:3599–608. doi: 10.1021/jf505557g
56. Liu J, Ma J, He CW, Li X, Zhang W, Xu F. Inhibition of cadmium ion uptake in rice (*Oryza Sativa*) cells by A wall-bound form of silicon. *New Phytol.* (2013) 200:691–9. doi: 10.1111/nph.12494
57. Qiu Q, Wang Y, Yang Z, Yuan J. Effects of phosphorus supplied in soil on subcellular distribution and chemical forms of cadmium in two Chinese flowering cabbage (*Brassica Parachinensis* L.) cultivars differing in cadmium accumulation. *Food Chem Toxicol.* (2011) 49:2260–7. doi: 10.1016/j.fct.2011.06.024
58. Zhang D, Ding A, Li T, Wu X, Liu Y, Naidu R. Immobilization of cd and Pb in A contaminated acidic soil amended with hydroxyapatite, bentonite, and biochar. *J Soils Sediments.* (2021) 21:2262–72. doi: 10.1007/s11368-021-02928-9
59. Mao P, Wu J, Li F, Sun S, Huang R, Zhang L, et al. Joint approaches to reduce cadmium exposure risk from Rice consumption. *J Hazard Mater.* (2022) 429:128263. doi: 10.1016/j.jhazmat.2022.128263
60. Mwamba TM, Li L, Gill RA, Islam F, Nawaz A, Ali B, et al. Differential subcellular distribution and chemical forms of cadmium and copper in *Brassica Napus*. *Ecotoxicol Environ Saf.* (2016) 134:239–49. doi: 10.1016/j.ecoenv.2016.08.021
61. Eder CS, Roberta de PM, Alexandra L, Marcelo M, Paulo AH, Zenilda LB. Effects of cadmium on growth, photosynthetic pigments, photosynthetic performance, biochemical parameters and structure of chloroplasts in the agarophyte *Gracilaria domingensis* (Rhodophyta, Gracilariaceae). *Am J Plant Sci.* (2012) 3:4. doi: 10.4236/ajps.2012.38129
62. Waisberg M, Black WD, Waisberg CM, Hale B. The effect of Ph, time and dietary source of cadmium on the bioaccessibility and adsorption of cadmium to/from lettuce (*Lactuca Sativa* L. cv. Ostinata). *Food Chem Toxicol.* (2004) 42:835–42. doi: 10.1016/j.fct.2004.01.007
63. Xu Q, Duan D, Cai Q, Shi J. Influence of humic acid on Pb uptake and accumulation in tea plants. *J Agric Food Chem.* (2018) 66:12327–34. doi: 10.1021/acs.jafc.8b03556
64. Montalvo D, McLaughlin MJ, Degryse F. Efficacy of hydroxyapatite nanoparticles as phosphorus fertilizer in Andisols and Oxisols. *Soil Sci Soc Am J.* (2015) 79:551–8. doi: 10.2136/sssaj2014.09.0373
65. Vijver MG, Van Gestel CAM, Lanno RP, Van Straalen NM, Peijnenburg WJ. Internal metal sequestration and its Ecotoxicological relevance: a review. *Environ Sci Technol.* (2004) 38:4705–12. doi: 10.1021/es040354g
66. Jiang HM, Yang JC, Zhang JF. Effects of external phosphorus on the cell ultrastructure and the chlorophyll content of maize under cadmium and zinc stress. *Environ Pollut.* (2007) 147:750–6. doi: 10.1016/j.envpol.2006.09.006
67. Chen X, Cui Y. Effects of dry and fresh states of *Brassica Chinensis* on the oral bioaccessibility of lead. *Asian J Ecotoxicol.* (2009) 4:793–9.
68. Wu Z, Mcgroutner K, Chen D, Wu W, Wang H. Subcellular distribution of metals within *Brassica Chinensis* L. in response to elevated Lead and chromium stress. *J Agric Food Chem.* (2013) 61:4715–22. doi: 10.1021/jf4005725
69. Campbell PGC, Giguère A, Bonneris E, Hare L. Cadmium-handling strategies in two chronically exposed indigenous freshwater organisms—the yellow perch (*Perca Flavescens*) and the floater Mollusc (*Pyganodon Grandis*). *Aquat Toxicol.* (2005) 72:83–97. doi: 10.1016/j.aquatox.2004.11.023



OPEN ACCESS

EDITED BY

Marco Iammarino,
Experimental Zooprophyllactic Institute
of Puglia and Basilicata (IZSPB), Italy

REVIEWED BY

Kangkan Saikia,
Ministry of Science and Technology, India
Facundo Ibañez,
National Institute for Agricultural Research
(INIA), Uruguay

*CORRESPONDENCE

Emanuel Vamanu
✉ emanuel.vamanu@gmail.com
Mahendra P. Singh
✉ mprataps01@gmail.com;
✉ mahendra.zool@ddugu.ac.in

†These authors have contributed equally to
this work

RECEIVED 23 November 2023

ACCEPTED 25 March 2024

PUBLISHED 17 April 2024

CITATION

Sajad M, Shabir S, Singh SK, Bhardwaj R,
Alsanie WF, Alamri AS, Alhomrani M,
Alsharif A, Vamanu E and Singh MP (2024)
Role of nutraceutical against exposure
to pesticide residues: power of bioactive
compounds.
Front. Nutr. 11:1342881.
doi: 10.3389/fnut.2024.1342881

COPYRIGHT

© 2024 Sajad, Shabir, Singh, Bhardwaj,
Alsanie, Alamri, Alhomrani, Alsharif, Vamanu
and Singh. This is an open-access article
distributed under the terms of the [Creative
Commons Attribution License \(CC BY\)](#). The
use, distribution or reproduction in other
forums is permitted, provided the original
author(s) and the copyright owner(s) are
credited and that the original publication in
this journal is cited, in accordance with
accepted academic practice. No use,
distribution or reproduction is permitted
which does not comply with these terms.

Role of nutraceutical against exposure to pesticide residues: power of bioactive compounds

Mabil Sajad^{1†}, Shabnam Shabir^{1†}, Sandeep Kumar Singh²,
Rima Bhardwaj³, Walaa F. Alsanie^{4,5}, Abdulhakeem S. Alamri^{4,5},
Majid Alhomrani^{4,5}, Abdulaziz Alsharif^{4,5}, Emanuel Vamanu^{6*}
and Mahendra P. Singh^{7,8*}

¹School of Bioengineering and Biosciences, Lovely Professional University, Phagwara, India, ²Indian Scientific Education and Technology Foundation, Lucknow, India, ³Department of Chemistry, Poona College, Savitribai Phule Pune University, Pune, India, ⁴Department of Clinical Laboratory Sciences, The Faculty of Applied Medical Sciences, Taif University, Taif, Saudi Arabia, ⁵Research Center for Health Sciences, Deanship of Graduate Studies and Scientific Research, Taif University, Taif, Saudi Arabia, ⁶Faculty of Biotechnology, University of Agricultural Sciences and Veterinary Medicine, Bucharest, Romania, ⁷Department of Zoology, Deen Dayal Upadhyay Gorakhpur University, Gorakhpur, India, ⁸Centre of Genomics and Bioinformatics, Deen Dayal Upadhyay Gorakhpur University, Gorakhpur, India

Pesticides play a crucial role in modern agriculture, aiding in the protection of crops from pests and diseases. However, their indiscriminate use has raised concerns about their potential adverse effects on human health and the environment. Pesticide residues in food and water supplies are a serious health hazards to the general public since long-term exposure can cause cancer, endocrine disruption, and neurotoxicity, among other health problems. In response to these concerns, researchers and health professionals have been exploring alternative approaches to mitigate the toxic effects of pesticide residues. Bioactive substances called nutraceuticals that come from whole foods including fruits, vegetables, herbs, and spices have drawn interest because of their ability to mitigate the negative effects of pesticide residues. These substances, which include minerals, vitamins, antioxidants, and polyphenols, have a variety of biological actions that may assist in the body's detoxification and healing of harm from pesticide exposure. In this context, this review aims to explore the potential of nutraceutical interventions as a promising strategy to mitigate the toxic effects of pesticide residues.

KEYWORDS

pesticides, nutraceuticals, reactive oxygen species, apoptosis, cytotoxicity

1 Introduction

Pesticides have become indispensable tools in modern agriculture, ensuring the protection of crops from pests and diseases, thus securing food production and global food security (1). Nevertheless, there are significant concerns about the unintended effects of pesticides on the environment and human health due to their widespread usage. Among these concerns, the presence of pesticide residues in food and water sources has emerged as a pressing issue, with potentially detrimental effects on both human and ecological systems

(2). On the other hand, nutraceuticals have gained significant attention as functional foods that offer potential health benefits beyond basic nutrition (3). Derived from natural food sources, nutraceuticals contain biologically active compounds, such as vitamins, minerals, antioxidants, and phytochemicals, which can promote health, prevent chronic diseases, and enhance overall wellbeing. The increasing demand for nutraceuticals stems from the desire to seek alternative approaches to traditional medicine for maintaining and improving health (4). However, the use of pesticides in conventional agricultural practices poses a significant challenge to the concept of food-based nutraceuticals. Pesticides, despite their intended purpose of safeguarding crops, can leave residues on fruits, vegetables, and other agricultural products. These residues can contaminate the food supply chain, leading to potential health risks for consumers (5).

The presence of pesticide residues in food has raised concerns about their adverse effects on human health. Some pesticides have been linked to various health problems, including developmental disorders, hormonal disruption, neurotoxicity, and even certain types of cancer. Thus, the substances used to protect and enhance food production can inadvertently become a threat to human health (6). In contrast, food-based nutraceuticals offer a promising solution to counterbalance the potential harm caused by pesticide residues (7). These natural compounds found in fruits, vegetables, whole grains, and other food sources possess significant antioxidant and anti-inflammatory properties (8). They can help combat oxidative stress, neutralize harmful free radicals, support immune function, and contribute to overall health and wellness. The key challenge lies in minimizing pesticide residues in food products to ensure the safety and efficacy of nutraceuticals (9). Adopting sustainable agricultural practices, such as organic farming, integrated pest management (IPM), and precision agriculture, can reduce reliance on synthetic pesticides and promote the production of cleaner, pesticide-free crops (10). The use of pesticides in agricultural practices raises concerns about their potential impact on human health and the environment. While pesticide residues can pose risks, food-based nutraceuticals derived from natural sources offer a potential solution to counteract these risks (11). By adopting sustainable agricultural practices and ensuring strict monitoring, it is possible to reduce pesticide residues and promote the production of safe, nutrient-rich crops. Striking a balance between the benefits of pesticides in crop protection and the potential harm they may cause is crucial for ensuring a healthy and sustainable food system (12).

The global pesticide consumption in 2019 was approximately 4.19 million metric tons, where China was by far the largest pesticide-consuming country (1.76 million metric tons), followed by the United States (408 thousand tons), Brazil (377 thousand tons), and Argentina (204 thousand tons) (13). In southeast Asia, the WHO reported an annual increase in pesticide usage, with 20% of developing countries as pesticide consumers, including Cambodia, Laos, and Vietnam. India belongs to one of the major pesticide producing countries in Asia, having 90 thousand tons annual production of organochlorine pesticides including benzene hexachloride (14).

An increase in the usage of pesticides can cause endocrine and neurological disturbances, influencing development, reproduction, and the immune system (15). Pesticides may also influence fundamental regulatory and homeostatic systems, drive reactive

oxygen species (ROS)-induced alteration of cellular components, and deplete antioxidant mechanisms, all of which contribute to the occurrence of oxidative stress (16). This review highlights various studies and research that have explored the presence of pesticide residues in food and their potential health implications. It delves into the adverse effects of chronic pesticide exposure, such as neurotoxicity, endocrine disruption, and carcinogenicity, among others. Additionally, it discusses the mechanisms by which pesticide residues can accumulate in the human body and the challenges associated with regulating their usage and monitoring their presence in food.

2 Classification of pesticides

Pesticides are categorized according to their toxicological attributes (17). The World Health Organization (WHO) has created a generally accepted pesticide classification system based on acute toxicity values. This method divides pesticides into four categories:

Class I: highly hazardous pesticides. They have high acute toxicity and constitute a serious risk to human health. Organophosphates and carbamates are examples (18).

Class II: moderately hazardous pesticides. They have moderate acute toxicity and constitute a substantial risk to human health. Some pyrethroids and herbicides are examples (19).

Class III: slightly hazardous pesticides. They have modest acute toxicity but can still be dangerous. Fungicides and insecticides are two examples (20).

Class IV: unlikely to present an acute hazard. Pesticides in this class have low toxicity. Some herbicides and insecticides are examples (21).

Here, we discuss that the classification of pesticides as highly hazardous is often based on their acute toxicity, which refers to the immediate detrimental effects that might emerge following short-term exposure. Pesticides designated very toxic can cause serious health problems even at modest levels of exposure (22).

2.1 Organochlorine

Organochlorine insecticides are organic compounds that are linked to five or even more chlorine atoms (also known as chlorinated hydrocarbons). They are used in agriculture and were among the first pesticides developed (23). There are two types of organochlorides: DDT-type substances and chlorinated alicyclic substances, comprising bornanes, cyclohexanes, and cyclodienes. Organochlorine is also a broad category of chlorinated hydrocarbons, which also includes chlorinated compounds of hexachlorobenzene (HCB), diphenyl ethane, cyclodiene (aldrin, endrin, and dieldrin), hexachlorocyclohexane (or lindane), nonachloride, chlordane, heptachlor, and heptachlor epoxide (24). Such chemicals have bioaccumulated in nature as a result of their extensive use, lipophilic nature, persistence, and narrow-spectrum action (25). The primary site of action for these substances or their metabolites in humans is the central nervous system, where

they alter the electrophysiological characteristics and enzymatic neuronal membranes. These changes in the dynamics of Na^+ and K^+ flow through the cell membranes of neurons result in the propagation of multiple nerve impulses for each external stimulus, which can cause symptoms such as seizures and acute respiratory poisoning or even death from respiratory failure (26).

2.2 Organophosphates

They are phosphoric acid esters, which are classified as wide-spectrum insecticides because they contain a diverse range of compounds (27). This class of compounds is differentiated by the covalent substitution of one of the four carbon-oxygen-phosphorus links of phosphate ester with the carbon-phosphate bond (28). Organophosphorus insecticides fall under a variety of other chemical categories, such as organothiophosphate, aliphatic amide, aliphatic organothiophosphate, oxime organothiophosphate, benzotriazine organothiophosphate, heterocyclic organothiophosphate, benzothiopyran organothiophosphate, isoxazole organothiophosphate, benzotriazine organothiophosphate, isoxazole organothiophosphate, pyrimidine organothiophosphate, pyridine organothiophosphate, thiadiazole organothiophosphate, quinoxaline organothiophosphate, triazole organothiophosphate, phosphonate phosphonothioate, phenyl organothiophosphate, phenyl ethylphosphonothioate, phosphoramidate, phenylphosphonothioate, phosphorodiamide, and phosphate oramidothioate (19). Organophosphorus pesticides include mipafox, diazinon, chlorpyrifos, ethion, dichlorvos, malathion, parathion, and fenthion. The cholinesterase-inhibiting effects of organophosphorus pesticides on invertebrates and vertebrates result in acetylcholine neurotransmitter superimposition across synapses. Because nerve impulses are unable to cross the synapse, voluntary muscles contract quickly, resulting in paralysis and death (18).

2.3 Carbamates

Pesticides made from organic carbamic acid are known as carbamates. These compounds comprise aminocarb, carbaryl, and carbofuran (29). Similar to carbamates, organophosphate pesticides also work by interfering with nerve signal transmission and destroying pests by poisoning them (30). Aldicarb, trimethacarb, carbofuran, carbaryl, propoxur, ethionocarb, methomyl, oxamyl, pirimicarb, and fenobucarb are common substances that cause hazardous exposure (31).

2.4 Pyrethroid

They are synthesized derivatives of natural pyrethrin. Compared to natural pyrethrins, they are more reliable and have prolonged residual effects (32). Although they are moderately poisonous to mammals, they are extremely detrimental to insects. For instance, cyclomethrin and decamethrin come under the pyrethroid category (33).

Overall, the classification of pesticides as highly hazardous serves as a crucial tool for identifying and managing the risks associated with their use. It emphasizes the significance of taking preventative precautions, following correct handling rules, and moving to safer and more sustainable pest management practices (34).

2.5 Pesticide exposure

Previous report demonstrated that pesticide exposure contributes to over 300,000 deaths worldwide annually (35). It is characterized by a state in which an individual ingests or inhales any pesticide beyond its threshold levels, which causes adverse effects. Pesticides can penetrate the organism by inhalation, contact with skin, and ingestion. Pesticide exposure can be occupational, as people who work in forestry, agriculture, the pesticide industry, and pesticide application are exposed to pesticides on the job (36). Domestic use (clothing) and dietary intake of tainted food and drink are the sources of nonoccupational exposure, which can lead to significant complications as they are absorbed by the environment and food chain. Although they can be eliminated through the skin, exhaled, and urine, pesticides are transported throughout the body by the bloodstream (37). Pesticides can penetrate the body through the mouth, skin, eye, and respiratory routes, which are the four most prevalent entry points. Pesticides are an essential component of fundamental agricultural processes all over the world, and farmer exposure to them is an inevitable occupational hazard (38). Farmers, according to various studies, are more prone to neurological, digestive, retinal, respiratory, and reproductive disorders than the general population and it is suspected to be influenced by the regular exposure to harmful chemicals but not only, as other factors related to way of life and hard work are also affecting their health (34). Pesticide exposure can cause immediate health problems such as acute poisoning, nausea, eye irritation, pain, and headaches. Diabetes, cancer, asthma, and other medical disorders might develop as a result of prolonged exposure. Pesticide exposure has a negative impact based on the quantity of pesticide used and the period of its retention, i.e., how prolonged it stays there. We are repeatedly exposed to pesticides in our regular activities, either directly or indirectly (39).

3 Mechanism of oxidative stress caused by some pesticides

Exposure to pesticides and many chemicals can lead to oxidative stress in living organisms. Oxidative stress occurs when there is an imbalance between the production of ROS and the body's antioxidant defense mechanisms. Pesticides can induce oxidative stress through various mechanisms (35). Some pesticides (such as rotenone) can directly generate ROS, such as superoxide anion ($\text{O}_2^{\cdot-}$), hydrogen peroxide (H_2O_2), and hydroxyl radicals ($\cdot\text{OH}$). These ROS can damage cellular components, including lipids, proteins, and DNA, leading to oxidative stress. Pesticides can deplete the body's antioxidant defenses, including enzymes such as superoxide dismutase (SOD), catalase (CAT), and glutathione peroxidase (GPx) (40). These enzymes play a crucial role in

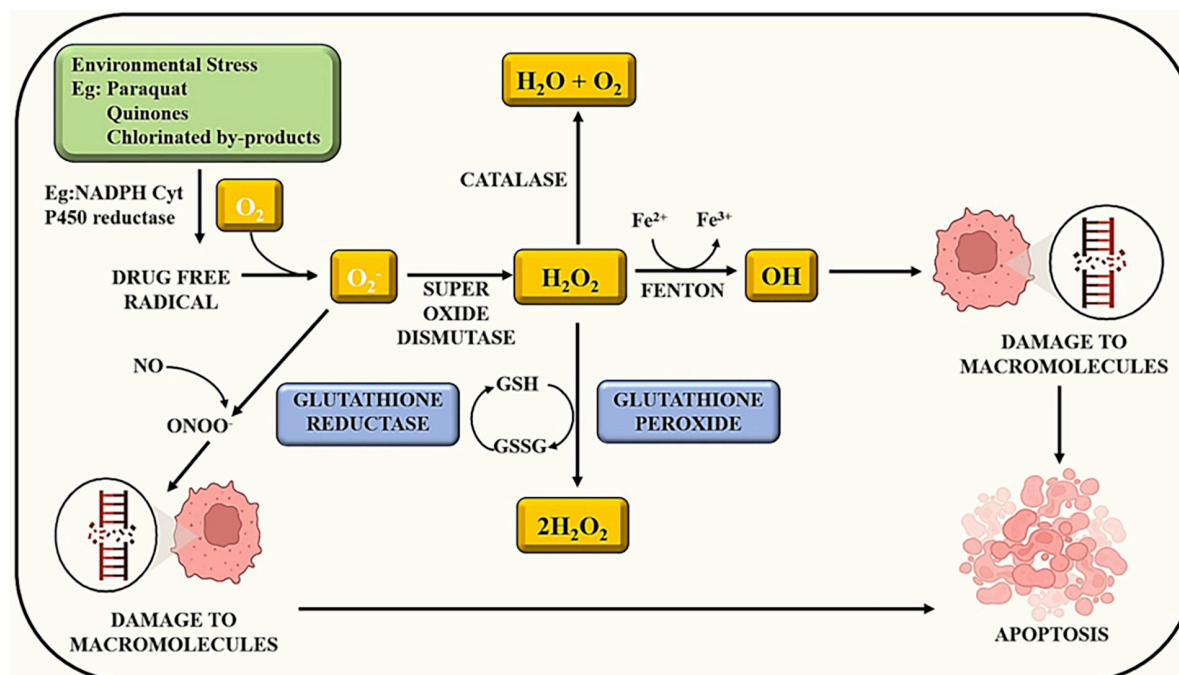


FIGURE 1

Chemical exposure induces reactive oxygen species and alters other signaling cascades, which results in cell apoptosis.

neutralizing ROS. Pesticides can inhibit or reduce the activity of these enzymes, impairing the antioxidant defense system. Some pesticide exposure can lead to lipid peroxidation; a process in which ROS attack and damage lipid molecules in cell membranes. This process generates lipid peroxides, which further exacerbate oxidative stress and cause membrane dysfunction. Some pesticides can directly interact with DNA, causing oxidative damage to DNA molecules (41). This can lead to mutations, DNA strand breaks, and impaired DNA repair mechanisms, which contribute to cellular dysfunction and oxidative stress. Some Pesticides can disrupt mitochondrial function, leading to increased ROS production. Mitochondria are a major source of ROS generation in cells. Pesticide-induced mitochondrial dysfunction can impair the electron transport chain, leading to increased electron leakage and ROS production. Pesticide exposure can trigger inflammation in tissues and organs. Inflammatory cells produce ROS as part of the immune response, contributing to oxidative stress. Pesticide-induced inflammation can further promote oxidative damage and disrupt cellular homeostasis (42).

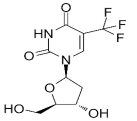
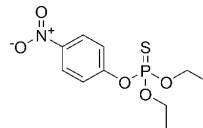
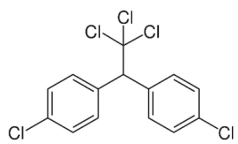
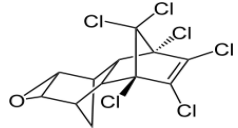
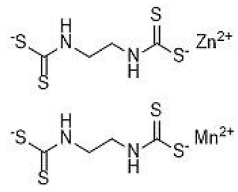
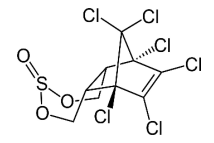
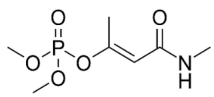
Exposure to certain chemicals or toxins can initiate a cascade of events within cells. Some compounds have the potential to produce reactive oxygen species. Oxidative stress develops when there is an imbalance between the creation of ROS and the ability of cells to detoxify them. ROS can cause damage to biological structures such as lipids, proteins, and DNA. ROS can disrupt several signaling pathways within the cell. ROS, for example, can trigger signaling cascades involving transcription factors such as NF- κ B and AP-1, which influence gene expression in inflammation and cell survival (43). Apoptosis, also known as programmed cell death, is a natural mechanism that aids in the elimination of damaged or undesirable cells. Apoptosis

can be triggered by excessive oxidative stress and disrupted signaling cascades. This is a defense mechanism designed to keep injured cells from causing more harm as illustrated in Figure 1 (25). Overall, the sequence of events demonstrates the complex link between chemical exposure, oxidative stress, altered signaling, and cellular responses (19). Understanding how pesticides cause oxidative stress can aid in the development of ways to minimize their adverse effects and encourage safer pesticide use (Table 1).

In contrast, high ROS concentrations cause cellular biomolecule damage, which results in the emergence of numerous illnesses (65). The human body contains a number of defense systems to mitigate the harm caused by oxidative stress. Antioxidative agents' action is the primary mechanism (66). Since they are stable enough to eliminate free radicals by donating electrons, antioxidants are molecules that prevent or limit oxidative injury (67). Many substances have recently been discovered to have antioxidative properties, but the human body has two types of antioxidant defense systems: enzymatic and nonenzymatic. By preserving a physiologic amount of ROS, they defend both cellular structural integrity and performance from ROS harm (68). The enzymatic antioxidants include catalase (present in peroxisomes), glutathione peroxidase, which contains selenium (Se-GPX) and resides in the matrix of mitochondria and cytosol, and glutathione reductase (GSH-R), which is considered a key enzyme for the glutathione (GSH) redistribution pathway. Copper and zinc-containing SOD (Cu, Zn-SOD) is present in peroxisomes and CAT. These factors maintain the cellular homeostasis of the human body (54).

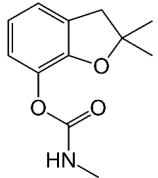
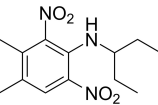
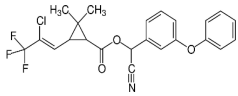
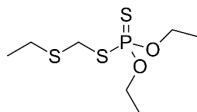
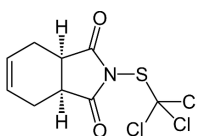
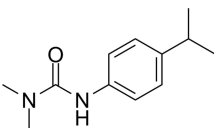
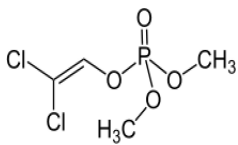
Elevated levels of oxidative stress and endocrine disruption have been linked to pesticide actions in the human body. Exposure

TABLE 1 Some examples of well-known pesticides and their oxidative stress response and related toxicity.

S No.	Name of pesticides	Chemical structure	Used for crop	Cellular responses	References
1	Triflorin		Glycine max, citrus, and <i>Coffea arabica</i>	It can induce microtubules in <i>Oreochromis niloticus</i> and is genotoxic to mice and <i>Drosophila melanogaster</i> . In humans it is fighting leishmaniasis.	(44)
2	Parathion		Barley, canola, corn, cotton, sorghum, sunflowers, and wheat	It causes immunotoxic reactions such as enhanced <i>in vitro</i> lymphocyte apoptosis, lowers IgM and germ cells center-positive B-lymphocyte numbers as well as antigen-specific immunotoxicology IgM responses.	(45)
3	DDT		Beans, sweet, potatoes, peanuts, cabbage, tomatoes, and cauliflower	In both humans and laboratory animals, dichlorodiphenyltrichloroethane (DDT) and its metabolite dichlorodiphenyldichloroethylene (DDE) have been linked to an increased risk of insulin resistance and obesity.	(46)
4	Dieldrin		Corn, cotton, and citrus fruit	Through a nuclear receptor CAR-mediated method of action, it causes liver cancers in mice.	(47)
5	Mancozeb		Tree fruits, vegetables crops, field crops, nuts, and ornamentals	In mice exposed to (mancozeb) MCZ, the ovarian structure was harmed, and apoptosis was elevated. MCZ can affect the abnormal function of mitochondrial respiratory chain, lead to oxidative phosphorylation decoupling, produce oxidative stress, and finally cause ovarian injury and apoptosis in mice.	(48)
6	Endosulfan		Soybean	Endosulfan was found to cause DNA damage in grass carp (<i>Ctenopharyngodon idella</i>).	(49)
7	Monocrotophos		Maize, rice, sugarcane, cotton, groundnut, soybeans, and vegetables	In nematodes (<i>Caenorhabditis elegans</i>) and arthropods (<i>Culex quinquefasciatus</i>), causes paralysis, acetylcholine inhibition, increased micronuclei, and a decrease in the DNA/RNA ratio.	(50)

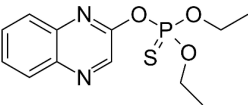
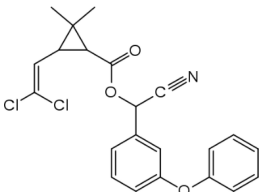
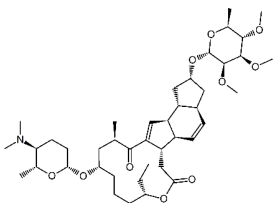
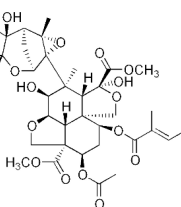
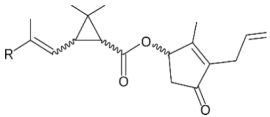
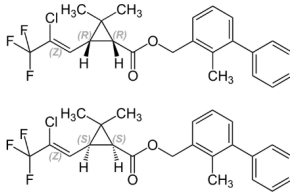
(Continued)

TABLE 1 (Continued)

S No.	Name of pesticides	Chemical structure	Used for crop	Cellular responses	References
8	Carbofuran		Potatoes, corn, soybeans, strawberries, grapes, wheat, and alfa-alfa	Because to its anticholinesterase function, which blocks the action of acetyl-cholinesterase and butyrylcholines, it is exceedingly deadly to animals, birds, fishes, and other species. Carbofuran is linked to endothelial dysfunction, anomalies in the reproductive cycle, and cytotoxicity and mutagenicity effects in humans.	(51)
9	Pendimethalin		Cereals, legumes, and vegetable crops	ROS production, apoptosis induction, and DNA damage were all detected in rat bone marrow and human lymphocytes.	(52)
10	Cyhalothrin		Cotton, cereals, hops, ornamentals, potatoes, and vegetables	It binds to the voltage-gated sodium channel in nerve and tremors in poisoned insects. Due to this insect lose control on nervous system.	(53)
11	Phorate		Corn, sugar beets, cotton, coffee, potatoes, beans, wheat, some ornamental peanuts, herbaceous plants, and bulb	It is observed in comet assay that the exposure of phorate to human lymphocytes results in DNA damage.	(54)
12	Captan		Apples, peaches, strawberries, almonds. Ornamental plants, turf, and seeds	Apoptotic and necrotic cell death caused by captan, it increases the intrinsic Ca^{2+} and Zn^{2+} , also increases hydrogen peroxide cytotoxicity and reduce the levels of cellular thiol compounds prior to cell death.	(55)
13	Isoproturon		Wheat, cereal, sugarcane, citrus, cotton, and asparagus	Isoproturon boosted kidney and heart weight while decreasing epididymis weight. Organ histopathological changes were dose dependent.	(56)
14	Dichlorvos		Cotton, coffee, tea, and cocoa	Elderly male Swiss mice exposed to dichlorvos experience reactive oxygen species generation, altered gene expression for acetylcholinesterase (AChE), and significantly higher levels of protein carbonyl content (PCC) and thiobarbituric acid reactive substances.	(57)

(Continued)

TABLE 1 (Continued)

S No.	Name of pesticides	Chemical structure	Used for crop	Cellular responses	References
15	Quinalphos		Wheat, rice, coffee, sugarcane, and cotton	Low expression of antioxidant biomarkers in the kidney tissue of wistar rats, which include total thiol groups, glutathione s-transferase, superoxide dismutase, glutathione peroxidase, catalase, and glutathione reductase, as well as enhanced thiobarbituric acid reacting substance levels, suggested that considerable oxidative damage to the renal tissue happened after multiple doses of quinalphos.	(58)
16	Cypermethrin		Cotton and fresh vegetables	In zebra fish, it has been found that there is a decrease in egg production, a delay in the growth of gonadotropins, significant changes in the levels of plasma 17-estradiol (E2) and testosterone, disruption of the release of sex hormones, and anomalies in the gene expression of the thalamic axis.	(59)
17	Spinosad		Cotton, corn, soybeans, and tomato	Due to Spinosad injection inhibition of acetylcholinesterase in the liver and brain of <i>Oreochromis niloticus</i> . Spinosad induces fast stimulation of the organism's nervous system by stimulating γ-aminobutyric acid (GABA) and nAChR receptors, resulting in paralysis and death.	(60)
18	Azadirachtin		Tomatoes, cabbage, potatoes, cotton, tea, tobacco, coffee, and protected crops	In silkworm, the Sf9 cell line's Ca ²⁺ Mg ²⁺ ATPase activity was significantly increased by azadirachtin, indicating that the calcium signaling pathway may be involved in growth control and the process of death in the prothoracic gland.	(61)
19	Pyrethroid		Cotton, tea, and vegetables	Pyrethroid produce oxidative damage in fish species such as tilapia, carp, and trout through ROS-mediated mechanisms.	(62)
20	Bifenthrin		Bananas, apples, pears, and ornamentals	Bifenthrin has the capacity to cause severe oxidative stress (lipid peroxidation) in the kidney, lung, and liver of rats and in insect <i>Spodoptera frugiperda</i> , it causes DNA damage and autophagy, and reduces viability of Sf9 cells.	(63, 64)

to pesticides is a major factor in the rise in oxidative stress, which might change a person's susceptibility to diseases. They have been discovered in the human placenta and have been linked to increased oxidative stress, intrauterine limitation, and decreased birth weight. In particular, lipid peroxidation (one of the key oxidative stress markers) and cytotoxicity have been observed in humans, primarily in pregnant women and agricultural producers (69). However, studies utilizing pesticides on mammals that directly connect the lethality of the contaminants and oxidative stress are exceedingly rare. As a result, research employing human cell lines started, and it is now being done more often. The effects of pesticides on the extent of oxidative stress in human tissues and changes in the endocrine system were demonstrated using human cell cultures. The precise action mechanisms of phenoxy analogs, triazolo pyrimidines, triazines, dinitroanilines, imidazolines, and other types of fungicides and insecticides are typically difficult to pinpoint. Particularly in cases where the effect is brought on by a dose of environmental exposure, these pathways in humans are not well understood (70).

As previously noted, in human cell lines, the oxidative stress variables under the action of pesticides were studied. It was discovered that the herbicide MCPA (4-chloro-2-methylphenoxyacetic acid) is carried across the membranes of Caco-2 cells, which is a useful study model of the human digestive tract. Caco-2 cells cultivated on semipermeable membranes were utilized to examine and characterize the mechanisms of transcellular transport of MCPA across the small intestine, where pesticides are absorbed (71). Another study looked at the impact of the sodium salts of 2,4-D-Na and 4-chloro-2-methylphenoxyacetic acid (MCPA-Na), two extensively used phenoxy herbicides, on the amount of carbonyl groups in protein substrates in erythrocytes. Because of their biological and structural simplicity, making them particularly suited for research on specific xenobiotic toxicity, human erythrocytes were chosen as such an experimental animal model (68). The results of the experiments showed that the location of the hydroxyl in the phenol ring has a significant impact on the pro-oxidative activity of phenoxy herbicides. According to previous literature, paraquat (1,1-dimethyl-4,40-bipyridinium chloride), one of the most commonly used herbicides, causes mitochondrial dysfunction in human bronchial BEAS-2B cells. Because these cells were developed from normal healthy bronchi, they are a suitable model system to investigate the pathogenic mechanisms of oxidative stress-induced respiratory ailments caused by pesticides. Furthermore, the mechanisms behind oxidative stress are frequently studied using this cell line (72).

4 Signaling mechanism related with oxidative stress in some pesticides

Although some pesticide exposure is acute or chronic, a number of events comprising various cellular pathways, including alterations in gene activation, expression, or suppression, take place (73). The exact molecular mechanism by which this happens is still unknown. Understanding the molecular and cellular level alterations is essential for determining the primary pathways associated with the induction of oxidative stress due to some

pesticides and evaluating potential defensive medications or therapies (74).

4.1 TNF- α pathway

According to several investigations, one of the potential mechanisms responsible for oxidative stress is the death receptor pathway (75). The signaling of caspase-8, which catalyzes the breakdown of the caspase-3 effector either indirectly or directly through the mitochondrial pathway, is brought on by the conjugation of cell surface death receptors, including the tumor necrosis factor receptor (TNFR), which facilitates the transmitted signal of tumor necrosis factor-alpha (TNF- α). TNF- is a potent pro-inflammatory cytokine that is produced during inflammation by macrophages and monocytes and is in control of many cell signaling pathways that trigger necrosis or apoptosis (76). The association between TNF- α and the two cell surface receptors TNF-R1 and TNF-R is what causes the inflammatory responses that it triggers. TNF- α is also responsible for the activation and transcription of adhesion molecules, the stimulation of inflammatory cytokines, and the promotion of growth. The mouse fibrosarcoma cell line (L929) could experience mitochondrial dysfunction and ROS production as a result of increased TNF- α levels alone (77). Based on an experiment on mice exposed to permethrin, a rise in TNF- levels induces ROS generation and reduces the redox equilibrium, which causes oxidative stress (78). Permethrin also enhanced TNF-mRNA expression in zebrafish exposed for a period of 72 h after fertilization in a concentration-dependent manner (65).

4.2 NF- κ B and Nurr1 pathway

The transcription factor orphan nuclear receptor-related 1 (Nurr1), a constituent of the nuclear receptor subclass 4 group A member 2 (NR4A2) family of proteins, is crucial for dopaminergic neuron metabolism. New research suggests that decreased Nurr1 activity may play a role in Parkinson's disease etiology. In brain cells, Nurr1 prevents NF-B (transcription factor NF-B), which has anti-inflammatory properties (79). The pro-inflammatory nuclear factor-B, i.e., transcription factor, is expressed more, while the Nurr1 gene expression is lowered by permethrin (80). Permethrin (insecticide) enhanced the production of the pro-inflammatory cytokine TNF- and inhibited the expression of IL-13, IL-2, and IL-1 in an additional investigation in older treated rats. These findings suggest that the Nurr1, NF- κ B, and TNF- α pathways may contribute to understanding some pathways associated with oxidative stress caused by pesticides (81).

4.3 STAT

According to a plethora of studies, chlorpyrifos (CPF) weakens antioxidant defenses by interfering with the electron transport chain in mitochondria (ETC) complex 1 activity, which increases the formation of free radicals and superoxide. According to an

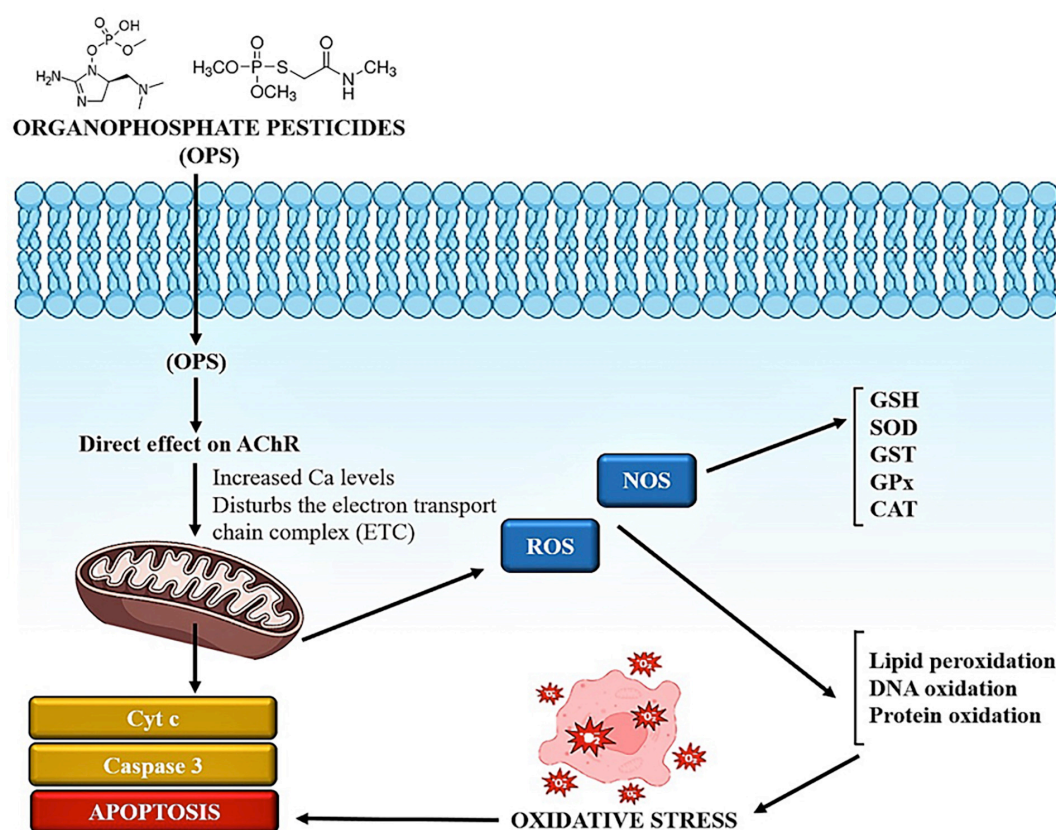


FIGURE 2

The role of oxidative stress in pesticide-induced toxicities.

earlier investigation, CPF increased cell mortality in a dose-dependent manner and caused oxidative stress by increasing ROS production and lowering GSH levels in dopaminergic neurons and human mesencephalic cells (82). The team hypothesized that signaling transducers and activators of transcription 1 (STAT-1) regulate CPF-induced ROS production and that higher ROS ultimately result in cell apoptosis based on the findings of CPF-induced dopaminergic cell damage (Figure 2). Apoptotic cell mortality subsequently results from increased reactive oxygen species. STAT proteins are members of a group of latent cytoplasmic transcriptional regulators that are crucial for cell type-specific differentiation, growth, apoptosis, and multiplication. Both neuronal viability and cell death depend on Janus kinase (JAK)-STAT signaling (83). The activation of JAK that results from the binding of mediators to their receptors phosphorylates STAT-1 on serine 727 and tyrosine 701 residues. Phospho STAT-1 dimerizes and moves into the nucleus, where it attaches to the GAS/ISRE found on the coding region of particular target genes that control NADPH oxidase (NOX), pro-inflammatory cytokines, apoptosis, and regulators of cell cycle arrest such as fas, caspases, and bax. Proapoptotic gene transcription-dependent expression as well as non-transcriptional signal transduction pathways are regulated by STAT-1 to control apoptosis. In yet another study, when organophosphate pesticides (OP) pesticides were used on STAT-1 suppression (KD) dopaminergic cells, they caused a 66% reduction in mitochondrial ROS levels compared to scrambled tiny interfering RNA (siRNA)-transfected cells subjected

to identical pesticides (84). NOX-1, an NADPH oxidase isoform that produces superoxide, controls the production of ROS in a variety of cell types, including but not limited to monocytes, macrophages, vascular endothelial cells, and smooth muscle cells. The primary ROS-producing enzyme throughout inflammation is NOX1. The fact that OP pesticides boosted the recruitment of STAT-1 to the constitutive NOX1 promoter suggests that STAT-1 is responsible for controlling the transcription of NOX1. In neural cells exposed to the OP pesticide CPF, STAT-1 is critical in controlling ROS production as well as GSH levels in a NOX1-dependent manner. In human monocytes, organochlorine pesticides increased NOX-dependent ROS production. These findings collectively imply that NOX-STAT-1 activation is critical for the production of ROS during OP pesticide-induced oxidative damage (85).

4.4 Endoplasmic reticulum stress

Assembly, folding, posttranslational alteration, and protein transport are only a few of the many tasks performed by the endoplasmic reticulum (ER). Additionally, calcium, which is necessary for muscular contractions, is stored in the ER. When the ER's (86) aptitude for folding peptides is exceeded, ER stress results, and cells with ER stress are characterized by a build-up of abnormal proteins within the ER lumen. Numerous factors, such as hypoxia, nutritional scarcity, and

pesticides, can cause ER stress. Cellular senescence might be produced in the event that ER stress is substantial or prolonged. It has been demonstrated that a number of pesticides, including 2,4-dichlorophenol, paraquat, chlorpyrifos, and deltamethrin, cause ER stress. Numerous of these pesticides also cause apoptosis, although research indicates that ER stress and apoptotic cell death are caused by separate chemical mechanisms (78).

4.5 Mitochondrial dysfunction pathway (mitochondrial apoptosis)

Mitochondrial dysfunction is a typical oxidative stress-related malfunction. ROS can induce mitochondrial damage in some circumstances, but they can also cause mitochondrial damage in other circumstances. Numerous pesticides have been found to block mitochondrial ensembles, which are the primary site for ROS generation (87). As a result, it is believed that the ROS generated by damaged mitochondria play a significant role in oxidative stress. In both mammals and fish, ER stress and apoptosis are frequently linked to mitochondrial malfunction (65). Pentachlorophenol (PCP) and its metabolite tetrachlorohydroquinone (TCHQ) massively increased lipid oxidation in the rat liver and lowered the antioxidant GSH level by producing large amounts of urine 8-iso-prostaglandin-F2 (8-iso-PG-F2). The mitochondrial apoptotic pathway is another possible mechanism that may be implicated in pesticide such as atrazine (ATR), organophosphorus (OP) compounds, carbamates, and pyrethroids induced mitochondrial dysfunction, according to the available and developing evidence (88). The primary regulators of mitochondrial coherence in this system are B-cell lymphoma 2 (BCL2) and BCL2-associated X (BAX). They also affect the release of cytochrome c and the activation of caspase. Several well-known proteins linked to cell damage, BAX and BCL2, have opposing roles. In contrast to the BAX peptide, which acts as an apoptosis activator, the BCL2 protein suppresses apoptosis by its own antioxidative action (89). Following mitochondrial injury, Bax is translocated from the cytoplasm to the mitochondria, and Bcl-2 expression is significantly reduced. Mitochondrial cytochrome c is released into the cytoplasm, which is a crucial terminal event, as a result of high amounts of ROS from exposure to pesticides. TCHQ increased the transcription of Hsp70 in hepatocytes while decreasing the expression of the BCL2/BAX ratio and cellular apoptotic sensitivity (CAS), two genes involved in apoptotic and necrotic processes (90).

5 Relationship of the toxicity of some pesticides with alteration of oxidative balance

5.1 Neurotoxicity

Neurotoxins are any compounds that can damage the central nervous system, along with the brain (80). The brain is particularly prone to OP toxicity, which disrupts the balance of oxidant

and antioxidant components in neuronal cells (91). OPs have a strong pro-oxidant action that disrupts neuronal mitochondrial function, resulting in a variety of neurological disorders. Higher level exposures from occupational exposures and closeness to agricultural spraying are linked to a variety of neurotoxicity in people (92).

Human neurodegenerative disorders and neurotoxicity have been associated with pyrethroid pesticides, organochlorine insecticides, and organophosphate insecticides. DDT has low toxicity (rat oral LD₅₀ = 113 mg/kg) (93). Furthermore, oral administration of 3.5 or 35 mg DDT/day to people for up to 18 months did not result in observable toxicity or neurotoxicity. Only a few human studies have examined DDT's possible neurotoxicity. DDT was identified more frequently in the brains of Alzheimer's sufferers. Nonoccupational DDT exposure can potentially result in cognitive impairments (94). Dieldrin caused substantial oxidative stress, mostly owing to mitochondrial malfunction, and was associated with considerable caspase overexpression and activation, resulting in apoptosis (95). Dieldrin-induced dopaminergic neurotoxicity is caused by caspase-3-dependent proteolytic cleavage of protein kinase C (PKC δ) (96). Dieldrin has also been shown to cause epigenetic dysregulation in cell and animal models of dieldrin neurotoxicity by hyperacetylation of core histones. Endosulfan is very neurotoxic in rats, inducing both chronic neurodegeneration and developmental neurotoxicity.

Aside from inducing apoptotic cell death through mitochondrial dysfunction. According to research (97), rats gavaged with 2 mg/kg endosulfan for 6 days had damaged brain mitochondria, as evidenced by significantly lower levels of SOD, GSH, and CAT, as well as enhanced lipid peroxidation.

5.2 Disruption of the endocrine system

Every hormone has a different molecular structure and a unique production process with numerous phases. The production of the hormone may be impaired or the characteristics of the hormones may change if one component or link in the chain of hormone synthesis is disrupted. Some pesticides, including prochloraz, fenarimol, and other fungicides (imidazole), have the capacity to block testosterone to oestrogen conversion by inhibiting cytochrome 19 aromatase *in vitro* (98). It was predicted that substances that may decrease the activity of aromatase *in vitro* might also be able to alter local oestrogen and androgen levels *in vivo*. Aromatase induction is a biological method of xenobiotic deactivation that does not typically result in toxicity. *In vitro* aromatase function is induced by the pesticides simazine, atrazine, and propazine. It has been proven that p,p-DDE induces aromatase both *in vivo* and *in vitro*. Additionally, the pesticide heptachlor may operate as an inducer of testosterone 16- α and 16- β hydroxylases, although pirimicarb, methomyl, iprodione, and propamocarb can only slightly stimulate aromatase activity (99). Dopamine- β -hydroxylase activity has been demonstrated to be suppressed by thiram, sodium N-methyl-di-thio-carbamate (SMD), and other di-thio-carbamates, which results in a reduced conversion of dopamine to norepinephrine. This might affect the hypothalamic catecholamines that produce the proestrus surge in

lutinizing hormone, which triggers the last stages of ovulation. It was determined that SMD has the ability to prevent rat ovulation and the LH surge. Ketoconazole blocks the synthesis of progesterone as well as a number of cytochrome 450-dependent monooxygenase enzymes (100).

5.3 Carcinogenicity

The large percentage of pesticides poses a risk to nontarget organisms, including humans. In laboratory animals, 56 pesticides have been identified as cancer-causing. In clinical studies, chemicals such as lindane, phenoxy acid herbicides, toxaphene, and several organophosphates have been linked to cancer (101). Due to the destructive effects of genotoxic substances, cellular genetic components (DNA and RNA) lose their genotoxic characteristics.

It has been studied *in vivo*, *in vitro*, and epidemiologically that certain pesticides can cause genomic toxicity (102). This genotoxicity is viewed as a fundamental health concern that, with repeated exposures, will have long-term consequences on reproductive, neurological, and cancerous systems. Pesticide use might cause mutagenic and non-mutagenic processes that cause genetic changes. Several studies have revealed a strong link between chronic pesticide exposure and a few proto-oncogenes in populations exposed owing to pesticide cytogenetic effects (103). It is linked to an increased risk of leukemia and non-lymphoma, Hodgkin's as well as cancers of the brain, skin, thyroid, esophagus, kidney, lung, prostate, testicles, cervix, bladder, and rectum (104). These may cause oxidative stress, which results in the production of free radicals and changes in enzymatic antioxidants such as catalase, glutathione transferase and SOD (105).

6 Nutraceuticals and bioactive compounds from medicinal plants

Medicinal plants have traditionally been utilized by humans as a traditional way of treating a variety of diseases. Despite significant improvements in therapeutic development, there is still a need for effective and potent analgesic drugs (106). In this context, it has been widely described that numerous plant-derived compounds serve an essential part in the process of developing novel techniques to treat various diseases. Recent research on herbal plants or medicine has resulted in significant advances in the pharmacological assessment of diverse plants utilized in traditional medical systems (107). Secondary metabolites or substances found in medicinal plants include tannins, terpenoids, alkaloids, and flavonoids, which determine the therapeutic effectiveness of the plant, particularly its antioxidant activity. Secondary metabolites are very diverse low molecular weight substances with a wide range of biological characteristics that interact with proteins, nucleic acids, and other bio membranes and are active and volatile targets of cells (108).

Herbal remedies play a crucial part in healthcare and have various therapeutic applications. Here are some key reasons highlighting the importance of medicinal plants and their therapeutic applications:

6.1 Traditional medicine

For ages, medicinal plants have been employed in traditional medical systems including Ayurveda, Traditional Chinese Medicine, and Indigenous healing practices. They form the foundation of these systems and have been trusted for their healing properties by communities worldwide (109).

6.2 Rich source of bioactive compounds

Medicinal plants contain numerous bioactive compounds including flavonoids, alkaloids, terpenoids, and tannins, which possess medicinal properties. These compounds can have diverse impacts on the human health, including analgesic, anti-inflammatory, antimicrobial, antioxidant, anticancer, and antidiabetic activities (110).

6.3 Drug discovery and development

Many modern pharmaceutical drugs are derived from or inspired by medicinal plants. Natural plant substances serve as the foundation for the creation of novel drugs. Examples include the use of the plant-derived compound paclitaxel for cancer treatment and the development of aspirin from willow bark (111). Medicinal herbs are often the primary source of healthcare in many developing countries, where access to conventional medicine may be limited. Local communities rely on traditional herbal remedies derived from medicinal plants for treating common ailments and maintaining their wellbeing (112). Medicinal plants are an integral part of complementary and alternative medicine practices. Many people seek natural and plant-based treatments as alternatives or supplements to conventional medicine. Herbal remedies and supplements made from medicinal plants are used for various purposes, including immune support, stress reduction, and overall wellness (113, 114).

6.4 Nutraceuticals and functional foods

Medicinal herbs are also used to create functional meals and nutraceuticals. These products go beyond basic nourishment to give additional health advantages. They are created with specialized plant extracts or bioactive chemicals to promote various areas of health, such as cardiovascular health, cognitive function, and digestive wellness (115, 116).

7 Protective effects of various nutraceuticals against some pesticide-induced injuries

Various nutraceuticals have been studied for their potential protective effects against pesticide-induced toxicities. These natural compounds derived from food sources can possess antioxidant,

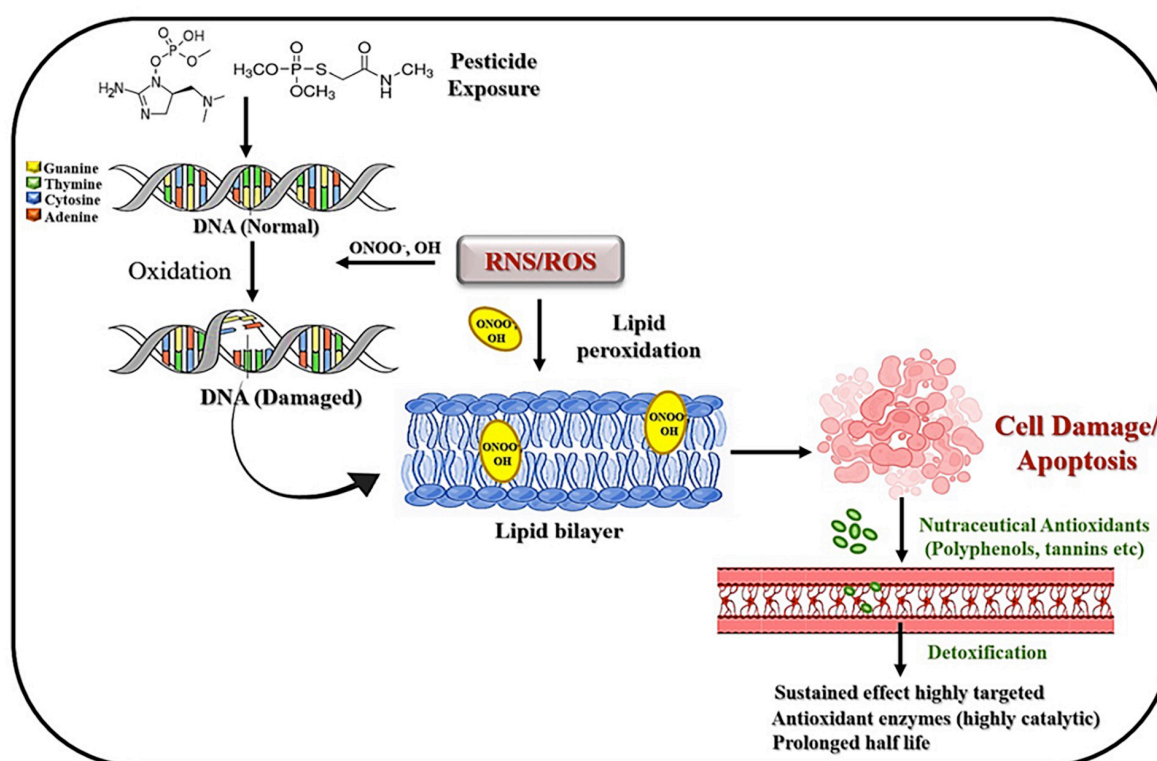


FIGURE 3

Schematic representation of the interplay between pesticide exposure and cellular responses, including DNA damage, lipid peroxidation, and cell apoptosis, alongside the protective effects of nutraceutical antioxidants through detoxification pathways.

anti-inflammatory, and detoxifying properties, which may help mitigate the harmful effects of some pesticides (Figure 3) (117).

Nutraceuticals rich in antioxidants, such as vitamins C and E, beta-carotene, and flavonoids, can counteract oxidative stress induced by pesticides. Examples include berries (blueberries and strawberries), citrus fruits, leafy greens (spinach and kale), and cruciferous vegetables (broccoli and cauliflower).

7.1 Curcumin

Curcumin, a bioactive component found in turmeric, has been examined for its possible protective mechanisms against pesticide-induced damage (118). While the particular methods may differ based on the pesticide and the target organ or system. Curcumin is a powerful antioxidant that can neutralize the damaging free radicals produced by pesticides (119). This helps to protect cells and tissues from oxidative damage and decreases inflammation (120). Curcumin has the ability to suppress a variety of inflammatory processes in the body. Pesticides can cause inflammation, and curcumin's anti-inflammatory qualities may assist to mitigate this impact. It may increase the activity of detoxification enzymes in the liver, such as glutathione S-transferases (GSTs), which are important in metabolizing and removing pesticides. Pesticide poisoning frequently targets the liver. Curcumin may help protect the liver from pesticide-induced damage by lowering oxidative stress and inflammation. Curcumin's anti-apoptotic characteristics may aid in the prevention

or reduction of cell death caused by pesticide exposure (121). Some pesticides have been related to an increased cancer risk. By suppressing tumor development and metastasis, curcumin's anticancer effects may help lessen the carcinogenic risk of some pesticides. Curcumin may boost the generation and activity of natural antioxidant enzymes including SOD and catalase, boosting the body's ability to counteract pesticide-induced oxidative stress. Curcumin can improve gut health by encouraging the development of good gut bacteria and decreasing inflammation in the gastrointestinal system. This can help reduce some of the negative effects of pesticides on the digestive system (122). A recent study demonstrated that rats treated with mancozeb alone exhibited significant liver damage, characterized by elevated levels of liver enzymes [aspartate transaminase (AST) and alanine transaminase (ALT)] and histopathological alterations indicative of hepatotoxicity. In contrast, rats co-administered with curcumin and mancozeb showed a significant reduction in liver enzyme levels and less severe histopathological changes, indicating the protective effects of curcumin against pesticide-induced hepatotoxicity (88).

7.2 Resveratrol

Resveratrol is a polyphenolic chemical found naturally in foods such as red grapes, red wine, and some berries. Its possible preventive mechanisms against pesticide-induced damage have been investigated. Resveratrol is a powerful antioxidant that may

neutralize pesticide-generated free radicals. This helps to minimize oxidative stress and tissue damage. Resveratrol has the ability to suppress a variety of inflammatory pathways in the body (123). Pesticides can cause inflammation, which resveratrol's anti-inflammatory qualities may help to mitigate. Resveratrol may increase the activity of liver detoxification enzymes such as GSTs. These enzymes are essential for pesticide metabolism and elimination. Pesticide poisoning frequently affects the liver. Some pesticides have the ability to cause cell death in diverse tissues. The anti-apoptotic characteristics of resveratrol may help prevent or minimize cell death in response to pesticide exposure (124). Resveratrol has been explored for its neuroprotective properties. It may help protect nerve cells from pesticide damage, potentially lowering the likelihood of neurodegenerative consequences. Some insecticides may be harmful to the cardiovascular system. The cardiovascular advantages of resveratrol, such as its capacity to enhance blood vessel function and lower inflammation, may protect against these consequences. Resveratrol has been linked to anticancer activity. By suppressing tumor development and metastasis, it may help lessen the carcinogenic risk of some pesticides. Resveratrol may promote metabolic health by regulating blood sugar levels and improving lipid profiles. These advantages may assist in mitigating some pesticide-induced metabolic abnormalities. Some pesticides have the potential to damage the endocrine system. The ability of resveratrol to promote hormonal homeostasis may assist to mitigate these abnormalities (94). Kumar et al. (119) provides evidence supporting the potential neuroprotective effects of resveratrol against pesticide-induced neurotoxicity in rats. The findings suggest that resveratrol may offer therapeutic benefits in mitigating the adverse neurological effects associated with pesticide exposure (125).

7.3 Flavonoids and flavone glycosides

Flavonoids and flavone glycosides constitute a diverse class of phytochemicals known for their potent antioxidant and anti-inflammatory properties. These compounds have demonstrated significant potential in preventing oxidative damage induced by pesticides. Quercetin is a flavonoid, which is a polyphenolic component present in a variety of fruits, vegetables, and cereals (126, 127). Quercetin is a powerful antioxidant that may neutralize pesticide-generated free radicals. This helps to minimize oxidative stress and tissue damage (128). Histopathological analysis of brain tissues revealed that rats treated with chlorpyrifos alone displayed neuronal damage and gliosis, whereas rats co-administered with quercetin and chlorpyrifos showed preservation of neuronal morphology and reduced gliosis, supporting the neuroprotective effects of quercetin. Rutin is well-known for its antioxidant properties. Pesticides can cause free radicals and oxidative stress in the body, which can lead to cell damage and inflammation (129, 130). Organophosphate insecticides, for example, cause toxicity by blocking cholinesterase enzymes. The ability of rutin to inhibit these enzymes may give protection against pesticide-induced toxicity (131). A recent study measured levels of pro-inflammatory cytokines (such as TNF- α and IL-6) and apoptotic markers (such as caspase-3 activity) in liver and kidney tissues. Rats treated with deltamethrin alone showed increased levels

of pro-inflammatory cytokines and caspase-3 activity, indicative of inflammation and apoptosis. However, rats co-administered with rutin and deltamethrin exhibited reduced levels of pro-inflammatory cytokines and caspase-3 activity, suggesting the anti-inflammatory and anti-apoptotic effects of rutin (132). Flavonols like kaempferol may be found in a variety of fruits and vegetables. It is useful in preventing oxidative stress brought on by pesticides because of its potent anti-inflammatory and antioxidant qualities. A prevalent flavone in celery, parsley, and chamomile tea is apigenin. By scavenging free radicals and adjusting the activity of antioxidant enzymes, it has been demonstrated to mitigate oxidative damage caused by pesticides (133).

7.4 N-acetylcysteine

N-acetylcysteine (NAC) is an amino acid supplement and pharmaceutical renowned for its mucolytic and antioxidant characteristics. NAC is a precursor of glutathione, one of the most essential antioxidants in the body. NAC can help neutralize damaging free radicals produced by pesticides by raising glutathione levels, lowering oxidative stress and cellular damage (134). NAC helps the body's detoxification functions, notably in the liver. It can aid in increasing the liver's ability to metabolize and remove pesticides and other pollutants. NAC is widely used to treat acetaminophen (paracetamol) overdoses. While not specifically related to pesticide toxicity, it demonstrates NAC's potential to combat toxic chemicals by increasing detoxification mechanisms in the liver. In situations of pesticide inhalation, NAC's mucolytic characteristics can assist lower the thickness of mucus in the respiratory system, making hazardous chemicals easier to remove from the lungs (135). NAC may have anti-inflammatory characteristics that can aid to reduce the inflammatory response caused by some pesticides. NAC may affect the immune system, perhaps improving the body's immunological response against pesticide-induced illnesses or inflammatory processes. NAC may protect against the negative effects of pesticides on several organs, including the liver, kidneys, and nervous system, by lowering oxidative stress and oxidative damage in cells and tissues. NAC has been examined for its possible neuroprotective benefits, and it may help protect nerve cells against pesticide damage, lowering the likelihood of neurodegeneration (136). A report assessed biochemical markers of oxidative stress and neuroinflammation in the brain tissues of rats. Rats treated with chlorpyrifos alone showed increased levels of oxidative stress markers (such as malondialdehyde) and pro-inflammatory cytokines (such as TNF- α and IL-1 β) compared to control rats. In contrast, rats co-administered with NAC and chlorpyrifos exhibited reduced levels of oxidative stress markers and pro-inflammatory cytokines, indicating the antioxidant and anti-inflammatory properties of NAC (137).

7.5 Omega-3 fatty acids

Omega-3 fatty acids, polyunsaturated fats present in foods such as fatty fish, flaxseeds, and walnuts, have been investigated for their possible protective mechanisms against pesticide-induced

toxicity. Anti-inflammatory properties of omega-3 fatty acids are well established. Pesticides, notably organophosphates and pyrethroids, have the potential to cause inflammation in the body (138). Omega-3 fatty acids can help decrease inflammation, potentially reducing pesticide harm. Omega-3 fatty acids have antioxidant qualities, which means they can help neutralize the damaging free radicals produced by pesticide exposure. Some research suggests that omega-3 fatty acids can boost the activity of detoxification enzymes in the liver, such as cytochrome P450 enzymes. These enzymes are in charge of breaking down and removing numerous poisons, including pesticides, from the body. Omega-3 fatty acids may alter the immune system's response to pesticide exposure. They may help the body deal with the harmful effects of pesticides by altering immunological function. Pesticides, particularly some organophosphates, can be neurotoxic (139). Docosahexaenoic acid (DHA), in particular, is critical for brain health and development. They may provide protection against pesticide-induced nervous system harm. Cell membranes rely heavily on omega-3 fatty acids. They can assist preserve the fluidity and integrity of cell membranes, which may protect cells against pesticide-induced disruption. Pro-inflammatory cytokines, which are chemicals involved in the inflammatory response, have been demonstrated to be reduced by omega-3s. This decrease in cytokine production may aid in reducing the inflammatory response caused by certain pesticides (140). The study evaluated the neurobehavioral effects of organophosphate pesticide exposure and the potential protective effects of omega-3 fatty acids using various behavioral tests, including the Y-maze test and the elevated plus maze test. Rats treated with organophosphate pesticide exhibited impaired spatial memory and increased anxiety-like behavior compared to control rats. However, rats co-administered with omega-3 fatty acids and pesticide showed significant improvements in spatial memory and reduced anxiety-like behavior, suggesting the neuroprotective effects of omega-3 fatty acids against pesticide-induced toxicity (141).

7.6 Vitamins

Vitamins are essential micronutrients known for their diverse physiological functions, including antioxidant defense and immune regulation. Vitamin C is a potent antioxidant that scavenges free radicals and regenerates other antioxidants, such as vitamin E. It plays a crucial role in protecting cells from oxidative damage induced by pesticides. Elzoghby et al. (139) evaluated markers of liver function, such as serum levels of ALT and AST, as well as histopathological changes in liver tissues. Rats treated with malathion alone exhibited elevated levels of ALT and AST, indicative of liver damage. However, rats co-administered with vitamin showed reduced levels of ALT and AST, suggesting the protective effects of vitamin C against pesticide-induced hepatotoxicity. Histopathological examination also revealed less severe liver damage (142). Vitamin E comprises a group of fat-soluble antioxidants, including alpha-tocopherol and gamma-tocotrienol. It acts as a lipid-soluble antioxidant, protecting cell membranes from oxidative stress caused by pesticides (143). The experimental study provides evidence supporting the protective effects of vitamin E against organophosphate pesticide-induced

oxidative stress in rats. The findings suggest that supplementation with vitamin E enhances the activity of key antioxidant enzymes, such as SOD, CAT, and GPx, thereby mitigating the adverse effects associated with pesticide exposure (144).

Vitamin A and its precursors, such as beta-carotene, possess antioxidant properties that contribute to cellular defense against pesticide-induced oxidative damage (145). Rats treated with atrazine alone showed decreased activities of antioxidant enzymes, such as SOD and catalase, and increased levels of lipid peroxidation, indicative of oxidative stress. In contrast, rats co-administered with vitamin E and atrazine exhibited restored antioxidant enzyme activities and reduced lipid peroxidation levels, suggesting the antioxidant properties of vitamin E (146). Additionally, vitamin A is involved in maintaining epithelial integrity and immune function. Vitamin D regulates calcium and phosphorus metabolism, thereby promoting bone health. Moreover, emerging research suggests its potential role in modulating immune responses and reducing inflammation, which may aid in mitigating pesticide-induced toxicity (147).

7.7 Coenzyme Q10

Coenzyme Q10 (CoQ10), also known as ubiquinone, is a naturally occurring molecule present in the body that plays an important role in the creation of cellular energy. CoQ10 is a powerful antioxidant that aids in the neutralization of damaging free radicals and the reduction of oxidative stress. Pesticides can cause free radicals to form in the body, causing cellular damage and inflammation (147). The antioxidant capabilities of CoQ10 may assist to offset these effects and reduce pesticide-induced oxidative stress. CoQ10 is essential in mitochondria, the energy-producing organelles found within cells. Pesticides can interfere with cellular energy generation, causing weariness and tissue damage. CoQ10 supplementation may maintain mitochondrial activity, guaranteeing an appropriate energy supply to cells and maybe assisting cells in coping with pesticide-induced stress. Some insecticides, especially those with neurotoxic characteristics, can cause mitochondrial damage. Because CoQ10 is an essential component of the mitochondrial electron transport chain, it may help shield mitochondria from such damage, sustaining cellular function (148). CoQ10 has been linked to anti-inflammatory properties. Pesticides can cause inflammation in the body, which can lead to tissue damage. CoQ10 has been shown to improve the body's natural defense systems against pollutants such as pesticides. It may boost the activity of detoxification enzymes in the liver and aid in the elimination of pesticides from the body. CoQ10 has being investigated for its neuroprotective effects. Some pesticides can injure the neurological system, and CoQ10 may provide protection. Some insecticides have been linked to cardiovascular damage. CoQ10 is proven to benefit heart health and may help guard against pesticide-related cardiovascular problems (129). A report provides evidence supporting the potential cardioprotective, antioxidant, and anti-inflammatory effects of coenzyme Q10 against pesticide-induced cardiac toxicity in rats. The findings suggest that coenzyme Q10 supplementation may offer therapeutic benefits in mitigating the adverse effects of pesticide exposure on cardiac health (149).

A report by Mohamed et al. (148) measured SOD activity in rat tissues as an indicator of antioxidant defense. Rats treated with

acetamiprid alone showed decreased SOD activity compared to control rats, indicative of reduced antioxidant capacity. However, rats co-administered with curcumin and pesticide exhibited

restored SOD activity, suggesting the ability of these phyto-protective nutraceuticals to enhance antioxidant defense against pesticide-induced oxidative stress (150). As an additional indicator

TABLE 2 List of commonly used plants and their medicinal properties against different toxicities.

S No.	Plant	Scientific name	Component(s)	Medicinal properties of nutraceuticals	References
1	Spinach	<i>Spinacia oleracea</i>	Leaves	Anticarcinogenic and anti-mutagenic activity	(155)
2	Nettle	<i>Urtica dioica</i>	Leaves	Anti-inflammatory, anticancer, and antioxidant activity	(156)
3	Okra	<i>Abelmoschus esculentus</i>	Leaves and fruits	Anti-inflammatory and antioxidant property	(157)
4	Drum stick	<i>Moringa oleifera</i>	Leaves, seeds, bark, and roots	Antidiabetic, anti-hypertensive, fertility enhancer, antioxidant, and anticancer property	(158)
5	Quinoa	<i>Chenopodium quinoa</i>	Seeds	Phenolics and antioxidant property	(159)
6	Inula	<i>Inula racemosa</i>	Roots	Antioxidant and anti-bacterial property	(160)
7	Shepherd's purse	<i>Capsella bursa-pastoris</i>	Stem, leaves, and flowers	Antioxidant and anti-inflammatory property	(161)
8	Curry leaves	<i>Murraya koenigii</i>	Leaves	Anti-inflammatory, anti-aging, and antioxidant property	(162)
9	Turmeric	<i>Curcuma longa</i>	Rhizome	Anti-inflammatory and anticancer property	(163)
10	Black pepper	<i>Piper nigrum</i>	Peppercorn	Antioxidant, antimicrobial, anti-inflammatory, antidiabetic, and anticancer property	(164)
11	Sweet pepper	<i>Capsicum annuum</i>	Peppercorn	Antioxidant and anti-inflammatory property	(165)
12	Ginger	<i>Zingiber officinale</i>	Rhizome	Antioxidant and anti-inflammatory property	(166)
13	Garlic	<i>Allium sativum</i>	Bulb, leaves, and flowers	Antioxidant, antidiabetic, anticancer, and anti-inflammatory property	(167)
14	Green tea	<i>Camellia sinensis</i>	Leaves	Antioxidant and anticancer property	(168)
15	Red ginseng	<i>Panax ginseng</i>	Leaves and roots	Antioxidant property	(169)
16	Purple coneflower	<i>Echinacea purpurea</i>	Leaves and flowers	Anti-inflammatory, antioxidant, and antiproliferative property	(170)
17	Fenugreek	<i>Trigonella foenum-graecum</i>	Leaves and seeds	Pro-apoptotic and anticancer property	(171)
18	Grapes	<i>Vitis vinifera</i>	Fruit	Anti-oxidative, anti-inflammatory, anticancer and anti-aging property	(172)
19	Raspberries	<i>Rubus idaeus</i>	Fruit	Antioxidant and anticancer property	(173)
20	Blueberries	<i>Vaccinium cyanococcus</i>	Fruit	Antioxidant and anti-proliferative property	(174)
21	Black cumin	<i>Nigella sativa</i>	Seeds	Antioxidant property	(175)
22	Fennel seed	<i>Foeniculum vulgare</i>	Seeds	Antioxidant property	(176)
23	Kale	<i>Brassica sabellica</i>	Leaves	Anticancer, antioxidant, and anti-inflammatory property	(177)
24	Broccoli	<i>Brassica oleracea</i>	Stem, leaves, and florets	Anti-proliferative and antioxidant property	(178)
25	Pomegranate	<i>Punica granatum</i>	Endocarp	Anticancer, anti-fungal, and anti-inflammatory property	(179)
26	Papaya	<i>Carica papaya</i>	Fruit	Antioxidative and anticancer property	(180)
27	Orange	<i>Citrus sinensis</i>	Fruit	Antioxidant property	(181)
28	Pineapple	<i>Ananas comosus</i>	Fruit	Antioxidant and anticancer property	(182)
29	Apple	<i>Malus domestica</i>	Fruit	Antioxidative and anticancer property	(183)
30	Mango	<i>Mangifera indica</i>	Fruit	Antioxidant, anti-inflammatory, and anticancer property	(184)
31	Jalapeno	<i>Capsicum annuum</i>	Seeds	Antioxidant, anti-obesity, antibiotic, and anticancer property	(185)
32	Amla	<i>Phyllanthus emblica</i>	Fruit	Anti-diabetes, anticancer, and antioxidant	(186)
33	Chamomile	<i>Matricaria chamomilla</i>	Flowers	Antioxidant and anti-aging properties	(187–189)

of antioxidant defense, CAT activity in rat tissues was evaluated in an earlier report. When compared to control rats, animals treated with deltamethrin alone had lower CAT activity, a sign of compromised antioxidant defense systems. On the other hand, rats who received both the pesticide and rutin concurrently showed increased CAT activity, indicating that these phyto-protective nutraceuticals can improve CAT-mediated antioxidant defense against oxidative stress caused by pesticides (151).

As another indicator of antioxidant defense, GPx activity was also evaluated in rat tissues in previous report. When compared to control rats, animals treated with metribuzin alone had lower GPx activity, a sign of impaired antioxidant defense systems. Rats co-administered with quercetin plus metribuzin, however, showed restored GPx activity, indicating that these phyto-protective nutraceuticals can improve GPx-mediated antioxidant protection against oxidative stress caused by pesticides (152). The findings suggest that supplementation with these phyto-protective nutraceuticals can enhance the activity of key antioxidant enzymes, such as SOD, CAT, and GPx, thereby mitigating the adverse effects associated with pesticide exposure.

The substances curcumin, resveratrol, flavonoids, n-acetylcysteine, omega-3 fatty acids, vitamins, and coenzyme Q10 are highlighted as representative examples due to their relevance in providing protective effects against certain injuries induced by pesticide exposure. These substances have been studied for their potential to counteract the harmful effects of pesticides on the body, such as oxidative stress, inflammation, and cellular damage. By presenting these examples, it is suggested that they may offer promising avenues for mitigating the negative impacts of pesticide exposure on human health (153).

These compounds also possess anti-inflammatory properties, further protecting against pesticide-induced injuries (154). Furthermore, certain nutraceuticals have been found to enhance detoxification mechanisms in the body. Similarly, certain herbs and spices, such as ginger and turmeric, have been found to alleviate pesticide-induced liver and kidney injuries through their antioxidant and anti-inflammatory properties (Table 2).

8 Conclusion

Specific pesticide-mediated toxicities pose significant risks to human health and the environment. Pesticides are widely used in agricultural practices to control pests and increase crop yield, but they can have detrimental effects on nontarget organisms, including humans. However, there is growing evidence that certain food-based nutraceuticals can help mitigate the toxic effects of pesticides. Natural compounds found in various foods, such as antioxidants, vitamins, minerals, and phytochemicals, possess protective properties against pesticide toxicity. These

nutraceuticals can act as scavengers of free radicals, reduce oxidative stress, enhance detoxification processes, and boost the immune system. Additionally, they may have the ability to repair damaged DNA and protect vital organs such as the liver and kidneys. Furthermore, incorporating a balanced diet rich in fruits, vegetables, whole grains, and legumes can provide essential nutrients that support overall health and resilience against pesticide toxicities. Additionally, further research is needed to better understand the mechanisms by which nutraceuticals protect against pesticide toxicity and to identify optimal dosages and combinations for effective amelioration.

Author contributions

MS: Formal analysis, Writing – original draft. SS: Investigation, Methodology, Writing – original draft. SKS: Resources, Writing – review & editing. RB: Formal analysis, Writing – original draft. WA: Resources, Writing – original draft. ASA: Software, Writing – original draft. MA: Formal analysis, Writing – original draft. AA: Methodology, Writing – original draft. EV: Resources, Writing – review & editing. MPS: Project administration, Writing – review & editing.

Funding

The author(s) declare that no financial support was received for the research, authorship, and/or publication of this article.

Conflict of interest

The authors declare that the research was conducted in the absence of any commercial or financial relationships that could be construed as a potential conflict of interest.

The author(s) declared that they were an editorial board member of Frontiers, at the time of submission. This had no impact on the peer review process and the final decision.

Publisher's note

All claims expressed in this article are solely those of the authors and do not necessarily represent those of their affiliated organizations, or those of the publisher, the editors and the reviewers. Any product that may be evaluated in this article, or claim that may be made by its manufacturer, is not guaranteed or endorsed by the publisher.

References

- Premanandh J. Factors affecting food security and contribution of modern technologies in food sustainability. *J Sci Food Agric*. (2011) 91:2707–14. doi: 10.1002/jsfa.4666
- Cerda R, Avelino J, Gary C, Tixier P, Lechevallier E, Allinne C. Primary and secondary yield losses caused by pests and diseases: Assessment and modeling in coffee. *PLoS One*. (2017) 12:e0169133. doi: 10.1371/journal.pone.0169133

3. Gaur N, Diwan B, Choudhary R. Bioremediation of organic pesticides using nanomaterials. nano-bioremediation: Fundamentals and Applications. *Micro Nano Technol.* (2022) 2022:517–40. doi: 10.1016/B978-0-12-823962-9.00024-6
4. Pandey MM, Rastogi S, Rawat AKS. Indian traditional ayurvedic system of medicine and nutritional supplementation. *Evid Based Complement Alternat Med.* (2013) 2013:376327. doi: 10.1155/2013/376327
5. Van Boxtael S, Habib I, Jacxsens L, De Vocht M, Baert L, Van de Perre E, et al. Food safety issues in fresh produce: Bacterial pathogens, viruses and pesticide residues indicated as major concerns by stakeholders in the fresh produce chain. *Food Control.* (2013) 32:190–7. doi: 10.1016/j.foodcont.2012.11.038
6. Simoglou KB, Roditakis E. Consumers' Benefit-risk perception on pesticides and food safety—a survey in Greece. *Agriculture.* (2022) 12:192. doi: 10.3390/agriculture12020192
7. Kim KH, Kabir E, Jahan SA. Exposure to pesticides and the associated human health effects. *Sci Total Environ.* (2017) 575:525–35. doi: 10.1016/j.scitotenv.2016.09.009
8. Bernardes MFF, Pazin M, Pereira LC, Dorta DJ. Impact of pesticides on environmental and human health. In: Andreazza A, Scola G editors. *Toxicology studies-cells, drugs, and environment.* London: IntechOpen (2015). p. 195–233. doi: 10.5772/59710
9. Fang Y, Nie Z, Die Q, Tian Y, Liu F, He J, et al. Organochlorine pesticides in soil, air, and vegetation at and around a contaminated site in southwestern China: Concentration, transmission, and risk evaluation. *Chemosphere.* (2017) 178:340–9. doi: 10.1016/j.chemosphere.2017.02.151
10. Liu Y, Mo R, Tang F, Fu Y, Guo Y. Influence of different formulations on chlorpyrifos behavior and risk assessment in bamboo forest of China. *Environ Sci Pollut Res.* (2015) 22:20245–54. doi: 10.1007/s11356-015-5272-2
11. Tudi M, Daniel Ruan H, Wang L, Lyu J, Sadler R, Connell D, et al. Agriculture development, pesticide application and its impact on the environment. *Int J Environ Res Public Health.* (2021) 18:1112. doi: 10.3390/ijerph18031112
12. Zhang W. Global pesticide use: Profile, trend, cost/benefit and more. *Proc Int Acad Ecol Environ Sci.* (2018) 8:1.
13. Pathak VM, Verma VK, Rawat BS, Kaur B, Babu N, Sharma A, et al. Current status of pesticide effects on environment, human health, and it is eco-friendly management as bioremediation: A comprehensive review. *Front Microbiol.* (2022) 13:962619. doi: 10.3389/fmicb.2022.962619
14. Ali Mekouar M. 15. Food and agriculture organization of the United Nations (FAO). *Yearbook Int Environ Law.* (2017) 28:506–20. doi: 10.1093/yiel/yvy073
15. Xavier R, Rekha K, Bairy KL. Health perspective of pesticide exposure and dietary management. *Malaysian J Nutr.* (2004) 10:39–51.
16. Sachdev S, Ansari SA, Ansari MI, Fujita M, Hasanuzzaman M. Abiotic stress and reactive oxygen species: Generation, signaling, and defense mechanisms. *Antioxidants.* (2021) 10:277. doi: 10.3390/antiox10020277
17. Nardelli V, D'Amico V, Ingegno M, Della Rovere I, Iammarino M, Casamassima F, et al. Pesticides contamination of cereals and legumes: Monitoring of samples marketed in Italy as a contribution to risk assessment. *Appl Sci.* (2021) 11:7283. doi: 10.3390/app11167283
18. Terziev V, Petkova-Georgieva S. Human health problems and classification of the most toxic pesticides. *Int E J Adv Soc Sci.* (2019) 5:8. doi: 10.2139/ssrn.3513837
19. Ahamad A, Kumar J. Pyrethroid pesticides: An overview on classification, toxicological assessment and monitoring. *J Hazard Mater Adv.* (2023) 10:100284. doi: 10.1016/j.hazadv.2023.100284
20. DiBartolomeis M, Kegley S, Mineau P, Radford R, Klein K. An assessment of acute insecticide toxicity loading (AITL) of chemical pesticides used on agricultural land in the United States. *PLoS One.* (2019) 14:e0220029. doi: 10.1371/journal.pone.0220029
21. Lushchak VI, Matviishyn TM, Husak VV, Storey JM, Storey KB. Pesticide toxicity: A mechanistic approach. *EXCLI J.* (2018) 17:1101.
22. Garcia FP, Ascencio SC, Oyarzún JCG, Hernandez AC, Alavarado PV. Pesticides: Classification, uses and toxicity. Measures of exposure and genotoxic risks. *J Res Environ Sci Toxicol.* (2012) 1:279–93.
23. Abubakar Y, Tijjani H, Egbuna C, Adetunji CO, Kala S, Kryeziu TL, et al. Pesticides, history, and classification. *Natural remedies for pest, disease and weed control.* Cambridge, MA: Academic Press (2020). p. 29–42. doi: 10.1016/B978-0-12-819304-4.00003-8
24. Lovleen. Differential specification of various insecticides and their environmental degradation. *Toxicol Int.* (2020) 26:110–28.
25. Chmiel T, Mieszkowska A, Kempńska-Kupczyk D, Kot-Wasik A, Namieśnik J, Mazerska Z. The impact of lipophilicity on environmental processes, drug delivery and bioavailability of food components. *Microchem J.* (2019) 146:393–406. doi: 10.1016/j.microc.2019.01.030
26. Kauts S, Shabir S, Yousuf S, Mishra Y, Bhardwaj R, Milibari AA, et al. The evidence of in-vivo and in-vitro studies on microplastic and nano plastic toxicity in mammals: A possible threat for an upcoming generation? *Phys Chem Earth.* (2023) 132:103511. doi: 10.1016/j.pce.2023.103511
27. Bhatt P, Zhou X, Huang Y, Zhang W, Chen S. Characterization of the role of esterases in the biodegradation of organophosphate, carbamate, and pyrethroid pesticides. *J Hazard Mater.* (2021) 411:125026. doi: 10.1016/j.jhazmat.2020.125026
28. Banjare P, Singh J, Roy PP. Predictive classification-based QSTR models for toxicity study of diverse pesticides on multiple avian species. *Environ Sci Pollut Res.* (2021) 28:17992–8003. doi: 10.1007/s11356-020-11713-z
29. Kaur R, Mavi GK, Raghav S, Khan I. Pesticides classification and its impact on environment. *Int J Curr Microbiol Appl Sci.* (2021) 8:1889–97. doi: 10.20546/ijcmas.2019.803.224
30. Yadav IC, Devi NL. Pesticides classification and its impact on human and environment. *Environ Sci Eng.* (2018) 6:140–58.
31. Mdeni NL, Adeniji AO, Okoh AI, Okoh OO. Analytical evaluation of carbamate and organophosphate pesticides in human and environmental matrices: A review. *Molecules.* (2022) 27:618. doi: 10.3390/molecules27030618
32. Oguh CE, Okpaka CO, Ubani CS, Okekeaji U, Joseph PS, Amadi EU. Natural pesticides (biopesticides) and uses in pest management—a critical review. *Asian J Biotechnol Genet Eng.* (2019) 2:1–18.
33. Field LM, Emyr Davies TG, O'reilly AO, Williamson MS, Wallace BA. Voltage-gated sodium channels as targets for pyrethroid insecticides. *Eur Biophys J.* (2017) 46:675–9. doi: 10.1007/s00249-016-1195-1
34. Damalas CA, Eleftherohorinos IG. Pesticide exposure, safety issues, and risk assessment indicators. *Int J Environ Res Public Health.* (2011) 8:1402–19. doi: 10.3390/ijerph8051402
35. Baghel AS, Bhardwaj A, Ibrahim W. Optimization of pesticides spray on crops in agriculture using machine learning. *Comp Intell Neurosci.* (2022) 2022:9408535. doi: 10.1155/2022/9408535
36. Sabarwal A, Kumar K, Singh RP. Hazardous effects of chemical pesticides on human health—Cancer and other associated disorders. *Environ Toxicol Pharmacol.* (2022) 63:103–14. doi: 10.1016/j.etap.2018.08.018
37. Vopham T, Bertrand KA, Hart JE, Laden F, Brooks MM, Yuan JM, et al. Pesticide exposure and liver cancer: A review. *Cancer Causes Control.* (2017) 28:177–90. doi: 10.1007/s10552-017-0854-6
38. Muhammad Muddassir MM, Muhammad Shahid MS, Altalab AAT, Ahsan SMW, Muhammad Mubushar MM, Zia MA, et al. Paradigm shift from non-Bt to Bt cotton and factors conducting Bt cotton production in a southern Punjab's district of Pakistan. *AgroLife Sci J.* (2017) 6.
39. Carvalho FP. Pesticides, environment, and food safety. *Food Energy Secur.* (2017) 6:48–60. doi: 10.1002/fes3.108
40. Yin K, Wang Y, Zhao H, Wang D, Guo M, Mu M, et al. A comparative review of microplastics and nanoplastics: Toxicity hazards on digestive, reproductive and nervous system. *Sci Total Environ.* (2021) 774:145758. doi: 10.1016/j.scitotenv.2021.145758
41. Fuhrmann S, Van den Brenk I, Atuhaire A, Mubeezi R, Staudacher P, Huss A, et al. Recent pesticide exposure affects sleep: A cross-sectional study among smallholder farmers in Uganda. *Environ Int.* (2022) 158:106878. doi: 10.1016/j.envint.2021.106878
42. Bhardwaj JK, Kumar V, Saraf P, Panchal H, Rathee V, Sachdeva SN. Efficacy of N-acetyl-L-cysteine against glyphosate induced oxidative stress and apoptosis in testicular germ cells preventing infertility. *J Biochem Mol Toxicol.* (2022) 36:e22979. doi: 10.1002/jbt.22979
43. Ali SN, Ahmad MK, Mahmood R. Sodium chlorate, an herbicide and major water disinfectant byproduct, generates reactive oxygen species and induces oxidative damage in human erythrocytes. *Environ Sci Pollut Res.* (2017) 24:1898–909. doi: 10.1007/s11356-016-7980-7
44. Khan AU, Jamshaid H, Ud Din F, Zeb A, Khan GM. Designing, optimization and characterization of Trifluralin transfersomal gel to passively target cutaneous leishmaniasis. *J Pharm Sci.* (2022) 111:1798–811. doi: 10.1016/j.xphs.2022.01.010
45. Fukuyama T, Kosaka T, Hayashi K, Miyashita L, Tajima Y, Wada K, et al. Immunotoxicity in mice induced by short-term exposure to methoxychlor, parathion, or piperonyl butoxide. *J Immunotoxicol.* (2013) 10:150–9. doi: 10.3109/1547691X.2012.703252
46. Vonder Embse AN, Elmore SE, Jackson KB, Habecker BA, Manz KE, Pennell KD, et al. Developmental exposure to DDT or DDE alters sympathetic innervation of brown adipose in adult female mice. *Environ Health.* (2021) 20:1–16. doi: 10.1186/s12940-021-00721-2
47. Wang Z, Wu Q, Li X, Klaunig JE. Constitutive androstane receptor (CAR) mediates dieldrin-induced liver tumorigenesis in mouse. *Arch Toxicol.* (2020) 94:2873–84. doi: 10.1007/s00204-020-02781-8
48. Bao J, Zhang Y, Wen R, Zhang L, Wang X. Low level of mancozeb exposure affects ovary in mice. *Ecotoxicol Environ Saf.* (2022) 239:113670. doi: 10.1016/j.ecoenv.2022.113670
49. Khisroon M, Hassan N, Khan A, Farooqi J. Assessment of DNA damage induced by endosulfan in grass carp (*Ctenopharyngodon idella* Valenciennes, 1844). *Environ Sci Pollut Res.* (2021) 28:15551–5. doi: 10.1007/s11356-021-12727-x

50. Singh S, Kumar V, Kanwar R, Wani AB, Gill JPK, Garg VK, et al. Toxicity, and detoxification of monocrotophos from ecosystem using different approaches: A review. *Chemosphere*. (2021) 275:130051. doi: 10.1016/j.chemosphere.2021.130051
51. Mishra S, Zhang W, Lin Z, Pang S, Huang Y, Bhatt P, et al. Carbofuran toxicity and its microbial degradation in contaminated environments. *Chemosphere*. (2020) 259:127419. doi: 10.1016/j.chemosphere.2020.127419
52. Arici M, Abudayyak M, Boran T, Özhan G. Does pendimethalin develop in pancreatic cancer induced inflammation? *Chemosphere*. (2020) 252:126644. doi: 10.1016/j.chemosphere.2020.126644
53. Alavi J, Maroufi A, Mirzaghaderi G. Trifluralin-mediated polyploidization of fenugreek (*Trigonella feonum-graecum* L.) using in vitro embryo culture. *Acta Physiol Plant*. (2022) 44:97. doi: 10.1007/s11738-022-03436-0
54. Saquib Q, Faisal M, Ansari SM, Wahab R. Phorate triggers oxidative stress and mitochondrial dysfunction to enhance micronuclei generation and DNA damage in human lymphocytes. *Saudi J Biol Sci*. (2019) 26:1411–7. doi: 10.1016/j.sjbs.2019.04.008
55. Inoue T, Kinoshita M, Oyama K, Kamemura N, Oyama Y. Captan-induced increase in the concentrations of intracellular Ca²⁺ and Zn²⁺ and its correlation with oxidative stress in rat thymic lymphocytes. *Environ Toxicol Pharmacol*. (2018) 63:78–83. doi: 10.1016/j.etap.2018.08.017
56. Sarkar S, Kotteeswaran V. Green synthesis of silver nanoparticles from aqueous leaf extract of Pomegranate (*Punica granatum*) and their anticancer activity on human cervical cancer cells. *Adv Nat Sci Nanosci Nanotechnol*. (2018) 9:025014. doi: 10.1088/2043-6254/aac590
57. Bist R, Chaudhary B, Bhatt DK. Defensive proclivity of bacoside A and bromelain against oxidative stress and AChE gene expression induced by dichlorvos in the brain of *Mus musculus*. *Sci Rep*. (2021) 11:1–11. doi: 10.1038/s41598-021-83289-8
58. Singh P, Verma PK, Raina R, Sood S, Sharma P. Maximum contaminant level of arsenic in drinking water potentiates quinalphos-induced renal damage on coadministration of both arsenic and quinalphos in Wistar rats. *Environ Sci Pollut Res*. (2020) 27:21331–40. doi: 10.1007/s11356-020-08643-1
59. Lu J, Wu Q, Yang Q, Li G, Wang R, Liu Y, et al. Molecular mechanism of reproductive toxicity induced by beta-cypermethrin in zebrafish. *Comp Biochem Physiol C Toxicol Pharmacol*. (2021) 239:108894. doi: 10.1016/j.cbpc.2020.108894
60. Piner P, Üner N. In vivo acetylcholinesterase inhibition in the tissues of spinosad exposed *Oreochromis niloticus*. *Environ Toxicol Pharmacol*. (2012) 34:473–7. doi: 10.1016/j.etap.2012.06.012
61. Zhang J, Liu H, Sun Z, Xie J, Zhong G, Yi X. Azadirachtin induced apoptosis in the prothoracic gland in *Bombyx mori* and a pronounced Ca²⁺ release effect in Sf9 cells. *Int J Biol Sci*. (2017) 13:1532. doi: 10.7150/ijbs.22175
62. Yang C, Lim W, Song G. Mediation of oxidative stress toxicity induced by pyrethroid pesticides in fish. *Comp Biochem Physiol C Toxicol Pharmacol*. (2020) 234:108758. doi: 10.1016/j.cbpc.2020.108758
63. Dar MA, Khan AM, Raina R, Verma PK, Wani NM. Effect of bifenthrin on oxidative stress parameters in the liver, kidneys, and lungs of rats. *Environ Sci Pollut Res*. (2019) 26:9365–70. doi: 10.1007/s11356-019-04362-4
64. Xu Z, Zhu L, Yang Y, Zhang Y, Lu M, Tao L, et al. Bifenthrin induces DNA damage and autophagy in *Spodoptera frugiperda* (Sf9) insect cells. *Vitro Cell Dev Biol Anim*. (2021) 57:264–71. doi: 10.1007/s11626-021-00554-w
65. Sule RO, Condon L, Gomes AV. A common feature of pesticides: Oxidative stress—The role of oxidative stress in pesticide-induced toxicity. *Oxid Med Cell Longev*. (2022) 2022:5563759. doi: 10.1155/2022/5563759
66. Cicchetti F, Drouin-Ouellet J, Gross RE. Environmental toxins, and Parkinson's disease: What have we learned from pesticide-induced animal models. *Trends Pharmacol Sci*. (2009) 30:475–83. doi: 10.1016/j.tips.2009.06.005
67. Kaur K, Kaur R. Occupational pesticide exposure, impaired DNA repair, and diseases. *Indian J Occup Environ Med*. (2018) 22:74. doi: 10.4103/ijoom.IJOEM_45_18
68. Shah HK, Sharma T, Banerjee BD. Organochlorine pesticides induce inflammation, ROS production, and DNA damage in human epithelial ovary cells: An in vitro study. *Chemosphere*. (2020) 246:125691. doi: 10.1016/j.chemosphere.2019.125691
69. Colle D, Farina M, Ceccatelli S, Raciti M. Paraquat and maneb exposure alters rat neural stem cell proliferation by inducing oxidative stress: New insights on pesticide-induced neurodevelopmental toxicity. *Neurotox Res*. (2021) 34:820–33. doi: 10.1007/s12640-018-9916-0
70. Gupta PK. Toxicity of herbicides. In: Gupta RC editor. *Veterinary toxicology*. Cambridge, MA: Academic Press (2018). p. 553–67. doi: 10.1016/B978-0-12-811410-0.00044-1
71. Chedik L, Bruyere A, Bacle A, Potin S, Le Vée M, Fardel O. Interactions of pesticides with membrane drug transporters: Implications for toxicokinetics and toxicity. *Expert Opin Drug Metab Toxicol*. (2018) 14:739–52. doi: 10.1080/17425255.2018.1487398
72. Maheshwari N, Khan FH, Mahmood R. Pentachlorophenol-induced cytotoxicity in human erythrocytes: Enhanced generation of ROS and RNS, lowered antioxidant power, inhibition of glucose metabolism, and morphological changes. *Environ Sci Pollut Res*. (2019) 26:12985–3001. doi: 10.1007/s11356-019-04736-8
73. Eleršek T, Filipič M. Organophosphorus pesticides-mechanisms of their toxicity. In: Stoytcheva M editor. *Pesticides-the impacts of pesticide exposure*. New York, NY: Intech (2011). p. 243–60.
74. Bhardwaj JK, Saraf PN-. acetyl-l-cysteine mediated regulation of DNA fragmentation, an apoptotic event, against methoxychlor toxicity in the granulosa cells of ovarian antral follicles. *Mutat Res Genet Toxicol Environ Mutagen*. (2020) 858:503222. doi: 10.1016/j.mrgentox.2020.503222
75. Li H, Wang F, Li J, Deng S, Zhang S. Adsorption of three pesticides on polyethylene microplastics in aqueous solutions: Kinetics, isotherms, thermodynamics, and molecular dynamics simulation. *Chemosphere*. (2021) 264:128556. doi: 10.1016/j.chemosphere.2020.128556
76. Decourt B, Lahiri D, Sabbagh M. Targeting tumor necrosis factor alpha for Alzheimer's disease. *Curr Alzheimer Res*. (2017) 14:412–25. doi: 10.2174/1567205013666160930110551
77. Zhu S, Liu Y, Li Y, Yi J, Yang B, Li Y, et al. The potential risks of herbicide butachlor to immunotoxicity via induction of autophagy and apoptosis in the spleen. *Chemosphere*. (2022) 286:131683. doi: 10.1016/j.chemosphere.2021.131683
78. Wang X, Martínez MA, Dai M, Chen D, Ares I, Romero A, et al. Permethrin-induced oxidative stress and toxicity and metabolism. A review. *Environ Res*. (2016) 149:86–104. doi: 10.1016/j.envres.2016.05.003
79. Murphy EP, Crean D. Molecular interactions between NR4A orphan nuclear receptors and NF-κB are required for appropriate inflammatory responses and immune cell homeostasis. *Biomolecules*. (2015) 5:1302–18. doi: 10.3390/biom5031302
80. Bordonì L, Nasuti C, Mirto M, Caradonna F, Gabbianelli R. Intergenerational effect of early life exposure to permethrin: Changes in global DNA methylation and in Nurr1 gene expression. *Toxics*. (2015) 3:451–61. doi: 10.3390/toxics3040451
81. Kamal S, Junaid M, Bibi I, Rehman S, Rehman K, Akash MSH. Role of pesticides as EDCs in metabolic disorders. In: Akash MS, Rehman K, and Hashmi MZ editors. *Endocrine disrupting chemicals-induced metabolic disorders and treatment strategies*. New York, NY: Springer International Publishing (2021). p. 265–300. doi: 10.1007/978-3-030-45923-9_17
82. Lee JH, Mohan CD, Basappa S, Rangappa S, Chinnathambi A, Alahmadi TA, et al. The IκB kinase inhibitor ACHP targets the STAT3 signaling pathway in human non-small cell lung carcinoma cells. *Biomolecules*. (2019) 9:875. doi: 10.3390/biom9120875
83. Khalifa AG, Moselhy WA, Mohammed HM, Khalil F, Shaban M, El-Nahass ES, et al. Deltamethrin and its nanoformulations induce behavioral alteration and toxicity in rat brain through oxidative stress and JAK2/STAT3 signaling pathway. *Toxics*. (2022) 10:303. doi: 10.3390/toxics10060303
84. Singh NS, Sharma R, Parween T, Patanjali PK. Pesticide contamination and human health risk factor. In: Oves M, Zain Khan M, Ismail M editors. *Modern age environmental problems and their remediation*. Cham: Springer (2018). p. 49–68. doi: 10.1007/978-3-319-64501-8_3
85. Sharma H, Hirko AC, King MA, Liu B. Role of NADPH oxidase in cooperative reactive oxygen species generation in dopaminergic neurons induced by combined treatment with diethrin and lindane. *Toxicol Lett*. (2018) 299:47–55. doi: 10.1016/j.toxlet.2018.09.006
86. Lee GH, Choi KC. Adverse effects of pesticides on the functions of immune system. *Comp Biochem Physiol C Toxicol Pharmacol*. (2020) 235:108789. doi: 10.1016/j.cbpc.2020.108789
87. Shabir S, Singh MP. *The aging: Introduction, theories, principles, and future prospective. Anti-aging drug discovery on the basis of hallmarks of aging*. Amsterdam: Elsevier (2022). p. 1–17. doi: 10.1016/B978-0-323-90235-9.00017-3
88. Farkhondeh T, Mehrpour O, Forouzanfar F, Roshanravan B, Samarghandian S. Oxidative stress and mitochondrial dysfunction in organophosphate pesticide-induced neurotoxicity and its amelioration: A review. *Environ Sci Pollut Res*. (2020) 27:24799–814. doi: 10.1007/s11356-020-09045-z
89. Bouaziz C, Graiet I, Salah A, Ben Salem I, Abid S. Influence of bifenthrin, a pyrethroid pesticide, on human colorectal HCT-116 cells attributed to alterations in oxidative stress involving mitochondrial apoptotic processes. *J Toxicol Environ Health*. (2020) 83:331–40. doi: 10.1080/15287394.2020.1755756
90. Dash AP, Raghavendra K, Pillai MKK. Resurrection of DDT: A critical appraisal. *Indian J Med Res*. (2007) 126:1.
91. Chopra G, Shabir S, Yousuf S, Kauts S, Bhat SA, Mir AH, et al. Proteinopathies: Deciphering physiology and mechanisms to develop effective therapies for neurodegenerative diseases. *Mol Neurobiol*. (2022) 59:7513–40. doi: 10.1007/s12035-022-03042-8
92. Richardson JR, Fitsanakis V, Westerink RH, Kanthasamy AG. Neurotoxicity of pesticides. *Acta Neuropathol*. (2019) 138:343–62. doi: 10.1007/s00401-019-02033-9
93. Singh MP, Chakrabarty R, Shabir S, Yousuf S, Obaid AA, Moustafa M, et al. Influence of the gut microbiota on the development of neurodegenerative diseases. *Mediat Inflamm*. (2022) 2022:3300903. doi: 10.1155/2022/3300903
94. Zeng X, Du Z, Ding X, Jiang W. Protective effects of dietary flavonoids against pesticide-induced toxicity: A review. *Trends Food Sci Technol*. (2021) 109:271–9. doi: 10.1016/j.tifs.2021.01.046

95. Wong HL, Garthwaite DG, Ramwell CT, Brown CD. Assessment of occupational exposure to pesticide mixtures with endocrine-disrupting activity. *Environ Sci Pollut Res.* (2019) 26:1642–53. doi: 10.1007/s11356-018-3676-5
96. Bretveld RW, Thomas CM, Scheepers PT, Zielhuis GA, Roelleveld N. Pesticide exposure: The hormonal function of the female reproductive system disrupted? *Reprod Biol Endocrinol.* (2006) 4:1–14. doi: 10.1186/1477-7827-4-30
97. Johansson HK, Christiansen S, Draskau MK, Svingen T, Boberg J. Classical toxicity endpoints in female rats are insensitive to the human endocrine disruptors diethylstilbestrol and ketoconazole. *Reprod Toxicol.* (2021) 101:9–17. doi: 10.1016/j.reprotox.2021.01.003
98. Jacobsen-Pereira CH, Dos Santos CR, Maraslis FT, Pimentel L, Feijó AJL, Silva CI, et al. Markers of genotoxicity and oxidative stress in farmers exposed to pesticides. *Ecotoxicol Environ Saf.* (2018) 148:177–83. doi: 10.1016/j.ecoenv.2017.10.004
99. Perumalla Venkata R, Rahman MF, Mahboob M, Indu Kumari S, Chinde S, Dumala N, et al. Assessment of genotoxicity in female agricultural workers exposed to pesticides. *Biomarkers.* (2017) 22:446–54. doi: 10.1080/1354750X.2016.1252954
100. Bolognesi C, Creus A, Ostrosky-Wegman P, Marcos R. Micronuclei, and pesticide exposure. *Mutagenesis.* (2011) 26:19–26. doi: 10.1093/mutage/geq070
101. Blair A, Freeman LB. Epidemiologic studies in agricultural populations: Observations and future directions. *J Agromed.* (2009) 14:125–31. doi: 10.1080/10599240902779436
102. Benigni R, Laura Battistelli C, Bossa C, Giuliani A, Fioravanzo E, Bassan A, et al. Evaluation of the applicability of existing (Q) SAR models for predicting the genotoxicity of pesticides and similarity analysis related with genotoxicity of pesticides for facilitating of grouping and read across. *EFSA Support Publ.* (2019) 16:1598E. doi: 10.1016/j.yrtph.2020.104658
103. Radha, Kumar M, Puri S, Pundir A, Bangar SP, Changan S, et al. Evaluation of nutritional, phytochemical, and mineral composition of selected medicinal plants for therapeutic uses from cold desert of Western Himalaya. *Plants.* (2021) 10:1429. doi: 10.3390/plants10071429
104. Pathak K, Pathak MP, Saikia R, Gogoi U, Sahariah JJ, Zothantluanga JH, et al. Cancer chemotherapy via natural bioactive compounds. *Curr Drug Discov Technol.* (2022) 19:4–23. doi: 10.2174/1570163819666220331095744
105. De Filippis LF. Plant secondary metabolites: From molecular biology to health products. In: Azooz MM, Ahmad P editors. *Plant-environment interaction: Responses and approaches to mitigate stress.* New York, NY: Wiley (2016). p. 263–99. doi: 10.1002/9781119081005.ch15
106. Keihanian F, Moohebaty M, Saedinia A, Mohajeri SA, Madaeni S. Therapeutic effects of medicinal plants on isoproterenol-induced heart failure in rats. *Biomed Pharmacother.* (2021) 134:111101. doi: 10.1016/j.biopha.2020.111101
107. Zhu T, Wang L, Wang LP, Wan Q. Therapeutic targets of neuroprotection and neurorestoration in ischemic stroke: Applications for natural compounds from medicinal herbs. *Biomed Pharmacother.* (2022) 148:112719. doi: 10.1016/j.biopha.2022.112719
108. Dutra RC, Campos MM, Santos AR, Calixto JB. Medicinal plants in Brazil: Pharmacological studies, drug discovery, challenges, and perspectives. *Pharmacol Res.* (2016) 112:4–29. doi: 10.1016/j.phrs.2016.01.021
109. Barkat MA, Goyal A, Barkat HA, Salauddin M, Pottoo FH, Anwer ET. Herbal medicine: Clinical perspective and regulatory status. *Comb Chem High Throughput Screen.* (2021) 24:1573–82. doi: 10.2174/1386207323999201110192942
110. Jahangir MA, Anand C, Muheem A, Gilani SJ, Taleuzzaman M, Zafar A, et al. Nano phytomedicine based delivery system for CNS disease. *Curr Drug Metab.* (2020) 21:661–73. doi: 10.2174/1389200221666200523161003
111. Maqbool Z, Arshad MS, Ali A, Aziz A, Khalid W, Afzal MF, et al. Potential role of phytochemical extract from saffron in development of functional foods and protection of brain-related disorders. *Oxid Med Cell Longev.* (2022) 2022:6480590. doi: 10.1155/2022/6480590
112. Dey P, Kundu A, Chakraborty HJ, Kar B, Choi WS, Lee BM, et al. Therapeutic value of steroidal alkaloids in cancer: Current trends and future perspectives. *Int J Cancer.* (2019) 145:1731–44. doi: 10.1002/ijc.31965
113. Tiwari P, Sangwan RS, Sangwan NS. Plant secondary metabolism linked glycosyltransferases: An update on expanding knowledge and scopes. *Biotechnol Adv.* (2016) 34:714–39. doi: 10.1016/j.biotechadv.2016.03.006
114. Pagare S, Bhatia M, Tripathi N, Pagare S, Bansal YK. Secondary metabolites of plants and their role: Overview. *Curr Trends Biotechnol Pharm.* (2015) 9:293–304.
115. Jafari-Nozad AM, Jafari A, Aschner M, Farkhondeh T, Samarghandian S. Curcumin combats against organophosphate pesticides toxicity: A review of the current evidence and molecular pathways. *Curr Med Chem.* (2023) 30:2312–39. doi: 10.2174/0929867329666220817125800
116. Jabłońska-Trypuc A, Wiater J. Protective effect of plant compounds in pesticides toxicity. *J Environ Health Sci Eng.* (2022) 20:1035–45. doi: 10.1007/s40201-022-00823-0
117. Hossen MS, Tanvir EM, Prince MB, Paul S, Saha M, Ali MY, et al. Protective mechanism of turmeric (*Curcuma longa*) on carbofuran-induced hematological and hepatic toxicities in a rat model. *Pharm Biol.* (2022) 55:1937–45. doi: 10.1080/13880209.2017.1345951
118. Alp H, Aytekin I, Hatipoglu NK, Alp A, Ogun M. Effects of sulforaphane and curcumin on oxidative stress created by acute malathion toxicity in rats. *Eur Rev Med Pharmacol Sci.* (2012) 16:144–8.
119. Kumar R, Ali M, Kumar A, Gahlot V. Comparative bioremedial effect of *Withania somnifera* and curcuma longa on ovaries of pesticide induced mice. *Eur J Pharm Med Res.* (2015) 2:249–53.
120. Saber TM, Abo-Elmaaty AMA, Abdel-Ghany HM. Curcumin mitigates mancozeb-induced hepatotoxicity and genotoxicity in rats. *Ecotoxicol Environ Saf.* (2019) 183:109467. doi: 10.1016/j.ecoenv.2019.109467
121. Sharma P, Huq AU, Singh R. Cypermethrin-induced reproductive toxicity in the rat is prevented by resveratrol. *J Hum Reprod Sci.* (2014) 7:99. doi: 10.4103/0974-1208.138867
122. Jahan S, Kumar D, Singh S, Kumar V, Srivastava A, Pandey A, et al. Resveratrol prevents the cellular damages induced by monocrotophos via PI3K signalling pathway in human cord blood mesenchymal stem cells. *Mol Neurobiol.* (2018) 55:8278–92. doi: 10.1007/s12035-018-0986-z
123. Kumar V, Tripathi VK, Singh AK, Lohani M, Kuddus M. Trans-resveratrol restores the damages induced by organophosphate pesticide-monocrotophos in neuronal cells. *Toxicol Int.* (2013) 20:48–55. doi: 10.4103/0971-6580.111571
124. Akinmoladun AC, Oladejo CO, Josiah SS, Famusiwa CD, Ojo OB, Olaleye MT. Catechin, quercetin and taxifolin improve redox and biochemical imbalances in rotenone-induced hepatocellular dysfunction: Relevance for therapy in pesticide-induced liver toxicity. *Pathophysiology.* (2018) 25:365–71. doi: 10.1016/j.pathophys.2018.07.002
125. Ahmadian E, Eftekhari A, Kavetsky T, Khosroushahi AY, Turksoy VA, Khalilov R. Effects of quercetin loaded nanostructured lipid carriers on the paraquat-induced toxicity in human lymphocytes. *Pestic Biochem Physiol.* (2020) 167:104586. doi: 10.1016/j.pestbp.2020.104586
126. Baldissera MD, Souza CF, Parmeggiani B, Vendrusculo RG, Ribeiro LC, Muenchen DK. Protective effects of diet containing rutin against trichlorfon-induced muscle bioenergetics disruption and impairment on fatty acid profile of silver catfish *Rhamdia quelen*. *Ecotoxicol Environ Saf.* (2020) 205:111127. doi: 10.1016/j.ecoenv.2020.111127
127. Banerjee BD, Seth V, Ahmed RS. Pesticide-induced oxidative stress: Perspective and trends. *Rev Environ Health.* (2001) 16:1–40. doi: 10.1515/rev.2001.16.1.1
128. Gandhi S, Abramov AY. Mechanism of oxidative stress in neurodegeneration. *Oxid Med Cell Longev.* (2012) 2012:428010. doi: 10.1155/2012/428010
129. Küküçler S, Kandemir FM, Özdemir S, Çomaklı S, Çağlayan C. Protective effects of rutin against deltamethrin-induced hepatotoxicity and nephrotoxicity in rats via regulation of oxidative stress, inflammation, and apoptosis. *Environ Sci Pollut Res Int.* (2021) 28:62975–90. doi: 10.1007/s11356-021-15190-w
130. Nimse SB, Pal D. Free radicals, natural antioxidants, and their reaction mechanisms. *RSC Adv.* (2015) 5:27986–8006. doi: 10.1039/C4RA13315C
131. Dhoubi IE, Jallouli M, Annabi A, Gharbi N, Elfazaa S, Lasram MM. A minireview on N-acetylcysteine: An old drug with new approaches. *Life Sci.* (2016) 151:359–63. doi: 10.1016/j.lfs.2016.03.003
132. Aboubakr HM, Elzohairy EA, Ali AA, Rashed LA, Elkady NK, Soliman AS. Therapeutic effects of N-acetylcysteine against malathion-induced hepatotoxicity. *Egypt J Forens Sci.* (2019) 9:1–9. doi: 10.1186/s41935-019-0142-6
133. Ahmed T, Tripathi AK, Ahmed RS, Das S, Suke SG, Pathak R, et al. Endosulfan-induced apoptosis, and glutathione depletion in human peripheral blood mononuclear cells: Attenuation by N-acetylcysteine. *J Biochem Mol Toxicol.* (2008) 22:299–304. doi: 10.1002/jbt.20240
134. Mahmoud SM, Abdel Moneim AE, Qayed MM, El-Yamany NA. Potential role of N-acetylcysteine on chlorpyrifos-induced neurotoxicity in rats. *Environ Sci Pollut Res Int.* (2019) 26:20731–41. doi: 10.1007/s11356-019-05366-w
135. Emam H, Ahmed E, Abdel-Daim M. Antioxidant capacity of omega-3-fatty acids and vitamin E against imidacloprid-induced hepatotoxicity in Japanese quails. *Environ Sci Pollut Res.* (2018) 25:11694–702. doi: 10.1007/s11356-018-1481-9
136. Moneim AEA, Dkhil MA, Al-Quraishy S. The potential role of *Portulaca oleracea* as a neuroprotective agent in rotenone-induced neurotoxicity and apoptosis in the brain of rats. *Pestic Biochem Physiol.* (2013) 105:203–12. doi: 10.1016/j.pestbp.2013.02.004
137. Aljadani NA, Elnaggar MH, Assaggaff AI. The role of fish oil and evening primrose oil against the toxicity of fenitrothion pesticide in male rats. *Int J Pharm Res Allied Sci.* (2020) 9:108–22.
138. Avci B, Bilge SS, Arslan G, Alici O, Darakci O, Baratzada T, et al. Protective effects of dietary omega-3 fatty acid supplementation on organophosphate poisoning. *Toxicol Ind Health.* (2018) 34:69–82. doi: 10.1177/0748233717737646
139. Elzoghby RR, Ahlam FH, Abdel-Fatah A, Farouk M. Protective role of vitamin C and green tea extract on malathion-induced hepatotoxicity and nephrotoxicity in rats. *Am J Pharmacol Toxicol.* (2014) 9:177. doi: 10.3844/ajptsp.2014.177.188
140. Aly N, Kawther EG, Mahmoud F, El-Sebae AK. Protective effect of vitamin C against chlorpyrifos oxidative stress in male mice. *Pestic Biochem Physiol.* (2010) 97:7–12. doi: 10.1016/j.pestbp.2009.11.007

141. Sun Y, Zhang J, Song W, Shan A. Vitamin E alleviates phoxim-induced toxic effects on intestinal oxidative stress, barrier function, and morphological changes in rats. *Environ Sci Pollut Res Int*. (2018) 25:26682–92. doi: 10.1007/s11356-018-2666-y
142. Sharma RK, Sharma B. In-vitro carbofuran induced genotoxicity in human lymphocytes and its mitigation by vitamins C and E. *Dis Mark*. (2012) 32:153–63. doi: 10.3233/DMA-2011-0870
143. Singh M, Kaur P, Sandhir R, Kiran R. Protective effects of vitamin E against atrazine-induced genotoxicity in rats. *Mutat Res Genet Toxicol Environ Mutagen*. (2008) 654:145–9. doi: 10.1016/j.mrgentox.2008.05.010
144. Eroglu S, Pandir D, Uzun FG, Bas H. Protective role of vitamins C and E in diclorvos-induced oxidative stress in human erythrocytes in vitro. *Biol Res*. (2013) 46:33–8. doi: 10.4067/S0716-97602013000100005
145. Malik V, Singh J, Kumar A, Kumar V. Protective effect of coenzyme Q10 nanoparticles against monocrotophos induced oxidative stress in kidney tissues of rats. *Biologia*. (2021) 76:1849–57. doi: 10.1007/s11756-021-00732-x
146. Amit K, Jagjeet S, Annu P, Vijay K. Protective effects of coenzyme Q10 nanoparticles on hepatotoxicity induced by monocrotophos in rats. *Res J Biotechnol*. (2022) 17:8. doi: 10.25303/1708rjbt001008
147. Mantle D, Hargreaves IP. Organophosphate poisoning and coenzyme Q10: An overview. *Br J Neurosci Nurs*. (2018) 14:206–14. doi: 10.12968/bjnn.2018.14.5.206
148. Mohamed Z, El-Kader AEK, Salah-Eldin AE, Mohamed O, Awadalla EA. Protective effects of curcumin against acetamiprid-induced neurotoxicity in male albino rats. *Biol Bull*. (2023) 24:1–13.
149. Kadeche L, Bourogaa E, Boumendjel A, Djeflal A, Abdennour C, El Feki A, et al. Quercetin attenuates metribuzin-induced biochemical and hematological toxicity in adult rats. *Int J Pharm Sci Rev Res*. (2016) 40:38–46.
150. Medithi S, Jonnalagadda PR, Jee B. Predominant role of antioxidants in ameliorating the oxidative stress induced by pesticides. *Arch Environ Occup Health*. (2021) 76:61–74. doi: 10.1080/19338244.2020.1750333
151. Saafi EB, Louedi M, Elfeki A, Zakhama A, Najjar MF, Hammami M, et al. Protective effect of date palm fruit extract (*Phoenix dactylifera* L.) on dimethoate induced-oxidative stress in rat liver. *Exp Toxicol Pathol*. (2011) 63:433–41. doi: 10.1016/j.etp.2010.03.002
152. Rice PJ, Rice PJ, Arthur EL, Barefoot AC. Advances in pesticide environmental fate and exposure assessments. *J Agric Food Chem*. (2007) 55:5367–76. doi: 10.1021/jf063764s
153. Alavanja MC, Hoppin JA, Kamel F. Health effects of chronic pesticide exposure: Cancer and neurotoxicity. *Annu Rev Public Health*. (2004) 25:155–97. doi: 10.1146/annurev.publhealth.25.101802.123020
154. Bhatia R, Wernham A. Integrating human health into environmental impact assessment: An unrealized opportunity for environmental health and justice. *Environ Health Perspect*. (2008) 116:991–1000. doi: 10.1289/ehp.11132
155. Al-Jawhari H, Bin-Thiyab H, Elbially N. In vitro antioxidant and anticancer activities of cupric oxide nanoparticles synthesized using spinach leaves extract. *Nano Struct Nano Objects*. (2022) 29:100815. doi: 10.1016/j.nano.2021.100815
156. Singh MP, Shabir S, Deopa AS, Raina SR, Bantun F, Jalal NA, et al. Synthesis of green engineered silver nanoparticles through *Urtica dioica*: An inhibition of microbes and alleviation of cellular and organismal toxicity in *Drosophila melanogaster*. *Antibiotics*. (2022) 11:1690. doi: 10.3390/antibiotics11121690
157. Yousuf S, Shabir S, Kauts S, Minocha T, Obaid AA, Khan AA, et al. Appraisal of the antioxidant activity, polyphenolic content, and characterization of selected himalayan herbs: Anti-proliferative potential in HepG2 cells. *Molecules*. (2022) 27:8629. doi: 10.3390/molecules27238629
158. Singh MP, Himalian R, Shabir S, Obaid AA, Alamri AS, Galanakis CM, et al. Protection of phytoextracts against rotenone-induced organismal toxicities in *drosophila melanogaster* via the attenuation of ROS generation. *Appl Sci*. (2022) 12:9822. doi: 10.3390/app12199822
159. Panighel G, Ferrarese I, Lupo MG, Sut S, Dall'Acqua S, Ferri N. Investigating the in vitro mode of action of okra (*Abelmoschus esculentus*) as hypocholesterolemic, anti-inflammatory, and antioxidant food. *Food Chem Mol Sci*. (2022) 5:100126. doi: 10.1016/j.fochms.2022.100126
160. Khor KZ, Lim V, Moses EJ, Abdul Samad N. The in vitro and in vivo anticancer properties of *Moringa oleifera*. *Evid Based Complement Alternat Med*. (2018) 2018:1071243. doi: 10.1155/2018/1071243
161. Sidorova YS, Shipelin VA, Petrov NA, Zorin SN, Mazo VK. Anxiolytic and antioxidant effect of phytoecdysteroids and polyphenols from *Chenopodium quinoa* on an in vivo restraint stress model. *Molecules*. (2022) 27:9003. doi: 10.3390/molecules27249003
162. Peng J, Hu T, Li J, Du J, Zhu K, Cheng B, et al. Shepherd's purse polyphenols exert its anti-inflammatory and antioxidative effects associated with suppressing MAPK and NF- κ B pathways and heme oxygenase-1 activation. *Oxid Med Cell Longev*. (2019) 2019:7202695. doi: 10.1155/2019/7202695
163. Shabir S, Yousuf S, Singh SK, Vamanu E, Singh MP. Ethnopharmacological Effects of *Urtica dioica*, *Matricaria chamomilla*, and *Murraya koenigii* on rotenone-exposed, *D. melanogaster*: An attenuation of cellular, biochemical, and organismal markers. *Antioxidants*. (2022) 11:1623. doi: 10.3390/antiox11081623
164. Termini D, Den Hartogh DJ, Jaglanian A, Tsiani E. Curcumin against prostate cancer: Current evidence. *Biomolecules*. (2020) 10:1536. doi: 10.3390/biom10111536
165. Banerjee S, Katiyar P, Kumar V, Saini SS, Varshney R, Krishnan V, et al. Black pepper and piperine induce anticancer effects on leukemia cell line. *Toxicol Res*. (2021) 10:169–82. doi: 10.1093/toxres/tfab001
166. Thuphairo K, Sornchan P, Suttisansanee U. Bioactive compounds, antioxidant activity and inhibition of key enzymes relevant to Alzheimer's disease from sweet pepper (*Capsicum annuum*) extracts. *Prevent Nutr Food Sci*. (2019) 24:327. doi: 10.3746/pnf.2019.24.3.327
167. Kulkarni RA, Deshpande AR. Anti-inflammatory, and antioxidant effect of ginger in tuberculosis. *J Complement Integr Med*. (2016) 13:201–6. doi: 10.1515/jcim-2015-0032
168. Yousuf S, Shabir S, Singh MP. Protection against drug-induced liver injuries through nutraceuticals via amelioration of Nrf-2 signaling. *J Am Nutr Assoc*. (2022) 42:495–515. doi: 10.1080/27697061.2022.2089403
169. Jiang Y, Jiang Z, Ma L, Huang Q. Advances in nano delivery of green tea catechins to enhance the anticancer activity. *Molecules*. (2021) 26:3301. doi: 10.3390/molecules26113301
170. Lee SJ, Oh S, Kim MJ, Sim GS, Moon TW, Lee J. Oxidative stability of extracts from red ginseng and puffed red ginseng in bulk oil or oil-in-water emulsion matrix. *J Ginseng Res*. (2018) 42:320–6. doi: 10.1016/j.jgr.2017.04.002
171. Shi Q, Lang W, Wang S, Li G, Bai X, Yan X, et al. Echinacea polysaccharide attenuates lipopolysaccharide induced acute kidney injury by inhibiting inflammation, oxidative stress and the MAPK signaling pathway. *Int J Mol Med*. (2021) 47:243–55. doi: 10.3892/ijmm.2020.4769
172. Sethi G, Shanmugam MK, Warriar S, Merarchi M, Arfuso F, Kumar AP, et al. Pro-apoptotic and anticancer properties of diosgenin: A comprehensive and critical review. *Nutrients*. (2018) 10:645. doi: 10.3390/nu10050645
173. Wijekoon C, Netticadan T, Siow YL, Sabra A, Yu L, Raj P, et al. Potential associations among bioactive molecules, antioxidant activity and resveratrol production in *Vitis vinifera* fruits of North America. *Molecules*. (2022) 27:336. doi: 10.3390/molecules27020336
174. Baby B, Antony P, Vijayan R. Antioxidant and anticancer properties of berries. *Crit rev Food Sci Nutr*. (2018) 58:2491–507. doi: 10.1080/10408398.2017.1329198
175. Maya-Cano DA, Arango-Varela S, Santa-Gonzalez GA. Phenolic compounds of blueberries (*Vaccinium* spp) as a protective strategy against skin cell damage induced by ROS: A review of antioxidant potential and antiproliferative capacity. *Heliyon*. (2021) 7:e06297. doi: 10.1016/j.heliyon.2021.e06297
176. Soleimanifar M, Niazmand R, Jafari SM. Evaluation of oxidative stability, fatty acid profile, and antioxidant properties of black cumin seed oil and extract. *J Food Measur Character*. (2019) 13:383–9. doi: 10.1007/s11694-018-9953-7
177. Zhao D, Wei J, Hao J, Han X, Ding S, Yang L, et al. Effect of sodium carbonate solution pretreatment on drying kinetics, antioxidant capacity changes, and final quality of wolfberry (*Lycium barbarum*) during drying. *LWT*. (2019) 99:254–61. doi: 10.1016/j.lwt.2018.09.066
178. Yu L, Gao B, Li Y, Wang TT, Luo Y, Wang J, et al. Home food preparation techniques impacted the availability of natural antioxidants and bioactivities in kale and broccoli. *Food Funct*. (2018) 9:585–93. doi: 10.1039/c7fo00948h
179. Hossain MN, De Leo V, Tamborra R, Laselva O, Ingrosso C, Daniello V, et al. Characterization of anti-proliferative and antioxidant effects of nanosized vesicles from *Brassica oleracea* L.(Broccoli). *Sci Rep*. (2022) 12:14362. doi: 10.1038/s41598-022-17899-1
180. Babu KD, Sharma J, Maity A, Singh NV, Patil PG, Shilpa P, et al. Pomegranate: An ancient fruit for health and nutrition. *Progr Hortic*. (2021) 53:3–13. doi: 10.5958/2249-5258.2021.00001.4
181. Hadadi SA, Li H, Rafie R, Kaseloo P, Witak SM, Siddiqui RA. Antioxidation properties of leaves, skin, pulp, and seeds extracts from green papaya and their anticancer activities in breast cancer cells. *J Cancer Metastas Treat*. (2018) 4:25. doi: 10.20517/2394-4722.2018.22
182. Jovanović M, Milutinović M, Kostić M, Miladinović B, Kitić N, Branković S, et al. Antioxidant capacity of pineapple (*Ananas comosus* (L.) Merr.) extracts and juice. *Lek Sirov*. (2018) 38:27–30. doi: 10.5937/lekir1838027
183. Rashad MM, Mahmoud AE, Ali MM, Nooman MU, Al-Kashef AS. Antioxidant and anticancer agents produced from pineapple waste by solid-state fermentation. *Int J Toxicol Pharmacol Res*. (2015) 7:287–96.
184. Alansari WS, Eskandrani AA. The anticarcinogenic effect of the apple polyphenol phloretin in an experimental rat model of hepatocellular carcinoma. *Arabian J Sci Eng*. (2020) 45:4589–97. doi: 10.1007/s13369-020-04478-7
185. Adilah ZM, Jamilah B, Hanani ZN. Functional and antioxidant properties of protein-based films incorporated with mango kernel extract for active packaging. *Food Hydrocoll*. (2018) 74:207–18. doi: 10.1016/j.foodhyd.2017.08.017
186. Hamed M. Estimation of capsaicinoid compounds and other nutritionally important compounds in Colorado grown pepper cultivars. Ph.D. thesis. Fort Collins, CO: Colorado State University (2021).

187. Yousuf S, Shabir S, Mehdi MM, Srivastav S, Mohammed Saleh ZM, Bassfar Z, et al. Investigation of the Protective Effects of *Urtica dioica*, *Capsella bursa-pastoris* and *Inula racemosa* on Acetaminophen-Induced nephrotoxicity in Swiss albino male mice. *Appl Sci*. (2023) 13:3925. doi: 10.3390/app13063925
188. Shabir S, Sehgal A, Dutta J, Devgon I, Singh SK, Alsanie WF, et al. Therapeutic potential of green-engineered ZnO nanoparticles on rotenone-exposed *D. melanogaster* (Oregon R+): Unveiling ameliorated biochemical, cellular, and behavioral parameters. *Antioxidants*. (2023) 12:1679. doi: 10.3390/antiox12091679
189. Zaheer A, Betül Ö, Mustafa S, Emre Cem, E, Zeliha, S, Celal BAL. Phenolic compound and antioxidant potential of Hebeloma sinapizans mushroom. *AgroLife Sci J*. (2023) 12:12–17. doi: 10.17930/AGL202322



OPEN ACCESS

EDITED BY

Maojun Jin,
Chinese Academy of Agricultural Sciences
(CAAS), China

REVIEWED BY

Ge Chen,
Chinese Academy of Agricultural Sciences,
China
Yihua Liu,
Chinese Academy of Forestry, China
Peipei Li,
Institute of Quality Standard and Testing
Technology for Agro-Products of CAAS,
China

*CORRESPONDENCE

Valeria Nardelli
✉ valeria.nardelli@izspb.it
Marco Iammarino
✉ marco.iammarino@tin.it

RECEIVED 19 March 2024

ACCEPTED 25 April 2024

PUBLISHED 10 May 2024

CITATION

Ingegno M, Zianni R, Della Rovere I,
Chiappinelli A, Nardelli V, Casamassima F,
Calitri A, Quinto M, Nardiello D and
Iammarino M (2024) Development of a highly
sensitive method based on QuEChERS and
GC–MS/MS for the determination of
polycyclic aromatic hydrocarbons in infant
foods.
Front. Nutr. 11:1403541.
doi: 10.3389/fnut.2024.1403541

COPYRIGHT

© 2024 Ingegno, Zianni, Della Rovere,
Chiappinelli, Nardelli, Casamassima, Calitri,
Quinto, Nardiello and Iammarino. This is an
open-access article distributed under the
terms of the [Creative Commons Attribution
License \(CC BY\)](https://creativecommons.org/licenses/by/4.0/). The use, distribution or
reproduction in other forums is permitted,
provided the original author(s) and the
copyright owner(s) are credited and that the
original publication in this journal is cited, in
accordance with accepted academic
practice. No use, distribution or reproduction
is permitted which does not comply with
these terms.

Development of a highly sensitive method based on QuEChERS and GC–MS/MS for the determination of polycyclic aromatic hydrocarbons in infant foods

Mariateresa Ingegno¹, Rosalia Zianni¹, Ines Della Rovere¹,
Andrea Chiappinelli¹, Valeria Nardelli^{1*},
Francesco Casamassima¹, Anna Calitri¹, Maurizio Quinto²,
Donatella Nardiello² and Marco Iammarino^{1*}

¹Struttura Complessa di Chimica, Istituto Zooprofilattico Sperimentale della Puglia e della Basilicata, Foggia, Italy, ²Department of Agriculture, Food, Natural Resources and Engineering (DAFNE), University of Foggia, Foggia, Italy

Polycyclic aromatic hydrocarbons (PAHs) are environmental contaminants that can be found in various food products, including those intended for infants. Due to their potential health risks, it is crucial to develop sensitive analytical methods for the accurate determination of PAHs in infant foods. This study describes the development and validation of a highly sensitive method for the quantification of European PAH markers, namely benzo[a]pyrene, benzo[a]anthracene, chrysene, and benzo[b]fluoranthene, using gas chromatography–tandem mass spectrometry (GC–MS/MS), in baby food samples. The first step was the optimization of the sample preparation procedure, performed using different methods based on the QuEChERS approach, also testing different extraction solvents. Several factors such as extraction efficiency, selectivity, and recovery were evaluated to choose the most effective procedure for sample preparation. Furthermore, the GC–MS/MS method was optimized, evaluating parameters such as linearity, sensitivity, accuracy, and robustness using spiked infant food samples. The method demonstrated excellent linearities with a correlation coefficient higher than 0.999 over a wide concentration range, and limits of detection and limits of quantification in the range 0.019–0.036 µg/kg and 0.06–0.11 µg/kg, respectively. Extraction recoveries were between 73.1 and 110.7%, with relative standard deviations always lower than 8%. These findings are compliant with the indications of the European Commission (Reg. 836/2011). To assess the applicability of the method to official control activities, a survey was conducted on commercially available infant food products. Four markers were determined in commercial samples belonging to different food categories for infants and young children. The outcome of this monitoring showed that PAH contamination, in all samples, was below the quantification limits. In conclusion, the developed GC–MS/MS method provides a highly sensitive and reliable approach for the determination of PAHs in baby foods. The optimized sample preparation, instrumental parameters, and validation results ensure accurate quantification of 4 PAHs even at trace levels. This method could contribute to the assessment of PAH exposure in infants and it could support regulatory efforts to ensure the safety and quality of infant food products with regular monitoring.

KEYWORDS

food safety, GC–MS/MS, infant foods, polycyclic aromatic hydrocarbons (PAHs), QuEChERS, validation

1 Introduction

Polycyclic aromatic hydrocarbons (PAHs) are a class of chemical contaminants, comprising over 200 organic compounds, that are originated from the incomplete combustion or pyrolysis of organic matter by natural and anthropogenic processes (1–3). PAHs contain two or more fused benzene rings in linear, angular, or cluster arrangements and they are classified in function of the number of condensed aromatic rings as light (2–3 rings) or heavy (4–6 rings) (4, 5). Due to particular physicochemical properties, such as high lipophilicity, thermostability, low solubility in water, and low biodegradability, these contaminants are ubiquitous and persistent, both in the environment and in the food chain (1, 6). These organic pollutants are highly toxic, mutagenic, carcinogenic, teratogenic, and immunotoxicogenic for several life forms, including humans (7). In particular, the heavy PAHs, such as benzo[*g,h,i*]perylene, benzo[*a*]pyrene (BAP), and indeno[1,2,3-*c,d*]pyrene, because of higher hydrophobicity, are more toxic and stable compared to the light ones (8).

Occurrence and toxicity of PAHs have been evaluated by numerous organizations, e.g., the United States Environmental Protection Agency (U.S. EPA), the International Agency for Research on Cancer (IACR), the Scientific Committee on Food (SCF), the Joint FAO/WHO Expert Committee on Food Additives (JECFA), the International Programme on Chemical Safety (IPCS), and the European Food Safety Authority (EFSA) (9). The two most important groups of PAHs monitored worldwide are the 16 PAHs, listed by U.S. EPA, and the 15+1 priority PAHs, defined by SCF for the European Union (EU) (10, 11). The 16 EPA PAHs are the following: acenaphthene, acenaphthylene, anthracene, fluoranthene, fluorene, naphthalene, phenanthrene, pyrene, benzo[*a*]anthracene, benzo[*b*]fluoranthene (BBF), benzo[*k*]fluoranthene, benzo[*ghi*]perylene, BAP, chrysene (CHY), dibenz[*a,h*]anthracene, and indeno[1,2,3-*cd*]pyrene (7, 9). The SCF assessed 33 PAHs and identified 15 PAHs that possess both genotoxic and carcinogenic properties, including 8 high molecular weight PAHs that are also part of the U.S. EPA list. The 15+1 EU priority PAHs are benz[*a*]anthracene (BAA), BBF, benzo[*j*]fluoranthene, benzo[*k*]fluoranthene, benzo[*ghi*]perylene, BAP, CHY, cyclopenta[*cd*]pyrene, dibenzo[*a,h*]anthracene, dibenzo[*a,e*]pyrene, dibenzo[*a,h*]pyrene, dibenzo[*a,i*]pyrene, dibenzo[*a,l*]pyrene, indeno[1,2,3-*cd*]pyrene, and 5-methylchrysene. These compounds show clear evidence of mutagenicity/genotoxicity and, with the exception of benzo[*ghi*]perylene, they also show clear carcinogenic effects in various bioassays of experimental animals (9). SFC suggested to use of BAP as a marker of occurrence of carcinogenic PAHs in food because it is based on examinations of PAH profiles in food and on evaluation of carcinogenicity studies (12). PAHs have several negative effects on human health, in particular on reproductive, developmental, cardiorespiratory, and immune systems, also causing asthma or chronic obstructive pulmonary disease and such as breast, skin, bladder, lung, and colon cancer (2). The main routes of human

exposure to PAHs are ingestion, dermal, and inhalation pathways, even if food ingestion contributes largely to overall PAH intake (13). Indeed, they can be present in cooked foods as a consequence of the cooking process (12), especially in grilling and deep-frying process, owing to the pyrolysis of fat at higher temperature and adsorption of PAHs emitted from combustion process. In raw foods PAHs may come from the deposition of ambient particles, contaminated soils and water (14). Dietary intake represents a very common and widespread route of exposure specifically for infants and young children, which are particularly vulnerable to food contaminants, due to their different physiological characteristics compared to adults (15–17). Exposure to potentially toxic substances is especially dangerous because of their higher food intake, higher ventilation, and greater body surface area (18). Chronic exposure to PAHs, which unfortunately already begins during gestation through the placenta, continuing with feeding, can lead to delays in cognitive development, disorders of the nervous, urinary and immune systems, and cardiovascular diseases (19). The legislation of the EU Commission established regulation guidelines for the presence of four substances, that is BAP, BAA, BBF, and CHY, known together as PAH4, in food matrices. The lower bound concentration, used as a limit and reference for adherence to safe standards, is calculated as the sum of PAH4 concentrations (20). Regulation (EU) 2023/915 sets maximum levels for PAH4 in foods for infants and young children at 1.0 µg/kg (21).

The extreme heterogeneity of PAHs in foods and their simultaneous presence, combined with their toxicity, require not only a robust regulatory framework but also advanced analytical techniques. The distribution of PAHs is influenced by different physical states of foods, therefore extraction and analysis methods must be adapted to the specific matrices to detect and quantify these contaminants (3). To provide repeatable data and satisfy legal criteria, proper sample preparation with adequate extraction procedures and improved cleaning strategies are required. Soxhlet extraction is probably the most widely used traditional extraction technique for PAHs from a wide range of foodstuffs. However, this conventional approach is laborious, time-consuming and requires great amounts of organic solvents (22, 23). To date, automated extraction techniques for PAHs in food have achieved popularity through their increased efficiency, shorter analytical times, and environmentally friendly characteristics. They include accelerated solvent extraction (ASE), microwave-assisted extraction (MAE), supercritical fluid extraction (SFE), high-temperature distillation (HTD), and fluidized-bed extraction (FBE) (1). Among the clean-up procedures, column chromatography, such as gel permeation chromatography (GPC), Florisil, and silica gel, is the standard approach which is characterized by an extensive quantity of reagents, solvents, and materials. The solid-phase extraction (SPE), along with dispersive liquid-liquid microextraction (DLLME), solid-phase microextraction (SPME), magnetic solid-phase extraction (MSPE), and QuEChERS (Quick, Easy, Cheap, Effective, Rugged, and Safe) are the clean-up procedures with high enrichment factor, automation capability, and less exposure

to organic solvents (9). In particular, the QuEChERS method is based on the green chemistry principles of multi-residue analysis, with several advantages such as lower costs, fewer solvents, time savings, increased yield, and great extraction performance (24–26). The QuEChERS strategy is characterized by great versatility and, for this reason, it has been systematically employed in routine analytical determinations of a wide range of analytes (e.g., pesticides, mycotoxins, pharmaceutical residues, illicit drugs, etc.) in environmental, food, feed, pharmaceutical, biological, and forensic matrices (27). The experimental layout of the QuEChERS method includes two steps: a solid–liquid extraction/partitioning with a salting–out effect and a dispersive solid-phase extraction (d-SPE) for sample clean-up. The extraction is performed with acetonitrile partitioned from an aqueous matrix using MgSO_4 and NaCl, followed by dispersive-SPE (d-SPE) with MgSO_4 , a primary secondary amine (PSA), and another sorbent such as octadecyl silica (C18) and graphitized carbon black (GCB) (24, 28).

In the QuEChERS d-SPE method, the choice of adsorbents is critical for the reduction of matrix interference in the following chromatographic analysis. In the original method proposed by Anastassiades et al. (24), the first extraction step was carried out under unbuffered conditions with acetonitrile as solvent, but this approach had some limitations. To overcome these drawbacks, citrate buffer (with a relatively low buffering capacity) (29) and/or acetate buffer (with a strong buffering capacity) (30) were used to enhance the extraction efficiency. Another important factor is the nature of the extraction solvent, which can be modified according to the target analyte. Acetonitrile is an excellent separator from water, after the salt addition, therefore it is suitable to extract the broadest range of organic compounds, without co-extraction of large amounts of lipophilic material, in different matrices (3, 27). However, to improve the extraction efficiency of target analytes some solvent modifications have been proposed, namely acidification or combination of acetonitrile with isooctane and/or ethyl acetate (31–33).

PSA is typically used as sorbent of the d-SPE step to remove fatty acids, sugars, organic acids, lipids, and some pigments. C18 is particularly effective for the removal of high lipid contents while GCB is used to remove co-extracted pigments, namely carotenoids and chlorophyll, typical from highly pigmented matrices (27, 33). For other complex matrices, more oriented adsorbents based on new materials have been developed, such as zirconium-coated silica (32). Furthermore, modifications of the QuEChERS procedure in terms of solvents, salts, and sorbents, are continuously proposed to improve and broaden even more the range of applications from food samples (9).

In this work, different extraction and purification methods, principally based on molecularly imprinted polymers (MIP) and QuEChERS with Enhanced Matrix Removal-Lipid (EMR-lipid), were considered. MIPs are a class of highly cross-linked polymer-based molecular recognition elements engineered to bind one specific target compound or a class of structurally related compounds with high selectivity. The MIP material is designed with cavities that are sterically and chemically complementary to the target analytes. As a result, multiple interactions (e.g., hydrogen bonding, ionic, Van der Waals, hydrophobic) can take place between the MIP cavity and the analytes. On the other side, EMR-Lipid is a new product used as a d-SPE to remove lipids. This technology, based on size exclusion and hydrophobic interactions, is very promising for the selective removal of lipids, ensuring minimal loss and ion suppression of target analytes,

and improving method reliability and ruggedness. Moreover, modified-QuEChERS procedures were tested, also using EMR-Lipid in combination with different extraction and purification salts.

For the identification and quantification of PAHs in a wide range of food matrices, common analytical approaches are adopted, such as high-performance liquid chromatography (HPLC) with an ultraviolet (UV) array detector photodiode array (PDA), and gas chromatography (GC) coupled to a flame ionization detector (FID). However, these techniques are not sensitive, not selective, time-consuming, and labor-intensive (9). High-resolution mass spectrometry (HRMS) detectors allow better performance than DAD and FLD, and for this reason, they are widely used in PAH determination in food matrices (1). In particular, GC coupled to tandem mass spectrometry (MS/MS) is the most common analytical tool, mainly due to its sensitivity, accuracy, and convenience even in official methods (34, 35). Current literature provides several investigations focused on the extraction and analysis of PAHs in baby food, comprising both traditional and novel approaches (32). Moazzen et al. (17) proposed the good performances of MSPE method coupled to GC–MS/MS to detect PAHs in the Iranian market. Recently, Prata et al. (36) provided a QuEChERS-based extraction procedure based on different salts composition in addition to MgSO_4 and PSA, such as Florisil, C18 and zirconium-coated silica. All these approaches are adequate for the determination of PAHs in baby food, but they are quite laborious also requiring particular laboratory equipment for sample preparation, which is not always available.

In this study, the preparative procedure based on modified-QuEChERS for the extraction and purification of four regulated PAHs was optimized, and the following efficient GC–MS/MS analytical method was validated to detect and quantify the target analytes in baby foods. Compared to the current methods, the proposed procedure involves a double initial extraction with acetonitrile and extract freezing at -20°C , before clean-up. Therefore, a method based on a simple modification of standard QuEChERS protocol for contaminants analysis was optimized and used for the first time to analyse the main PAHs in several types of baby food. The developed method was found to be accurate, efficient, sensitive, and selective for the analysis of food products of different types, based on meat, fish, legumes, and vegetables, subject to official control for the presence of BAP, BAA, BBE, and CHF. To the best of our knowledge, there is a lack of information regarding the determination of PAHs in the Italian markets. Therefore, this procedure was used to analyze food samples present on the Italian market and intended for infant nutrition, demonstrating its suitability for baby food control. Cooking methods, i.e., microwave and steam cooking, were also considered to verify PAH contamination as a consequence of heat treatments.

2 Materials and methods

2.1 Samples and chemical standards

A total of 60 samples, consisting of meat (chicken) and mixed meat, mixed fish, and mixed legumes were used for validation. A total of 100 samples, consisting of meat (chicken, beef, lamb, ham) and mixed meat, fish (salmon and trout) and mixed fish, legumes (white beans, chickpeas, lentils) and mixed legumes, and vegetables (green peas and courgettes) were analyzed for monitoring purposes. All samples, listed in Table 1, were purchased in local markets and

subsequently stored in their original packaging, properly labeled, and refrigerated ($4 \pm 1^\circ\text{C}$) until analysis. In Italy, in accordance with the European Regulation (37), the dietary guidelines suggest introducing homogenized products into infant complementary feeding, particularly during weaning, thanks to their consistency and specific composition.

Analytical grade cyclohexane, ethyl acetate, and acetonitrile were supplied by Merck Life Science s.r.l. (Darmstadt, Germany). Isooctane was purchased from Panreac Química S.L.U. (Castellar del Vallès, Barcelona, Spain). Deionized water ($18.2\text{ M}\Omega/\text{cm}$) was obtained from a Milli-Q purification system (Millipore, Milan, Italy). Polychlorinated biphenyl (PCB) 209 (purity >99.0%; 10 mg/L in isooctane, Lab Instruments Castellana Grotte, Bari, Italy) was used as internal standard. From this stock standard solution, PCB 209 working standard solutions of 1,000 $\mu\text{g/L}$ in isooctane were prepared and used to spike food samples at 100 $\mu\text{g/L}$. Within the subsequent monitoring survey of PAH levels in tested samples, PCB 209 was added to the samples before extraction, to perform reliable quantifications of target analytes with correction of errors due to ion suppression/enhancement caused by the presence of matrix co-extracts in the injector and ion source. Certified mix standard solution, indicated as IL8 constituted by benzo[a]pyrene (BAP), benz[a]anthracene (BAA), benzo[b]fluoranthene (BBF), chrysene (CHR) and their relative deuterated (PAHs-d12), that is BAP-d12, BAA-d12, BBF-d12 and CHR-d12 (purity >99.0%; 100 mg/L in toluene, Lab Instruments Castellana Grotte, Bari, Italy) was used for the method validation. Working standard solutions of 1,000 $\mu\text{g/L}$, 100 $\mu\text{g/L}$, 25 $\mu\text{g/L}$, and 10 $\mu\text{g/L}$ were obtained by diluting the stock IL8 in isooctane. All standard solutions were stored at -20°C and were taken out to allow them to reach room temperature and sonicated before use. Matrix-matched calibration (MMC) curves were obtained using 0.1, 0.5, 1.0, 2.0, 5.0 $\mu\text{g/L}$ working standard solutions of IL8 in the blank sample. The presence of the matrix effect was considered in the optimization and validation steps and in the monitoring study. MMCs were used because the different substances investigated had a different composition from each other, i.e., lipid, protein, carbohydrate and salt content (Table 1).

SupelMIP SPE – PAHs cartridges (50 mg/3 mL) were purchased from Merck Life Science s.r.l. (Darmstadt, Germany). Bond Elut Enhanced Matrix Removal - Lipid dispersive SPE (Bond Elut-EMR lipid dSPE) Agilent Technologies were purchased from Analitica sas (Gioia del Colle, Bari, Italia).

For QuEChERS procedures, all extraction and purification salts were listed below and were supplied by Lab Instruments (Castellana Grotte, Bari, Italy):

- QuE-Lab® EMR dSPE Lipid Tube (15 mL) with the following composition: 0.40 g NaCl and 1.60 g MgSO_4 ;
- QuE-Lab® Citrate tube (15 mL) with the following composition: 4.00 g MgSO_4 , 1.00 g NaCl, 0.50 g $\text{Na}_2\text{HC}_6\text{H}_5\text{O}_7 \cdot 1.5\text{H}_2\text{O}$ and 1.00 g $\text{C}_6\text{H}_5\text{Na}_3\text{O}_7 \cdot 2\text{H}_2\text{O}$;
- QuE-Lab® PSA Tube (15 mL) with the following composition: 950 mg MgSO_4 and 150 mg Primary secondary amine sorbent (PSA);
- QuE-Lab® PSA/C18 Tube (15 mL) with the following composition: 900 mg MgSO_4 , 150 mg PSA, and 150 mg C18 end-capped (C18EC);
- QuE-Lab® LLE tube EMR method (50 mL), with the following composition: 3.00 g NaCl, 0.50 g $\text{Na}_2\text{HC}_6\text{H}_5\text{O}_7 \cdot 1.5\text{H}_2\text{O}$ and 1.00 g $\text{C}_6\text{H}_5\text{Na}_3\text{O}_7 \cdot 2\text{H}_2\text{O}$;
- QuE-Lab® dSPE MgSO_4 tube EMR method (15 mL), with the following composition: 0.50 g MgSO_4 .

2.2 Extractions and clean-up procedures

The optimization of PAH extractions and clean-up protocols were performed on smoked salmon samples and chicken baby foods, following what was suggested by literature and on the base of our earlier knowledge relevant to the multi-residual analysis of foodstuffs (38, 39). During the development of analytical procedures, an ultrasonic bath (LIARRE s.r.l., Casalfiumanese, Bologna, Italy), a TX4

TABLE 1 Declared composition of investigated baby food matrices.

Matrix	Protein content (%)	Salt content (%)	Carbohydrates content (%)	Total lipid (%)	Fatty saturated (%)
Chicken	6.1	0.08	6.3	2.4	1.6
Beef	5.8	0.06	5.7	3.7	1.3
Lamb	5.5	0.05	6.8	3.1	1.5
Ham	7.9	0.20	8.7	3.6	1.2
Mixed Meat	7.5	0.10	6.6	2.1	0.5
Salmon	4.0	0.03	8.7	2.4	0.5
Trout	3.7	0.03	9.2	1.4	0.3
Mixed Fish	4.0	0.08	10	2.4	0.5
White beans	3.5	0.01	6.4	0.005	0.001
Chickpeas	2.5	0.01	4.9	0.9	0.1
Lentils	2.4	0.04	6.5	0.2	0.001
Mixed legumes	3.4	0.05	5.9	0.004	0.002
Green peas and courgettes	1.9	0.003	7.9	0.3	0.002

Digital vortex mixer (Velp Scientifica, Usmate Velate, Italy) and a BKC-DL5M centrifuge (BiobaseMeihua Trading Co., Ltd., Jinan, China) were used to sonicate, vortex and centrifuge, respectively.

2.2.1 Protocol I

SupelMIP SPE – PAH for extraction and clean-up. Aliquots of 2.5 g of homogenized samples were weighed into 10 mL screw-cap vials, 7.5 mL of cyclohexane were added, and then stirred for 2 min with a TX4 Digital VortexMixer (Velp Scientifica, Usmate, Italy) to disperse the sample. Afterwards, the mixture was sonicated for 20 min using an ultrasonic bath (LIARRE s.r.l., Casalfiumanese, Bologna, Italy), and centrifuged at 1,500 rpm for 15 min at 4°C with a BKC-DL5M centrifuge (BiobaseMeihua Trading Co., Ltd., Jinan, China). A SupelMIP column was conditioned with 1 mL of cyclohexane, then the sample was loaded, discarding the first eluate, avoiding its complete drying. After column washing with 2 mL of cyclohexane, for the elution of PAHs, 3 mL of ethyl acetate were used, collecting the eluate in a 10 mL glass vial, completely drying the column under vacuum. The extract was evaporated to dryness at 55°C under N₂ flow using an automated solvent evaporation system TurboVap® II (Biotage AB, Uppsala, Sweden). Finally, the dried extracts were suspended with 0.5 mL of working standard solution of PCB 209 and transferred into a glass vial for the following GC–MS/MS analysis in duplicate.

2.2.2 Protocol II

QuEChERS method using Bond Elut-EMR lipid dSPE for extraction and purification salts a) for clean-up. Aliquots of 5.0 g of homogenized samples were weighed into a 10 mL polypropylene tube, and 10 mL of acetonitrile were added. The mixture was vortexed for 2 min and centrifuged at 3,000 rpm for 5 min at 4°C. The resulting supernatant was then added to a tube containing 1.0 g of EMR-Lipid adsorbent and was vortexed for 2 min. The phases were separated by centrifugation at 3,000 rpm for 5 min at 4°C, and subsequently, the supernatant was put into a dispersive SPE tube containing a mixture of salts MgSO₄ and NaCl, vortexed for 2 min and then centrifuged at 3,000 rpm for 5 min at 4°C. The supernatant (8 mL) was evaporated to dryness under a N₂ stream at 55°C.

2.2.3 Protocol III

QuEChERS method using Bond Elut-EMR lipid dSPE for a double extraction and purification salts a) for clean-up. This protocol is the same as *Protocol II*, but the extraction procedure was repeated twice. Indeed, this step was carried out by adding acetonitrile and Bond Elut-EMR lipid two times consecutively, therefore the final volume of supernatant to be evaporated to dryness was 16 mL.

2.2.4 Protocol IV

QuEChERS method using dispersive salts b) for extraction step, and purification salts c) for clean-up. In this procedure, a double extraction with acetonitrile was performed and then the resulting supernatant was extracted with the following dispersive salts MgSO₄, NaCl, Na₂HC₆H₅O₇·1.5H₂O and C₆H₅Na₃O₇·2H₂O. Afterward, the mixture was vortexed for 2 min and the phases were separated by centrifugation 3,000 rpm for 5 min at 4°C; subsequently, the supernatant was purified with a mixture of salts MgSO₄ and PSA, vortexed for 2 min, and then centrifuged at 3,000 rpm for 5 min at

4°C. The supernatant (16 mL) was evaporated to dryness under an N₂ stream at 55°C.

2.2.5 Protocol V

QuEChERS method using dispersive salts b) for extraction step and purification salts d) for clean-up. This protocol is the same as Protocol IV for the three extractions, but the clean-up was performed using MgSO₄, PSA, and C18EC as dispersive salts. The supernatant (16 mL) was evaporated to dryness under an N₂ stream at 55°C.

2.2.6 Protocol VI

QuEChERS method using dispersive salts e) for extraction step and Bond Elut-EMR lipid dSPE and purification salts f) for clean-up. In this procedure, a double extraction with acetonitrile was performed and then the resulting supernatant was extracted with the following dispersive salts NaCl; Na₂HC₆H₅O₇·1.5H₂O and C₆H₅Na₃O₇·2H₂O. The extracted supernatant, firstly with Bond Elut-EMR lipid and after with MgSO₄, was then purified. Between the two purification steps, the sample was vortexed for 2 min and centrifuged at 3000 rpm for 5 min at 4°C. The supernatant (5 mL) was evaporated to dryness under an N₂ stream at 55°C.

2.2.7 Protocol VII

QuEChERS method using Bond Elut-EMR lipid dSPE and purification salts a) for clean-up. In this procedure, a double extraction with acetonitrile was performed and then the resulting supernatant was again extracted with EMR-lipid. Afterward, the supernatant was refrigerated at –20°C for 1 h and then purified with MgSO₄ and NaCl, vortexed for 1 min, and then centrifuged at 3,000 rpm for 10 min at 4°C. The supernatant (16 mL) was evaporated to dryness under an N₂ stream at 55°C.

Finally, all the dried extracts obtained from protocols II up to VII were suspended with 1.0 mL of working standard solution of PCB 209, as internal standard, and transferred into a glass vial for the following GC/MS/MS analysis in duplicate.

2.3 Gas chromatography/tandem mass spectrometry analyses (GC–MS/MS)

An Agilent 7693A Automatic Liquid Sampler and an Agilent 8,890 N gas chromatograph coupled with an Agilent 7,000 Triple Quadrupole detector (Little Falls, DE, United States) were used for GC–MS/MS analyses. Data were acquired using MSD ChemStation software (Agilent, Little Falls, DE, United States). The GC–MS/MS operating conditions are shown in [Table 2](#). Backflushing was used to prevent contamination with compounds strongly retained in the primary column by reversing a continuous flow of carrier gas, thus avoiding, through the second column, reaching the MS detector. According to European directive (40), the number of identification points that GC–MS/MS can earn, namely three points, one for ion precursor and 1.5 for each of two daughter ions. The identification point can be five if there are two precursor ions, each with 1 daughter of five points. The list of precursor ions, both quantifiers and qualifiers, their transitions, as well as the chosen collision energies (CEs), were shown for each of the 4 PAHs and the 4 PAHs-d12, in [Table 3](#).

TABLE 2 Operating conditions of GC–MS/MS.

Chromatographic parameters	
Liner	Ultra Inert Liner of 78.5 mm, ID 4 mm, OD 6.47 mm, volume 900 µL and single taper (Agilent technologies Little Falls, DE, United States)
Column 1 and Column 2	Ultra Inert 15 m x 0.25 mm, 0.25 µm film thickness (Agilent J&W. Scientific, Folsom, United States)
Carrier gas and flow mode	Helium carrier gas (99.999%); Flow in Colum 1: 1.0 mL/min Flow in Colum 2: 1.2 mL/min
Injection mode, temperature, and volume	Splitless mode, 280°C, 1 µL, hold time 3.0 min
Oven temperature	60°C (held 1.0 min); 170°C (rate 40°C/min, held 3.75 min) and 310°C (rate 10°C/min)
Blackflush	320°C (held 5.0 min)
Run time	18 min + 5 min blackflush

Mass spectrometer parameters	
Detector	MS operating in electron ionization mode: 70 eV
	Temperature of MS1 and MS2: 150°C
	Source temperature: 280°C
	Transfer line: 290°C
	Acquisition in Multiple Reaction Monitoring mode (MRM),
	Resolution MS ₁ = 1.5
	Resolution MS ₂ = 1.5

TABLE 3 List of quantifier and qualifier ions (m/z) used in GC–MS/MS method for PAHs, PAHs-d12, and PCB-209 determination.

Analyte	RT ^a	Quantifier ion	Transition	CE ^b	Qualifier ion	Transition	CE ^b
BAP	16.97	252	252 → 250	45	252	252 → 224	60
BAP-d12	16.92	264	264.1 → 260.1	40	265.1	265.1 → 261.1	40
BAA	13.93	228	228 → 226	40	228	228 → 227	25
BAA-d12	13.88	240	240 → 236	40	240	240 → 238	30
BBF	16.33	252	252 → 248	60	252	252 → 224	60
BBF-d12	16.28	264.1	264.1 → 260.1	40	265.1	265.1 → 261.1	40
CHR	14.02	228	228 → 226	40	228	228 → 227	25
CHR-d12	13.96	240	240 → 238	20	240	240 → 236	38
PCB 209	17.08	497.7	497.7 → 427.7	30	495.8	495.8 → 425.7	30

^aRT Retention time (min).

^bCE collision energy (V).

3 Results and discussion

3.1 Optimization of extraction and clean-up procedure

The identification of BAP, BAA, BBF, and CHR in GC–MS/MS analysis was performed by comparing the retention time of each compound with that of the relevant standard and verifying the presence of precursor ions (Table 3). The ratios between the peak areas of quantifier ions and PCB 209 were used for the compound quantification.

The first two extraction and clean-up protocols were tested using MMC curves with smoked salmon samples. MMC curves of SupelMIP SPE and QuEChERS based on Bond Elut-EMR lipid dSPE showed correlation coefficients ≥ 0.99 . The recovery percentage at 2 µg/kg was

also evaluated, carrying out 3 replicates for both protocols, also comparing two different solvents, i.e., acetonitrile and toluene, for the preparation of the IL8 working standard solution used to spike the samples. The results, shown in Table 4, demonstrated that the QuEChERS approach gave higher recovery values (71.4–83.0%) compared to SupelMIP SPE (29.8–48.8%). In Figure 1, the chromatographic separation and mass spectrometric identification of the analytes were reported for protocol based on the QuEChERS procedure. Therefore, the QuEChERS method was selected as the best procedure and was further optimized, modifying the extraction and purification steps in the other 5 Protocols (III, IV, V, IV, and VII). No significant differences emerged changing the solvent for standard solutions preparation, therefore, considering the high toxicity of toluene compared to acetonitrile, the latter was selected for further experiments.

TABLE 4 Mean values ($N = 3$) of recovery % of smoked salmon samples, spiked at 2 $\mu\text{g/kg}$, obtained from Protocol I and II, using IL8 working standard solution prepared with two solvents, toluene and acetonitrile, respectively.

Extraction and clean-up procedure	Solvents	BAA	BAP	BBF	CHR
Protocol I	Toluene	40.3%	29.6%	33.4%	40.4%
	Acetonitrile	48.8%	36.5%	40.4%	48.1%
Protocol II	Toluene	80.6%	71.4%	77.6%	83.0%
	Acetonitrile	80.3%	71.4%	78.2%	80.0%

Protocols from III to VII were tested with chicken baby food samples, performing two replicates for the recovery evaluation at 0.5 $\mu\text{g/kg}$. Protocols III, IV, V, and VI provided recovery values <10%, as shown in Table 5. Protocol VII provided the best results with recovery values ranging from 70 to 90% and, for this reason, it was chosen as the extraction and cleaning procedure for subsequent validation and monitoring. In particular, concerning other tested procedures, the step at -20°C overnight, together with chosen salts, enhanced the clean-up with better removal of co-extracted fat lipids. Then, protocol VII was also tested on other infant food matrices based on meat, fish, legumes, and mixed fruits. The full dataset obtained from this study was evaluated by using Box Plot, a useful tool of graphic representation used for managing quantitative data. This tool allows the comparison of many distributions in the same graph, highlighting the most significant characteristics such as symmetry, range, variance, and possible outliers. The median value, first and third interquartile, upper and lower limits within Tukey's limit, and outliers (if any) can be visualized in a single graphical representation. Moreover, the use of median and quartiles in describing the distribution makes the considerations about possible outliers in the dataset more robust. The dataset obtained during the method validation showed similar accuracy parameters for 4 PAHs, but different behavior in different matrices. A more detailed data analysis showed that the mean recovery percentage obtained by analysing baby food samples of mixed meats, legumes, fish products, and chicken were comparable, in the range of 80–100%, with higher variance in chicken samples, while a lower value (~60%) was obtained from homogenized mixed fruits analysis. Regarding method sensitivity, evaluated by elaborating the linear regression, the higher performance was obtained for BAA, followed by CHR, BAP, and BBF. The Box Plot, shown in Figure 2, was successfully applied for optimizing the analytical method for the detection of 4 PAHs in baby food since it allows rapid and effective visualization of all statistical parameters that characterize the procedure.

3.2 Method validation

The following validation parameters, namely the linearity of MMC curves, the limit of detection (LOD), the limit of quantification (LOQ), the selectivity, the precision, the recovery percentage, and the ruggedness were determined to assure the efficiency of the proposed GC–MS/MS method and to guarantee the validity of routine analysis. The MMC curve for the 4 PAHs was evaluated from 0.1 to 5 $\mu\text{g/kg}$, considering the framework of European legislation for residues in baby foods (40). MMC curves were used for the validation method,

TABLE 5 Mean values ($N = 3$) of recovery % of smoked salmon samples, spiked at 2 $\mu\text{g/kg}$, obtained from Protocol III to Protocol VII, using IL8 working standard solution prepared with acetonitrile.

Extraction and clean-up procedure	BAA	BAP	BBF	CHR
Protocol III	9.8%	7.3%	9.5%	4.3%
Protocol IV	8.8%	7.9%	9.5%	8.9%
Protocol V	7.5%	10.1%	10.2%	9.5%
Protocol VI	8.3%	7.3%	10.1%	10.2%
Protocol VII	70.5%	84.5%	89.2%	71.0%

analyzing each level in triplicate. All validation parameters, obtained using matrix chicken baby food (Table 6) resulted in compliance with EU provision No. 836/2011 and 808/2021 (41, 42).

The coefficients of determination (R^2 values) were in the range of 0.998–0.999, indicating good calibration linearity in investigated matrices. Mandel test was used to assess whether the data best fitted a linear function. The test was verified with a p -value <0.05. The significance of the slope (b), of the regression line obtained from the MMC curve, at $\alpha = 0.05$, was verified with a t -test. The t -Student was calculated for ratios s_b/b , where s_b was the standard deviation of the slope b , obtained for each of the studied analytes. All the values resulted lower than 0.22. Figure 3 shows MMC curves for each PAHs.

LODs and LOQs were calculated, according to the following equations: $\text{LOD} = 3.3s_a/b$ and $\text{LOQ} = 10s_a/b$, where s_a was the standard deviation of the intercept. The calculated values of LOD and LOQ (Table 6), indicated high sensitivity for the determination of these analytes at trace levels, reducing the risk of false-negative results. Selectivity ensures the correct identification of analytes of interest without interference from other components that could be present in the sample, such as impurities, degradants, matrix components, etc. To verify method selectivity, 20 sample blanks representative of the chosen matrices were analysed. The 20 specificity tests were carried out on the following baby food samples: chicken, beef, lamb, ham, salmon, trout, white bean, chickpea, legumes, pea and courgettes, mixed meat, and mixed fish. The absence of significant interferences in the maximum tolerance range of ± 0.1 min for analyte retention times compared to a spiked sample was verified.

The trueness and precision of measurements were assessed in accordance with Decision 2021/808/EC (40) through the analysis of spiked samples, prepared starting from blank material by additions of known amounts of the analytes. The precision of a method measures the repeatability, evaluating the degree of agreement among individual test results. The recovery percentage is used to indicate trueness and to express the distance between the mean and the reference value. Precision and trueness were determined by analyzing two sets of blank matrices (six replicates each), spiked at a concentration of 0.1 $\mu\text{g/kg}$ for each analyte. Precision was expressed as deviation standard (SD) and relative deviation standard (RSD), while trueness was expressed as recovery %. The intra-day RSD values were well below the reference values of 20%, derived by the Horwitz equation, under repeatability conditions, demonstrating a good method precision (43). Calculated values of recoveries % and RDS % were in the range of 73–110% and always lower than 8.75%, respectively. Homoscedasticity of data was evaluated using ANOVA ($p = 0.05$), calculating the mean of recoveries %, obtained for the level at 0.1 $\mu\text{g/Kg}$. The recovery factors resulted from 0.903 to 1.368 for the 4 PAHs. In Figure 4, an example of a

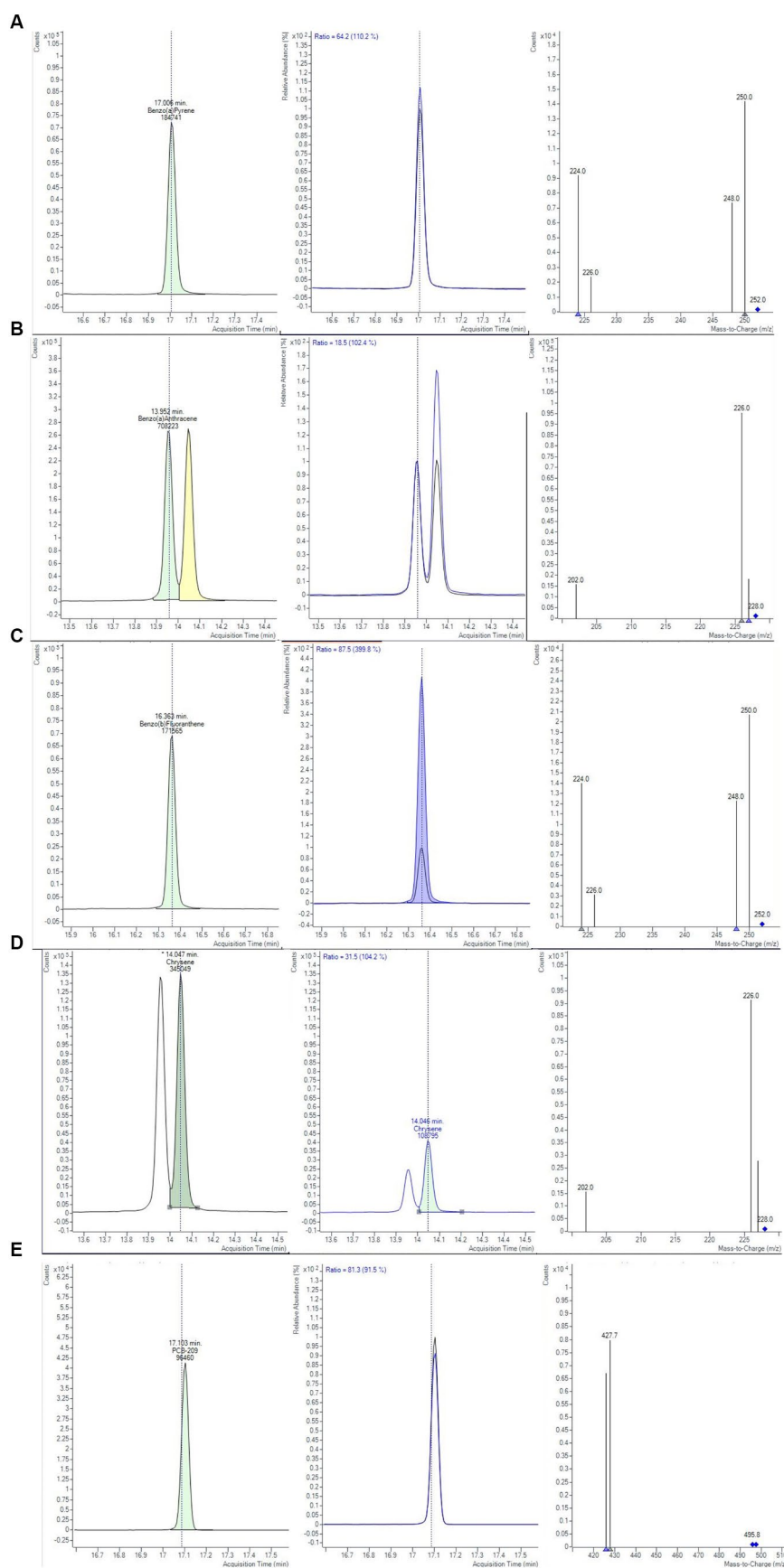


FIGURE 1

Chromatograms and mass spectra of quantifier and qualifier ions (m/z) used in GC-MS/MS method for (A) BAP, (B) BAA, (C) BBF, (D) CHR, (E) PCB-209 determination, obtained from smoked salmon samples, extracted with Protocol II based on QuEChERS method (Bond Elut-EMR lipid dSPE for extraction and purification salts for clean-up, see text for details).

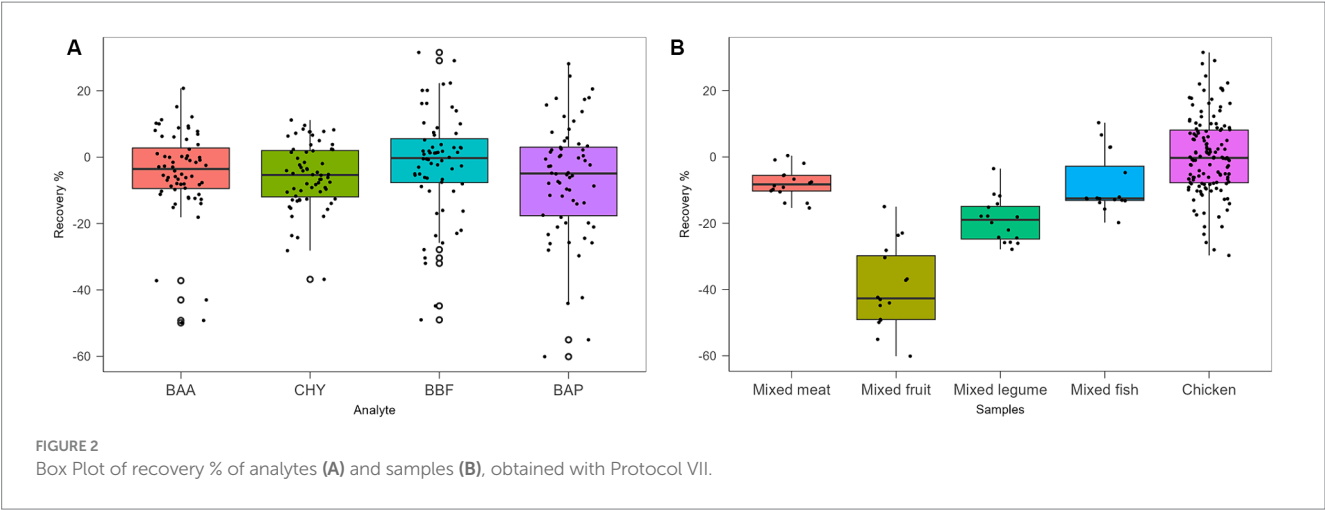
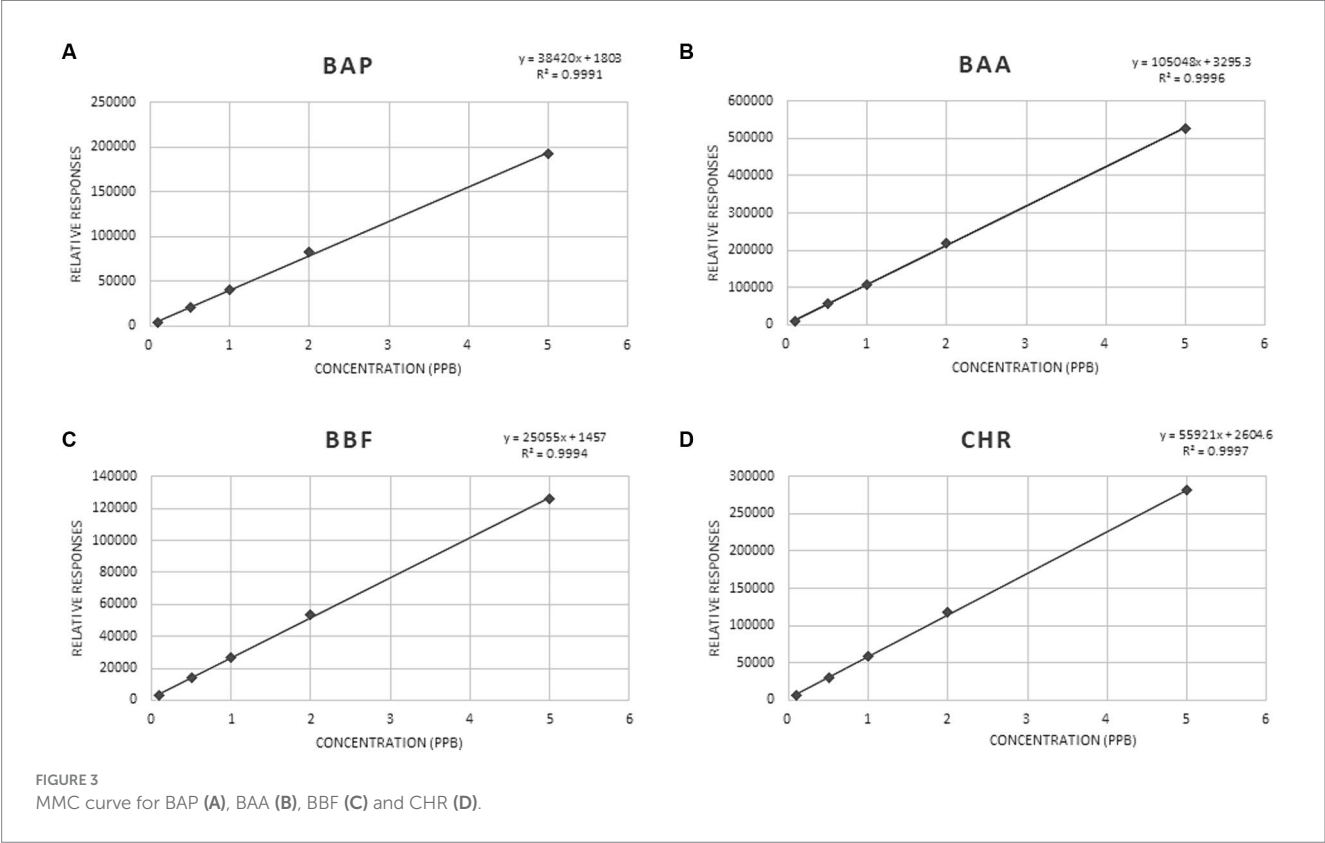


TABLE 6 Validation parameters of BAP, BAA, BBF, and CHR, determined by means of GC–MS/MS analysis of chicken samples, extracted and cleaned-up with Protocol VII.

PAH	$t s_b/b < 0.22^a$	Intercept	R^{2b}	LOD ^c	LOQ ^d	SD \pm RSD % ^e	Recovery % \pm RSD % ^e	Uncertainty % ^f
BAP	0.056	1.803×10^{-3}	0.999	0.036	0.110	0.004 ± 5.56	73.08 ± 4.06	10.15
BAA	0.035	3.295×10^{-3}	0.999	0.023	0.070	0.005 ± 5.43	94.25 ± 5.12	9.98
BBF	0.043	1.457×10^{-3}	0.999	0.028	0.080	0.005 ± 7.29	76.07 ± 5.54	12.57
CHY	0.030	2.604×10^{-3}	0.999	0.019	0.060	0.009 ± 7.91	110.70 ± 8.75	13.47

^a t -Student of the ratios s_b/b , where s_b is the standard deviation of the slope of MMC curve (b).
^b R^2 is the coefficients of determination of MMC curve.
^cLimit of detection (LOD) = $3.3s_b/b$ where s_b was the standard deviation of the intercept.
^dLOQ = $10s_b/b$, both calculated from MMC curve.
^eMean values \pm standard deviations ($n=6$) of blank matrices fortified at 0.1 $\mu\text{g/kg}$ for each analyte.
^fMean values determined of blank matrices fortified at 0.1 $\mu\text{g/kg}$ for each analyte ($n=6$).



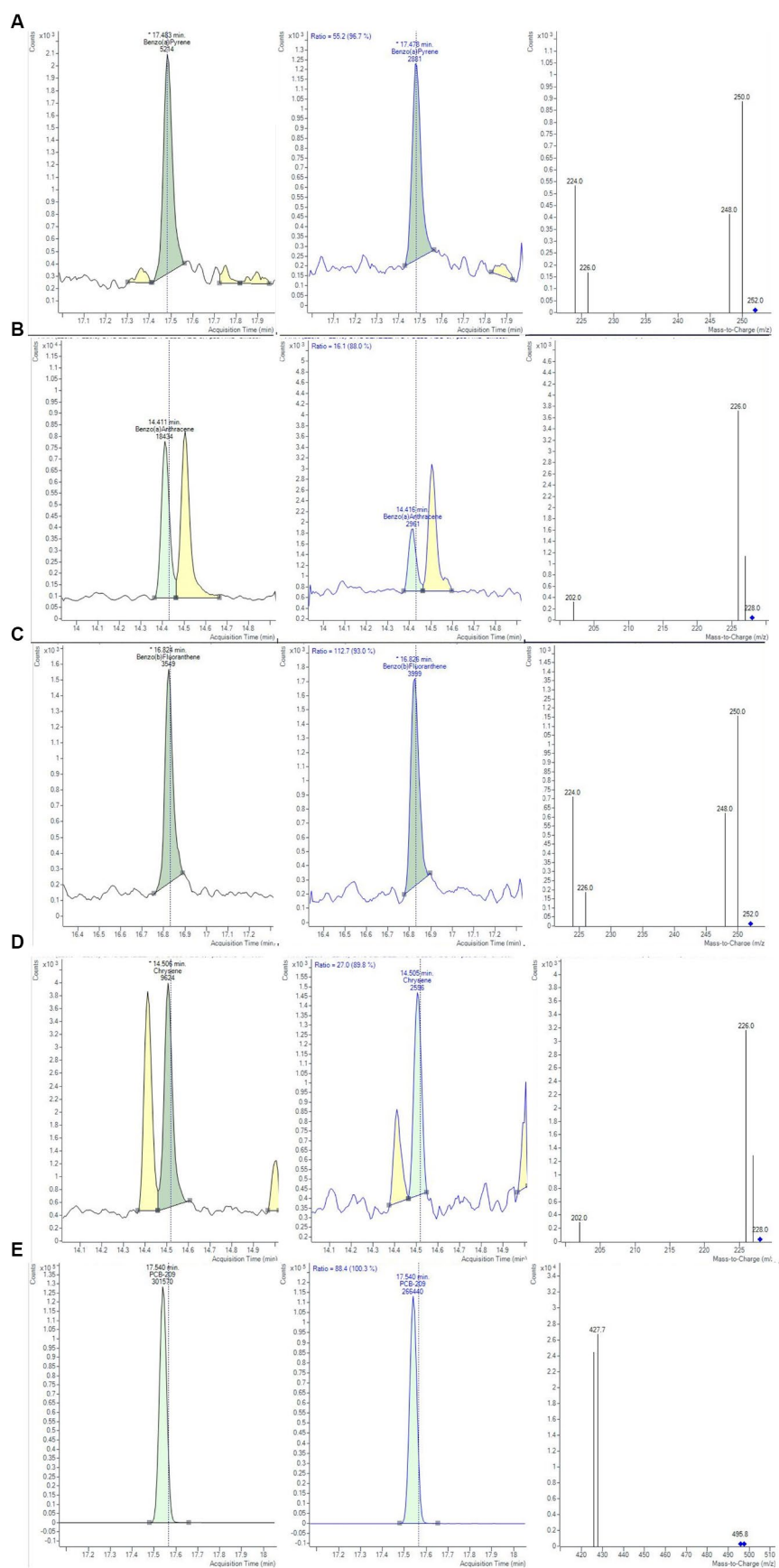


FIGURE 4

Chromatograms and mass spectra of quantifier and qualifier ions (m/z) used in GC-MS/MS method for (A) BAP, (B) BAA, (C) BBF, (D) CHR, (E) PCB-209 determination, obtained at 0.1 µg/Kg for the evaluation of method precision.

TABLE 7 Repeatability and recovery % of BAP, BAA, BBF, and CHR, determined by means of GC–MS/MS analysis of fish and legume baby foods samples, extracted and cleaned-up with Protocol VII.

Analyte	Fish baby foods ^a		Legume baby foods ^b	
	$ C_1 - C_2 < s_r \times t\sqrt{2}$	Recovery %	$ C_1 - C_2 < s_r \times t\sqrt{2}$	Recovery %
BAP	$ 0.063 - 0.066 < 0.014$	64.5	$ 0.743 - 0.756 < 0.400$	74.95
BAA	$ 0.096 - 0.095 < 0.018$	95.5	$ 0.848 - 0.859 < 0.233$	85.35
BBF	$ 0.080 - 0.071 < 0.018$	75.5	$ 0.721 - 0.742 < 0.334$	73.15
CHR	$ 0.110 - 0.103 < 0.032$	106.5	$ 0.758 - 0.822 < 0.214$	79.00

^aCollected data by performing the analysis on sets of six replicates of blank matrices fortified at a concentration of 0.1 µg/kg for each analyte.

^bCollected data by performing the analysis on sets of six replicates of blank matrices fortified at a concentration of 1.0 µg/kg for each analyte.

TABLE 8 Repeatability standard deviation (s_r) at 0.1, 1.0 and 1.5 µg/kg of BAP, BAA, BBF and CHR, calculated in step of validation method by means of GC–MS/MS analysis of chicken baby foods samples, extracted and cleaned-up with Protocol VII.

s_r	BAP	BAA	BBF	CHR
0.1 µg/kg	0.004	0.005	0.005	0.008
1.0 µg/kg	0.108	0.064	0.092	0.060
1.5 µg/kg	0.161	0.101	0.053	0.083

chromatographic separation obtained at 0.1 µg/kg was reported, showing the chromatogram of quantifier ions and relative studied transition for all 4 PAHs in chicken baby food samples. For the evaluation of the uncertainty of measurements, the metrological approach was adopted, using the validation data obtained from each step of the analytical procedure. Taking into consideration the uncertainties propagation law, the concentration relative uncertainty was calculated for 4 PAHs, as reported in a previous work (39). A relative expanded measurement uncertainty was calculated using a coverage factor k of 2, corresponding approximately to a 95% confidence level.

The robustness of this analytical method was evaluated by Youden's test, introducing several changes at once (44). The application of the method to other matrices was considered as changes to be applied. Hence, mixed meat and fish were also spiked at 1.0 µg/Kg of each PAH and then analyzed and compared with chicken samples. The standard deviation of the differences D_i (SD_i) was calculated according to the equation reported by Karageorgou and Samanidou (45). SD_i resulted not significantly larger than the standard deviation of the method carried out on validated matrices (chicken samples), confirming that the proposed method is sufficiently robust against the chosen modification.

Moreover, other matrices such as fish and legume baby foods were considered. Further analyses on two sets of blank matrices (four replicates each) were also carried out. Fish and legume blank samples were spiked at a concentration of 0.1 and 1.0 µg/kg for each analyte, respectively. To evaluate the method reproducibility, the absolute difference between independent single test results (C_1 and C_2) was considered. The $|C_1 - C_2|$ values were not found to be higher than the repeatability limit, calculated against the expected 95% probability interval of $s_r \times t\sqrt{2}$, where s_r is the repeatability standard deviation at 1.0 µg/kg, as shown in Table 7. For fish samples, values of recovery % resulted in the range of 83–105%, while for the legume matrix, they were in the range of 73–85%. Also, these data were compliant with the acceptability criteria of European regulation (41, 42).

3.3 Evaluation of four PAHs in baby food samples

The monitoring was performed over 2 years, by analyzing a total of 60 samples of baby food, of common brands present on the Italian market, and of different compositions (meat, fish, legumes, and vegetables). The samples were analyzed in duplicate, verifying that the concentrations of each analyte satisfied the repeatability criteria, i.e., the absolute difference of two values $|C_1 - C_2|$ must not exceed the repeatability limit ($s_r \times t\sqrt{2}$). In Table 8 values of s_r , obtained during the validation step, were calculated at three levels (0.1, 1.0, and 1.5 µg/kg). If $|C_1 - C_2|$ satisfied these criteria, a mean value of concentration was calculated and reported together with its measurement uncertainty, also considering the coverage and recovery factors. The final results were expressed as the sum of 4 PAHs. The results showed that the mean level of total PAHs, for all the investigated samples, was always below the lowest LOQ. Moreover, as reported in the literature, cooking methods could influence the production of PAHs (46). Considering that microwave and steaming cooking are the most used methods to conserve nutrients and quality of baby foods, 40 samples of chicken, salmon, lentils, and mixed legumes and vegetables, were analyzed after these heat treatments. Twenty samples were heated for 5 min in a water bath at 100°C and the other 20 samples were heated for 30 s in a microwave at full power. As in the previous case, PAH contents resulted under the LODs and then they were not detected and quantified (Figure 5). However, in this regard, further studies are needed to evaluate the formation of 4 PAHs also considering other setting parameters (temperature, time, power etc...) but also different cooking treatments.

4 Conclusion

Different extraction and clean-up procedures were evaluated and compared for the analytical determination of four regulated PAHs in different infant foods, aiming to achieve high recovery rates and low detection and quantification limits. The QuEChERS method based on

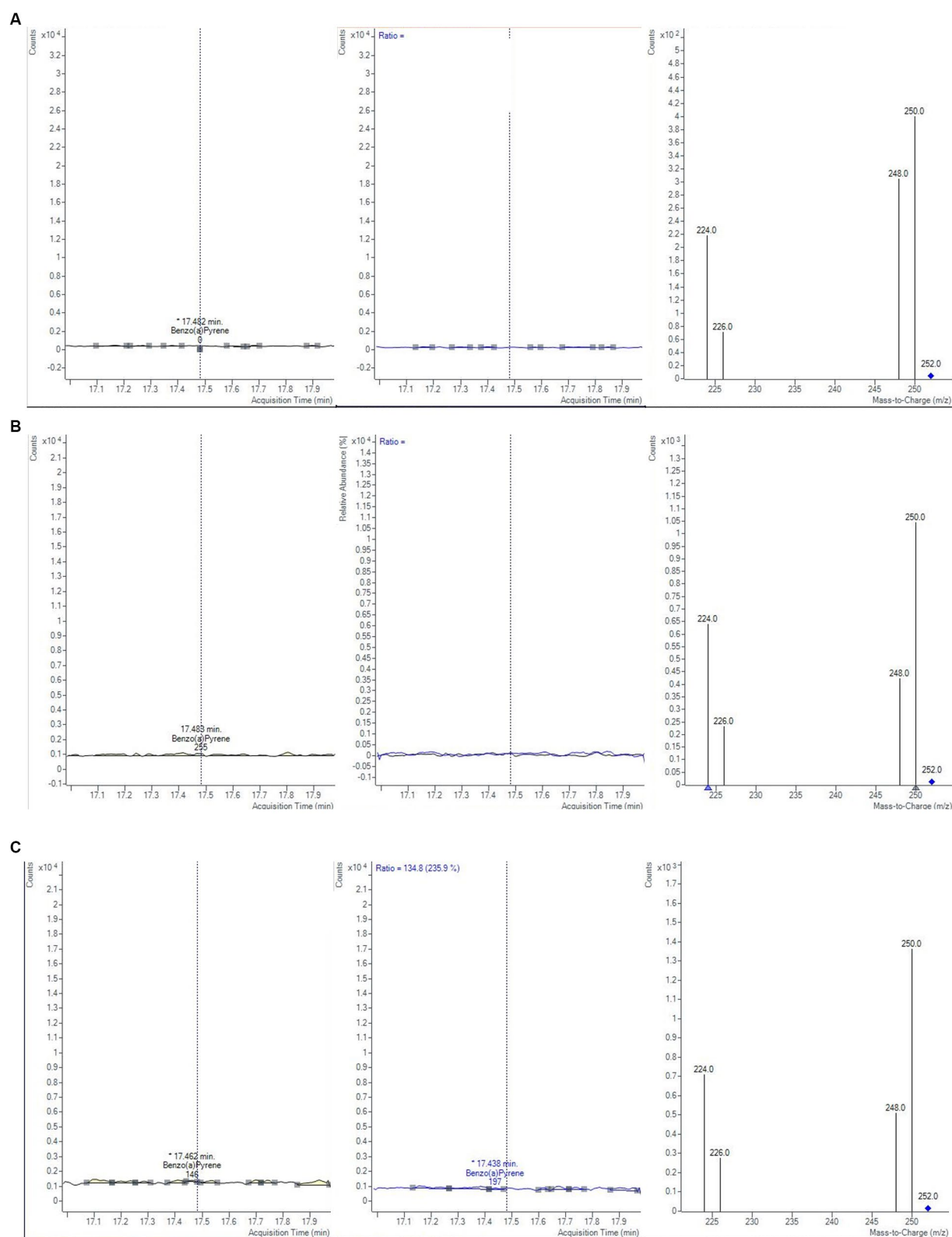


FIGURE 5

Chromatograms and mass spectra of quantifier and qualifier ions (m/z) used in GC-MS/MS method for BAP determination in fish baby food samples (A) not-cooked, (B) after microwave cooking and (C) after steaming cooking.

a triple extraction, twice with acetonitrile and once with Bond Elut-EMR lipid dSPE, followed by a subsequent purification with salts NaCl and $MgSO_4$ 1:4 and $-20^\circ C$ overnight, was found to be the best

procedure, with recoveries in the range of 70–90% for the target analytes. The proposed method, based on GC-MS/MS analysis, was validated and used to analyze baby food samples (meat, fish, legumes,

and vegetables), collected in the Italian market. The monitoring was performed on untreated, steamed, and microwaved baby foods, confirming that the concentration levels of BAP, BAA, BBF, and CHR were lower than LOQs and consequently lower than the EU standard limit (1 µg/kg) in all samples. Moreover, considering the high toxicity and carcinogenicity of BAP, this monitoring has provided reassuring results for children's common products on the Italian market. In conclusion, the developed GC/MS/MS method provided a highly sensitive and reliable approach for the determination of PAHs in different types of baby foods, even at trace levels. This method can contribute to the assessment of PAH exposure in infants and support regulatory efforts to ensure the safety and quality of infant food products with regular monitoring.

Data availability statement

The raw data supporting the conclusions of this article will be made available by the authors, without undue reservation.

Author contributions

MI: Writing – original draft, Writing – review & editing, Conceptualization, Data curation, Formal analysis, Investigation, Methodology, Software, Validation. RZ: Writing – original draft, Writing – review & editing, Investigation, Visualization. ID: Data curation, Formal analysis, Validation, Writing – original draft. ACh: Data curation, Formal analysis, Writing – original draft, Validation. VN: Conceptualization, Funding acquisition, Investigation, Project administration, Resources, Supervision, Visualization, Writing – original draft. FC: Conceptualization, Data curation, Investigation, Visualization, Writing – original draft. ACa: Formal analysis, Writing

– original draft. MQ: Conceptualization, Investigation, Methodology, Visualization, Writing – original draft, Writing – review & editing. DN: Conceptualization, Investigation, Visualization, Writing – original draft. MIa: Conceptualization, Investigation, Project administration, Resources, Supervision, Visualization, Writing – original draft, Writing – review & editing.

Funding

The author(s) declare that financial support was received for the research, authorship, and/or publication of this article. This research was supported by the Italian Ministry of Health, Roma, Italy (Project code: IZSPB-08/2020 RC).

Conflict of interest

The authors declare that the research was conducted in the absence of any commercial or financial relationships that could be construed as a potential conflict of interest.

The author(s) declared that they were an editorial board member of Frontiers, at the time of submission. This had no impact on the peer review process and the final decision.

Publisher's note

All claims expressed in this article are solely those of the authors and do not necessarily represent those of their affiliated organizations, or those of the publisher, the editors and the reviewers. Any product that may be evaluated in this article, or claim that may be made by its manufacturer, is not guaranteed or endorsed by the publisher.

References

- Palade LM, Negoită M, Adascăluţ AC, Mihai AL. Polycyclic aromatic hydrocarbon occurrence and formation in processed meat, edible oils, and cereal-derived products: a review. *Appl Sci.* (2023) 13:7877. doi: 10.3390/app13137877
- Shoaei F, Talebi-Ghane E, Amirsadeghi S, Mehri F. The investigation of polycyclic aromatic hydrocarbons (PAHs) in milk and its products: a global systematic review, meta-analysis and health risk assessment. *Int Dairy J.* (2023) 142:105645. doi: 10.1016/j.idairyj.2023.105645
- Sampaio GR, Guizellini GM, da Silva SA, de Almeida AP, Pinaffi-Langley ACC, Rogero MM, et al. Polycyclic aromatic hydrocarbons in foods: biological effects, legislation, occurrence, analytical methods, and strategies to reduce their formation. *Int J Mol Sci.* (2021) 22:6010. doi: 10.3390/ijms22116010
- Habe H, Omori T. Genetics of polycyclic aromatic hydrocarbon metabolism in diverse aerobic bacteria. *Biosci Biotechnol Biochem.* (2003) 67:225–43. doi: 10.1271/bbb.67.225
- Purcaro G, Moret S, Conte LS. Overview on polycyclic aromatic hydrocarbons: occurrence, legislation and innovative determination in foods. *Talanta.* (2013) 105:292–305. doi: 10.1016/j.talanta.2012.10.041
- Hirano M, Tanaka S, Asami O. Classification of polycyclic aromatic hydrocarbons based on mutagenicity in lung tissue through DNA microarray. *Environ Toxicol.* (2013) 28:652–9. doi: 10.1002/tox.20761
- Patel AB, Shaikh S, Jain KR, Desai C, Madamwar D. Polycyclic aromatic hydrocarbons: sources, toxicity, and remediation approaches. *Front Microbiol.* (2020) 11:562813. doi: 10.3389/fmicb.2020.562813
- Kang HJ, Lee SY, Kwon JH. Physico-chemical properties and toxicity of alkylated polycyclic aromatic hydrocarbons. *J Hazard Mater.* (2016) 312:200–7. doi: 10.1016/j.jhazmat.2016.03.051
- Zelinkova Z, Wenzl T. The occurrence of 16 EPA PAHs in food – a review. *Polycycl Aromat Compd.* (2015) 35:248–84. doi: 10.1080/10406638.2014.918550
- European Food Safety Authority. Polycyclic aromatic hydrocarbons in food—scientific opinion of the panel on contaminants in the food chain. *EFSA J.* (2008) 6:724. doi: 10.2903/j.efsa.2008.724
- Huertas-Pérez JF, Bordajandi LR, Sejerøe-Olsen B, Emteborg H, Baù A, Schimmel H, et al. PAHs in baby food: assessment of three different processing techniques for the preparation of reference materials. *Anal Bioanal Chem.* (2015) 407:3069–81. doi: 10.1007/s00216-015-8490-z
- Darwish WS, Chiba H, El-Ghareeb WR, Elhelaly AE, Hui S-P. Determination of polycyclic aromatic hydrocarbon content in heat-treated meat retained in Egypt: health risk assessment, benzo[a]pyrene induced mutagenicity and oxidative stress in human colon (CaCo-2) cells and protection using rosmarinic and ascorbic acids. *Food Chem.* (2019) 290:114–24. doi: 10.1016/j.foodchem.2019.03.127
- Polachova A, Gramblícká T, Parizek O, Sram RJ, Stupak M, Hajslova J, et al. Estimation of human exposure to polycyclic aromatic hydrocarbons (PAHs) based on the dietary and outdoor atmospheric monitoring in the Czech Republic. *Environ Res.* (2020) 182:108977. doi: 10.1016/j.envres.2019.108977
- Duan X, Shen G, Yang H, Tian J, Wei F, Gong J, et al. Dietary intake polycyclic aromatic hydrocarbons (PAHs) and associated Cancer risk in a cohort of Chinese urban adults: inter- and intra-individual variability. *Chemosphere.* (2016) 144:2469–75. doi: 10.1016/j.chemosphere.2015.11.019
- Hokkanen M, Mikkilä A, Pasonen P, Tuominen P, Uusitalo L, Erkkola M, et al. Children's dietary exposure to polycyclic aromatic hydrocarbons in Finland. *Polycycl Aromat Compd.* (2022) 42:4651–65. doi: 10.1080/10406638.2021.1903951
- Huang X, Deng X, Li W, Liu S, Chen Y, Yang B, et al. Internal exposure levels of polycyclic aromatic hydrocarbons in children and adolescents: a systematic review and meta-analysis. *Environ Health Prev Med.* (2019) 24:50. doi: 10.1186/s12199-019-0805-9
- Moazzen M, Shariatifar N, Arabameri M, Hosseini H, Ahmadloo M. Measurement of polycyclic aromatic hydrocarbons in baby food samples in Tehran, Iran with

magnetic-solid-phase-extraction and gas-chromatography/mass-spectrometry method: a health risk assessment. *Front Nutr.* (2022) 9:833158. doi: 10.3389/fnut.2022.833158

18. Mielech A, Puścion-Jakubik A, Socha K. Assessment of the risk of contamination of food for infants and toddlers. *Nutrients.* (2021) 13:2358. doi: 10.3390/nu13072358

19. Drwal E, Rak A, Gregoraszcuk EL. Review: polycyclic aromatic hydrocarbons (PAHs)—action on placental function and health risks in future life of newborns. *Toxicology.* (2019) 411:133–42. doi: 10.1016/j.tox.2018.10.003

20. Bansal V, Kim K-H. Review of PAH contamination in food products and their health hazards. *Environ Int.* (2015) 84:26–38. doi: 10.1016/j.envint.2015.06.016

21. European Commission. Commission regulation (EU) 2023/915 of 25 April 2023 on maximum levels for certain contaminants in food and repealing regulation (EC) no 1881/2006. *OJEU.* (2023) L 119: 66:103–57.

22. Agus BAP, Rajentran K, Selamat J, Lestari SD, Umar NB, Hussain N. Determination of 16 EPA PAHs in food using gas and liquid chromatography. *J Food Compos Anal.* (2023) 116:105038. doi: 10.1016/j.jfca.2022.105038

23. Zianni R, Mentana A, Campaniello M, Chiappinelli A, Tomaiuolo M, Chiaravalle AE, et al. An investigation using a validated method based on HS-SPME-GC-MS detection for the determination of 2-dodecylcyclobutanone and 2-tetradecylcyclobutanone in X-ray irradiated dairy products. *LWT.* (2022) 153:112466. doi: 10.1016/j.lwt.2021.112466

24. Anastassiades M, Lehotay SJ, Štajnbaher D, Schenck FJ. Fast and easy multiresidue method employing acetonitrile extraction/partitioning and “dispersive solid-phase extraction” for the determination of pesticide residues in produce. *J AOAC Int.* (2003) 86:412–31. doi: 10.1093/jaoac/86.2.412

25. He Z, Wang L, Peng Y, Luo M, Wang W, Liu X. Multiresidue analysis of over 200 pesticides in cereals using a QuEChERS and gas chromatography–tandem mass spectrometry-based method. *Food Chem.* (2015) 169:372–80. doi: 10.1016/j.foodchem.2014.07.102

26. Santana-Mayor A, Rodríguez-Ramos R, Herrera-Herrera AV, Socas-Rodríguez B, Rodríguez-Delgado MA. Updated overview of QuEChERS applications in food, environmental and biological analysis (2020–2023). *Trends Anal Chem.* (2023) 169:117375. doi: 10.1016/j.trac.2023.117375

27. Perestrelo R, Silva P, Porto-Figueira P, Pereira JAM, Silva C, Medina S, et al. QuEChERS - fundamentals, relevant improvements, applications and future trends. *Anal Chim Acta.* (2019) 1070:1–28. doi: 10.1016/j.jaca.2019.02.036

28. Surma M, Sadowska-Rociek A, Cieślík E. The application of d-SPE in the QuEChERS method for the determination of PAHs in food of animal origin with GC-MS detection. *Eur Food Res Technol.* (2014) 238:1029–36. doi: 10.1007/s00217-014-2181-4

29. Anastassiades M, Scherbaum E, Taşdelen B, Štajnbaher D. Recent developments in QuEChERS methodology for pesticide multiresidue analysis. *Pesticide Chem.* (2007) 46:439–58. doi: 10.1002/9783527611249.ch46

30. Lehotay SJ. Collaborators: determination of pesticide residues in foods by acetonitrile extraction and partitioning with magnesium sulfate: collaborative study. *J AOAC Int.* (2007) 90:485–520. doi: 10.1093/jaoac/90.2.485

31. Sun Y, Wu S. Analysis of PAHs in oily systems using modified QuEChERS with EMR-lipid clean-up followed by GC-QqQ-MS. *Food Control.* (2020) 109:106950. doi: 10.1016/j.foodcont.2019.106950

32. Chen B-H, Inbaraj BS, Hsu K-C. Recent advances in the analysis of polycyclic aromatic hydrocarbons in food and water. *J Food Drug Anal.* (2022) 30:494–522. doi: 10.38212/2224-6614.3429

33. Sadowska-Rociek A, Surma M, Cieślík E. Comparison of different modifications on QuEChERS sample preparation method for PAHs determination in black, green, red

and white tea. *Environ Sci Pollut Res Int.* (2014) 21:1326–38. doi: 10.1007/s11356-013-2022-1

34. ITeh Stand (n.d.) EN 16619:2015 - food analysis - determination of benzo[a]pyrene, benz[a]anthracene, chrysene and benzo[b]fluoranthene in foodstuffs by gas chromatography mass spectrometry (GC-MS). Available at: <https://standards.iteh.ai/catalog/standards/cen/ca6d5bc8-3a90-4857-a250-7cfcb9096c4b/en-16619-2015> (Accessed January 19, 2024).

35. Wenzl T, Simon R, Anklaam E, Kleiner J. Analytical methods for polycyclic aromatic hydrocarbons (PAHs) in food and the environment needed for new food legislation in the European Union. *Trends Anal Chem.* (2006) 25:716–25. doi: 10.1016/j.trac.2006.05.010

36. Prata R, López-Ruiz R, Nascimento LES, Petrarca MH, Godoy HT, French AG, et al. Method validation for GC-measurable pesticides and PAHs in baby foods using QuEChERS-based extraction procedure. *J Food Compos Anal.* (2024) 129:106062. doi: 10.1016/j.jfca.2024.106062

37. European Commission 2013/609/E commission regulation (EU) 2013/609 regulation (EU) of 12 June 2013 on food intended for infants and young children, food for special medical purposes, and total diet replacement for weight control and repealing council directive 92/52/EEC, commission directives 96/8/EC, 1999/21/EC, 2006/125/EC and 2006/141/EC, directive 2009/39/EC of the European Parliament and of the council and commission regulations (EC) no 41/2009 and (EC) no 953/2009 (text with EEA relevance) (2023) Available at: <http://data.europa.eu/eli/reg/2013/609/2023-03-21>

38. Nardelli V, D'Amico V, Della Rovere I, Casamassima F, Marchesiello WMV, Nardiello D, et al. Box Behnken design-based optimized extraction of non-dioxin-like PCBs for GC-ECD and GC-MS analyses in milk samples. *Emerg Contam.* (2020) 6:303–11. doi: 10.1016/j.emcon.2020.08.002

39. Nardelli V, D'Amico V, Ingegno M, Della Rovere I, Iammarino M, Casamassima F, et al. Pesticides contamination of cereals and legumes: monitoring of samples marketed in Italy as a contribution to risk assessment. *Appl Sci.* (2021) 11:7283. doi: 10.3390/app11167283

40. European Commission. 2002/657/EC Commission decision of 12 august 2002 implementing council directive 96/23/EC concerning the performance of analytical methods and the interpretation of results (notified under document number C(2002) 3044). *OJEU.* (2002) 45:8–36.

41. European Commission. 2011/836/EC Commission regulation (EU) no. 836/2011 amending regulation (EC) no. 333/2007 laying down the methods of sampling and analysis for the official control of the levels of lead, cadmium, mercury, inorganic tin, 3-MCPD and benzo(a)pyrene in foodstuffs. *OJEU.* (2011) 4:9–116.

42. European Commission. 2021/808/EC Commission implementing regulation (EU) 2021/808 of 22 march 2021 on the performance of analytical methods for residues of pharmacologically active substances used in food-producing animals and on the interpretation of results as well as on the methods to be used for sampling and repealing decisions 2002/657/EC and 98/179/EC (text with EEA relevance). *OJEU.* (2021) 64:84–109.

43. Thompson M. Recent trends in inter-laboratory precision at ppb and sub-ppb concentrations in relation to fitness for purpose criteria in proficiency testing. *Analyst.* (2000) 125:385–6. doi: 10.1039/B000282H

44. César IDC, Pianetti GA. Robustness evaluation of the chromatographic method for the quantitation of lumefantrine using Youden's test. *Braz J Pharm Sci.* (2009) 45:235–40. doi: 10.1590/S1984-82502009000200007

45. Karageorgou E, Samanidou V. Youden test application in robustness assays during method validation. *J Chromatogr A.* (2014) 1353:131–9. doi: 10.1016/j.chroma.2014.01.050

46. Siddique R, Zahoor AF, Ahmad H, Zahid FM, Karrar E. Impact of different cooking methods on polycyclic aromatic hydrocarbons in rabbit meat. *Food Sci Nutr.* (2021) 9:3219–27. doi: 10.1002/fsn3.2284



OPEN ACCESS

EDITED BY

Ricardo Calheta,
Centro de Investigação de Montanha (CIMO),
Portugal

REVIEWED BY

Jing Si,
Beijing Forestry University, China
Lara Pires,
Centro de Investigação de Montanha (CIMO),
Portugal

*CORRESPONDENCE

Xin Zhang
✉ chenxl@necita.org.cn
Wengang Zheng
✉ greenwave214@163.com

[†]These authors have contributed equally to this work and share first authorship

RECEIVED 21 March 2024

ACCEPTED 29 April 2024

PUBLISHED 27 May 2024

CITATION

Chen X, Liu Y, Guo W, Wang M, Zhao J, Zhang X and Zheng W (2024) The development and nutritional quality of *Lyophyllum decastes* affected by monochromatic or mixed light provided by light-emitting diode.
Front. Nutr. 11:1404138.
doi: 10.3389/fnut.2024.1404138

COPYRIGHT

© 2024 Chen, Liu, Guo, Wang, Zhao, Zhang and Zheng. This is an open-access article distributed under the terms of the [Creative Commons Attribution License \(CC BY\)](https://creativecommons.org/licenses/by/4.0/). The use, distribution or reproduction in other forums is permitted, provided the original author(s) and the copyright owner(s) are credited and that the original publication in this journal is cited, in accordance with accepted academic practice. No use, distribution or reproduction is permitted which does not comply with these terms.

The development and nutritional quality of *Lyophyllum decastes* affected by monochromatic or mixed light provided by light-emitting diode

Xiaoli Chen^{1†}, Yihan Liu^{1,2†}, Wenzhong Guo¹, Mingfei Wang¹, Jiuxiao Zhao¹, Xin Zhang^{1*} and Wengang Zheng^{1*}

¹Intelligent Equipment Research Center, Beijing Academy of Agriculture and Forestry Sciences, Beijing, China, ²College of Horticultural and Landscape Architecture, Tianjin Agricultural University, Tianjin, China

Edible fungi has certain photo-sensitivity during the mushroom emergence stage, but there has been few relevant studies on the responses of *Lyophyllum decastes* to different light quality. *L. decastes* were planted in growth chambers with different light qualities that were, respectively, white light (CK), monochromatic red light (R), monochromatic blue light (B), mixed red and blue light (RB), and the mixture of far-red and blue light (FrB). The photo-sensitivity of *L. decastes* was investigated by analyzing the growth characteristics, nutritional quality, extracellular enzymes as well as the light photoreceptor genes in mushroom exposed to different light treatments. The results showed that R led to mycelium degeneration, fungal skin inactivation and failure of primordial formation in *L. decastes*. The stipe length, stipe diameter, pileus diameter and the weight of fruiting bodies exposed to RB significantly increased by 8.0, 28.7, 18.3, and 58.2% respectively, compared to the control ($p < 0.05$). B significantly decreased the stipe length and the weight of fruiting body, with a decrease of 8.5 and 20.2% respectively, compared to the control ($p < 0.05$). Increased color indicators and deepened simulated color were detected in *L. decastes* pileus treated with B and FrB in relative to the control. Meanwhile, the expression levels of blue photoreceptor genes such as *WC-1*, *WC-2* and *Cry-DASH* were significantly up-regulated in mushroom exposed to B and FrB ($p < 0.05$). Additionally, the contents of crude protein and crude polysaccharide in pileus treated with RB were, respectively, increased by 26.5 and 9.4% compared to the control, while those in stipes increased by 5.3 and 58.8%, respectively. Meanwhile, the activities of extracellular enzyme such as cellulase, hemicellulase, laccase, manganese peroxidase, lignin peroxidase and amylase were significant up-regulated in mushroom subjected to RB ($p < 0.05$), which may promote the degradation of the culture materials. On the whole, the largest volume and weight as well as the highest contents of nutrients were all detected in *L. decastes* treated with RB. The study provided a theoretical basis for the regulation of light environment in the industrial production of high quality *L. decastes*.

KEYWORDS

edible fungi, *Lyophyllum decastes*, nutritional quality, light quality, extracellular enzymes, photoreceptor

1 Introduction

Lyophyllum decastes (*L. decastes*), also known as fried chicken mushroom, belongs to the order Agaricales, family Tricholomataceae, and genus *Lyophyllum*. It is named for its resemblance to the medicinal plant pilose antler (1). *L. decastes* is a large fungus widely distributed in temperate regions of the northern hemisphere, which can be used for both food and medicine. The substances such as protein, vitamins, dietary fiber, minerals, amino acids and trace elements in the mycelium and fruiting body have high nutritional value, while the crude polysaccharides have medicinal functions such as antioxidant, anti-tumor, blood pressure lowering, cholesterol lowering, and immune function improving (2, 3). Nowadays, the market prospect of *L. decastes* is promising due to its rich nutritional composition, good medicinal properties and rich flavor.

The growth and development process of edible fungi can be divided into the nutritional growth stage and the reproductive growth stage, and the transition between these two stages is mainly achieved through changes in environmental factors. Among them, light is one of the important environmental factors affecting the growth and development of edible fungi. Some studies have shown that certain mushrooms such as *Agaricus bitorquis*, *Agaricus bisporus*, and underground *Poria cocos* can produce fruiting bodies in total darkness. However, light is indispensable during the reproductive growth stage of most edible mushrooms. Meanwhile, studies have reported that the light requirements of edible fungi are related to the variety and growth stage (4–6). Previous studies have reported that light quality can affect the mycelium activity, as well as the color, size and weight of the fruiting bodies, and edible fungi exhibited different fruiting body morphologies under different light environments. Wu et al. (7) showed that red and yellow light promoted the mycelial growth of *Pleurotus eryngii* in solid culture compared with the white light. Dong et al. (8) showed that pink light increased the dry matter content of *Cordyceps militaris* fruiting body compared with the blue light. Yu et al. (9) investigated the effects of light quality on the growth of mycelium and fruiting bodies of *Volvariella volvacea*, and found that blue-green light was beneficial for the growth of mycelium, and the number and yield of fruiting bodies were also the highest under blue-green light. Song et al. (10) found that the length and diameter of the *Hypsizygus marmoreus* stipe were the largest in the dark, while the pileus diameter was the largest under blue light and the combination of red, green and blue light. Light quality not only affected the growth of mycelium and fruiting body, but also affected the synthesis and accumulation of nutrient substance in edible fungi. Jang and Lee (11) showed that the yield and ergot content of *Pleurotus ostreatus* were higher under mixed blue and white light in relative to the white light. Wu et al. (7) showed that the exopolysaccharides (EPS) production of *Pleurotus eryngii* was highest under blue light conditions. In addition, studies have shown that light exposure time also had impacts on the development of edible fungi. Li et al. (12) reported that 6 h of light exposure was beneficial for the appearance and total yield (per bottle) of fruiting bodies, while 18 h of light exposure was beneficial for the weight of individual fruiting body.

The nutrients required for the growth and development of edible fungi are mainly provided by cultivation materials. Edible fungi decompose macromolecular substances into micromolecular substances under the catalytic action of extracellular enzymes. The small molecule substances which are easily absorbed and

transformed by the mycelium and fruiting bodies, can provide nutrients for the hypha growth, primordial formation, and fruiting body growth. Therefore, extracellular enzymes play a crucial role in edible fungi growth and development. The main extracellular enzymes during the growth of edible fungi include cellulase system, hemicellulase system, lignin degrading enzyme system, and amylase system (13–15). Cellulases include endo-1,4- β -D-glucanohydrolase (E.C.3.2.1.4), exo-1,4- β -D-glucanase (E.C.3. 2.1.91) and β -1,4-glucosidase (E.C.3.2.1.21), etc. Hemicellulases include endo-1,4- β -xylanase (E.C.3.2.1.8) and exo-1,4- β -xylosidase (E.C.3.2.1.37), etc. Lignin degrading enzymes include Lignin peroxidase (E.C.1.11.1.14), Manganese peroxidase (E.C.1.11.1.13) and Laccase (E.C.1.10.3.2). Amylase includes α -Amylase (E.C.3.2.1.1), β -Amylase (E.C.3.2.1.2), Glucoamylase (E.C.3.2.1.3.) and Isoamylase (E.C.3.2.1.68) (16). Study has shown that green light can increase the activities of total cellulase, endo-1,4- β -D-glucanohydrolase, and xylanase in *Pleurotus ostreatus*, but reduce the activity of laccase (17). The extracellular enzyme activity of edible fungi varies in different environments, which reflects the growth rate of mycelium and its ability to absorb small molecule nutrients, thereby affecting the yield and nutrient quality of edible fungi. Therefore, it is of great practical significance to study the response of extracellular enzymes in edible fungi to different light qualities.

So far, studies on the effects of light on the growth and development of edible fungi mainly focus on *Auricularia auricula*, *Flammulina velutipes*, *Ganoderma lucidum*, and *Lentinula edodes*, etc. On the contrary, there have been few studies on the effects of artificial lights on the characteristic mushroom *L. decastes*. This study not only analyzed the impacts of light quality on *L. decastes* from the perspective of phenotype, but also further explored the mechanism of light's influence on the mushroom at the molecular level. Meanwhile, light emitting diodes (LED) control system with all-round adjustable light formula has been applied in the experiment, ensuring the stability and accuracy of the lighting environment. The results are expected to provide a theoretical basis for the light regulation in the industrial production of high-quality *L. decastes*.

2 Materials and methods

2.1 Experimental design

This experiment was conducted in a growth chamber of BAAFS, Beijing, China, using an LED system that can set any light formula. The *L. decastes* mushroom-sticks were treated with different light qualities from the day when the mycelium was full. The growth cycle of the mushrooms were divided into four stages that were hyphal stage [needle shaped primordium, undifferentiated fruiting body, 0–14 days after treatment (DAT)], bud stage (hemispherical pileus, 15–25 DAT), coralline stage (oblate hemispherical pileus, 26–31 DAT), and mature stage (flat pileus, diameter ≥ 35 mm, 32–37 DAT) (18).

Five treatments were set up in the experiment, namely white light (CK), pure blue light (B), pure red light (R), red and blue light (RB), and far-red and blue light (FrB), with a total light intensity of $15 \mu\text{mol}\cdot\text{m}^{-2}\cdot\text{s}^{-1}$ for each treatment. The wavelength peak of blue light, red light and far-red light were, respectively, 450 nm, 660 nm and 735 nm. The light intensity and spectrum were all measured approximately 10 cm below the light source using a spectrometer (LI-180, LI-COR, USA).

The light/dark (L/D) period at hyphal stage, bud stage, coralline stage and mature stage were, respectively, 12 h/12 h, 12 h/12 h, 22.5 h/1.5 h and 21 h/3 h (Supplementary Figure S1 and Table 1). The temperature and the CO₂ concentration in the growth chamber was, respectively, 17 ± 1 °C and 1,550 μmol·mol⁻¹, and the relative humidity of air was, respectively, (80 ± 1)%, (80 ± 1)%, (90 ± 1)% and (90 ± 1)% at hyphal stage, bud stage, coralline stage and mature stage. Purified water was sprayed three time per day with a spray bottle during the growth period.

2.2 Sampling and phenotypic measurement

The length and diameter of mushroom stipe, the pileus diameter as well as the mushroom-sticks weight of *L. decastes* were dynamically measured at 25, 28, 31, 34 and 37 DAT. The weight of fruiting body was measured at harvest (37 DAT). Eight fruiting bodies randomly taken from per treatment was regarded as a repetition, and there were three repetitions in each treatment.

The color parameters and the spectral reflectance ranging 400 ~ 700 nm of the fruiting body were measured by spectrophotometer (Shenzhen San'enshi Technology Co., Ltd., Guangzhou, China) at harvest. The color tone was obtained using various color space parameters (L*, a* and b*). L* represents the gloss brightness, with a value range of [0,100]. The larger L*, the brighter surface of the fruiting body. a* and b* represent color components, with values ranging from [-60,60]. Among them, a* represents the displacement of mushrooms from green to red, where positive values represent the red color tone and negative values represent the green color tone. b* represents the displacement of the mushrooms from blue to yellow, where positive values represent the yellow color tone and negative values represent the blue color tone. The color parameters such as the hue angle (Hue), the color saturation (C), the color index (CCI) and the chromatism (ΔE) were calculated to further compare color

differences of the mushrooms exposed to different light treatments. The calculation formula was as follows:

Hue = tan⁻¹(b* / a*), if a* > 0; and 180 + tan⁻¹(b* / a*), if a* < 0

C = √(a*² + b*²)

CCI = 1000 x a* / (L* x b*)

ΔE = √(ΔL*² + Δa*² + Δb*²)

2.3 Determination of nutrient content and extracellular enzyme activities

0.1 g mushroom tissue (ground in liquid nitrogen) mixed with 0.9 mL PBS buffer (pH = 7.4) were centrifuged at 4 °C and 8,000 rpm/min for 30 min, then the supernatant was collected and stored at 4 °C for use. The nutritional indicators and extracellular enzyme activities of *L. decastes* were determined using the Elisa assay kit purchased from Shanghai C-reactive Biotechnology Co. Ltd. The contents of crude polysaccharides (19), crude proteins (19), and total triterpenes (20) were determined according to the instructions of the biochemical analysis kit. The activities of extracellular enzymes including cellulase, hemicellulase, laccase, manganese peroxidase, lignin peroxidase and amylase were measured according to the instructions of the enzyme-linked immunosorbent assay kit (21–25).

TABLE 1 Irradiation modes of LED light in different treatments.

Treatment		Light supply mode	Light intensity (μmol·m ⁻² ·s ⁻¹)			
			Blue light	Red light	White light	Far-red light
Hyphal stage (0–14 DAT) & Bud stage (15–25 DAT) L(12 h) / D(12 h)	B	pure blue light	15	0	0	0
	R	pure red light	0	15	0	0
	CK	white light	0	0	15	0
	RB	red and blue light	7.5	7.5	0	0
	FrB	far-red and blue light	7.5	0	0	7.5
Coralline stage (26–31 DAT) L(22.5 h) / D(1.5 h)	B	pure blue light	15	0	0	0
	R	pure red light	0	15	0	0
	CK	white light	0	0	15	0
	RB	red and blue light	7.5	7.5	0	0
	FrB	far-red and blue light	7.5	0	0	7.5
Mature stage (32–37 DAT) L(21 h) / D(3 h)	B	pure blue light	15	0	0	0
	R	pure red light	0	15	0	0
	CK	white light	0	0	15	0
	RB	red and blue light	7.5	7.5	0	0
	FrB	far-red and blue light	7.5	0	0	7.5

2.4 Photoreceptor related gene expression analysis by quantitative real-time reverse-transcription polymerase chain reaction (qRT-PCR)

The total RNA of *L. decastes* was extracted using a polyphenolic polysaccharide plant total RNA extraction kit (Magen Biotechnology Co., Ltd., Guangzhou, China). The real-time PCR primers were designed using Premier 6.0, and gene quantitative analysis was performed on a fluorescence quantitative PCR instrument (Applied Biosystems, USA) using the SYBR green method. The 10 μ L reaction mix was obtained using 5 μ L of 1 \times SYBR Green Master Mix, 1 μ L of upstream and downstream primers, 2 μ L of cDNA, and RNase-free Water. The relative transcript levels were calculated using the $2^{-\Delta\Delta CT}$ method (26). GPD gene was used as internal gene in the test. The design of primer sequences for target gene and internal parameter gene was shown in [Supplementary Table S1](#).

2.5 Statistical analysis

The relative spectral curve was extracted using Avasoft 8, and data was organized and plotted using Excel and SPSS Statistics 22. Cluster analysis was performed using Hplot, and correlation analysis was performed using Origin 2021. The data was presented as mean \pm errors.

3 Results

3.1 The growth and development of *Lyophyllum decastes* under different light treatments

As shown in [Figure 1A](#), the mycelium of mushroom treated with monochromatic red light (R) degenerated and the activity of fungal skin decreased. The primordium formation was inhibited and no fruiting body formed under R treatment, indicating that monochromatic red light was not conducive to the growth of *L. decastes*.

As shown in [Figure 1B](#), the stipe length was increased by RB and FrB, while decreased by B, compared with the control. The stipe length of mushroom exposed to RB treatment kept the longest throughout the entire growth period, while that subjected to B treatment displayed the lowest. At 37 DAT, the stipe length of mushroom under RB and FrB treatments was increased by, respectively, 8.0 and 3.5% relative to the control, while that under B was significantly decreased by 8.5% ($p < 0.05$). It indicated that monochromatic blue light combined with red light or far-red light promoted the elongation of the stipe, on the contrary, the monochromatic blue light restrained the stipe elongation. The highest elongation rate of stipe was detected during the mature stage which was 5.7–6.6 mm·d⁻¹ under different treatments.

The diameter of both stipe and pileus were increased by all the treatments compared with the control, displaying an order as RB > FrB > B > CK. At 37 DAT, the stipe diameter of mushroom exposed to RB, B and FrB treatments was significantly increased by, respectively, 28.7, 27.4 and 26.4% compared with the control ($p < 0.05$). The highest growth rate of stipe diameter was detected during the bud stage which was 0.9–1.0 mm·d⁻¹ under different treatments ([Figure 1C](#)). At 37 DAT, the pileus diameter of mushroom exposed to

RB, B and FrB treatments was significantly increased by, respectively, 18.3, 14.8 and 8.2% compared with the control ($p < 0.05$). The highest growth rate of pileus diameter was observed during the coralline stage which was 3.4–4.7 mm·d⁻¹ under different treatments ([Figure 1D](#)).

The total weight of nutrients and fruiting bodies declined with the nutrient consumption in the bacterial bag over time, however, no significant difference was detected among different treatments ([Figure 1E](#)). In addition, as regards of the body weight at harvest, the weight of fruiting bodies subjected to RB and FrB treatments were significantly increased by, respectively, 58.2 and 31.9% ($p < 0.05$) compared to the control. On the contrary, B treatment significantly decreased the fruiting body weight by 20.2% relative to the control ($p < 0.05$) ([Figure 1F](#)). On the whole, compared with white light, blue light mixed with red light or far-red light were beneficial for increasing the size and weight of *L. decastes*. Monochromatic blue light inhibited the stipe elongation and the weight accumulation of the fruiting body, but promoted the lateral growth of *L. decastes* compared with white light.

3.2 The coloring of pileus and stipe of *Lyophyllum decastes* under different light treatments

Color is an important factor affecting the appearance and commercial value of mushrooms. C represents color saturation, with higher values indicating higher chromaticity and lower values indicating a color closer to gray. Hue represents the color angle, reflecting the coloring of the fruiting body. CCI stands for color index which can be used to evaluate the color changes of mushroom, and the color ratio a^*/b^* is the comprehensive color index. ΔE represents color difference, the larger the value, the greater the color difference. As shown in [Table 2](#), all color parameters showed higher in the pileus than the stipe, which might be due to the stipe being obscured by the pileus and receiving less light. Compared with the control, mushroom pileus exposed to B and FrB treatments showed significantly higher value of Hue, CCI, a^*/b^* and ΔE , together with darker simulated color ($p < 0.05$). It indicated that monochromatic blue or mixed blue and far-red light irradiation was beneficial for the coloring of the pileus. In contrast, the color change of stipe under different treatments was not as significant as that of the pileus from the result of simulated color.

3.3 The reflectance of pileus and stipe of *Lyophyllum decastes* under different light treatments

As shown in [Figure 2](#), the reflection spectrum curves of mushroom were basically similar among treatments, and the reflectance of the pileus and stipe increased with the increasing wavelength. The reflectance of mushroom pileus in each treatment was lower than that of the control, as follows: CK > RB > FrB > B, the difference between each treatment reached a significant level ($p < 0.05$). This indicated that light treatments especially B and FrB enhanced the light absorption of pileus ([Figure 2A](#)), which was corresponded with the color parameters in [Table 2](#). Similarly, the reflectance of the stipe was also found the lowest in mushroom exposed to B (significantly lower than the other treatments, $p < 0.05$), it might imply that monochromatic blue light was conducive for light absorption of mushroom. The reflectance difference in the stipe among

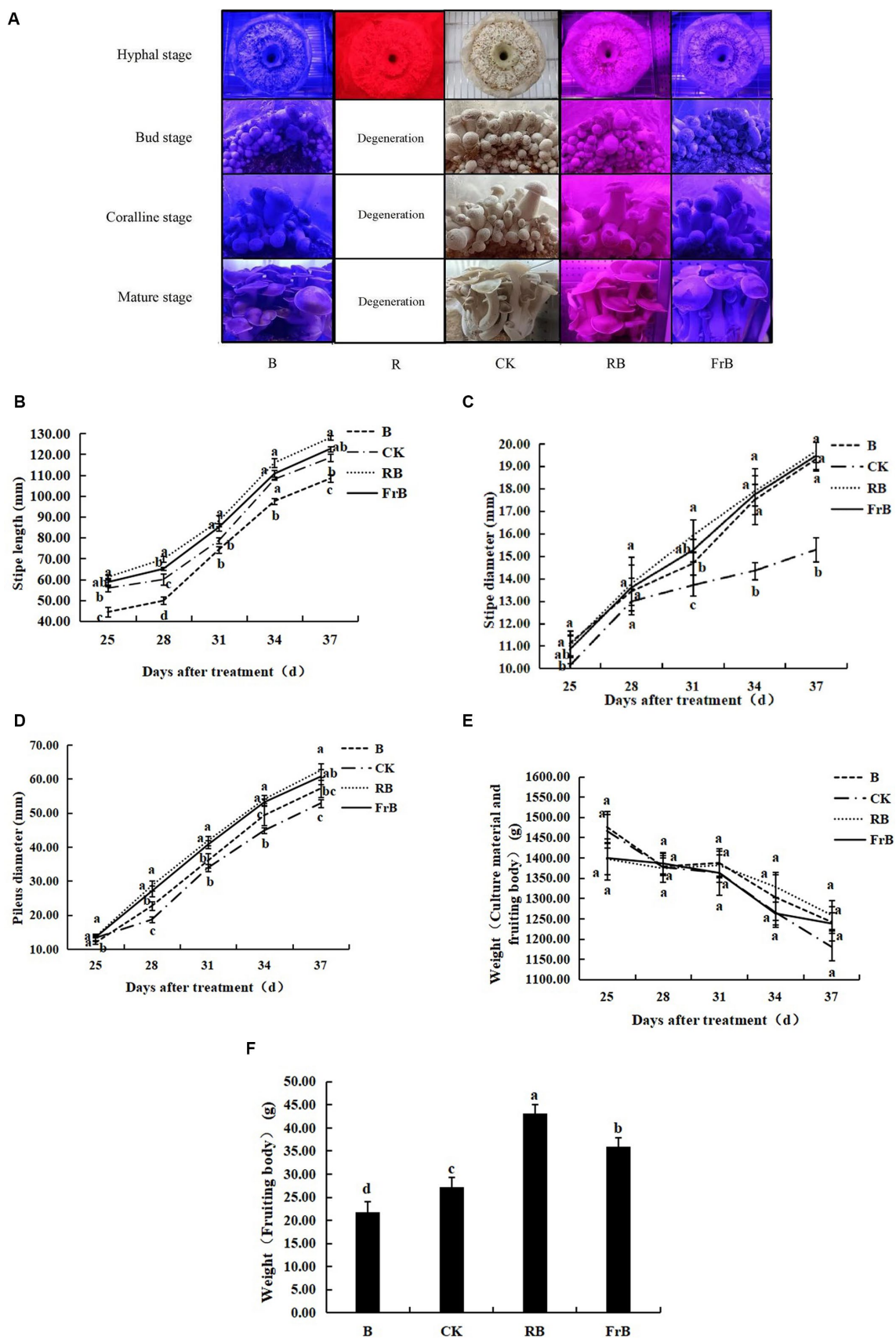







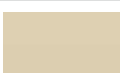
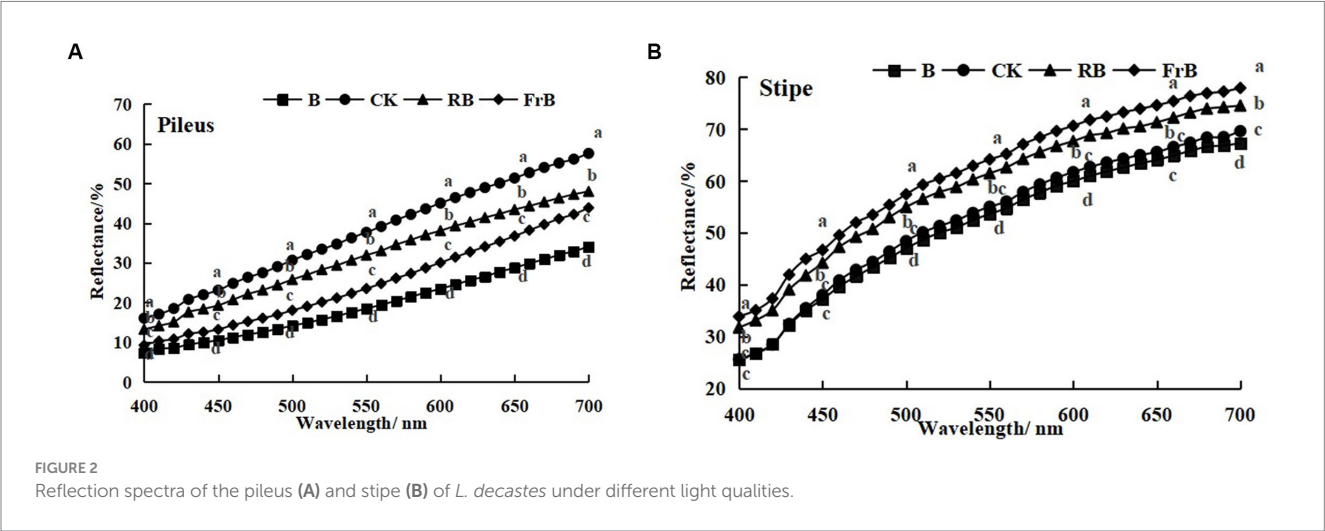


FIGURE 1 Growth and development of *L. decastes* under different light qualities. **(A)** Photos of *L. decastes* at different stages; **(B)** The stipe length of *L. decastes* at 25, 28, 31, 34, and 37 days after treatment (DAT); **(C)** The stipe diameter of *L. decastes* at 25, 28, 31, 34, and 37 DAT; **(D)** The pileus diameter of *L. decastes* at 25, 28, 31, 34, and 37 DAT; **(E)** The weight of culture material and fruiting body of *L. decastes* at 25, 28, 31, 34, and 37 DAT; **(F)** The weight of fruiting body of *L. decastes* at 37 DAT. Different lowercase letters indicate significant differences between groups ($p < 0.05$). The following figure is the same.

TABLE 2 The color and simulated color of the pileus and stipe of *L. decastes* under different light qualities.

	Treatment	C	Hue	CCI	a*/b*	ΔE	Simulated color
Pileus	B	21.0±0.68a	3.53±2.00b	5.86±0.86a	0.30±0.03a	16.84±2.78a	
	CK	21.39±1.18a	0.32±0.10c	3.19±0.29b	0.22±0.02b	0d	
	RB	21.73±0.54a	0.65±0.73c	3.66±0.48b	0.23±0.03b	4.16±1.13c	
	FrB	22.40±1.14a	8.30±1.15a	5.96±0.06a	0.33±0.00a	12.45±1.87b	
Stipe	B	16.86±1.21a	1.70±0.80a	0.84±0.19a	0.06±0.02a	3.66±2.37ab	
	CK	19.96±1.14a	0.15±0.11b	0.99±0.33a	0.08±0.02a	0b	
	RB	17.90±2.61a	0.12±0.07b	0.69±0.42a	0.06±0.03a	4.13±3.13ab	
	FrB	16.76±1.12a	0.30±0.17b	1.02±0.17a	0.08±0.01a	7.45±2.19a	

Different letters in the same industry indicate significant differences ($p < 0.05$), as shown in the table below. Calculate ΔE using CK as the standard.



treatments seemed smaller than that of the pileus, indicating that the pileus was more sensitive to light quality than the stipe (Figure 2B).

3.4 The nutrient quality of *Lyophyllum decastes* under different light treatments

As seen in Figure 3, all treatments raised the contents of crude protein, crude polysaccharide and total triterpenoids in the fruiting bodies in various degrees compared with the control. The crude

protein content in pileus exposed to B, RB and FrB treatments was significantly increased by, respectively, 14.0, 26.5 and 18.8% ($p < 0.05$) in relative to the control, while that in stipe was increased by, respectively, 19.0, 5.3 and 6.5% (Figure 3A).

The crude polysaccharide content in pileus exposed to B, RB and FrB treatments was increased by, respectively, 2.1, 9.4 and 17.4% compared with the control, however no significant difference was observed. B and RB treatments significantly enhanced the crude polysaccharide content in stipe by, respectively, 38.0 and 58.8% ($p < 0.05$) compared with the control (Figure 3B). In addition, no

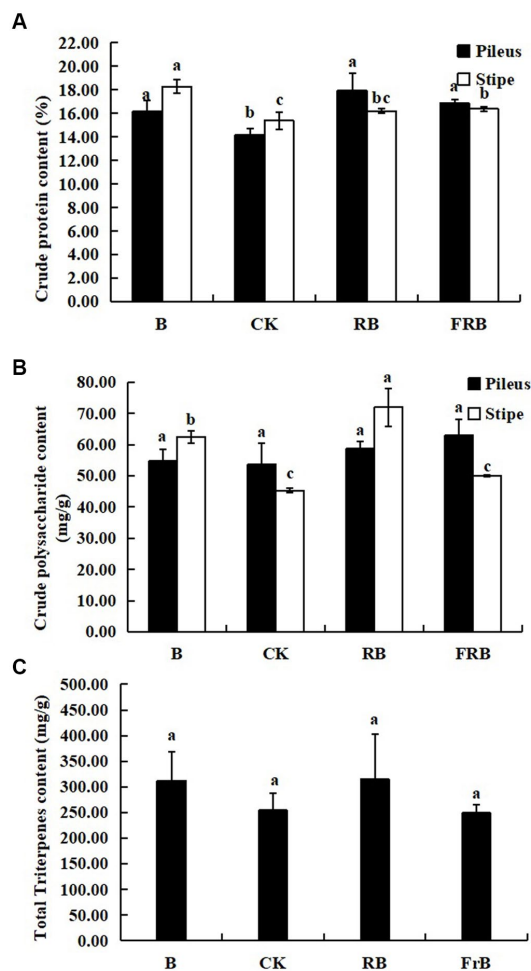


FIGURE 3
The contents of crude protein (A), crude polysaccharide (B), and total triterpenoid (C) in *L. decastes* under different light treatments.

significant difference was detected in the content of total triterpenoids in the fruiting bodies subjected to different light treatments (Figure 3C).

3.5 The extracellular enzyme activities of *Lyophyllum decastes* under different light treatments

As shown in Figure 4, the activities of cellulase, hemicellulase, laccase, manganese peroxidase, lignin peroxidase and amylase were all significantly ($p < 0.05$) raised in fruiting bodies exposed to RB and FrB treatments compared with the control, and the highest activities for these six extracellular enzymes were all detected under RB treatment, which were, respectively, 13.7%~46.2% (in pileus) and 19.0%~63.3% (in stipe) higher than those treated with the control. The increase of extracellular enzyme activities stimulated the degradation of the culture medium, thereby promoting the growth of fruiting bodies, which might explain the significantly higher weight of fruiting bodies in RB and FrB treatments. In contrast, the laccase activity of the fruiting body subjected to B treatment was significantly decreased compared with the

other treatments, it might indicate that short wavelength irradiation was not conducive to the enhancement of laccase activity.

3.6 The relative expression level of photoreceptor genes in *Lyophyllum decastes* exposed to different light treatments

To further investigate the responses of *L. decastes* to different light qualities, RT-PCR technology was used to analyze the expression of photoreceptor genes in the fruiting bodies under different light qualities. As shown in Figure 5, B and FrB treatments significantly increased the expression levels of both blue light photoreceptor gene (*WC-1*, *WC-2* and *Cry-DASH*) and red light photoreceptor gene (*Phy*) compared with the control ($p < 0.05$). The highest expression levels of *WC-2* and *Cry-DASH* were both detected in mushroom exposed to B treatment, significantly increased by 3 times and 1 times compared to the control ($p < 0.05$), respectively. The highest expression level of *WC-1* and *Phy* were both detected in mushroom exposed to FrB treatment, significantly increased by 1 time and 3 times relative to the control ($p < 0.05$), respectively. In contrast, no significant difference was detected in the expression level of photoreceptor genes in mushroom exposed to RB treatment compared to the control. The better coloring and higher light absorption of pileus subjected to B and FrB observed in Table 2 and Figure 2 might be due to the up-regulated expression level of photoreceptor genes by the two treatments.

3.7 Correlation analysis among the phenotype, nutrient qualities and extracellular enzyme activities of *Lyophyllum decastes* exposed to different light treatments

As shown in Figure 6, significant positive relationship was observed between the stipe length and the activities of laccase and cellulase in the stipe ($p < 0.05$). The diameter of the stipe and pileus was significantly positively correlated with the activities of cellulase, hemicellulase, manganese peroxidase, lignin peroxidase as well as amylase ($p < 0.05$). Moreover, the weight of the fruiting body was positively correlated with the activities of hemicellulase, manganese peroxidase, and lignin peroxidase in the stipe and pileus. It can be seen that the size and weight of *L. decastes* seemed generally positively correlated with extracellular enzyme activities.

As for the correlation between the nutrients and extracellular enzyme activity in the fruiting body, it was observed that the crude protein content was significantly positively correlated with the activities of cellulase and laccase in pileus, while the crude polysaccharide content was significantly positively correlated with the activity of amylase in pileus ($p < 0.05$). However, the crude protein content was negatively correlated with the activities of hemicellulase, manganese peroxidase, or lignin peroxidase in the stipe. Moreover, there is no significant correlation between triterpenoid substances and extracellular enzyme activity in the fruiting body. Therefore, the interaction mechanism between extracellular enzymes and the nutrient accumulation in the fruiting body was relatively complex.

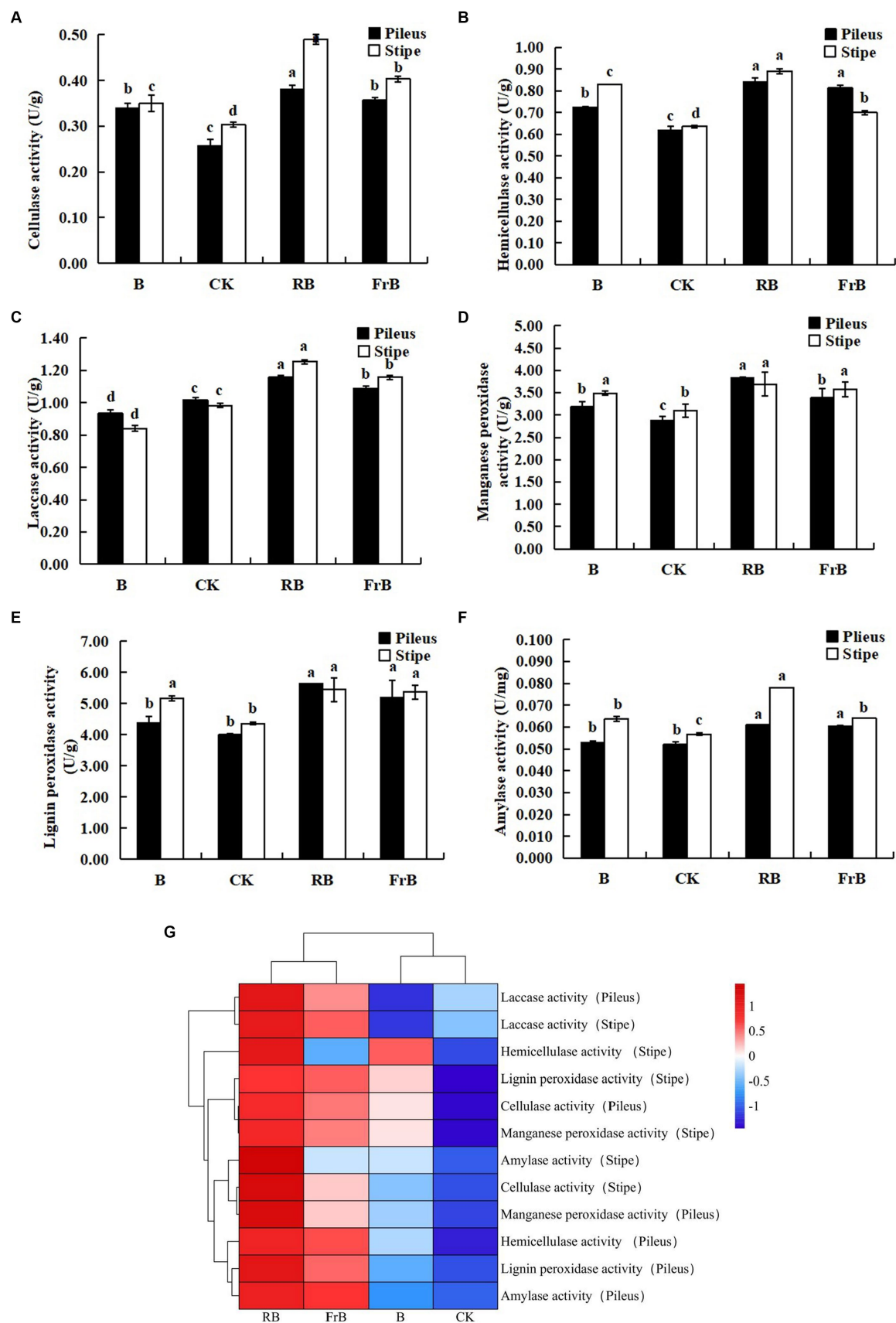


FIGURE 4 The enzyme activities of cellulase (A), hemicellulase (B), laccase (C), manganese peroxidase (D), lignin peroxidase (E) and laccase (F) in *L. decastes* under different light treatments, and the cluster heatmap of extracellular enzyme activity (G).

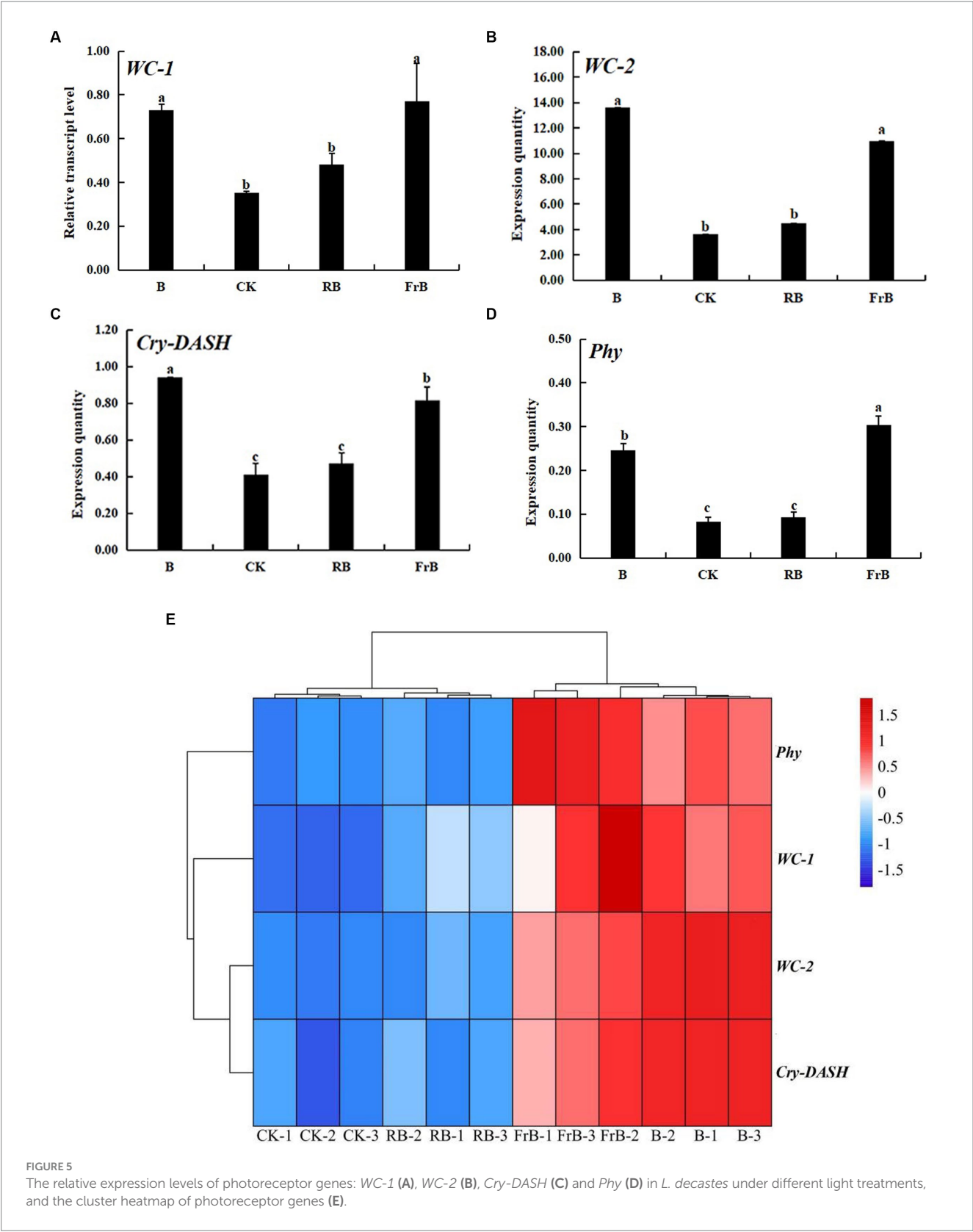


FIGURE 5 The relative expression levels of photoreceptor genes: *WC-1* (A), *WC-2* (B), *Cry-DASH* (C) and *Phy* (D) in *L. decastes* under different light treatments, and the cluster heatmap of photoreceptor genes (E).

4 Discussion

The fruiting stage of edible fungi is light sensitive stage, light can either stimulate or inhibit fungal development, so light is an

important factor in the growth and development of edible fungi. Our study indicated that the highest average growth rate of stipe diameter, pileus diameter, and stipe length of *L. decastes* was, respectively, detected at bud stage (DAT 15-Day 25), coralline

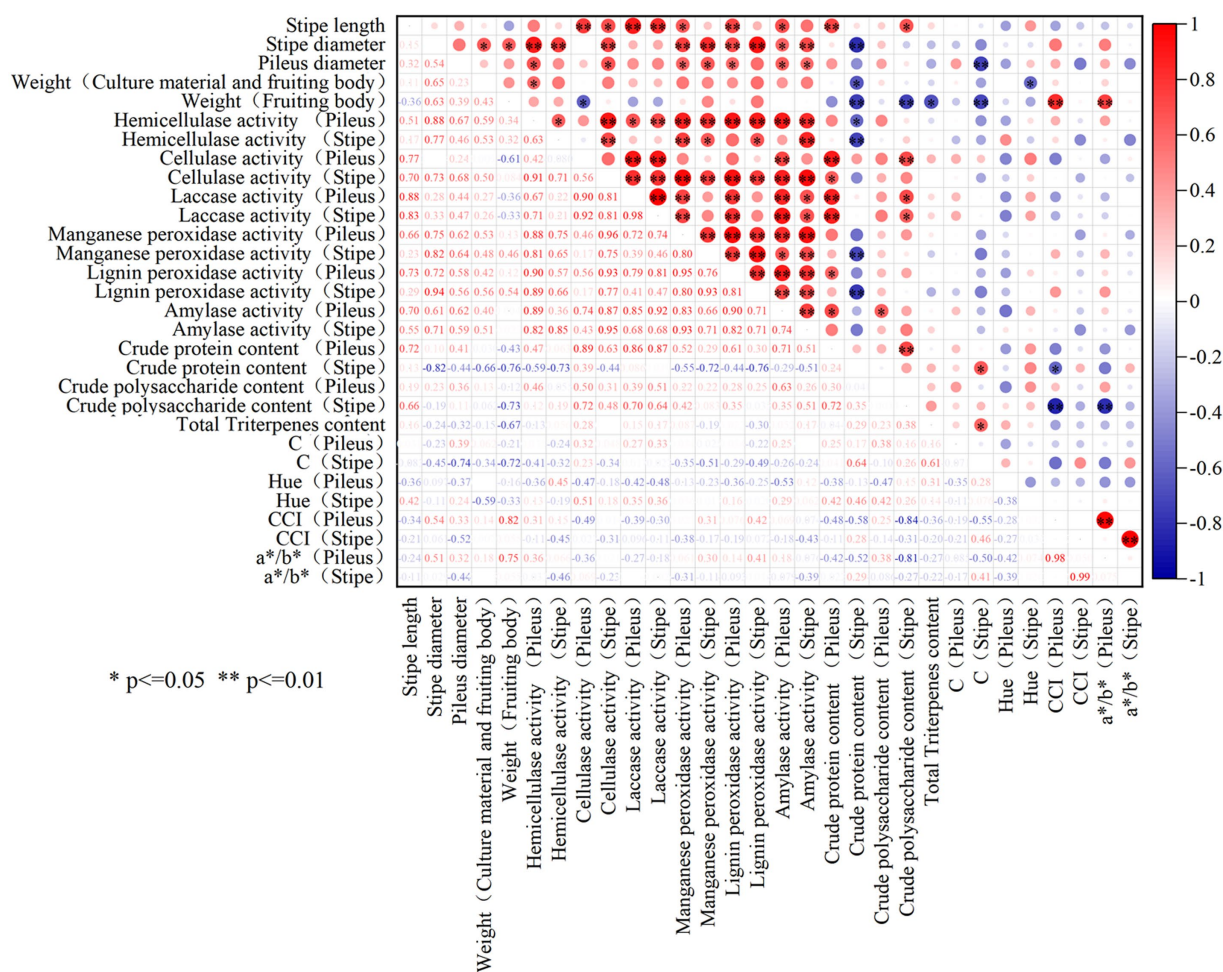


FIGURE 6

The correlation analysis among the phenotype, nutrient qualities and extracellular enzyme activities of *L. decastes*. * represents p -value less than 0.05, **represents p -value less than 0.01.

stage (Day 26–Day 31) and the mature stage (Day 32–Day 37) regardless of different treatments. Arjona et al. (27) reported that blue light was the triggering signal for the formation of *Pleurotus ostreatus* primordia, and the formation of primordia could not be achieved in a light environment lacking blue light. Ellis et al. (28) found that blue light with wavelengths of 440–470 nm was the most favorable for the formation of *Coprinus comatus* primordia. Kim et al. (29) found that blue light irradiation increased the expression level of FAD-NAD binding proteins related to primordial formation in *Lentinula edodes* by four times compared with the darkness. Li et al. (30) also observed that blue light up-regulated the expression of conidiation and hydrophobin proteins, which was related to the composition of fungal cell wall and cell membrane synthesis during the primordial formation in *Trichoderma*. These studies indicated that blue light played an important role in the formation of the primordium of edible fungi. In the present study, normal primordia formation of *L. decastes* occurred under CK, B, RB and FrB treatments. However, the mycelium of *L. decastes* degenerated and the fungal skin activity decreased under R treatment. It indicated that blue light was indispensable during the primordium formation of

L. decastes, confirming the importance of blue light for edible fungi mentioned above. In addition, studies also have shown that several important biosynthetic pathways in mushrooms such as the membrane transport protein synthesis and the amino acid biosynthetic were found inactive under monochromatic red light irradiation. The function of membrane transporters was to perceive external stimuli and transmit signals to cells, maintaining the activity of mycelial (31, 32). Therefore, the degradation of *L. decastes* mycelium under R treatment in this study might be due to the lack of blue light irradiation or a decreased expression level of membrane transporter protein in *L. decastes* caused by monochromatic red light.

Our study found that RB treatment significantly enhanced the size and weight of the *L. decastes* fruiting body compared with the control ($p < 0.05$). On the contrary, B treatment significantly decreased the stipe length and the fruiting body weight. This was consistent with Jang et al.'s study (33), which showed that the stipe of *Hypsizygus marmoreus* was the shortest under the pure blue light compared with the other light treatments such as mixed blue and white light, mixed green and white light, combined blue and green light. It implied that although blue light acted a crucial role in the primordium formation of *L. decastes*,

monochromatic blue light was not optimum light quality for the size or weight of fruiting body of *L. decastes*. In addition, the correlation analysis showed that the stipe length, the diameter of stipe and pileus were positively correlated with the activities of cellulase, hemicellulase, laccase, manganese peroxidase, lignin peroxidase, and amylase. Meanwhile, the fruiting body weight was positively correlated with the activities of hemicellulase, manganese peroxidase, and lignin peroxidase in both pileus and stipe. In the present study, the highest extracellular enzyme activity accompanied with the highest size and fruiting body weight were all detected in *L. decastes* treated with RB treatment. The mixed red and blue light might promote the degradation of the cultivation materials and absorption of nutrients by *L. decastes* via increasing the activities of the extracellular enzyme, which might account for the best growth and weight of the fruiting bodies detected under RB treatment.

The color of edible mushroom is one of the main factors affecting consumer choices (34). Carotenoid is one of the main pigments that contribute to the coloration of fungi, providing characteristic yellow, orange or reddish colors (35). Studies have shown that the synthesis of carotenoids in *Fusarium* and *Cordyceps militaris* was associated with the blue light signaling pathway and was synergically regulated by blue light photoreceptor, while red light wave band was ineffective for the carotenoids synthesis (36, 37). The current study displayed that higher color spectral parameters such as Hue, CCI, a^*/b^* , and ΔE values as well as deeper simulated color of the pileus were detected in *L. decastes* under B and FrB treatments compared with the other treatments. It demonstrated that blue light or mixed far-red and blue light were beneficial for the coloring of *L. decastes*. This might be due to that B or FrB irradiation up-regulated the expression level of light photoreceptor genes such as *WC-1*, *WC-2* and *Cry-DASH*, which might participate to regulate carotenoid biosynthesis pathway in edible fungi (38).

Light quality not only affected the morphology formation of edible fungi, but also acted on the synthesis and accumulation of nutrient substance in the fruiting body. Tang et al. (39) used transcriptomics to study the photoresponse mechanism of *Lentinus edodes* and found that light would affect the transportation and metabolism of carbohydrates. The studies by Wang et al. (40) and Zhu et al. (41) showed that blue light was conducive to the synthesis of polysaccharides and protein in *Ganoderma lucidum* and *Hypsizygus marmoreus* compared with red light. Similarly, our study found that the contents of crude protein and crude polysaccharide in *L. decastes* exposed to B, RB, FrB treatments were all increased compared with the control. The possible reason was that organic metabolism related genes such as hydrophobin genes (*SC1* and *SC3*), lignin-modifying genes (*LAC1*, *LCC2* and *LCC3*) and Tyrosinase-encoding genes (*TYR1* and *MELC2*) were up-regulated under the those light qualities (29, 39, 42, 43).

Extracellular enzyme activity reflects the ability of mushrooms to absorb and utilize small molecule nutrients. It has been reported that extracellular enzyme stimulated the degradation of the culture medium, thereby promoting the organic metabolism and the growth of fruiting bodies (14). Cao et al. (44) found that higher activities of cellulase and laccase appeared with higher contents of polysaccharides in *Lentinula edodes*. In the present study, the correlation analysis in Figure 6 showed that the crude protein content was significantly positively correlated with the cellulase and laccase activities in the pileus, while the crude polysaccharide content was significantly positively correlated with the

amylase activity in the stipe ($p < 0.05$). The results confirmed the positive correlations between the extracellular enzyme and the organic metabolism. In addition, our study found that the activities of cellulase, hemicellulase, manganese peroxidase, lignin peroxidase and amylase were all raised in fruiting bodies exposed to B, RB and FrB compared with the control. Thus, the increased activity of cellulase, hemicellulase, peroxidase and amylase in *L. decastes* treated with B, RB, FrB may also accounted for the higher contents of organic substance observed in those light treatments. Xie et al. (45) studied the effects of blue light on the activity of manganese peroxidase in *Pleurotus eryngii*, to find that blue light inhibited the activity of manganese peroxidase compared with darkness. Ramírez et al. (46) reported that blue light significantly reduced the activity of lignin peroxidase in *Phanerochaete chrysosporium* Burds in relative to white light. On the contrary, Gan et al. (47) and Zhu et al. (48) reported that blue light increased the activity of amylase in *Pseudopestalotiopsis theae*, *Fusarium solani*, *Xylaria venustula* and *Aspergillus niger* compared with the white light. The results in our study displayed that the activities of the manganese peroxidase, lignin peroxidase and amylase were all increased in *L. decastes* treated with B compared with the control. This might indicate that the effects of light quality on extracellular enzymes in edible fungi was variety dependent. Furtherly, when comparing the effects of these three light qualities (B, RB and FrB) on extracellular enzymes in the current study, it was found that the up-regulation effect of RB and FrB were more significant compared with B. It implied that blue light mixed with red light or far-red light were more effective to the extracellular enzyme activities in *L. decastes*.

Light signals were first transmitted into cells through photoreceptor proteins, and then the protein complexes acted as transcription factors to regulate the expression of many downstream genes, thereby regulating various life activities such as the development and nutrient synthesis in edible fungi (49–51). The results in our study showed that all treatments up-regulated the expression levels of the four photoreceptor genes (*WC-1*, *WC-2*, *Cry-DASH*, and *Phy*) compared with the control. Additionally, it was noticed that all treatments enhanced the activities of extracellular enzymes such as cellulase, hemicellulase, manganese peroxidase, lignin peroxidase and amylase in *L. decastes*. This may because that photoreceptor genes were involved in the regulation of extracellular enzyme (52). Nevertheless, since light environment elements include light intensity, light period, light quality and light distribution, the current study only analyzed the effects of light quality on *L. decastes*, further studies are needed to reveal the effects and mechanisms of the other light factors on the growth and development of *L. decastes*.

5 Conclusion

R led to the degeneration of the mycelium and decreased the activity of fungal skin, without forming the primordia. RB significantly promoted the increase of volume and weight in *L. decastes* and up-regulated the activities of extracellular enzyme in mushrooms, while B significantly decreased the stipe length and the weight of mushroom fruiting body compared to the white light. B or FrB were beneficial for the coloring of *L. decastes*, in that blue light photoreceptors (*WC-1*, *WC-2* and *Cry-DASH*) which synergically regulated the main pigments contributing to the coloration of fungi were up-regulated by B and FrB. On the whole, the largest volume and weight as well as the highest contents of crude polysaccharide, crude

protein and total triterpenoids were all detected in the *L. decastes* fruiting bodies treated with RB, compared with the other treatments.

Data availability statement

The original contributions presented in the study are included in the article/[Supplementary material](#), further inquiries can be directed to the corresponding authors.

Author contributions

XC: Writing – original draft, Writing – review & editing. YL: Writing – original draft, Writing – review & editing. WG: Data curation, Software, Writing – review & editing. MW: Data curation, Software, Writing – review & editing. JZ: Data curation, Software, Writing – review & editing. XZ: Supervision, Writing – review & editing. WZ: Supervision, Writing – review & editing.

Funding

The author(s) declare that financial support was received for the research, authorship, and/or publication of this article. This work was financially supported by the National Edible Fungi Industry Technology

System (CARS-20) and the Beijing Edible Fungi Innovation Team (BAIC03-2024).

Conflict of interest

The authors declare that the research was conducted in the absence of any commercial or financial relationships that could be construed as a potential conflict of interest.

Publisher's note

All claims expressed in this article are solely those of the authors and do not necessarily represent those of their affiliated organizations, or those of the publisher, the editors and the reviewers. Any product that may be evaluated in this article, or claim that may be made by its manufacturer, is not guaranteed or endorsed by the publisher.

Supplementary material

The Supplementary material for this article can be found online at: <https://www.frontiersin.org/articles/10.3389/fnut.2024.1404138/full#supplementary-material>

References

- Xu L, Yang W, Qiu T, Gao X, Zhang H, Zhang S, et al. Complete genome sequences and comparative secretomic analysis for the industrially cultivated edible mushroom *Lyophyllum decastes* reveals insights on evolution and lignocellulose degradation potential. *Front Microbiol.* (2023) 14:1137162. doi: 10.3389/fmicb.2023.1137162
- Hu Y, Li J, Lin H, Liu P, Zhang F, Lin X, et al. Ultrasonic treatment decreases *Lyophyllum decastes* fruiting body browning and affects energy metabolism. *Ultrason Sonochem.* (2022) 89:106111. doi: 10.1016/j.ulsonch.2022.106111
- Ukawa Y, Furuichi Y, Kokean Y, Nishii T, Hisamatsu M. Effect of Hatakeshimeji (*Lyophyllum decastes* sing.) mushroom on serum lipid levels in rats. *J Nutr Sci Vitaminol.* (2002) 48:73–6. doi: 10.3177/jnsv.48.73
- Janusz G, Sulej J, Jaszek M, Osinska-Jaroszuk M. Effect of different wavelengths of light on laccase, cellobiose dehydrogenase, and proteases produced by *Cerrena unicolor*, *Pycnoporus sanguineus* and *Phlebia lindmeri*. *Acta Biochim Pol.* (2016) 63:223–8. doi: 10.18388/abp.2015_1235
- Kamada T, Sano H, Nakazawa T, Nakahori K. Regulation of fruiting body photomorphogenesis in *Coprinopsis cinerea*. *Fungal Genet Biol.* (2010) 47:917–21. doi: 10.1016/j.fgb.2010.05.003
- Mei XL, Zhao Z, Chen XD, Lan J. Light quality regulation of growth and endogenous IAA metabolism of *Ganoderma lucidum* mycelium. *China J Chin Mater Med.* (2013) 38:1887–92. doi: 10.4268/cjcm.20131209
- Wu JY, Chen HB, Chen MJ, Lan SC, Shieh CJ. Quantitative analysis of LED effects on edible mushroom *Pleurotus eryngii* solid and submerged cultures. *J Chem Technol Biotechnol.* (2013) 88:1841–6. doi: 10.1002/jctb.4038
- Dong JZ, Lei C, Zheng XJ, Ai XR, Wang Y, Wang Q. Light wavelengths regulate growth and active components of *Cordyceps militaris* fruit bodies. *J Food Biochem.* (2013) 37:578–84. doi: 10.1111/jfbc.12009
- Yu CX, Li ZP, Cha L, Zhao Y, Chen MJ, Hou LJ, et al. Effects of light quality on mycelial growth and fruiting body characteristics of *Volvariella volvacea*. *Acta Edulis Fungi.* (2021) 28:72–7. doi: 10.16488/j.cnki.1005-9873.2021.03.009
- Song HB, Li Y, Huang JH, Duan JY, Zhang QS, Xie BG, et al. Growth and development of *Hypsizygus marmoreus* and response expression of light receptor white collar genes under different light quality irradiation. *Acta Horticulturae Sin.* (2020) 47:467–76. doi: 10.16420/j.issn.0513-353x.2019-0510
- Jang M, Lee Y. The suitable mixed LED and light intensity for cultivation of oyster mushroom. *J Mushrooms.* (2014) 12:258–62. doi: 10.14480/JM.2014.12.4.258
- Li QZ, Yang Y, Zhou F, Li Y, Guo LG, Bao DP, et al. Effect of light on *Pleurotus eryngii* fruit body size and yield. *Acta Edulis Fungi.* (2014) 21:32–5. doi: 10.16488/j.cnki.1005-9873.2014.02.010
- Gupta VK, Kubicek CP, Berrin JG, Berrin JG, Wilson DW, Couturier M, et al. Fungal enzymes for bio-products from sustainable and waste biomass. *Trends Biochem Sci.* (2016) 41:633–45. doi: 10.1016/j.tibs.2016.04.006
- Paramjeet S, Manasa P, Korrapati N. Biofuels: production of fungal-mediated ligninolytic enzymes and the modes of bioprocesses utilizing agro-based residues. *Biocatal Agric Biotechnol.* (2018) 14:57–71. doi: 10.1016/j.bcab.2018.02.007
- Rabemanantsoa H, Saka S. Various pretreatments of lignocellulosics. *Bioresour Technol.* (2016) 199:83–91. doi: 10.1016/j.biortech.2015.08.029
- Shon YH, Nam KS. Antimutagenicity and induction of anticarcinogenic phase II enzymes by basidiomycetes. *J Ethnopharmacol.* (2001) 77:103–9. doi: 10.1016/s0378-8741(01)00276-8
- Araújo NL, Avelino KV, Halabura MIW, Marim RA, Kassem ASS, Linde GA, et al. Use of green light to improve the production of lignocellulose-decay enzymes by *Pleurotus spp* in liquid cultivation. *Enzym Microb Technol.* (2021) 149:109860. doi: 10.1016/j.enzymtec.2021.109860
- Huang L, Si C, Shi H, He C, Duan J. Research on the stipe cracking of wine-cap mushroom (*Stropharia rugosoannulata*) in different humidity conditions. *Sci Rep.* (2023) 13:21122. doi: 10.1038/s41598-023-48608-1
- Tang YY, Zhou YL, Jie HD, Liu XC, Lü XY, Jie YC. Effects of different cultures on the yield and quality of *Pleurotus ostreatus*. *J Anhui Agric Sci.* (2023) 51:37–41. doi: 10.3969/j.issn.0517-6611.2023.08.010
- Zhu PL, Zhang J, Li SY, Cui XY, Yuan YJ, Wang W, et al. Purification of total triterpenoids from fruiting body and spore powder of *Ganoderma lucidum* by macroporous adsorption resins. *Food Res Dev.* (2023) 44:79–85. doi: 10.12161/j.issn.1005-6521.2023.04.012
- Chai S, Zhang X, Jia Z, Xu X, Zhang Y, Wang S, et al. Identification and characterization of a novel bifunctional cellulase/hemicellulase from a soil metagenomic library. *Appl Microbiol Biotechnol.* (2020) 104:7563–72. doi: 10.1007/s00253-020-10766-x
- Jin J, Kang WL, Sheng JP, Cheng FS, Wang QS, Zhang YX, et al. Enzymological characteristics of lignin peroxidase (LiP) from *Coriolus versicolor*. *Food Sci.* (2010) 31:224–7. doi: 10.7506/spkx1002-6630-201017050
- Peng H, Li R, Li F, Zhai L, Zhang X, Xiao Y, et al. Extensive hydrolysis of raw rice starch by a chimeric α -amylase engineered with α -amylase (AmyP) and a starch-binding

domain from *Cryptococcus* sp. S-2. *Appl Microbiol Biotechnol.* (2018) 102:743–50. doi: 10.1007/s00253-017-8638-1

24. Silva EM, Milagres AMF. Production of extracellular enzymes by *Lentinula edodes* strains in solid-state fermentation on lignocellulosic biomass sterilized by physical and chemical methods. *Curr Microbiol.* (2023) 80:395. doi: 10.1007/s00284-023-03501-y

25. Valle JS, Vandenberghe LP, Oliveira AC, Tavares MF, Linde GA, Colauto NB, et al. Effect of different compounds on the induction of laccase production by *Agaricus blazei*. *Genet Mol Res.* (2015) 14:15882–91. doi: 10.4238/2015.December.1.40

26. Wang H, Tong X, Tian F, Jia C, Li C, Li Y. Transcriptomic profiling sheds light on the blue-light and red-light response of oyster mushroom (*Pleurotus ostreatus*). *AMB Express.* (2020) 10:10. doi: 10.1186/s13568-020-0951-x

27. Arjona D, Aragón C, Aguilera JA, Ramírez L, Pisabarro AG. Reproducible and controllable light induction of in vitro fruiting of the white-rot basidiomycete *Pleurotus ostreatus*. *Mycol Res.* (2009) 113:552–8. doi: 10.1016/j.mycres.2008.12.006

28. Ellis RJ, Bragdon GA, Schlosser BJ. Properties of the blue light requirements for primordia initiation and basidiocarp maturation in *Coprinus stercorarius*. *Mycol Res.* (1999) 103:779–84. doi: 10.1017/S0953756298007722

29. Kim JY, Kim DY, Park YJ, Jang MJ. Transcriptome analysis of the edible mushroom *Lentinula edodes* in response to blue light. *PLoS One.* (2020) 15:e0230680. doi: 10.1371/journal.pone.0230680

30. Li YF, Sun TT, Guo DG, Gao J, Zhang J, Cai J, et al. Comprehensive analysis of the regulatory network of blue-light-regulated conidiation and hydrophobin production in *Trichoderma guizhouense*. *Environ Microbiol.* (2021) 23:6241–6256. doi: 10.1111/1462-2920.15748

31. Dou Y, Du F, Hu QX, Zou YJ, Bai X. Transcriptome analysis reveals candidate genes involved in light-induced primordium differentiation in *Pleurotus eryngii*. *Int J Mol Sci.* (2022) 23:435. doi: 10.3390/ijms23010435

32. Liu JY, Wang RJ, Zhang D, Xu Z, Lu H, Song CY, et al. Transcriptome analysis revealed effect of blue light on primordium formation of *Flammulina filiformis*. *Acta Edulis Fungi.* (2021) 28:29–36. doi: 10.16488/j.cnki.1005-9873.2021.05.004

33. Jang MJ, Lee YH, Ju YC, Kim SM, Koo HM. Effect of color of light emitting diode on development of fruit body in *Hypsizygus marmoreus*. *Mycobiology.* (2013) 41:63–6. doi: 10.5941/MYCO.2013.41.1.63

34. Yang Y, Zhang Y, Huang C, Chen Q, Gao W. Development of cleaved amplified polymorphic sequence marker for cap color identification in *Pleurotus cornucopiae*. *Horticulturae.* (2023) 9:1238. doi: 10.3390/horticulturae9111238

35. Phadwal K. Carotenoid biosynthetic pathway: molecular phylogenies and evolutionary behavior of crt genes in eubacteria. *Gene.* (2005) 345:35–43. doi: 10.1016/j.gene.2004.11.038

36. Avalos J, Estrada AF. Regulation by light in *Fusarium*. *Fungal Genet Biol.* (2010) 47:930–8. doi: 10.1016/j.fgb.2010.05.001

37. Zhang J, Wang F, Yang Y, Wang Y, Dong C. *CmVVD* is involved in fruiting body development and carotenoid production and the transcriptional linkage among three blue-light receptors in edible fungus *Cordyceps militaris*. *Environ Microbiol.* (2020) 22:466–82. doi: 10.1111/1462-2920.14867

38. Krobanan K, Liang S, Chiu H, Shen W. The blue-light photoreceptor *Sfwc-1* gene regulates the phototropic response and fruiting-body development in the homothallic

ascomycete *Sordaria fimicola*. *Appl Environ Microbiol.* (2019) 85:e02206–18. doi: 10.1128/AEM.02206-18

39. Tang LH, Jian HH, Song CY, Bao DP, Shang XD, Wu DQ, et al. Transcriptome analysis of candidate genes and signaling pathways associated with light-induced brown film formation in *Lentinula edodes*. *Appl Microbiol Biotechnol.* (2013) 97:4977–89. doi: 10.1007/s00253-013-4832-y

40. Wang LH, Chen XD, Wang QY, Hao JJ, Lan J. Effect of different light of LED light quality on growth and antioxidant enzyme activities of *Ganoderma lucidum*. *China J. Chin. Mater. Med.* (2011) 36:2471–4. doi: 10.4268/cjmm20111804

41. Zhu LP, Su Y, Ma ZH, Guo LZ, Yang S, Yu H. Comparative proteomic analysis reveals differential protein expression of *Hypsizygus marmoreus* in response to different light qualities. *Int J Biol Macromol.* (2022) 223:1320–34. doi: 10.1016/j.ijbiomac.2022.11.037

42. Deshpande N, Wilkins MR, Packer N, Nevalainen H. Protein glycosylation pathways in filamentous fungi. *Glycobiology.* (2008) 18:626–37. doi: 10.1093/glycob/cwn044

43. Nishizawa H, Miyazaki Y, Kaneko S, Shishido K. Distribution of hydrophobin 1 gene transcript in developing fruiting bodies of *Lentinula edodes*. *Biosci Biotechnol Biochem.* (2002) 66:1951–4. doi: 10.1271/bbb.66.1951

44. Cao YY, Li Y, Zhang Y, Xiang QJ, Zhang LZ, Gu YF. Effects of trehalose on lentinan metabolism and expression of key enzyme genes of *Lentinula edodes*. *Mycosystema.* (2023) 42:2244–56. doi: 10.13346/j.mycosystema.230099

45. Xie C, Gong W, Zhu Z, Yan L, Hu Z, Peng Y. Comparative transcriptomics of *Pleurotus eryngii* reveals blue-light regulation of carbohydrate-active enzymes (CAZymes) expression at primordium differentiated into fruiting body stage. *Genomics.* (2018) 110:201–9. doi: 10.1016/j.ygeno.2017.09.012

46. Ramírez DA, Muñoz SV, Atehortua L, Michel FC Jr. Effects of different wavelengths of light on lignin peroxidase production by the white-rot fungi *Phanerochaete chrysosporium* grown in submerged cultures. *Bioresour Technol.* (2010) 101:9213–20. doi: 10.1016/j.biortech.2010.06.114

47. Gan PT, Lim YY, Ting ASY. Influence of light regulation on growth and enzyme production in rare endolichenic fungi. *Folia Microbiol.* (2023) 68:741–55. doi: 10.1007/s12223-023-01050-2

48. Zhu JC, Wang XJ. Effect of blue light on conidiation development and glucoamylase enhancement in *Aspergillus niger*. *Acta Microbiol Sin.* (2005) 45:275–8. doi: 10.13343/j.cnki.wsbx.2005.02.024

49. Froehlich AC, Chen CH, Belden WJ, Madeti C, Roenneberg T, Merrow M, et al. Genetic and molecular characterization of a cryptochrome from the filamentous fungus *Neurospora crassa*. *Eukaryot Cell.* (2010) 9:738–50. doi: 10.1128/EC.00380-09

50. He Q, Cheng P, Yang Y, Wang L, Gardner KH, Liu Y. White collar-1, a DNA binding transcription factor and a light sensor. *Science.* (2002) 297:840–3. doi: 10.1126/science.1072795

51. Salomon M, Christie JM, Knieb E, Lempert U, Briggs WR. Photochemical and mutational analysis of the FMN-binding domains of the plant blue light receptor, phototropin. *Biochemistry.* (2000) 39:9401–10. doi: 10.1021/bi000585+

52. Schmoll M, Tian C, Sun J, Tisch D, Glass NL. Unravelling the molecular basis for light modulated cellulase gene expression – the role of photoreceptors in *Neurospora crassa*. *BMC Genomics.* (2012) 13:127. doi: 10.1186/1471-2164-13-127



OPEN ACCESS

EDITED BY

Lijun Sun,
Northwest A&F University, China

REVIEWED BY

Lijun Chen,
Beijing Sanyuan Foods Co., Ltd., China
Qiping Zhan,
Nanjing Agricultural University, China

*CORRESPONDENCE

Xu Wu

✉ wuxulz@126.com

Zhi Li

✉ lizhi_swmu@126.com

[†]These authors have contributed equally to this work

RECEIVED 12 May 2024

ACCEPTED 26 June 2024

PUBLISHED 08 July 2024

CITATION

Wei S, Li M, Zhao L, Wang T, Wu K, Yang J, Tang M, Zhao Y, Shen J, Du F, Chen Y, Deng S, Xiao Z, Wei M, Li Z and Wu X (2024) Fingerprint profiling for quality evaluation and the related biological activity analysis of polysaccharides from Liuweizhiji Gegen-Sangshen beverage. *Front. Nutr.* 11:1431518. doi: 10.3389/fnut.2024.1431518

COPYRIGHT

© 2024 Wei, Li, Zhao, Wang, Wu, Yang, Tang, Zhao, Shen, Du, Chen, Deng, Xiao, Wei, Li and Wu. This is an open-access article distributed under the terms of the [Creative Commons Attribution License \(CC BY\)](#). The use, distribution or reproduction in other forums is permitted, provided the original author(s) and the copyright owner(s) are credited and that the original publication in this journal is cited, in accordance with accepted academic practice. No use, distribution or reproduction is permitted which does not comply with these terms.

Fingerprint profiling for quality evaluation and the related biological activity analysis of polysaccharides from Liuweizhiji Gegen-Sangshen beverage

Shulin Wei^{1,2†}, Mingxing Li^{1,2†}, Long Zhao^{3†}, Tiangang Wang³, Ke Wu^{1,2}, Jiayue Yang^{1,2}, Mingyun Tang³, Yueshui Zhao^{1,2}, Jing Shen^{1,2}, Fukuan Du^{1,2}, Yu Chen^{1,2}, Shuai Deng^{1,2}, Zhangang Xiao^{1,2}, Mei Wei³, Zhi Li^{3,4*} and Xu Wu^{1,2*}

¹Cell Therapy & Cell Drugs of Luzhou Key Laboratory, Department of Pharmacology, School of Pharmacy, Southwest Medical University, Luzhou, China, ²South Sichuan Institute of Translational Medicine, Luzhou, China, ³Department of Spleen and Stomach Diseases, The Affiliated Traditional Chinese Medicine Hospital, Southwest Medical University, Luzhou, China, ⁴The Key Laboratory of Integrated Traditional Chinese and Western Medicine for Prevention and Treatment of Digestive System Diseases of Luzhou City, The Affiliated Traditional Chinese Medicine Hospital, Southwest Medical University, Luzhou, China

Introduction: Liuweizhiji Gegen-Sangshen beverage (LGS) is popular in China, which has been used for alleviating alcohol-mediated discomfort and preventing alcoholic liver disease (ALD). This beverage is consisted of six herbal components that are known as functional foods and fruits. LGS is rich in polysaccharides, however, the activity and quality evaluation of LGS-derived polysaccharides remain unexplored. The purpose of this study is thus to establish a comprehensive quality control methodology for the assessment of LGS polysaccharides (LGSP) and to further explore the anti-oxidant, anti-inflammatory as well as prebiotic effect of LGSP.

Methods: LGSP was extracted, followed by analysis of molecular weight distribution, monosaccharide content and structural characterization via integrating the application of high-performance size exclusion chromatography (HPSEC), 1-phenyl-3-methyl-5-pyrazolone-HPLC (PMP-HPLC), fourier transform infrared spectroscopy (FT-IR) as well as nuclear magnetic resonance spectroscopy (NMR) techniques. The anti-oxidation activity of LGSP was determined by DPPH, ABTS, hydroxyl radical scavenging capacity and total antioxidant capacity. The anti-inflammation of LGSP were assessed on the RAW 264.7 cells. The effect of LGSP on growth of *Lactobacillus*, *Bifidobacterium bifidum* and *Bifidobacterium adolescentis* was evaluated.

Results: The results demonstrated that LGSP had two molecular weight distribution peaks, with the average molecular weights of $(6.569 \pm 0.12) \times 10^4$ Da and $(4.641 \pm 0.30) \times 10^4$ Da. LGSP was composed of 8 monosaccharides, with galacturonic acid, glucose rhamnose and galactose representing the highest molar ratios. Homogalacturonic acid (HG) type and rhamnosegalacturonic acid glycans I (RG-I) type and α -1,4-glucan were present in LGSP. LGSP concentration in LGS was 17.94 ± 0.28 mg/mL. Furthermore, fingerprint analysis combined with composition quantification of 10 batches of LGSP demonstrated that there was a high similarity among batches. Notably, LGSP exhibited anti-oxidant effect and inhibited expressions of pro-inflammatory factors (TNF- α and IL-6) in LPS-stimulated RAW 264.7 cells. In addition, LGSP remarkably promoted

the proliferation of probiotics *Lactobacillus*, *Bifidobacterium bifidum* and *Bifidobacterium adolescentis*, showing good prebiotic activity.

Discussion: The results of present study would be of help to gain the understanding of structure–activity relationship of LGSP, provide a reference for quality evaluation of bioactive LGSP, and facilitate development of unique health and functional products in the future.

KEYWORDS

Gegen-Sangshen beverage, polysaccharide, fingerprint, anti-inflammation, *Lactobacillus*, *Bifidobacterium*

Introduction

Liuweizhiji® Gegen-Sangshen beverage (LGS), consisting of six functional and herbal foods, including *Puerariae lobatae radix* (The dried radix of *Pueraria lobata* (Willd.) Ohwi), *Hoveniae semen* (The dried fruit and seed of *Hovenia dulcis* Thunb), *Imperatae rhizoma* (The dried rhizome of *Imperata cylindrica* Beauv. var. *major* (Nees) C. E. Hubb), *Crataegi fructus* (The dried fructus of *Crataegus pinnatifida* Bge.), *Mori fructus* (The dried fructus of *Morus alba* L.) and *Canarli fructus* (The dried fructus of *Canarium album* Raeusch.), is available in market and is popular in southwest China, which has been used for alleviating alcohol-mediated discomfort and preventing alcoholic liver disease (ALD) (1). This functional drink and its components have been traditionally used to treat digestive tract disorders including liver dysfunction. The main components of LGS included flavonoids, polyphenols, organic acids, as well as the macromolecular polysaccharides. It was demonstrated that some flavonoids and organic acids, including puerarin and its derivatives, vitexin, rutin and gallic acid, showed anti-oxidant, anti-inflammatory and gut microbiota regulating activities and contributed to the ALD alleviating effect of LGS (2–5). Current studies on active ingredients of LGS are mainly focused on the small-molecule components (1), however, the polysaccharide fraction is largely unexplored. The activity and quality control of polysaccharides from LGS necessitate further studies.

Polysaccharides derived from varied sources exhibit potent biological effects, such as antioxidant, antitumor, immunomodulatory, hypoglycemic, and hepatoprotective properties (6–8). Previously, it was reported that *Pueraria lobata* polysaccharides, possessed antioxidant and immunomodulatory activities, and regulated gut microbiome (9, 10). Polysaccharides from *Crataegi fructus* modulated lipid metabolism and restored the imbalance of intestinal microbiota (11). Similarly, polysaccharides from *Mori fructus* showed anti-inflammation, antioxidant, and hepatoprotective properties (12, 13). Biologically active polysaccharides were also identified from rest of the three herbs (14–16). It is thus speculated that polysaccharides are an important fraction of LGS. However, after complex processing and manufacturing, the structure of LGS polysaccharides (LGSP) may be altered significantly. Moreover, whether LGSP exerts biological effects (including antioxidant, anti-inflammatory and prebiotic effects) related to the anti-ALD effect of LGS remains unclear.

Owing to the complicate structure and large molecular weight of polysaccharides, quality control of polysaccharides is considered difficult. Natural plant polysaccharides are complex carbohydrate polymers consisting of varied long-chain monosaccharide units, and the quantification of a single marker substance is difficult and cannot specifically reflect the whole structural characteristics of polysaccharides (17). Integrated techniques to evaluate polysaccharide

quality from different aspects, including monosaccharide contents, molecular weight, and distinctive structures, is thus of great significance (18). Multiple fingerprinting using spectroscopic and chromatographic methods as well as chemometrics have been proposed for the quality assessment (19). The determination of monosaccharide composition is indispensable in polysaccharide fingerprinting, and the commonly used detection methods include 1-phenyl-3-methyl-5-pyrazolone-HPLC (PMP-HPLC), gas chromatography–mass spectrometry (GC–MS), high-performance size exclusion chromatography (HPSEC), and high performance anion exchange chromatography-pulsed amperometric detector (HPAEC-PAD) (20, 21). In addition, gel permeation chromatography has been used for molecular weight distribution fingerprinting (22). Structural characteristic fingerprinting by fourier transform infrared spectroscopy (FT-IR) as well as nuclear magnetic resonance spectroscopy (NMR) analysis affords sufficient structural information of polysaccharides (21). Thus, multi-fingerprinting analysis combined with quantitative analysis present as an efficient and effective method for evaluation of the quality consistency of polysaccharides, especially those derived from complex herbal preparations with potential batch-to-batch differences.

Based on the limitations on current studies of LGSP, the purpose of this study is to establish a multiple-fingerprint-based methodology for quality control assessment of LGSP and to investigate the related biological activity of LGSP. In this study, the LGSP were extracted from LGS, and multi-fingerprint analysis based on HPSEC, PMP-HPLC, FT-IR, and NMR were performed to analyze the molecular weight, the types and proportions of constituent monosaccharides, the types of characteristic functional groups and glycosidic bonds of LGSP from 10 batches of samples. The contents of total polysaccharides, total acidic sugars, and the content distribution of different molecular weight components were also investigated. Eventually, the antioxidant, anti-inflammatory and prebiotic activities of LGSP were analyzed by *in vitro* assays. The results of current study would gain better understanding towards the structure of LGSP, provide basis for the quality evaluation, and support for the functional use of the active polysaccharide fraction of LGS.

Materials and methods

Materials and chemicals

Amyloglucosidase, heat-stabilized α -amylase, D-glucuronic acid, L-rhamnose monohydrate, D-(+)-glucose, D-(+)-mannose, L-arabinose, D-galacturonic acid, KBr (AR grade), bovine serum albumin (BSA) and coomassie brilliant blue were obtained via Shanghai Yuanye Bio-Technology (Shanghai, China). D-xylose and D-galactose

were provided by Shanghai Aladdin Biochemical Technology (Shanghai, China). PMP, trifluoroacetic acid (TFA) and dextran were obtained from Sigma-Aldrich (St. Louis, MO, United States). Glucose, lipopolysaccharide (LPS), 5-diphenyltetrazolium bromide (MTT) and dimethyl sulfoxide (DMSO) were obtained from Shanghai Macklin Biochemical Technology Co., Ltd. (Shanghai, China). MRS medium without glucose was got from Shandong Tuopu Biol-engineering (Shandong, China). DMEM culture medium and fetal bovine serum (FBS) were purchased from Shanghai Xiaopeng Biotechnology Co., Ltd. (Shanghai, China). Primers were purchased from Tsingke Biotechnology Co., Ltd. (Beijing, China). Acetonitrile and methanol (HPLC grade) were obtained from Chron Chemicals (Chengdu, China). Ultra-pure water was prepared by Milli-Q (Merck, Germany).

Lactobacillus (CICC 6269), *Bifidobacterium bifidum* (CICC 6071), *Bifidobacterium adolescentis* (CICC 6070) and *Escherichia coli* (CICC 10899) were purchased from the China Center of Industrial Culture Collection (CICC, Beijing, China). Under anaerobic condition at 37°C, *Lactobacillus* was cultured in MRS medium, *E. coli* was cultured in LB medium, while *B. bifidum* and *B. adolescentis* were cultured in CM0233 medium.

RAW264.7 macrophages were obtained from Cyagen Biotechnology Co., Ltd. (Guangdong, China). Macrophages were inoculated into DMEM medium supplemented with 10% FBS, 100 U/mL penicillin, and 100 U/mL streptomycin. The cells were then placed at 37°C in an incubator with 5% CO₂ humidified atmosphere.

A total of 10 batches of LGS (S1–S10) were supplied by Sichuan Tongyou Life Health Technology Co., Ltd. (Sichuan, China). Voucher specimens (Batch Number: 230101–230,110) were deposited at School of Pharmacy, Southwest Medical University, Luzhou, China.

Extraction and purification of LGSP

An aliquot of 30 mL LGS was mixed with 40 mL of ultrapure water. Thermostable α -amylase was added at 10 U/mL, maintaining at 70°C for 8 h. After cooling down, amyloglucosidase was added at 10 U/mL for removing starch. The reaction was taken at 59°C for 12 h, and finally heated to 95°C for 30 min to inactivate the enzyme. After further centrifugation at 4000 \times g for 15 min, 4 volumes of alcohol (95%, v/v) were mixed with the supernatant for precipitating crude polysaccharides. Next, crude polysaccharides were washed and redissolved and freeze-dried to obtain LGSP, which was stored at 4°C.

HPSEC fingerprint

The molecular weight and distribution of LGSP were analyzed by HPSEC connecting to a multi-angle laser light scattering and differential index detector (HPSEC-MALLS-RID), and molecular weight fingerprint of polysaccharides of LGS was established. The column used was Shodex OHpak SB-804 HQ column (8.0 \times 300 mm). The 0.9% NaCl in water served as the mobile phase. The flow rate was 0.5 mL/min. The injection volume was set to 100 μ L.

PMP-HPLC fingerprint

Complete acid hydrolysis

The complete acid hydrolysis of LGSP analyzed by PMP derivatization was conducted as previously reported (23). In brief,

6 mg of LGSP is precisely weighed and dissolved in 1 mL of ultrapure water and hydrolyzed by with 1 mL of 4 mM TFA at 95°C for 12 h. After complete removal of TFA residues under a vacuum evaporator, it is dissolved in 1 mL of ultrapure water for follow-up PMP derivatization. The monosaccharide standard solutions (0.5 mg/mL; including galacturonic acid, mannose, rhamnose, glucose, glucuronic acid, galactose, xylose, and arabinose) or the hydrolysate samples (50 μ L; 6 mg/mL) were, respectively, added with 50 μ L of sodium hydroxide (0.6 mM) and 100 μ L of PMP solution (0.5 mM) for reaction for 100 min at 70°C. After neutralization with 30 μ L of 0.3 mM HCl and removing PMP by chloroform extraction, the derivatization solution was filtered for further analysis.

Derivatized samples were analyzed on a Thermo UHPLC-3000 SL system with a ZORBAX Eclipse XDB-C18 column (150 mm \times 4.6 mm, 5 μ m) equipped with a diode array detector (DAD). The column temperature was controlled at 35°C. Isocratic elution was performed using the mixed mobile phase of A (0.1 M PBS, pH=6.7) and B (acetonitrile) with a v/v ratio of 83.5:16.5. The flow rate was 1.0 mL/min. Injection volume was 20 μ L. The detection wavelength was set at 245 nm for DAD analysis.

Partial acid hydrolysis

The partial acid hydrolysis of LGSP was conducted by reaction of 0.5 mM TFA with 6 mg/mL LGSP at 95°C for 5 h. The other procedures including PMP derivatization and ultra-high performance liquid chromatography (UHPLC) analysis were identical to those for complete acid hydrolysis.

FT-IR fingerprint

The FT-IR spectra (ranged 4,000–500 cm⁻¹) of LGSP were acquired on a PerkinElmer Spectrum 3 FT-IR spectrometer.

NMR fingerprint

The LGSP samples were dissolved in D₂O. The one-dimensional hydrogen spectra (¹H) and one-dimensional carbon spectra (¹³C) of LGSP were analyzed by a Bruker Ascend 600 MHz spectrometer using a z-gradient probe. The information acquisition temperature was 25°C, the carbon frequency was 150.90 MHz, and the proton frequency was 600.13 MHz.

Chemical composition analysis

Using the following formula, the extraction rate of LGSP was calculated: yields (%) = (weight of LGSP / volume of LGS) \times 100%. Components of LGSP, such as total polysaccharides, total proteins and total uronic acids, were determined using the colorimetric method. In brief, total contents of polysaccharides were quantified using phenol-sulfuric acid method with galactose and galacturonic acid as standards. Using galacturonic acid as the standard, the m-hydroxybiphenyl method was applied to detect the quantity of uronic acid. The protein contents were analyzed by the Bradford method with BSA used as the standard.

TABLE 1 Molecular weight distribution of polysaccharides in different batches of LGSP.

No.	Fraction 1 $M_w \times 10^4$ (Da)	Relative peak areas (%)	M_w/M_n	Fraction 2 $M_w \times 10^4$ (Da)	Relative peak areas (%)	M_w/M_n
S1	6.436	32.1	1.168	4.242	67.9	1.092
S2	6.443	33.2	1.189	4.068	66.8	1.109
S3	6.763	32.5	1.162	4.880	67.5	1.076
S4	6.531	32.8	1.150	4.881	67.2	1.075
S5	6.667	31.4	1.154	4.886	68.6	1.088
S6	6.689	33.7	1.159	4.681	66.3	1.082
S7	6.570	30.8	1.165	4.353	69.2	1.115
S8	6.621	32.1	1.169	4.851	67.9	1.076
S9	6.387	33.1	1.155	4.930	66.9	1.094
S10	6.583	32.8	1.163	4.640	67.2	1.089
Average	6.569	32.45	1.163	4.641	67.55	1.090

M_w , weight-average molecular weight; M_n , number-average molecular weight; M_w/M_n , index of molecular weight distribution.

Activity of LGSP

Antioxidant activity

The antioxidant activity of LGSP was assessed by the DPPH free radical scavenging assay, the hydroxyl radical scavenging assay, the ABTS free radical scavenging assay and the total antioxidant capacity test according to the kit manufacturer's instructions.

Anti-inflammatory effect

The anti-inflammation of LGSP were assessed on the RAW 264.7 cells. The impact of LGSP on macrophage proliferation was firstly detected using the MTT method. For the anti-inflammation study, pre-cultured RAW 264.7 cells were collected and seeded in 6-well plates (6×10^5 /mL). LPS ($1 \mu\text{g/mL}$) was added for induction for 4h, and then the cell morphology changes were observed before adding the LGSP ($0\text{--}200 \mu\text{g/mL}$). After 24h of drug treatment, cells were collected, and total RNA was extracted with Trizol reagent. Reverse transcription into cDNA was conducted by using a reverse transcription kit (Vazyme), and GAPDH was used as the internal control. The mRNA expression level was determined by quantitative PCR (qPCR). The primer sequences were as follows: *GAPDH* (forward, AGGTCGGTGTGAACGGATTTG; reverse, TGTAGACC ATGTAGTTGAGGTCA); *IL-6* (forward, TCTATACCACTTCACA AGTCGGA; reverse, CGATCACCCGAAGTTCAGTAG); *TNF- α* (forward, CAGGCGGTGCCTATGTCTC; reverse, CGATCA CCCCAGTTCAGTAG). The culture supernatants were used for determination of the concentrations of IL-6 and TNF- α using the enzyme linked immunosorbent assay (ELISA) kits (Jiangsu Meibiao Biotechnology Co., Ltd., Jiangsu, China).

Prebiotic activity

During experimentation, sugar-free culture medium was used. In order to evaluate whether LGSP had an effect on bacterial growth, LGSP at 4000 mg/L was supplemented as the carbon source. Glucose added at 4000 mg/L was used as a positive control. The bacterial growth was recorded at the time points of 0, 4, 8, 12, and 24 h, respectively, through determining the optical density (OD) at 600 nm with a spectrophotometer. In addition, to test the

particularity of LGSP in promoting the growth of beneficial bacteria, the impact of LGSP on the growth of *E. coli* was further investigated.

Statistical analysis

GraphPad Prism 6.0 was used for data analysis. All data are displayed as mean \pm standard deviation (SD). Statistical analysis was carried out using one-way analysis of variance (ANOVA) followed by Tukey's test.

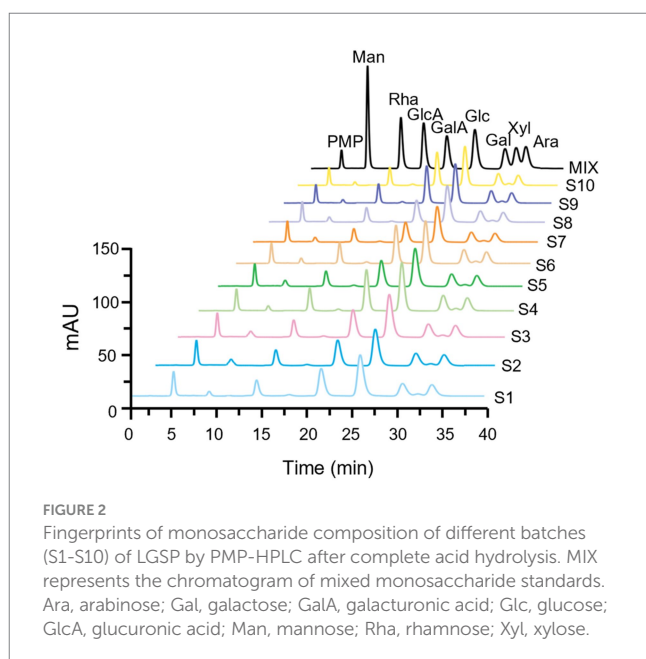
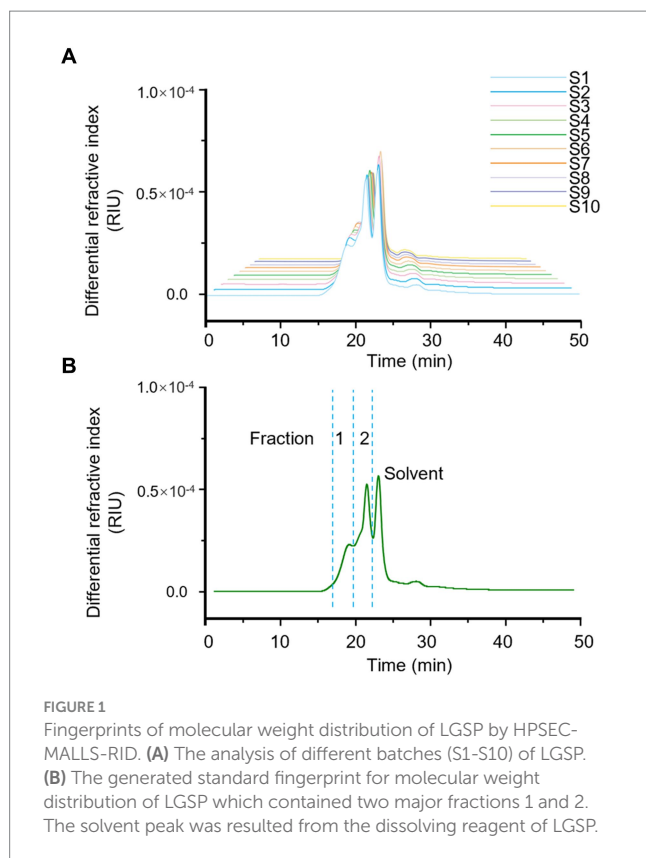
Results

Quality evaluation

Fingerprint based on molecular weight distribution

HPSEC fingerprint of 10 batches of LGSP was first conducted to reveal the characteristics of molecular weight distribution. The results are shown in Table 1 and Figure 1. The solvent background peaks that appeared after 21 min were removed, and the 10 batches of LGSP had similar spectra and molecular weight distributions, which contained two molecular weight distribution peaks, namely the fraction 1 and fraction 2.

The molecular weight of fraction 1 ranged from $6.387 \times 10^4 \text{ Da}$ to $6.763 \times 10^4 \text{ Da}$, with the average molecular weight of $6.569 \times 10^4 \text{ Da}$. It is worth noting that sample 3 had the highest molecular weight of fraction 1, while sample 9 had the lowest molecular weight of fraction 1. The relative proportion of fraction 1 accounted for 30.8–33.7% (average: 32.45%) of the total peak area. The molecular weight range of fraction 2 of different batches of LGSP was $4.068 \times 10^4 \text{ Da}$ – $4.930 \times 10^4 \text{ Da}$, and the average molecular weight was $4.641 \times 10^4 \text{ Da}$. The sample 9 had the highest molecular weight of fraction 2 and sample 2 had the lowest molecular weight. The relative proportion of the peak area of fraction 2 was 66.3–69.2%, with the average proportion of 67.55%. The peak area ratio of fraction 2 in different batches of LGSP was about twice that of fraction 1.



Fingerprint based on monosaccharide composition

Monosaccharides serve as the fundamental building blocks of polysaccharides, playing a crucial role in identifying their structural characteristics. The monosaccharide composition and the molar percentage among different batches of LGSP were analyzed by complete hydrolysis followed by HPLC analysis after

pre-column PMP derivatization. As shown in Figure 2, the monosaccharide compositions of different batches of LGSP were basically the same, which were composed of 8 monosaccharide components: mannose (Man), glucose (Glc), galactose (Gal), xylose (Xyl), rhamnose (Rha), arabinose (Ara), glucuronic acid (GlcA), and galacturonic acid (GalA). The molar ratios of 10 batches of LGSP are shown in Table 2. The molar percentages of different batches of LGSP were similar, among which Ara, Glc, GalA, Gal and Rha were the predominant monosaccharides.

In general, GalA, Gal, Ara, Rha, and GlcA are the typical monosaccharides of homogalacturonic acid (HG) type and rhamnosegalacturonic acid glycans I (RG-I) type polysaccharides. The molar ratio (MR) of monosaccharides can unveil the structural characteristics of polysaccharides. MR1 is the ratio of GalA/Rha, indicating the proportion of HG to RG-I domains. In addition, MR2 is the ratio of (Ara + Gal)/Rha, which reflects the degree of branching of RG-I. Higher values indicate that the RG-I region contains more or longer side chains. The results showed that the MR1 of different batches of LGSP ranged from 1.84 to 2.65, while MR2 ranged from 1.76 to 2.03. Therefore, according to the MR values, HG and RG-I pectin polysaccharides were present in the LGSP. In addition, although the samples were destarched with amylase and saccharification enzyme, Glc was still present in the LGSP, which may be resistant starch that could not be removed by the two enzymes. This indicated that different batches of LGSP also contained dextran.

Fingerprint based on controllable partial acid hydrolysis

Partial acid hydrolysis can simplify the complex structure of polysaccharides and degrade them into oligosaccharides with different degrees of polymerization. Unlike complete acid hydrolysis, partial acid hydrolysis is different in acid concentration or treatment time, which leads to different final hydrolysate products, and polysaccharide structure can be analyzed from different aspects (24). Thus, controllable partial acid hydrolysis of LGSP was carried out using low-concentration TFA, and the analysis of the controllable partial acid hydrolysate and the molar percentage of monosaccharide compositions were analyzed by HPLC after pre-column PMP derivatization. Fingerprints for both complete and partial acid hydrolysates would provide a more comprehensive information for chemical compositions of LGSP.

As shown in Figure 3, the monosaccharide compositions in the partial hydrolysate of LGSP were generally similar, which were composed of five monosaccharide components: Rha, Glc, Gal, Xyl and Ara. This indicated that the controllable partial acid hydrolysis did not destroy the HG pectin domain in the LGSP. In addition, the molar compositions of monosaccharides in the partial acid hydrolysate of different batches of LGSP were slightly different, and the composition of each monosaccharide in the partial hydrolysate of LGSP is shown in Table 3. The main monosaccharides in the partial acid hydrolysate of LGSP were Rha, Glc, Gal and Ara, among which the molar percentage of Rha was 10.46–14.04% averaged at 12.14%. The molar percentage of Glc was 41.23–48.65% averaged at 44.39%. The molar percentage of Gal was 14.92–17.36% averaged at 16.10%. The molar mass percentage of Ara was 22.86–25.43% averaged at 24.24%. Notably, the MR2 ratio of different batches of LGSP was 2.88–3.78, and the average value was 3.35.

TABLE 2 Monosaccharide composition and molar ratio of different batches of LGSP by complete acid hydrolysis.

No.	Man	Rha	GlcA	GalA	Glc	Gal	Xyl	Ara	MR1	MR2
S1	0.0132	0.1141	0.009	0.2499	0.3767	0.1141	0.0202	0.1028	2.19	1.90
S2	0.0438	0.1186	0.0082	0.2397	0.3481	0.1183	0.0197	0.1035	2.02	1.87
S3	0.0356	0.1172	0.008	0.2348	0.3696	0.1142	0.0196	0.101	2.00	1.84
S4	0.0183	0.111	0.0094	0.269	0.3487	0.116	0.018	0.1094	2.42	2.03
S5	0.0837	0.1086	0.009	0.2313	0.3414	0.1117	0.0177	0.0967	2.13	1.92
S6	0.0185	0.1118	0.0093	0.2813	0.3397	0.1145	0.0185	0.1065	2.52	1.98
S7	0.0609	0.1153	0.0078	0.2125	0.3824	0.1074	0.0184	0.0953	1.84	1.76
S8	0.0522	0.1167	0.0078	0.2197	0.3726	0.114	0.0191	0.098	1.88	1.82
S9	0.0167	0.1112	0.0093	0.2947	0.3375	0.11	0.0178	0.1029	2.65	1.91
S10	0.0178	0.1106	0.0091	0.2725	0.3534	0.1121	0.0177	0.1067	2.46	1.98
Average	0.0361	0.1135	0.0087	0.2505	0.3570	0.1132	0.0187	0.1023	2.21	1.90

Ara, arabinose; Gal, galactose; GalA, galacturonic acid; Glc, glucose; GlcA, glucuronic acid; Man, mannose; Rha, rhamnose; Xyl, xylose; MR1, the molar ratio of GalA/Rha; MR2, the molar ratio of (Ara + Gal)/Rha.

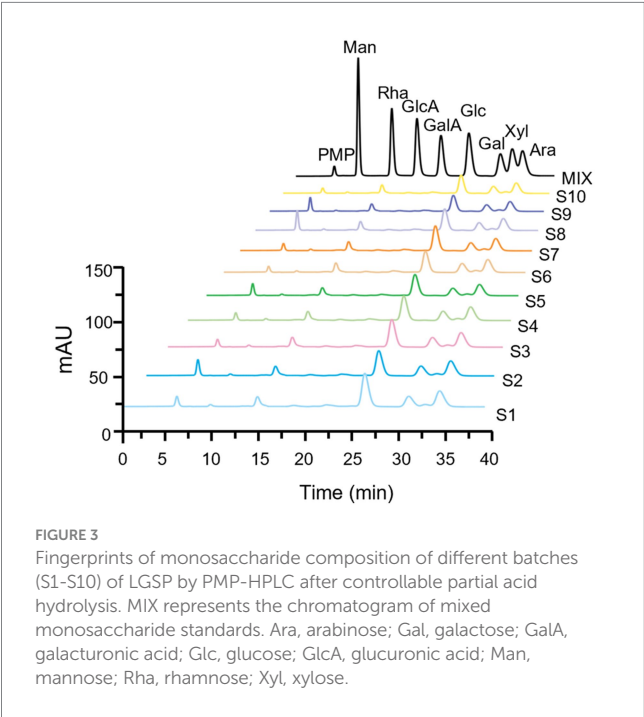


FIGURE 3 Fingerprints of monosaccharide composition of different batches (S1-S10) of LGSP by PMP-HPLC after controllable partial acid hydrolysis. MIX represents the chromatogram of mixed monosaccharide standards. Ara, arabinose; Gal, galactose; GalA, galacturonic acid; Glc, glucose; GlcA, glucuronic acid; Man, mannose; Rha, rhamnose; Xyl, xylose.

Fingerprint based on FT-IR

The FT-IR spectrometer was used to record the infrared spectra in the wavelength range of 4,000–500 cm⁻¹, and the FT-IR fingerprint of different batches of LGSP was established. As shown in Figure 4, the FT-IR spectra of different batches of LGSP were similar. The vibrational region shown between 3,200 cm⁻¹ and 3,600 cm⁻¹ was the featured band of the hydroxyl groups, and the peak at 3400 cm⁻¹ indicated the stretching vibration of hydroxyl group, representing the presence of hydroxyl groups. The fluctuations in the range of 3,000 cm⁻¹–2800 cm⁻¹ (2,929 cm⁻¹) were the C-H absorption peaks, which included the stretching vibrations of CH, CH₂, and CH₃. The strong peak at 1636 cm⁻¹ was the asymmetric stretching vibration of C=O in the carboxylic acid

TABLE 3 The composition and proportion of monosaccharides in the partial acid hydrolysate of different batches of LGSP.

No.	Rha	Glc	Gal	Xyl	Ara	MR2
S1	0.1046	0.4865	0.1506	0.0283	0.2300	3.64
S2	0.1187	0.4299	0.1658	0.0313	0.2543	3.54
S3	0.1062	0.4616	0.1600	0.0305	0.2417	3.78
S4	0.1179	0.4415	0.1662	0.0301	0.2443	3.48
S5	0.1157	0.4568	0.1582	0.0306	0.2388	3.43
S6	0.1311	0.4134	0.1736	0.0337	0.2482	3.22
S7	0.1227	0.4695	0.1492	0.0299	0.2286	3.08
S8	0.1193	0.4434	0.1592	0.0329	0.2452	3.39
S9	0.1378	0.4123	0.1669	0.0335	0.2495	3.02
S10	0.1404	0.4245	0.1606	0.0312	0.2433	2.88
Average	0.1214	0.4439	0.1610	0.0312	0.2424	3.35

Ara, arabinose; Gal, galactose; Glc, glucose; Rha, rhamnose; Xyl, xylose; MR2, molar ratio of (Ara + Gal)/Rha.

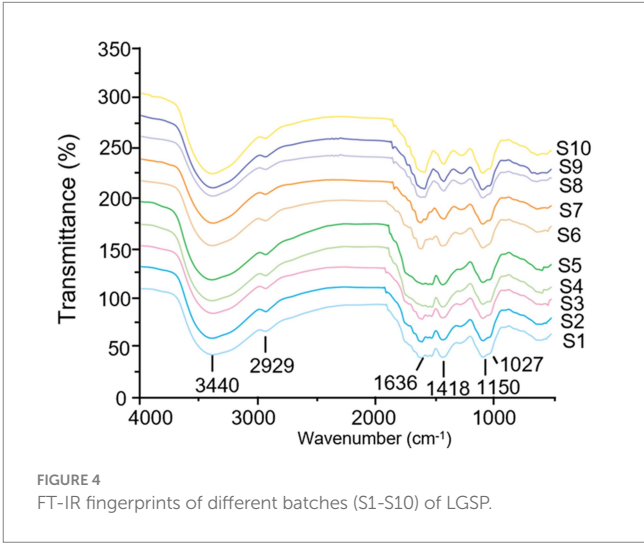


FIGURE 4 FT-IR fingerprints of different batches (S1-S10) of LGSP.

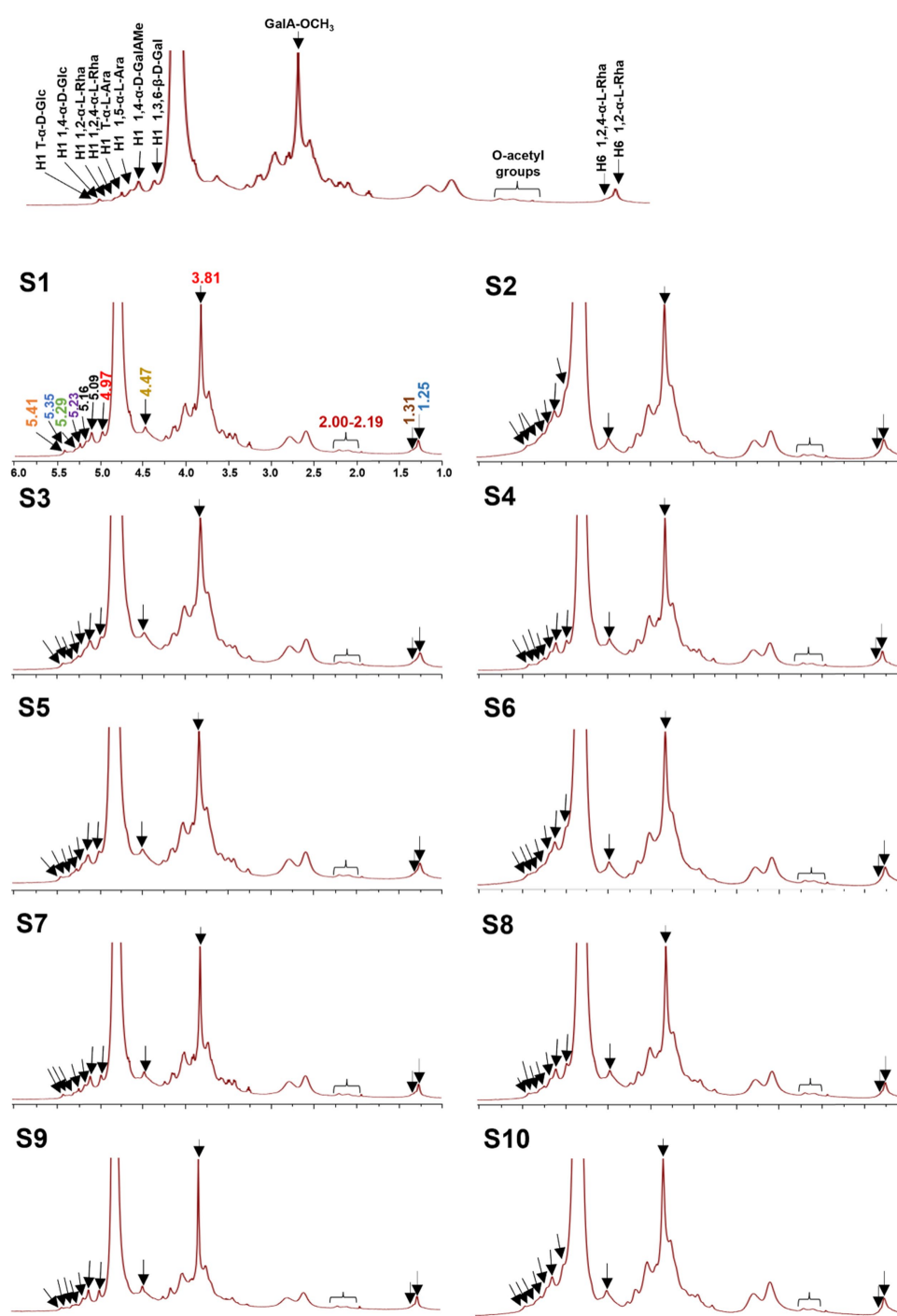


FIGURE 5

¹H NMR fingerprints of different batches (S1-S10) of LGSP with structural assignments of key signals.

group, which represented the presence of uronic acid. The vibration at 1418 cm^{-1} was attributed to the bending vibration of C-H or O-H, and the vibration at 1150 cm^{-1} was an asymmetrical C-O-C vibration, representing the presence of a methoxy group. In addition, the vibrational range ($1,000\text{ cm}^{-1}$ - $1,200\text{ cm}^{-1}$) was caused by the vibration of the ester glycan group (CO-C) and the C-O-H of the pyranose ring, which proved that the LGSP contained pyranonose.

Fingerprint based on NMR

To better understand the precise structure of the LGSP, the ¹H and ¹³C NMR spectra of 10 batches of LGSP were measured and analyzed by Bruker NMR spectroscopy (Figures 5, 6). The ¹H and ¹³C NMR spectra of the 10 batches of LGSP were similar, indicating that they had similar primary chemical structures.

Typical signals of pectins (HG and RG-I) as well as α-glucan, were observed from ¹H and ¹³C NMR. For example, from the ¹H spectra, the

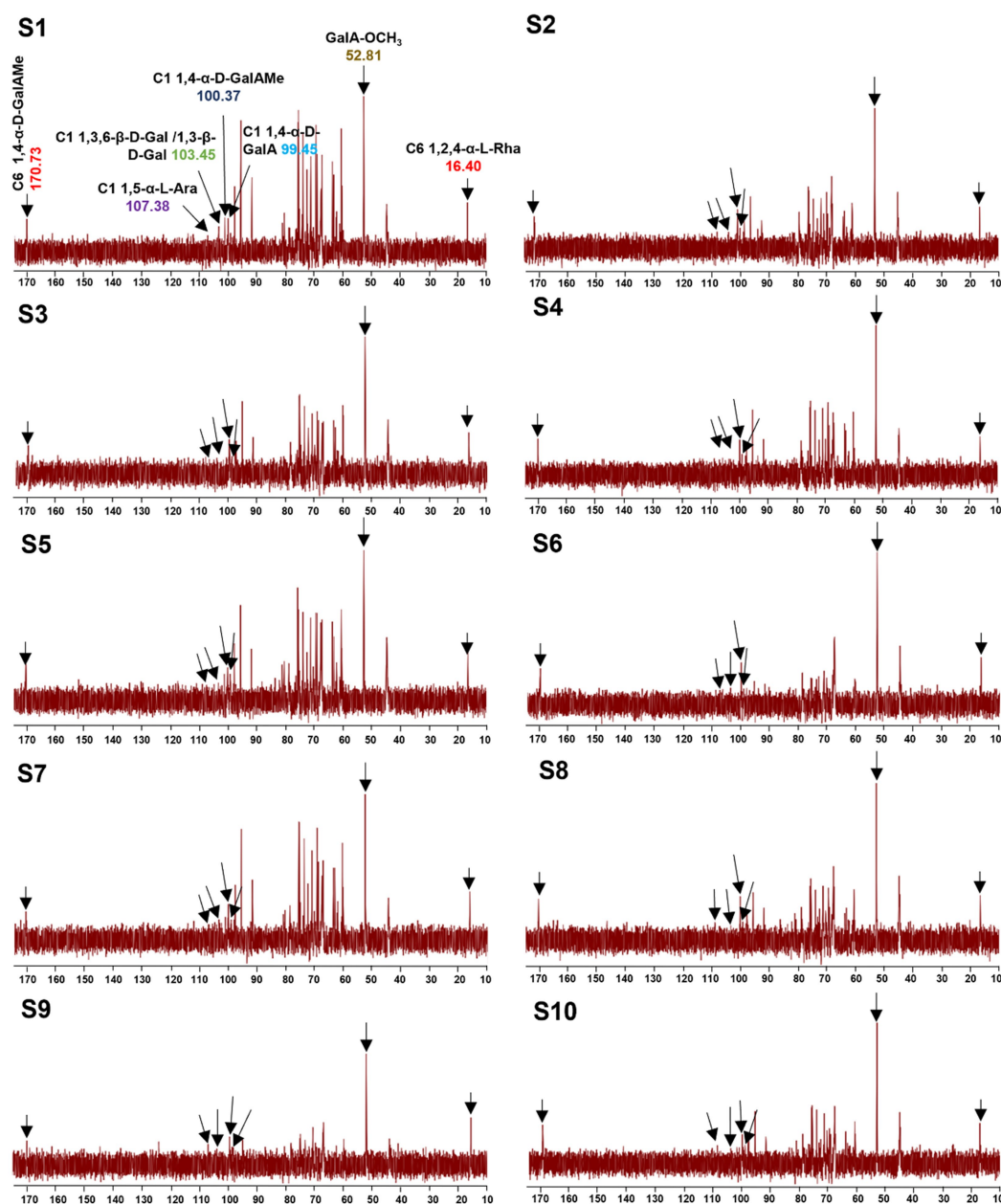


FIGURE 6
 ^{13}C NMR fingerprints of different batches (S1-S10) of LGSP with structural assignments of key signals.

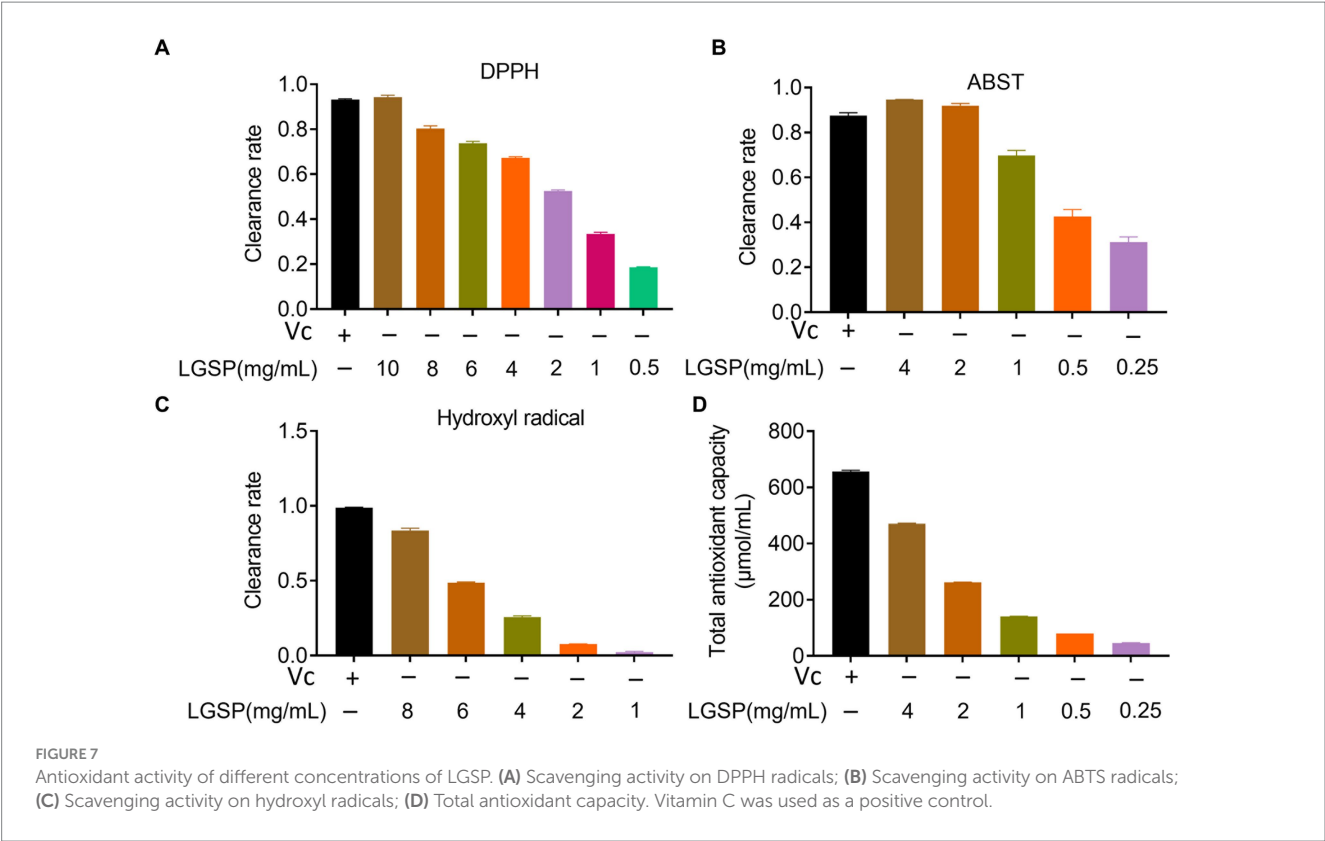
^1H NMR signals in the range of 5.09 to 5.29 ppm were attributed to the α -L-Ara and α -L-Rha residues. The signals in the range of 4.40 to 4.53 ppm were attributed to the β -D-Gal residue. The signals in the range of 4.97 ppm and 3.81 ppm were attributed to the GalAMep residue. The presence of signals (5.41 and 5.35 ppm) suggested the presence of T- α -D-Glc and 1,4- α -D-Glc, which further confirmed the presence of resistant starch in the LGSP. The signals at 5.29 ppm and 5.23 ppm were corresponded to the presence of 1,2- α -L-Rha and 1,2,4- α -L-Rha, respectively, while the 5.16 ppm and 5.09 ppm ^1H NMR signals were attributed to T- α -L-Ara and 1,5- α -L-Ara, respectively. The signal of 4.97 ppm was suggestive of the presence of 1,4- α -D-GalAMep, while the signal at GalA-OCH₃ was observed at 3.81 ppm. The signal at 4.47 ppm suggested the presence of 1,3,6- β -D-Gal. The signal at

2.00–2.09 ppm indicated the presence of the O-acetyl chemical group. Signals at 1.25 ppm and 1.31 ppm indicated the presence of 1,2- α -L-Rha and 1,2,4- α -L-Rha, respectively.

Based on ^{13}C spectra, the signals at 170.73 and 100.37 ppm were due to the presence of 1,4- α -D-GalAMep, while the signal of GalA-OCH₃ was observed at 52.81 ppm. The signal at 107.38 ppm indicated the presence of 1,5- α -L-Ara, while the signal at 103.45 ppm suggested the presence of 1,3,6- β -D-Gal. The signal at 99.45 ppm indicated the 1,4- α -D-GalA, while the signal at 16.40 ppm indicated the 1,2,4- α -L-Rha. According to the data of monosaccharide composition analysis combined with NMR analysis, HG, RG-I and α -1,4-glucan were indeed found in 10 batches of LGSP.

TABLE 4 Total polysaccharides, total uronic acid, and total protein content of different batches of LGSP.

Batch	Extraction rate (mg/mL)	Polysaccharide (%)	Uronic acid (%)	Protein (%)
S1	17.43±0.13	82.64±0.68	21.23±0.16	2.78±0.02
S2	17.98±0.49	83.18±0.76	22.20±0.17	3.39±0.01
S3	17.91±0.65	78.78±0.45	21.33±0.11	3.25±0.08
S4	17.54±0.15	76.44±0.13	21.84±0.05	3.19±0.01
S5	17.34±0.01	77.18±0.29	21.99±0.04	3.19±0.04
S6	17.35±0.17	80.97±0.55	22.40±0.11	2.96±0.04
S7	18.68±0.33	78.36±0.44	22.24±0.12	2.83±0.03
S8	17.69±0.17	76.86±0.30	22.00±0.27	2.72±0.06
S9	18.84±0.53	79.49±1.76	22.77±0.04	3.11±0.08
S10	18.62±0.13	80.31±0.39	22.15±0.06	2.89±0.07
Average	17.94±0.28	79.42±0.58	22.02±0.11	3.03±0.04



Quantitative analysis

The total polysaccharides, extraction rate, total uronic acids and total protein contents of different batches of LGS are shown in Table 4. The results showed that the yield of LGSP ranged from 17.34±0.01 mg/mL to 18.84±0.53mg/mL of LGS averaged at 17.94±0.28mg/mL. Different batches of LGSP contained a small amount of protein, with the content ranging from 2.72 to 3.39% averaged at 3.03%. The total polysaccharide content in different batches of LGSP ranged from 76.44 to 83.18%, and the average content was 79.42%. The total uronic acid content in different batches of LGSP ranged from 21.23 to 22.77%, and the average content was 22.02%.

Activity evaluation

Anti-oxidant activity

The anti-oxidation activity of LGSP was determined by DPPH, ABTS, hydroxyl radical scavenging capacity and total antioxidant capacity. The DPPH radical, characterized by a lone electron, exhibits notable stability despite its status as a free radical. Reacting with a scavenger, the solution undergoes a color change. (25). As can be seen in Figure 7A, the scavenging efficiency of LGSP on DPPH free radicals increased in direct proportion to the polysaccharide concentration, ranging from 1 to 10 mg/mL., and at a concentration of 10 mg/mL, the

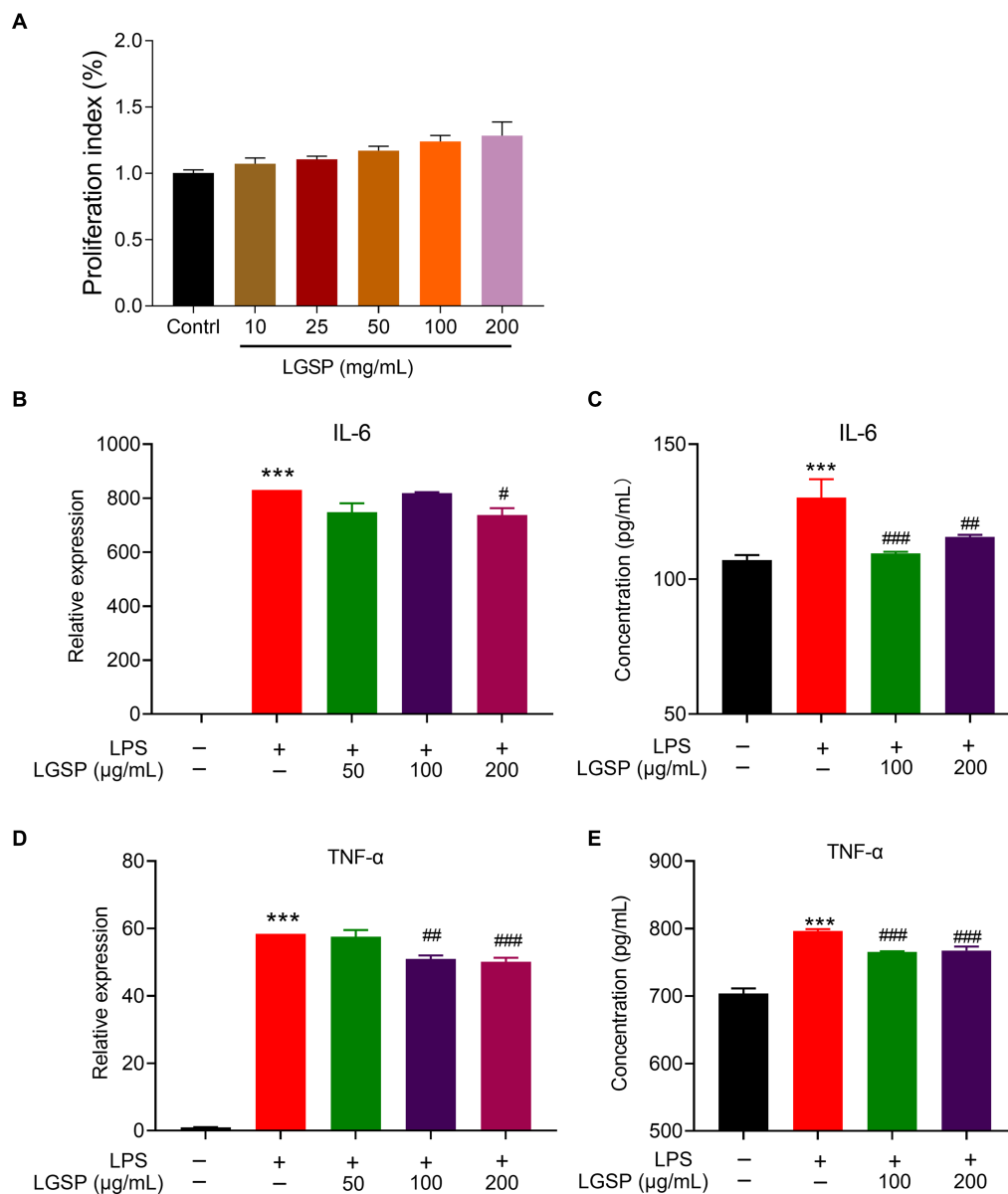


FIGURE 8

Anti-inflammatory effects of LGSP in LPS-induced RAW 264.7 cells. (A) Effects of LGSP on cell viability (24 h) of RAW 264.7 cells determined using MTT assays. (B) The mRNA expression of *IL-6* in LPS-induced RAW 264.7 cells. (C) The concentration of *IL-6* in culture supernatant of LPS-induced RAW 264.7 cells detected by ELISA kit. (D) The mRNA expression of *TNF-α* in LPS-induced RAW 264.7 cells. (E) The concentration of *TNF-α* in culture supernatant of LPS-induced RAW 264.7 cells detected by ELISA kit. *** $p < 0.001$ vs. blank group; * $p < 0.05$, ** $p < 0.01$, *** $p < 0.001$ vs. LPS alone group.

DPPH free radical scavenging rate reached 94.27%, slightly surpassing that of vitamin C (Vc) at 1 mg/mL.

ABTS has been used to evaluate the antioxidation ability of the substance (26). As displayed in Figure 7B, the ABTS free radical scavenging activity of LGSP was also positively correlated with dose. At the concentration was 4 mg/mL, the scavenging rate reached 94.66%, surpassing that of Vc at 0.05 mg/mL. These data indicate that LGSP exhibited significant efficacy in scavenging ABTS free radicals.

Among reactive oxygen species, hydroxyl radicals are very active, which may cause genetic alterations in cells and promote disease or cell death (27). As shown in Figure 7C, in the range of concentrations of 1–8 mg/mL, the scavenging ability of LGSP was gradually decreased. At the concentration of 8 mg/mL, its

scavenging rate reached 82.97%, which was slightly lower than that of Vc at 10 mg/mL.

The total antioxidant capacity represents the level of various antioxidant substances in the system. As shown in Figure 7D, similarly, with the increase of LGSP concentration, total antioxidant capacity increased. At a concentration of 8 mg/mL, its total antioxidant capacity was 471.19 μmol/mL.

Anti-inflammatory effect

The effect of LGSP on cell viability of macrophages is analyzed by MTT assay before evaluating anti-inflammatory effect of LGSP. The result showed that LGSP was non-cytotoxic to macrophages at dose range of 10–200 μg/mL (Figure 8A).

RAW 264.7 cells were further stimulated by LPS to establish the experimental inflammation model. The relative expression levels of pro-inflammatory cytokines (IL-6 and TNF- α) in cells stimulated by LPS were detected by qPCR and ELISA kits. As shown in Figures 8B–D, the expression levels of these pro-inflammatory cytokines in LPS-induced RAW 264.7 cells were significantly higher than that in the non-LPS-induced group, suggestive of successfully establishment of the inflammatory cell model. Remarkably, LGSP treatment significantly inhibited both the gene and protein expression levels of IL-6 (Figures 8B,C) and TNF- α (Figures 8D,E) in RAW 264.7 cells in a dose-dependent manner, especially at the concentration of 100 and 200 $\mu\text{g/mL}$.

The above results indicated that LGSP had an anti-inflammatory activity on LPS-stimulated macrophages.

Prebiotic activity

Three strains of probiotics (*Lactobacillus*, *Bifidobacterium bifidum* and *B. adolescentis*), which have been demonstrated to alleviate liver dysfunctions, were used in this study (28, 29).

Carbon sources were important for bacterial growth. To avoid interference of glucose, glucose-free medium was used for study. The results showed that supplementation of glucose-free medium with glucose or LGSP significantly promoted the growth of *Lactobacillus* (Figure 9A), *B. adolescentis* (Figure 9B) and *B. bifidum* (Figure 9C) when compared to the Medium group (using glucose-free medium only). Notably, for the growth of *Lactobacillus* (Figure 9A), the promoting effect of LGSP was smaller than that of glucose, while for the growth of *B. adolescentis* (Figure 9B) and *B. bifidum* (Figure 9C) the promoting effect of LGSP was comparable to that of glucose. The bacterial precipitation images at different time points also showed the same trend as the growth curve. In contrast, *in vitro* incubation experiments with *E. coli*, LGSP did not show an *in vitro* proliferative effect compared to the Medium group (Figure 9D). These results indicate that *Lactobacillus*, *B. bifidum* and *B. adolescentis* could ferment and use LGSP as a carbon source to support their proliferation *in vitro*, and LGSP displayed a prebiotic effect.

Discussion

In this study, for the first time, we provided a comprehensive understanding on the chemical compositions and structural characteristics of LGSP through performing multiple-fingerprint analysis. Moreover, the anti-oxidant, anti-inflammatory and prebiotic effects of LGSP were revealed.

Quality control of polysaccharides poses a significant bottleneck in the development of novel polysaccharide-based pharmaceuticals. As a macromolecular substance, polysaccharides have a multi-level structure like proteins, which makes it difficult to evaluate their quality by content determination alone or by a specific spectrum (30). Recently, fingerprinting has been used as the preferred quality control method for complex natural polysaccharides due to its efficiency and convenience. From the aqueous extract of *Astragalus membranaceus*, Wang et al. purified polysaccharides, and the quality control of the polysaccharides was carried out by assessing polysaccharide content, monosaccharide composition and molecular weight (31). Jiang et al. isolated polysaccharides from sea cucumbers by anion exchange and gel permeation chromatography (32). HPSEC, PMP-HPLC, FT-IR spectroscopy, gas chromatography–mass spectrometry (GC–MS) and NMR spectroscopy were used to characterize the preliminary

structure, and the results showed that the molecular weight of the polysaccharide was 9.3×10^5 Da and the polysaccharide was composed of Glc, Gal, Ara and GlcA, with the major backbone of (1 \rightarrow 4)-linked α -Glc, (1 \rightarrow 6)-linked β -Glc, and (1, 4 \rightarrow 6)-linked β -Glc (32). Generally, polysaccharides are mainly controlled by molecular weight distribution, the types and proportions of constituent sugars, the types of characteristic functional groups, and the determination of characteristic glycosidic bond types and contents. In this study, LGSP contained two molecular weight distribution peaks, which were divided into fraction 1 and 2, with the average molecular weight of $(6.569 \pm 0.12) \times 10^4$ Da, and $(4.641 \pm 0.30) \times 10^4$ Da. LGSP was composed of 8 monosaccharides, including Man, Rha, Ara, Glc, Xyl, Gal, GlcA, GalA, with GalA and Glc representing the highest composition followed by Rha and Gal. FT-IR analysis suggested the presence of uronic acid, pyranonose and methoxy groups. NMR analysis found that HG, RG-I and α -1,4-glucan were present in LGSP. Quantitative analysis showed that LGSP yields 17.94 ± 0.28 mg/mL from LGS, with a protein content of 3.03% and total uronic acid content of 22.02%. Notably, batch-to-batch analysis of LGSP indicated that the quality of different batches of LGSP were generally consistent. The quality control research system established is thus considered complete and reliable.

The antioxidation activity of polysaccharides is related to the capacity to scavenge free radicals (24, 33). It is worth noting that the activity of polysaccharides is directly determined by the polysaccharide backbone and glycosidic bond type. Studies showed that the smaller the molecular weight of the polysaccharide, the higher the activity. The probable reason for this is that low-molecular-weight polysaccharides have more reducing ends and can bind better to free radicals (34–36). In addition to molecular weight, uronic acid, fucose, galactose, and galacturonic acid have also been identified as significant contributors to antioxidant activity. High composition of uronic acid in polysaccharides may lead to activation of isomeric hydrogen atoms to scavenge free radicals (37–39). In this study, the good free radical scavenging capacity of LGSP may be attributable to the relatively low molecular weight (10^4 Da) and relatively high molar ratio of GalA (25.05%) and Gal (11.32%).

Macrophages are widely distributed and are important cells associated with inflammation, which are critical for immune stimulation and pathogen phagocytosis (40). Macrophages can differentiate into M1 type induced by LPS and generate the pro-inflammatory TNF- α , IL-1 β and IL-6 (41). Numerous naturally occurring active polysaccharides demonstrate anti-inflammatory effects through modulating the secretion of inflammatory factors (42). The anti-inflammatory effect of polysaccharides is closely associated with the structural properties, and the content of galacturonic acid may directly affect their anti-inflammatory activity (43). In this study, it is found that LGSP has good anti-inflammatory activity by suppressing LPS-induced macrophage activation via inhibiting TNF- α , IL-1 β and IL-6.

Polysaccharides with specific structures have good prebiotic activity (44). Increased probiotics may inhibit the systemic level of pro-inflammatory factors by correcting the imbalance of intestinal microbiota, increasing the proportion of probiotics, promoting the repair of intestinal wall and mucous membrane, inhibiting translocation of harmful bacterial metabolites (45, 46). Intestinal probiotics can decrease the lipid burden of the liver by regulating the intestinal microbial community, affecting the production of alcohol metabolites and the absorption of nutrients in the gut (47). Intestinal probiotics play a critical role in preserving immune balance within gut-liver axis, and their anti-inflammatory modulates the host's immune system, improving alcohol-related liver damage and hepatic oxidative stress (48,

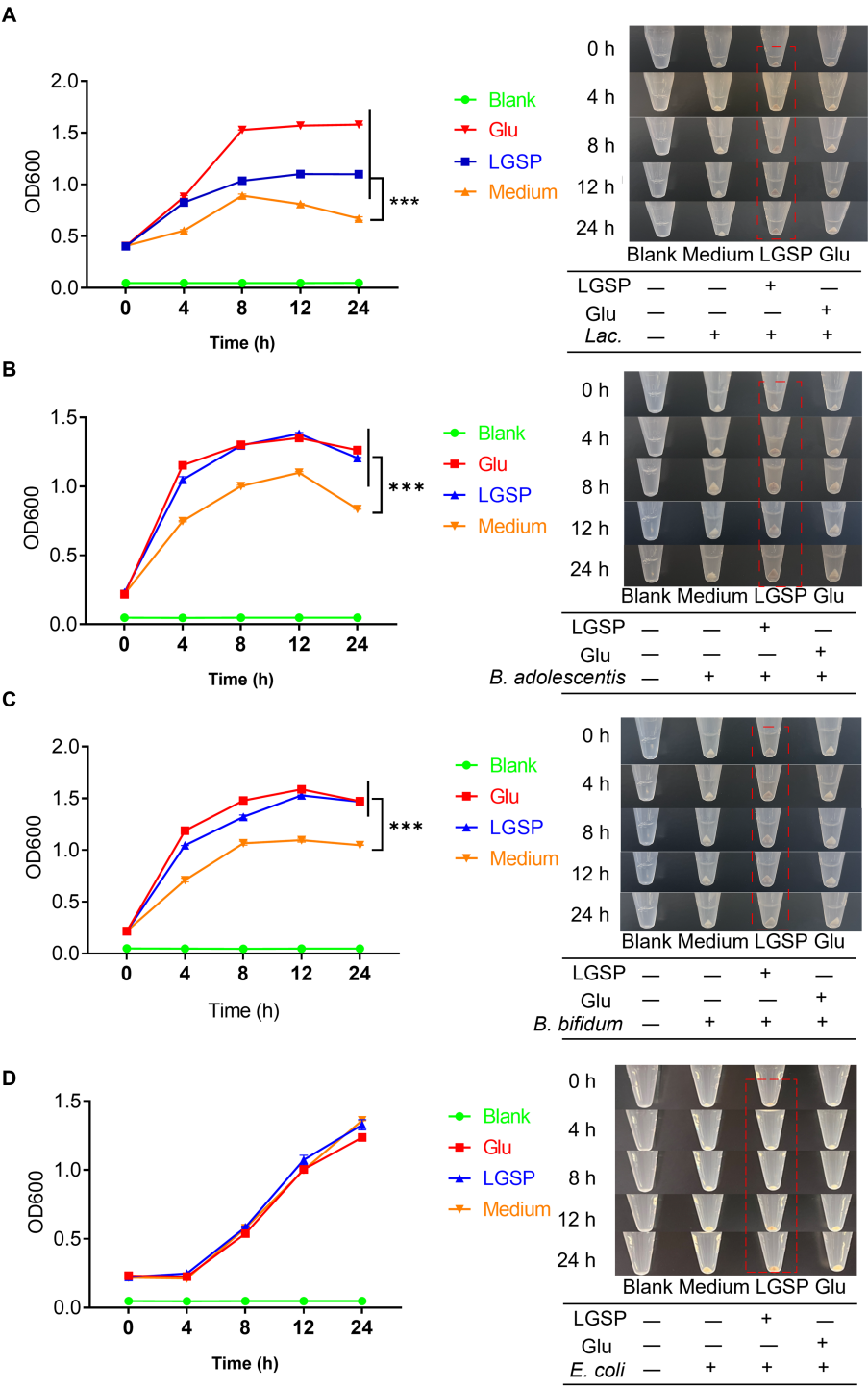


FIGURE 9
LGSP promoted the growth of three probiotic bacteria strains. **(A)** Growth curve of *Lactobacillus* (*Lac.*); **(B)** Growth curve of *Bifidobacterium adolescentis* (*B. adolescentis*). **(C)** Growth curve of *Bifidobacterium bifidum* (*B. bifidum*). **(D)** Growth curve of *Escherichia coli* (*E. coli*). Glucose (*Glu*) was used as positive control. ****p* < 0.001 vs. Medium group.

49). Previously, *Bifidobacterium* have been shown to increase glutathione peroxidase (GSH-Px) and glutathione (GSH) levels, reduce liver oxidative stress, while also reducing the expression of anti-inflammatory factors, reducing liver damage caused by ALD and ALD-associated intestinal dysbiosis (50, 51). In addition, *Lactobacillus* intake attenuates hepatic steatosis and liver injury, significantly reduces serum alanine aminotransferase (ALT) and aspartate transaminase (AST) levels, and

ameliorates hepatic lipid droplet accumulation (28). Interestingly, *Lactobacillus* also has the effect of regulating intestinal bacteria (28). Therefore, modulating gut microbiota by applying probiotics such as *Bifidobacterium* and *Lactobacillus* has been regarded as promising therapeutic strategy for handling ALD and other liver diseases. In this study, we found that LGSP could remarkably promote the growth of *Bifidobacterium* and *Lactobacillus*, displaying prebiotic effect. The

results provide evidence for understanding the polysaccharides as an active fraction of LGS to treat ALD. Furthermore, as the predominant pectin polysaccharide found in plants, HG-type pectin polysaccharides have the functions of regulating the intestinal microbiome and modulating the secretion of anti-inflammatory factors (52, 53). The finding that LGSP contains high content of GalA may suggest the potential association of typical structure of LGSP with its prebiotic effect. Although the starch fraction of LGS was removed during the extraction of LGSP, resistant starch (NMR signals showing T- α -D-Glc as well as 1,4- α -D-Glc) has been detected in LGSP. Resistant starch has also been investigated with prebiotic effect. Thus, the resistant starch in LGSP may also contribute to its prebiotic effect.

The main limitation of current study is that the anti-inflammatory and prebiotic effects of LGSP have not been validated *in vivo*. How these positive effects contribute to the anti-ALD effect of LGS warrants further investigation. Polysaccharides, polyphenols, flavonoids and others are mainly included in LGS, among which LGSP accounts for a high proportion (17.94 ± 0.28 mg/mL). The results of this study would help support the market use of LGS as a functional beverage and open up possible research directions (e.g., mechanisms of action and effective components) in the future.

Conclusion

Multiple fingerprint profiling combined with composition quantification for quality evaluation of LGSP was established based on HPSEC, PMP-HPLC, FT-IR and NMR. The quality consistency of different batches of LGSP was assessed. The molecular weight distribution, monosaccharide contents and structural characteristics of LGSP were obtained. LGSP demonstrated anti-oxidant, anti-inflammatory and prebiotic effects, which correlated well with its structures. The results of current study would gain better understanding towards the structure of LGSP, provide guidance for the quality control, and support for the treatment of ALD by the active polysaccharide fraction of LGS.

Data availability statement

The original contributions presented in the study are included in the article/supplementary material, further inquiries can be directed to the corresponding authors.

Ethics statement

Ethical approval was not required for the studies on humans in accordance with the local legislation and institutional requirements because only commercially available established cell lines were used.

References

1. Wei S, Jiang Y, Li M, Zhao L, Wang T, Wei M, et al. Chemical profiling and quality evaluation of Liuweizhiji Gegen-Sangshen oral liquid by UPLC-Q-TOF-MS and HPLC-diode array detector fingerprinting. *Phytochem Anal.* (2024) 35:860–72. doi: 10.1002/pca.3333
2. Lu KH, Liu CT, Raghu R, Sheen LY. Therapeutic potential of chinese herbal medicines in alcoholic liver disease. *J Tradit Complement Med.* (2012) 2:115–22. doi: 10.1016/s2225-4110(16)30084-0
3. Zhang H, Wei Z, Tong Y, Song X, Li S, Sun Y, et al. Spectrum-effect relationship study to reveal the pharmacodynamic substances in Flos Puerariae-semen Hoveniae medicine pair for the treatment of alcohol-induced liver damage. *J Ethnopharmacol.* (2023) 314:116628. doi: 10.1016/j.jep.2023.116628
4. Chen J, Wang X, Xia T, Bi Y, Liu B, Fu J, et al. Molecular mechanisms and therapeutic implications of dihydromyricetin in liver disease. *Biomed Pharmacother.* (2021) 142:111927. doi: 10.1016/j.biopha.2021.111927

Author contributions

SW: Writing – original draft, Formal analysis, Investigation, Validation. ML: Formal analysis, Investigation, Validation, Writing – original draft. LZ: Formal analysis, Investigation, Validation, Writing – original draft. TW: Formal analysis, Validation, Writing – review & editing. KW: Formal analysis, Validation, Writing – review & editing. JY: Formal analysis, Validation, Writing – review & editing. MT: Formal analysis, Writing – review & editing. YZ: Formal analysis, Writing – review & editing. JS: Formal analysis, Writing – review & editing, Validation. FD: Formal analysis, Validation, Writing – review & editing. YC: Formal analysis, Validation, Writing – review & editing. SD: Formal analysis, Validation, Writing – review & editing. ZX: Writing – review & editing, Resources. MW: Resources, Writing – review & editing, Project administration. ZL: Writing – review & editing, Conceptualization, Funding acquisition, Supervision. XW: Conceptualization, Funding acquisition, Supervision, Writing – review & editing, Project administration, Writing – original draft.

Funding

The author(s) declare that financial support was received for the research, authorship, and/or publication of this article. The present study was financially supported by the Sichuan Science and Technology Program, China (Grant No.: 2023NSFSC0614 and 2022YFS0624), the Luzhou Science and Technology Program, China (Grant No.: 2022-YJY-127, 2022YFS0624-B1, 2022YFS0624-C1 and 2022YFS0624-B3), the grant from Sichuan Province Administration of Traditional Chinese Medicine (Grant No.: 2023zd008 and 2024MS219) and SCU-Luzhou Platform Construction of Scientific and Technological Innovation (Grant No. 2022CDLZ-20).

Conflict of interest

The authors declare that the research was conducted in the absence of any commercial or financial relationships that could be construed as a potential conflict of interest.

Publisher's note

All claims expressed in this article are solely those of the authors and do not necessarily represent those of their affiliated organizations, or those of the publisher, the editors and the reviewers. Any product that may be evaluated in this article, or claim that may be made by its manufacturer, is not guaranteed or endorsed by the publisher.

5. Cao W, Wu J, Zhao X, Li Z, Yu J, Shao T, et al. Structural elucidation of an active polysaccharide from *Radix Puerariae lobatae* and its protection against acute alcoholic liver disease. *Carbohydr Polym.* (2024) 325:121565. doi: 10.1016/j.carbpol.2023.121565
6. Zhu XM, Xu R, Wang H, Chen JY, Tu ZC. Structural properties, bioactivities, and applications of polysaccharides from okra [*Abelmoschus esculentus* (L.) Moench]: a review. *J Agric Food Chem.* (2020) 68:14091–103. doi: 10.1021/acs.jafc.0c04475
7. Yin M, Zhang Y, Li H. Advances in research on Immunoregulation of macrophages by plant polysaccharides. *Front Immunol.* (2019) 10:145. doi: 10.3389/fimmu.2019.00145
8. Xue H, Hao Z, Gao Y, Cai X, Tang J, Liao X, et al. Research progress on the hypoglycemic activity and mechanisms of natural polysaccharides. *Int J Biol Macromol.* (2023) 252:126199. doi: 10.1016/j.ijbiomac.2023.126199
9. Chen R, Liu B, Wang X, Chen K, Zhang K, Zhang L, et al. Effects of polysaccharide from *Pueraria lobata* on gut microbiota in mice. *Int J Biol Macromol.* (2020) 158:740–9. doi: 10.1016/j.ijbiomac.2020.04.201
10. Yang Y, Li M, Wang Q, Huang H, Zhao Y, Du F, et al. *Pueraria lobata* starch regulates gut microbiota and alleviates high-fat high-cholesterol diet induced non-alcoholic fatty liver disease in mice. *Food Res Int.* (2022) 157:111401. doi: 10.1016/j.foodres.2022.111401
11. Wang Y, Zheng Y, Liu Y, Shan G, Zhang B, Cai Q, et al. The lipid-lowering effects of fenugreek gum, hawthorn pectin, and burdock inulin. *Front Nutr.* (2023) 10:1149094. doi: 10.3389/fnut.2023.1149094
12. Huang Y, Xie W, Tang T, Chen H, Zhou X. Structural characteristics, antioxidant and hypoglycemic activities of polysaccharides from *Mori Fructus* based on different extraction methods. *Front Nutr.* (2023) 10:1125831. doi: 10.3389/fnut.2023.1125831
13. Deng Q, Wang X, Chen H, Zhao C, Gong X, Zhou X. Structural characterization, modification and hepatoprotective effects of polysaccharide from *Mori Fructus*. *Int J Biol Macromol.* (2020) 153:357–63. doi: 10.1016/j.ijbiomac.2020.02.300
14. Zeng H, Miao S, Zheng B, Lin S, Jian Y, Chen S, et al. Molecular structural characteristics of polysaccharide fractions from *Canarium album* (Lour.) Raeusch and their antioxidant activities. *J Food Sci.* (2015) 80:H2585–96. doi: 10.1111/1750-3841.13076
15. Shu Y, He D, Li W, Wang M, Zhao S, Liu L, et al. Hepatoprotective effect of *Citrus aurantium* L. against APAP-induced liver injury by regulating liver lipid metabolism and apoptosis. *Int J Biol Sci.* (2020) 16:752–65. doi: 10.7150/ijbs.40612
16. Zou W, Dong Y, Yang S, Gong L, Zhang Y, Shi B, et al. Imperatae rhizoma-Hedyotis diffusa Willd. Herbal pair alleviates nephrotic syndrome by integrating anti-inflammatory and hypolipidaemic effects. *Phytomedicine.* (2021) 90:153644. doi: 10.1016/j.phymed.2021.153644
17. Chen YW, Hu DJ, Cheong KL, Li J, Xie J, Zhao J, et al. Quality evaluation of lentianin injection produced in China. *J Pharm Biomed Anal.* (2013) 78:79:176–82. doi: 10.1016/j.jpba.2013.02.012
18. Wang W, Liu X, Wang L, Song G, Jiang W, Mu L, et al. *Ficus carica* polysaccharide extraction via ultrasound-assisted technique: structure characterization, antioxidant, hypoglycemic and immunomodulatory activities. *Ultrason Sonochem.* (2023) 101:106680. doi: 10.1016/j.ultrsonch.2023.106680
19. Jing P, Zhao SJ, Lu MM, Cai Z, Pang J, Song LH. Multiple-fingerprint analysis for investigating quality control of *Flammulina velutipes* fruiting body polysaccharides. *J Agric Food Chem.* (2014) 62:12128–33. doi: 10.1021/jf504349r
20. Su LL, Li X, Guo ZJ, Xiao XY, Chen P, Zhang JB, et al. Effects of different steaming times on the composition, structure and immune activity of *Polygonatum* polysaccharide. *J Ethnopharmacol.* (2023) 310:116351. doi: 10.1016/j.jep.2023.116351
21. Sun X, Wang H, Han X, Chen S, Zhu S, Dai J. Fingerprint analysis of polysaccharides from different *Ganoderma* by HPLC combined with chemometrics methods. *Carbohydr Polym.* (2014) 114:432–9. doi: 10.1016/j.carbpol.2014.08.048
22. Li CY, Chen HY, Liu WP, Rui W. Multi-fingerprint profiling combined with chemometric methods for investigating the quality of *Astragalus* polysaccharides. *Int J Biol Macromol.* (2019) 123:766–74. doi: 10.1016/j.ijbiomac.2018.11.037
23. Zhi F, Yang TL, Wang Q, Jiang B, Wang ZP, Zhang J, et al. Isolation, structure and activity of a novel water-soluble polysaccharide from *Dioscorea opposita* Thunb. *Int J Biol Macromol.* (2019) 133:1201–9. doi: 10.1016/j.ijbiomac.2019.04.087
24. Li H, Cao J, Wu X, Deng Y, Ning N, Geng C, et al. Multiple fingerprint profiling for quality evaluation of polysaccharides and related biological activity analysis of Chinese patent drugs: Zishen Yutai pills as a case study. *J Ethnopharmacol.* (2020) 260:113045. doi: 10.1016/j.jep.2020.113045
25. Zou C, Du Y, Li Y, Yang J, Zhang L. Preparation and in vitro antioxidant activity of lacquer polysaccharides with low molecular weights and their sulfated derivatives. *Int J Biol Macromol.* (2010) 46:140–4. doi: 10.1016/j.ijbiomac.2009.11.010
26. Wang H, Ma JX, Wu DM, Gao N, Si J, Cui BK. Identifying bioactive ingredients and antioxidant activities of wild *Sanguangporus* species of medicinal Fungi. *J Fungi.* (2023) 9:242. doi: 10.3390/jof9020242
27. He J, Xu Y, Chen H, Sun P. Extraction, structural characterization, and potential antioxidant activity of the polysaccharides from four seaweeds. *Int J Mol Sci.* (2016) 17:1988. doi: 10.3390/ijms17121988
28. Chen L, Yang P, Hu L, Yang L, Chu H, Hou X. Modulating phenylalanine metabolism by *L. acidophilus* alleviates alcohol-related liver disease through enhancing intestinal barrier function. *Cell Biosci.* (2023) 13:24. doi: 10.1186/s13578-023-00974-z
29. Hizo GH, Rampelotto PH. The impact of probiotic *Bifidobacterium* on liver diseases and the microbiota. *Life.* (2024) 14:239. doi: 10.3390/life14020239
30. Wang Y, Jin H, Dong X, Yang S, Ma S, Ni J. Quality evaluation of *Lycium barbarum* (wolfberry) from different regions in China based on polysaccharide structure, yield and bioactivities. *Chin Med.* (2019) 14:49. doi: 10.1186/s13020-019-0273-6
31. Wang S, Peng Y, Zhuang Y, Wang N, Jin J and Zhan Z. Purification, Structural analysis and cardio-protective activity of polysaccharides from *Radix Astragali*. *Molecules* (2023) 28:4167. doi: 10.3390/molecules28104167
32. Jiang XL, Ma GF, Zhao BB, Meng Y, Chen LL. Structural characterization and immunomodulatory activity of a novel polysaccharide from *Panax notoginseng*. *Front Pharmacol.* (2023) 14:1190233. doi: 10.3389/fphar.2023.1190233
33. Liu Y, Sun Y, Huang G. Preparation and antioxidant activities of important traditional plant polysaccharides. *Int J Biol Macromol.* (2018) 111:780–6. doi: 10.1016/j.ijbiomac.2018.01.086
34. Xu Y, Niu X, Liu N, Gao Y, Wang L, Xu G, et al. Characterization, antioxidant and hypoglycemic activities of degraded polysaccharides from blackcurrant (*Ribes nigrum* L.) fruits. *Food Chem.* (2018) 243:26–35. doi: 10.1016/j.foodchem.2017.09.107
35. Li X, Chen C, Leng A, Qu J. Advances in the extraction, purification, structural characteristics and biological activities of *Eleutherococcus senticosus* polysaccharides: a promising medicinal and edible resource with development value. *Front Pharmacol.* (2021) 12:753007. doi: 10.3389/fphar.2021.753007
36. Zhu R, Zhang X, Wang Y, Zhang L, Zhao J, Chen G, et al. Characterization of polysaccharide fractions from fruit of *Actinidia arguta* and assessment of their antioxidant and antitiglycated activities. *Carbohydr Polym.* (2019) 210:73–84. doi: 10.1016/j.carbpol.2019.01.037
37. Chiu CH, Chiu KC, Yang LC. Amelioration of obesity in mice fed a high-fat diet with Uronic acid-rich polysaccharides derived from *Tremella fuciformis*. *Polymers.* (2022) 14:1514. doi: 10.3390/polym14081514
38. Zhu J, Zhou H, Zhang J, Li F, Wei K, Wei X, et al. Valorization of polysaccharides obtained from dark tea: preparation, physicochemical, antioxidant, and hypoglycemic properties. *Food Secur.* (2021) 10:2276. doi: 10.3390/foods10102276
39. Wu H, Min T, Li X, Li L, Lai F, Tang Y, et al. Physicochemical properties and antioxidant activities of acidic polysaccharides from wampee seeds. *Int J Biol Macromol.* (2013) 59:90–5. doi: 10.1016/j.ijbiomac.2013.04.020
40. Zeng J, Li M, Zhao Q, Chen M, Zhao L, Wei S, et al. Small molecule inhibitors of ROR γ t for Th17 regulation in inflammatory and autoimmune diseases. *J Pharm Anal.* (2023) 13:545–62. doi: 10.1016/j.jpba.2023.05.009
41. Zou M, Hu X, Wang Y, Wang J, Tang F, Liu Y. Structural characterization and anti-inflammatory activity of a pectin polysaccharide HBHP-3 from *Houttuynia cordata*. *Int J Biol Macromol.* (2022) 210:161–71. doi: 10.1016/j.ijbiomac.2022.05.016
42. Chang S, Chen X, Chen Y, You L, Hileuskaya K. UV/H₂O₂-degraded polysaccharides from *Sargassum fusiforme*: purification, structural properties, and anti-inflammatory activity. *Mar Drugs.* (2023) 21:561. doi: 10.3390/md21110561
43. Zhang Y, Pan X, Ran S, Wang K. Purification, structural elucidation and anti-inflammatory activity in vitro of polysaccharides from *Smilax china* L. *Int J Biol Macromol.* (2019) 139:233–43. doi: 10.1016/j.ijbiomac.2019.07.209
44. Yang Y, Li M, Liu Q, Zhao Q, Zeng J, Wang Q, et al. Starch from *Pueraria lobata* and the amylose fraction alleviates dextran sodium sulfate induced colitis in mice. *Carbohydr Polym.* (2023) 302:120329. doi: 10.1016/j.carbpol.2022.120329
45. Pereira APA, Lauretti LBC, Alvarenga VO, Paulino BN, Angolini CFF, Neri-Numa IA, et al. Evaluation of fruta-do-lobo (*Solanum lycocarpum* St. hill) starch on the growth of probiotic strains. *Food Res Int.* (2020) 133:109187. doi: 10.1016/j.foodres.2020.109187
46. Wang L, Lian J, Zheng Q, Wang L, Wang Y, Yang D. Composition analysis and prebiotics properties of polysaccharides extracted from *Lepista sordida* submerged cultivation mycelium. *Front Microbiol.* (2022) 13:1077322. doi: 10.3389/fmicb.2022.1077322
47. Chen L, Zhu Y, Hou X, Yang L, Chu H. The role of gut Bacteria and Fungi in alcohol-associated liver disease. *Front Med.* (2022) 9:840752. doi: 10.3389/fmed.2022.840752
48. Ki SH, Park O, Zheng M, Morales-Ibanez O, Kolls JK, Bataller R, et al. Interleukin-22 treatment ameliorates alcoholic liver injury in a murine model of chronic-binge ethanol feeding: role of signal transducer and activator of transcription 3. *Hepatology.* (2010) 52:1291–300. doi: 10.1002/hep.23837
49. Li H, Wang Y, Shao S, Yu H, Wang D, Li C, et al. *Rabdosia* *Serra* alleviates dextran sulfate sodium salt-induced colitis in mice through anti-inflammation, regulating Th17/Treg balance, maintaining intestinal barrier integrity, and modulating gut microbiota. *J Pharm Anal.* (2022) 12:824–38. doi: 10.1016/j.jpba.2022.08.001
50. He Q, Yang C, Kang X, Chen Y, Zhang T, Zhang H, et al. Intake of *Bifidobacterium lactis* ProBio-M8 fermented milk protects against alcoholic liver disease. *J Dairy Sci.* (2022) 105:2908–21. doi: 10.3168/jds.2021-21265
51. Zhou F, Jiang X, Wang T, Zhang B, Zhao H. *Lycium barbarum* polysaccharide (LBP): a novel prebiotics candidate for *Bifidobacterium* and *Lactobacillus*. *Front Microbiol.* (2018) 9:1034. doi: 10.3389/fmicb.2018.01034
52. Wu Y, Zhou H, Wei K, Zhang T, Che Y, Nguyễn AD, et al. Structure of a new glycyrrhiza polysaccharide and its immunomodulatory activity. *Front Immunol.* (2022) 13:1007186. doi: 10.3389/fimmu.2022.1007186
53. Wu Y, Wu C, Che Y, Zhang T, Dai C, Nguyễn AD, et al. Effects of Glycyrrhiza polysaccharides on Chickens' intestinal health and homeostasis. *Front Vet Sci.* (2022) 9:891429. doi: 10.3389/fvets.2022.891429

Glossary

ALD	alcoholic liver disease
Ara	arabinose
ALT	alanine aminotransferase
AST	aspartate transaminase
BSA	bovine serum albumin
DMSO	dimethyl sulfoxide
FBS	fetal bovine serum
FT-IR	fourier transform infrared spectroscopy
Gal	galactose
GaIA	galacturonic acid
Glc	glucose
GlcA	glucuronic acid
GSH	glutathione
GSH-Px	glutathione peroxidase
HG	homogalacturonic acid
HPAEC-PAD	high performance anion exchange chromatography-pulsed amperometric detector
HPSEC	high-performance size exclusion chromatography
LGS	Liuweizhiji Gegen-Sangshen beverage
LGSP	LGS polysaccharide
LPS	lipopolysaccharide
Man	mannose
MR	molar ratio
MTT	5-diphenyltetrazolium bromide
NMR	nuclear magnetic resonance
OD	optical density
PMP-HPLC	1-phenyl-3-methyl-5-pyrazolone-HPLC
Rha	rhamnose
RG-I	rhamnosegalacturonic acid glycans I
SD	standard deviation
TFA	trifluoroacetic acid
UHPLC	ultra-high performance liquid chromatography
Xyl	xylose



OPEN ACCESS

EDITED BY

Yun Deng,
Shanghai Jiao Tong University, China

REVIEWED BY

Javier Carballo,
University of Vigo, Spain
Xia Qiang,
Ningbo University, China

*CORRESPONDENCE

Rosaria Marino
✉ rosaria.marino@unifg.it

RECEIVED 24 June 2024

ACCEPTED 25 July 2024

PUBLISHED 23 August 2024

CITATION

Marino R, Albenzio M, della Malva A, Racioppo A, Speranza B and Bevilacqua A (2024) Valorization of fish from the Adriatic Sea: nutritional properties and shelf life prolongation of *Aphia minuta* through essential oils. *Front. Nutr.* 11:1454228. doi: 10.3389/fnut.2024.1454228

COPYRIGHT

© 2024 Marino, Albenzio, della Malva, Racioppo, Speranza and Bevilacqua. This is an open-access article distributed under the terms of the [Creative Commons Attribution License \(CC BY\)](#). The use, distribution or reproduction in other forums is permitted, provided the original author(s) and the copyright owner(s) are credited and that the original publication in this journal is cited, in accordance with accepted academic practice. No use, distribution or reproduction is permitted which does not comply with these terms.

Valorization of fish from the Adriatic Sea: nutritional properties and shelf life prolongation of *Aphia minuta* through essential oils

Rosaria Marino*, Marzia Albenzio, Antonella della Malva, Angela Racioppo, Barbara Speranza and Antonio Bevilacqua

Department of Agriculture, Food, Natural Resources, and Engineering (DAFNE), University of Foggia, Foggia, Italy

This study aimed to exploit the nutritional and microbiological qualities of *Aphia minuta*, which are still largely unknown; they are collected from Golfo di Manfredonia (Adriatic Sea). Chemical composition, fatty acids, and amino acid profiles were evaluated during winter, spring, and summer (two samples each season). The protein content was highest in spring, while no significant differences were found for fat and ash contents across all sampling periods. Fatty acid profile analyses revealed that monounsaturated and polyunsaturated fatty acids were affected by the sampling season. Notably, the value of n-3 polyunsaturated fatty acids increased in spring and summer compared to the winter season. The highest content of essential amino acids was measured during the spring and summer seasons ($P < 0.01$), with leucine and lysine being the most dominant. Regardless of the fishing season, from a nutritional point of view, this species is an excellent source of bioactive compounds. This study also focused on the microbiological quality and shelf life of *Aphia minuta*. Initially, the bioactivity of three different essential oils (thymol, lemon, and citrus extract) was tested on *Pseudomonas fluorescens*, *Staphylococcus aureus*, and *Escherichia coli*. These essential oils were then combined with various packaging materials (conventional, maize starch, and polylactate) and packaging atmosphere (air, vacuum, and a modified atmosphere with reduced oxygen content). The results indicated that combining citrus extract with vacuum packaging significantly reduced the psychrotrophic viable count to undetectable levels after 7 days. This study suggests some important considerations for exploiting and expanding the market of the *Aphia minuta*.

KEYWORDS

Aphia minuta, n-3 fatty acids, essential amino acids, essential oils, shelf life

1 Introduction

Aphia minuta (1) is a small neretic pelagic species, reaching a maximum size of 6 cm. It belongs to the Gobiidae family, one of the largest groups of fish in coastal marine waters. This species has a transparent or whitish-reddish body, compressed laterally, with chromatophores along the base of the median fin and on the head. It is found throughout the northeastern Atlantic region, from the western Baltic and Norway to Morocco and the Mediterranean and Black Seas (2). This species is highly valued in the Mediterranean region for its taste, making it a thriving business.

In Italy, the *Aphia minuta* fishery, referred to as “Rossetto,” has a long history and represents one of the most important small-scale activities; it is usually caught by small-scale fleets disseminated throughout the Ligurian Sea (3), Tyrrhenian Sea (4), Adriatic Sea (5, 6), and around the coast of Sicily and Sardinia (7, 8). Particularly, catches are about 160 tons per year, most of them in the southern Adriatic, and the fishing fleet comprises about 400 vessels (8).

It is known that fish provide significant amounts of bioavailable nutrients such as proteins, lipids, and micronutrients such as vitamins, iron, selenium, or zinc with well-recognized health benefits (9). In particular, fish are a good source of long-chain polyunsaturated fatty acids, supporting human health through various metabolic functions. In order to harness the potential of any food item to its fullest extent, its nutritional composition must be known. This is particularly important in the case of fish, which represent a large biodiversity with varieties of species and consequent differences in nutritional composition. To date, no studies are available on the nutritional properties of *Aphia minuta*; most studies on this fish concern the growth and reproduction aspects (5, 8, 10).

The high water activity, neutral pH, high content of low molecular weight molecules, and cold-adapted microbial flora make fish highly perishable. As a result, traditional fish preservation methods (salting, drying, and freezing) drastically reduce water activity. However, consumers now prefer fresh food that has been minimally processed. Many consumers perceive the use of synthetic preservatives as a potential health risk, so the use of natural preservatives is being investigated (11). Essential oils (EOs) are aromatic extracts (mainly terpenes and other aromatic compounds) of whole plants or specific parts of plants whose bioactive components confer biological properties (antioxidants, insecticides, antimicrobials, and so on). These properties depend on the plant and many other factors (agronomy, plant part, extraction process, application process). The solubility of the EO and the type of bacteria (gram-negative bacteria are more resistant than gram-positive bacteria) strongly influence the antimicrobial properties; furthermore, the food matrix can interfere with the activity of the EO (12). EOs are valued for food preservation because they are natural products; many are widely used and historically safe, and their addition to foods is part of the current trend toward clean labeling.

Several authors have demonstrated significant antimicrobial and antioxidant effects of various EOs. The efficacy of EOs depends on chemical structure, concentration, comparison of antimicrobial spectrum with target microorganisms, interactions with food matrix, and method of application (13). Regarding the food matrix, some authors have suggested that the fat level in fish may affect the efficacy of essential oils, as some essential oils have been reported to be more effective in low-fat fish (cod) than in fatty fish (salmon). Several systems have been tested for the application of EO to fish: (i) direct application to the food, such as dipping or direct application, (ii) as part of an active packaging, such as vapor phase application (14), or (iii) film packaging embedded in edible coatings (chitosan, starch, gelatin, blends, and others) with varying degrees of emulsification (nanoemulsions). The latter two allow a gradual release of the active compound and are more effective than direct application (12). Cooling combined with vacuum or modified atmosphere packaging are the most commonly used technologies

in combination with EO to preserve fish. In this context, the use of essential oils/natural extracts, combined with packaging and modified atmosphere, could be a promising strategy to promote and valorize *Aphia minuta* commercialization.

Therefore, the main aims of this research were as follows:

- a) Nutritional characterization (chemical composition, fatty acids, and amino acid profile) of *Aphia minuta* from the Adriatic Sea and its compositional changes throughout the fishing season;
- b) Preliminary optimization of packaging, treatment with natural compounds, and storage conditions are needed to increase the shelf-life and promote the diffusion of this product in other regions.

2 Materials and methods

2.1 Study area and sample collection

Aphia minuta was collected in five specific areas (A, B, C, D, and E, Figure 1), located along the Gulf of Manfredonia, at different distances from the coast and with different natures of the seabed or surrounding biocenoses. The more abundant samples of *Aphia minuta* were collected in B, D, and E areas. **Area A** was chosen near the coast, 2.5 km from the southwestern limit of Mattinata Bay, and is characterized by dense meadows of *Cymodocea nodosa* on a sandy-muddy bottom, up to a depth of 7–9 meters. **Area B** is ~5 km from the coast, with depths between 11 and 13 m. The bottom is predominantly inconsistent but characterized by the presence of mud and bio-constructions. **Area C**, about 6 km away from the port of Manfredonia and 3 km at the closest point to the coast, has a depth of 11–13 m, a muddy bottom, and small formations of scattered bio-constructions. **Area D** is ~4.4 miles away, transverse from the coast, and ~14.3 miles from the port of Manfredonia, with depths between 18 and 20 m. It is featured by coral formations of limited development and detrital beds; the samplings were carried out only along the mud/sandy channels present among the environments mentioned. **Area E** concerns the Maërl and Rodoliti funds, overlooking the Saline di Margherita di Savoia.

The Gulf of Manfredonia is located along the Italian coast of the Adriatic Sea in the Apulia region. Many factors contribute to determining the oceanographic characteristics of the Gulf of Manfredonia, such as the WAC (Western Adriatic Current), which is powered by northeast winds and moves the water masses along the Italian coasts in a north vs. south direction. The climate of the area is temperate Mediterranean with alternating dry and rainy seasons. In the last 10 years, rainfall has not exceeded 700 mm/year, which determines the accumulation of nutrients in the river basin. In the event of torrential rains, large quantities of nutrient-rich water are discharged into the gulf, which can cause local eutrophication. Due to its physiographic characteristics, the Gulf of Manfredonia is characterized by shallow, low hydrodynamic, and very productive waters. The abundance of phytoplankton in the area is the basis of the high fish density.

According to the fishing season of the South Adriatic Sea and the current guidelines in Italy (Council Regulation No 1967/2006),



FIGURE 1
Five specific sampling areas (A, B, C, D, and E) of *Aphia Minuta* located along the Gulf of Manfredonia. Map Data: Google Earth ©2021/ Data SIO, NOAA, U.S. Navy, NGA, GEBCO.

samples were collected at each site at six different times of the year ($n = 30$): two sampling in winter (in January and February), two in spring (at March and April), and two sampling in Summer (at June and July). During each sampling, local fishing vessels from 10 to 40 m depth on the seabed follow the seasonal migrations and shoaling of *Aphia minuta*. A small meshed semipelagic trawl with three concentric bags coded from 16 to 5 mm (stretched) mesh size was used for the sampling. The chemical-physical parameters of the seawater were also recorded for each catch. At every sampling point, the samples of *Aphia minuta* were placed in self-draining polystyrene boxes, packed in flake ice, and delivered to the laboratory on the same day.

2.2 Nutritional analyses

2.2.1 Chemical composition and fatty acid methyl esters profile

Fish samples were homogenized using a laboratory blender and frozen at -20°C until the subsequent analysis. The grounded mass was used as the representative sample for the analyses, and the results were expressed as a particular content/edible portion (EP).

Moisture, protein, lipid, and ash contents were performed according to AOAC methods (15), and all the chemical determinations were performed in triplicate.

The analysis for the determination of fatty acid composition was performed according to the method of O'Fallon et al. (16) with some modifications as previously described by Marino et al. (17). Briefly, 1 g of each sample was placed into a screw cap Pyrex reaction tube, added with 5.3 mL of MeOH, 0.7 mL of 10 N KOH in water, and 0.5 mg of C13:0/mL of the internal standard. Then, the tubes were incubated in a water bath at 55°C for 90 min, with handshaking for 5 s every 20 min. After incubation, the tubes were

cooled to room temperature, and subsequently, 580 μL of 24 N H_2SO_4 were added. After cooling, 3 mL of hexane was added into each tube, vortexed, and then centrifuged at $500 \times g$ (Eppendorf 5810 R, Hamburg, Germany) for 5 min at 21°C . The hexane layer containing the fatty acids methyl esters (FAME) was collected and transferred into a gas-chromatographic vial. The fatty acid profile was quantified through an Agilent 6890 N instrument (Agilent Technologies, Santa Clara, CA, USA) equipped with an HP-88 fused-silica capillary column (length 100 m, internal diameter 0.25 mm, film thickness 0.25 μm). Operating conditions were as follows: carrier gas (helium) at a constant flow of 1 mL/min; split-splitless injector at 260°C ; split ratio 1:25; injected sample volume 1 μL ; FID detector at 260°C . The temperature program of the column was 5 min at 100°C , then increased to 240°C ($3.5^{\circ}\text{C}/\text{min}$) and held for 15 min. The retention time and area of each peak were computed using the 6890 N NETWORK GC system software. Fatty acids were identified by comparing their retention times with the fatty acid methyl standards (FIM-FAME-7-Mix, Matreya LLC, Pleasant Gap PA, USA), added of C18:1-11t, C18:2-9c,11t, C18:2-9c, 11c, C18:2-9t, 11t, and C18:2-10t, 12c (Matreya LLC, Pleasant Gap PA, USA). The fatty acid concentration was expressed as g fatty acids/100 g total fatty acids. Nutritional indices such as PUFA/SFA, n6/n3, % EPA+DHA, atherogenic and thrombogenic indices, and fish lipid quality were calculated according to Marino et al. (18).

All the chemical and fatty acid determinations were performed in triplicate.

2.2.2 Amino acid determination

Amino acid extraction was carried out according to Marino et al. (19). Briefly, 20 mg of freeze-dried samples were placed in hydrolysis tubes with 500 μL of 6 M HCl. Tubes were sealed under vacuum and placed in a ventilated oven at 160°C for 75 min.

Hydrolyzed samples were filtered through Whatman 0.45 µm filters, and filtered solutions were diluted 1:10 with ultrapure water before being submitted to automated online derivatization and injection. The HPLC system consisted of an Agilent 1260 Infinity Series chromatograph (Agilent Technologies, Santa Clara, CA, USA) equipped with a binary pump (G1312B), a diode-array detector (1315C), and a fluorescence detector (G1321B). The analyses were performed using a Zorbax Eclipse AAA column (150 × 4.6 mm i.d., 3.5 µm particles; Agilent Technologies, Palo Alto, CA, USA). Individual amino acid peaks were identified by comparing their retention times with those of standards. Results for amino acids were expressed as mg/100 g meat. Amino acid determinations were performed in triplicate.

2.3 Microbiological analyses

2.3.1 Determination of antimicrobial activity of essential oils *in vitro*

Thymol (Sigma, Pool, UK), citrus extract (Biocitro, Probenza s.l., Zaragoza, Spain), and lemon extract (Spencer Food Industrial, Amsterdam, The Netherlands) were tested to evaluate their antimicrobial activity against three specific spoilage microorganisms. Stock solutions (200–300–400–500 mg/L) of thymol were prepared in water-ethanol (1:1), while the other compounds were dissolved in distilled water. All solutions were freshly prepared before each use and sterilized by filtering through membranes (0.20 µm; Sartorius, Goettingen, Germany). The strains used were *Pseudomonas fluorescens* DSM 50090 purchased from a Public Collection (Deutsche Sammlung von Mikroorganismen und Zellkulturen), *Staphylococcus* spp., and *Escherichia coli* belonging to the culture collection of the Laboratory of Predictive Microbiology, University of Foggia. The microorganisms were stored at –20°C in nutrient broth (Oxoid, Milan, Italy) added with 33% sterile glycerol and grown under aerobic conditions in nutrient broth at 25°C for 48 h for *P. fluorescens* and at 37°C for 24 h for both strains. The effectiveness of natural compounds against fish spoilage microorganisms was determined by inhibition zone assays inoculating the substrates with 1 ml of cell suspension (10⁶ CFU/mL). For each natural compound, 0.1 mL of the active solutions, for each concentration, was poured into wells (9 mm diameter) previously cut with a sterilized cork-borer into the agar medium. The plates inoculated with *P. fluorescens* were incubated at 25°C for 48 h, while those with *Staphylococcus* spp. and *E. coli* were incubated at 37°C for 24 h. As a control for the antimicrobial activity of thymol, 0.1 ml of a water-ethanol (1:1) solution was poured into wells; for the other active compounds, 0.1 ml of distilled water was used. After incubation, the inhibition diameter was measured in three directions, and the average was tabulated. Three replications of this experiment were made.

2.3.2 Challenge test in model system

Agar diskettes containing technical agar No. 3 (Oxoid, Milan) and 2% meat extract (Beef Extract, Oxoid) were used to simulate a fish filet model system. Before use, *P. fluorescens* and *E. coli* strains

were grown in nutrient broth and incubated at 25°C for 48 h and 37°C for 24 h, respectively. The microorganisms were centrifuged at 4,000 × g for 10 min, the supernatant was discarded, and the pellet was suspended in a sterile saline solution (0.9% NaCl). After two dilutions of the stock solution, 200 µL of cell suspension was added to a test tube containing liquid agar and meat extract (19 mL; 55°C) and 1 mL of a 2 g/L citrus extract. Immediately after inoculation, the agar solution was put in Petri dishes and left to dry for 1 h; the concentration of citrus extract in the final sample was 100 mg/L, while the microorganisms were 3 log CFU/g. Samples were stored at 37°C for *E. coli* and 25°C for *P. fluorescens* and analyzed after 24, 48, and 72 h. Agar pieces (20 g) were taken and diluted in 180 mL of saline solution in a Stomacher bag (Seward, London, England), then homogenized for 1 min in a Seward Stomacher Lab Blender 400. Serial dilutions of the homogenates were inoculated on nutrient agar and incubated at 37°C for 24 h (*E. coli*) or 25°C for 48–72 h (*P. fluorescens*). All tests were performed in duplicate over two different batches. Samples not containing the citrus extract but inoculated with the test microorganisms were used as a control.

2.3.3 Influence of citrus extract and different packages on the microbial stability of *Aphia minuta*

Aphia minuta samples were dipped for 5 min in a 100 mg/L citrus extract solution; after treatment, excess liquid was removed by air drying under a laminar flow hood. Samples immersed in distilled water were used as controls. Then, the samples were packaged in three different kinds of packaging materials: Nylon/Polyethylene bags (95 µm, Tecnovac, San Paolo D'Argon, Bergamo, Italy) using S100-Tecnovac equipment were 170 mm × 250 mm long, with O₂ permeability of 50.65 cm³/m² day atm and a water vapor transmission rate of 1.64 g/m² day, as specified by the manufacturer; PLA polylactic bags [OTR: 45*10³ cc/(m²*day)]; corn starch based [OTR: 45*10³ cc/(m²*day)] under three conditions: (A) under vacuum (UV); (B) ordinary Atmosphere (AO); and (C) modified atmosphere (65% N₂-30% CO₂-5% O₂; MA). Samples were stored at 4°C for 7 days and periodically analyzed as described in the following. All analyses were conducted twice.

For microbiological analyses, the following media were used: plate count agar (PCA) incubated at 5°C for 1 week and at 30°C for 48 h under aerobic conditions for psychrophilic microorganisms and total bacteria count, respectively; Baird Parker Agar Base, supplemented with Egg Yolk supplement, for coagulase-positive staphylococci; *Pseudomonas* agar base (PAB) supplemented with *Pseudomonas* CFC supplement, incubated at 25°C for 48 h for *Pseudomonadaceae*; Violet Red Bile Glucose Agar (VRBGA) incubated at 37°C for 24 h for *Enterobacteriaceae*. All the media and the supplements were sourced from Oxoid (Milan, Italy).

2.4 Statistic

Nutritional properties data were subjected to analysis of variance (ANOVA) using the GLM procedure of the SAS statistical software (20). The mathematical model included the fixed effect of

TABLE 1 Chemical composition (%) of *Aphia minuta* as affected by the sampling season (means \pm SEM).

	Sampling season				Effect, <i>P</i>
	Winter (<i>n</i> = 10)	Spring (<i>n</i> = 10)	Summer (<i>n</i> = 10)	SEM	
Moisture	79.70 ab	78.85 b	80.91 a	0.45	**
Fat	1.20	1.14	0.98	0.12	NS
Protein	15.86 ab	16.09 a	14.66 b	0.32	**
Ash	3.09	3.66	3.10	0.18	NS

NS, not significant.

***P* < 0.01.

Letters indicate significant differences in a row.

sampling season and random residual error. All effects were tested for statistical significance (to *P* < 0.05), and significant effects were reported in tables. When significant differences were found (at *P* < 0.05 unless otherwise noted), Tukey's test was performed for multiple comparisons among means.

For microbiological studies, significant differences were pointed out through a *t*-test for paired comparison, while ANOVA was used for the challenge test, using the time, the packaging and modified atmosphere, and treatment (control vs. dipping in citrus extract) as categorical predictors.

3 Results and discussion

3.1 Chemical composition and fatty acid profile

The chemical composition of *Aphia minuta* as affected by sampling season is shown in Table 1. No significant differences were found for fat and ash contents during the seasons, remaining relatively stable throughout the year (0.98–1.20 and 3.19–3.66% for fat and ash, respectively). A significant seasonal variation concerning protein (14.56–16.09%) and moisture content (78.85–80.91%) was noticed. Higher protein content was found in spring (*P* < 0.01) compared to the other seasons, while moisture content in this season showed the lowest content (*P* < 0.01). The highest value of protein observed in spring coincides with the high feeding period of *Aphia minuta*, as there is a peak in the primary production (planktonic blooms) during spring and summer. Particularly, *Aphia minuta* has a diet consisting of zooplankton (decapods, crustaceans, copepods, and cirripedes), a protein source.

The composition of *Aphia minuta*'s fatty acids during the winter, spring, and summer seasons is shown in Table 2. The percentage of saturated fatty acids (SFA) did not change during the winter, spring, and summer seasons, while monounsaturated and polyunsaturated fatty acid content was affected by sampling season (*P* < 0.05 and *P* < 0.01, respectively). Monounsaturated fatty acids (MUFA) were higher in winter compared to the percentage found in spring and summer seasons, with the highest content of oleic acid (*P* < 0.01). The content of polyunsaturated fatty acids (PUFA) was the highest in spring and summer. Particularly during summer, *Aphia minuta* showed the lowest content of n-6 PUFA and the highest content of n-3 PUFA. In contrast, the highest content of n-6 and the lowest content of n-3 PUFA were found in the winter. Among n-3 PUFAs, linolenic, eicosapentaenoic (EPA; C20:5 n-3),

docosapentaenoic (DPA; C22:5 n-3), and docosaeasenoic (DHA; C22:5 n-3) fatty acids showed a higher value (*P* < 0.01) in spring and summer compared to the winter season.

As reported in a previous study, the fatty acid composition of fish varies throughout the year due to factors such as the fish's life cycle and external influences, such as their food's temperature, salinity, and fatty acid composition (21). The seasonal changes in the fatty acid profile observed in *Aphia minuta* are consistent with variations observed in European sardine (*Sardina pilchardus*), which show the highest levels of PUFA and n-3 PUFA during intensive feeding in the summer season (22). In particular, European sardine is recognized as a highly nutritious and important species of Mediterranean Sea fisheries (23). It is popular for its rich of long-chain polyunsaturated fatty acids. The n-3 PUFA levels found in *Aphia minuta* are higher than those reported in sardines.

Regardless of the sampling season, it is worth noting that in *Aphia minuta*, the content of palmitic acid (C16:0) was lower than other little fishes of the Adriatic Sea. In particular, previous studies reported palmitic acid as the most abundant fatty acid in sardine in anchovy and picarel (24). On the contrary, in the *Aphia minuta*, the fatty acids with the highest percentages were DHA and EPA, resulting in 88% of the total polyunsaturated fatty acids. This is an important result from a nutritional point of view because n-3 eicosapentaenoic (EPA) and docosahexaenoic (DHA) fatty acids are essential for human development and have different beneficial effects on human health, performing important anti-inflammatory and antithrombotic functions and playing a very important role in the prevention and treatment of coronary heart disease (25). In contrast, palmitic acids are positively associated with a risk of atherosclerosis and other cardiovascular diseases.

The positive effects of n-3 PUFA on human health are related to the actual dietary intake of n-3 PUFA. In the present study, 100 g of *Aphia minuta* provided nearly 1,800 mg of EPA+ DHA. On a quantitative basis, the values of this fish accounted for 90% of the recommended intake of long-chain (LC) n-3 PUFA [2g EPA+ DHA per day; (26)]. Thus, *Aphia minuta* can be considered a high source of n-3 and a very good choice of fish all year round.

Based on the fatty acid profile, nutritional indices were calculated (Table 3). Samples of *Aphia minuta* collected in spring and in summer showed higher values of P/S (*P* < 0.05), EPA+DHA percentage (*P* < 0.01), and fish lipid quality index (*P* < 0.05) than samples collected during the winter season, while n-6/n-3 was the lowest in summer sampling (*P* < 0.05). This result confirms that *Aphia minuta* fished in spring and summer had better nutritional

TABLE 2 Fatty acid profile (%) of *Aphia minuta* as affected by the sampling season (means ± SEM).

	Sampling season			SEM	Effect, <i>P</i>
	Winter (<i>n</i> = 10)	Spring (<i>n</i> = 10)	Summer (<i>n</i> = 10)		
C12:0	0.05	0.05	0.11	0.05	NS
C14:0	3.31	2.98	3.53	0.19	NS
C15:0	0.63	0.55	0.54	0.10	NS
C16:0	14.80	14.84	14.27	0.28	NS
C17:0	1.43	1.38	1.55	0.12	NS
C18:0	4.15	3.96	3.95	0.15	NS
C21:0	0.34	0.25	0.31	0.06	NS
Other SFA	0.49	0.36	0.49	0.05	NS
SFA	25.20	24.37	24.75	0.45	NS
C16:1	3.80	3.34	3.75	0.18	NS
C17:1	0.11	0.13	0.10	0.03	NS
C18:1t9	0.16	0.11	0.15	0.03	NS
C18:1c9	5.32 a	4.55 b	3.95 b	0.31	*
C20:1	0.26	0.25	0.30	0.05	NS
Other MUFA	0.42	0.19	0.18	0.09	NS
MUFA	10.08 a	8.57 b	8.43 b	0.41	*
C18:2t9t12	0.07	0.05	0.05	0.03	NS
C18:2c9c12	0.94	0.89	0.91	0.11	NS
C20:2n6	5.58 a	5.24 ab	4.75 b	0.25	**
C20:3n6	0.01	0.03	0.02	0.01	NS
C20:4n6	0.64 a	0.50 b	0.48 b	0.02	**
C22:2n6	0.04	0.02	0.05	0.02	NS
C18:3n3	0.84 b	1.28 a	1.32 a	0.15	**
C20:3n3	0.05 b	0.13 a	0.16 a	0.02	*
C20:5n3 (EPA)	16.80 b	17.63 a	17.75 a	0.23	**
C22:6n3 (DHA)	39.74 b	41.27 a	41.32 a	0.25	***
n6	7.28 a	6.74 ab	6.26 b	0.19	**
n3	57.43 b	60.31 a	60.55 a	0.28	**
PUFA	64.71 a	67.05 b	66.81 b	0.31	**

NS, not significant.
**P* < 0.05.
***P* < 0.01.
****P* < 0.001.
Other SFA = C 20:0, C22:0, C23:0, C24:0; other MUFA = C 14:1, C15:1, C22:1, C24:1.
Letters indicate significant differences in a row.

properties. It has been demonstrated that FAs play positive or negative roles in the prevention and treatment of diseases; in the last years, many studies (18, 27) have been addressed to evaluate the nutritional value of fatty acids and to explore their potential usage in disease prevention and treatment to accurately select appropriate indices.

The n-6/n-3 ratio is an important index for determining the quality of fat, as a higher amount of n-6 fatty acids promotes the

pathogenesis of many diseases, including cancer, inflammatory, and autoimmune diseases, whereas increased levels of n-3 PUFA exert suppressive effects (28). Reducing the ratio of n-6/n-3 fatty acids in the human diet was essential to help prevent coronary heart disease and reduce the risk of cancer (28). In the current study, the ratio of n-6/n-3 fatty acids found in *Aphia minuta* ranged from 0.10 to 0.13; this value is much lower compared to previous studies (29) and to the threshold value (<4) indicated by the World Health

TABLE 3 Nutritional indices of *Aphia minuta* as effected by the sampling season (means \pm SEM).

	Sampling season			SEM	P, effect
	Winter (n = 10)	Spring (n = 10)	Summer (n = 10)		
P/S	2.57 b	2.75 a	2.70 a	0.05	*
n6/n3	0.13 a	0.11 ab	0.10 b	0.01	*
Atherogenic index (AI)	0.38	0.35	0.38	0.04	NS
Thrombogenic index (TI)	0.12	0.11	0.11	0.04	NS
EPA+DHA (%)	56.54 b	58.90 a	59.07 a	0.18	**
Fish lipid quality (FQL)	224.38 b	241.74 a	238.67 a	1.55	*

NS, not significant.

*P < 0.05.

**P < 0.01.

***P < 0.001.

AI = (C12:0 + 4 × C14:0 + C16:0)/(MUFA + Σ n6 + Σ n3).

TI = (C14:0 + C16:0 + C18:0)/[(0.5 × MUFA) + (0.5 × Σ n-6 PUFA) + (3 × Σ n-3 PUFA) + (Σ n-3 PUFA/ Σ n-6 PUFA)].

FLQ = 100 × (C20:5n-3 + C22:6n-3)/(Σ Saturated Fatty Acids).

Letters indicate significant differences in a row.

Organization (WHO). Similarly, Atherogenic and Thrombogenic indices ranged from 0.35 to 0.38 and from 0.11 to 0.12, respectively, showing values much lower than the threshold values (atherogenic index <0.5 and thrombogenic index <1.0) suggested as desirable to minimize the risks of cardiovascular diseases.

3.2 Amino acids

Next to providing essential fatty acids, fish is a source of high-quality proteins; particularly, fish protein is considered a complete source of protein, as it is only the protein source that contains a well-balanced amino acid composition that has eight essential and eight non-essential amino acids (30).

The amino acid composition of *Aphia minuta* during the winter, spring, and summer seasons is shown in Table 4. The highest content of essential amino acids was measured during the spring and summer ($P < 0.01$), with leucine and lysine being the most dominant amino acids. Essential amino acids are basic in the diet, particularly for certain populations with specific needs, such as those of children and sick and old people. In particular, leucine can stimulate the synthesis of muscle protein, while lysine has been shown to improve growth performance in the body (31).

The highest value was found in spring ($P < 0.05$) related to the total amino acid content. This result is consistent with the highest protein percentage found in this season. It is worth noting that *Aphia minuta* showed a very high percentage of essential amino acids/total amino acids, ranging from 58.4 to 62.7%, with the highest ratio in summer ($P < 0.05$). Furthermore, *Aphia minuta* has a high arginine content; being a functional amino acid, it plays an important role in the regulation of metabolic pathways to improve health, survival, growth, development, lactation, and reproduction of the organisms (32). These results highlight that the amino acid content of the *Aphia minuta* has many similarities with the amino acid profile of sardines (22), which is a rich source of essential and functional amino acids.

3.3 Microbiology

The antimicrobial activity of the three natural compounds at different concentrations (200–500 mg/L) was measured against three well-defined fish spoilage/pathogen bacteria, used as targets for the following reasons: *P. fluorescens*, such as all pseudomonads, is among the most resistant strains to EOS, while *E. coli* and *Staphylococcus* spp. are hygiene indicators. The diameter of the growth inhibition zone (measured in mm) was used as the criterion for antimicrobial activity. Table 5 shows the inhibitory effect of the active compounds on the growth of the target strains. The inhibitory effect of thymol was not observed against *Staphylococcus* spp., whereas for citrus and lemon extracts, the zone of inhibition was between 2 and 2.5 mm at all concentrations tested. For *P. fluorescens* and *E. coli*, at the lowest concentrations (200–300 mg/L) of citrus and lemon extracts, the inhibition zone was around 1.5–2 mm, without statistically significant differences between the compounds used. On the other hand, thymol concentrations up to 500 mg/L were required to obtain the same antibacterial activity.

The antibacterial activity of citrus and lemon extract was concentration-independent, as their antibacterial activity did not increase proportionally with increasing concentrations. In fact, against *Staphylococcus* spp. and *E. coli*, the inhibitory effect of these natural compounds was independent of the concentration, and the diameter of the inhibition zone was ~2–2.5 mm by using 200, 300, 400, or 500 mg/L. The trend of thymol was different from the other active compounds; the inhibition zone was very low, up to 300 mg/L, while at the highest concentration, an inhibition diameter of about 1.5 mm was recorded. Thymol is one of the most known and widely studied EO, extracted among others from *Thymus vulgaris* and *Ocimum gratissimum* and with a variety of biological functions (antimicrobial, anti-inflammatory, antioxidant, antimutagenic, larvicidal, analgesic, and radioprotective effects) (33). Although many authors in the past suggested a higher sensitivity of Gram-negative microorganisms (34, 35), the results hereby collected confirm the findings of the meta-analysis of Speranza et al. (36), who found a strong resistance of some Gram-negative bacteria, mainly those belonging to *E. coli* species and *Pseudomonas* genus.

TABLE 4 Aminoacids composition (mg/100 g fish) of *Aphia minuta* as affected by the sampling season (means \pm SEM).

	Sampling season			SEM	Effect, <i>P</i>
	Winter (<i>n</i> = 10)	Spring (<i>n</i> = 10)	Summer (<i>n</i> = 10)		
Arginine	969.6	977.7	936.6	22.3	NS
Histidine	452.4	395.1	382.0	24.7	NS
Threonine	924.2	995.4	949.2	44.7	NS
Valine	876.7	946.6	906.9	38.9	NS
Methionine	713.3	746.9	744.2	22.6	NS
Phenylalanine	629.2	688.7	696.6	31.3	NS
Isoleucine	740.5	839.0	849.7	42.8	NS
Leucine	1,622.2 B	1,852.7 a	1,938.3 a	66.5	*
Lysine	1,865.5 B	2,079.0 a	2,159.0 a	77.5	**
Aspartate	1,551.0	1,618.5	1,634.5	63.5	NS
Glutamate	2,112.4	2,170.6	2,275.6	76.5	NS
Serine	571.9	536.5	504.6	55.6	NS
Glycine	722.7	682.2	641.5	45.8	NS
Alanine	908.8	990.4	1,100.5	48.7	NS
Tyrosine	618.7	553.4	536.3	31.5	NS
Cystein	336.5	247.3	263.0	25.5	NS
Proline	391.3	480.5	404.4	22.5	NS
AAT	15,056.8 B	16,104.4	15,242.8 b	250.5	*
EAAT	8,793.4 B	9,521.2 a	9,562.5 a	99.5	**
NEAAT	7,213.4	7,279.2	7,360.3	68.8	NS
EAA/NEAA	1.2	1.3	1.3	0.3	NS
%EA/AAT	58.4 B	59.1 b	62.7 a	0.65	*

Letters indicate significant differences in a row.

NS, not significant.

* $P < 0.05$.

** $P < 0.01$.

*** $P < 0.001$.

AAT, amino acid total; EAAT, essential amino acid total; NEAAT, non-essential amino acid total.

On the other hand, the antimicrobial activity recorded by citrus and lemon extracts confirms the potentiality of oils and active components extracted from *Citrus* spp.; some authors reported in the past the ability to eradicate several *Pseudomonas* and/or *E. coli* strains by different mechanisms, including among others the disturbance of quorum sensing, biofilm eradication, or affecting cell surface hydrophobicity (37–39).

Based on these findings, lemon and citrus extracts were regarded as promising antimicrobials for the second step, but lemon extract was not used in the second phase of the experiment because its antimicrobial activity was not reproducible due to its variable and complex composition; in fact, some preliminary analyses by authors revealed that its antimicrobial activity changed as a function of the batch used. Furthermore, the organoleptic impact on the matrix should not be underestimated when using essential oils. Therefore, based on the preliminary results, the citrus extract was chosen for the next steps, as the commercial preparation used is less organoleptically harmful, as also found by authors for other applications. Thus, a solution of citrus extract at

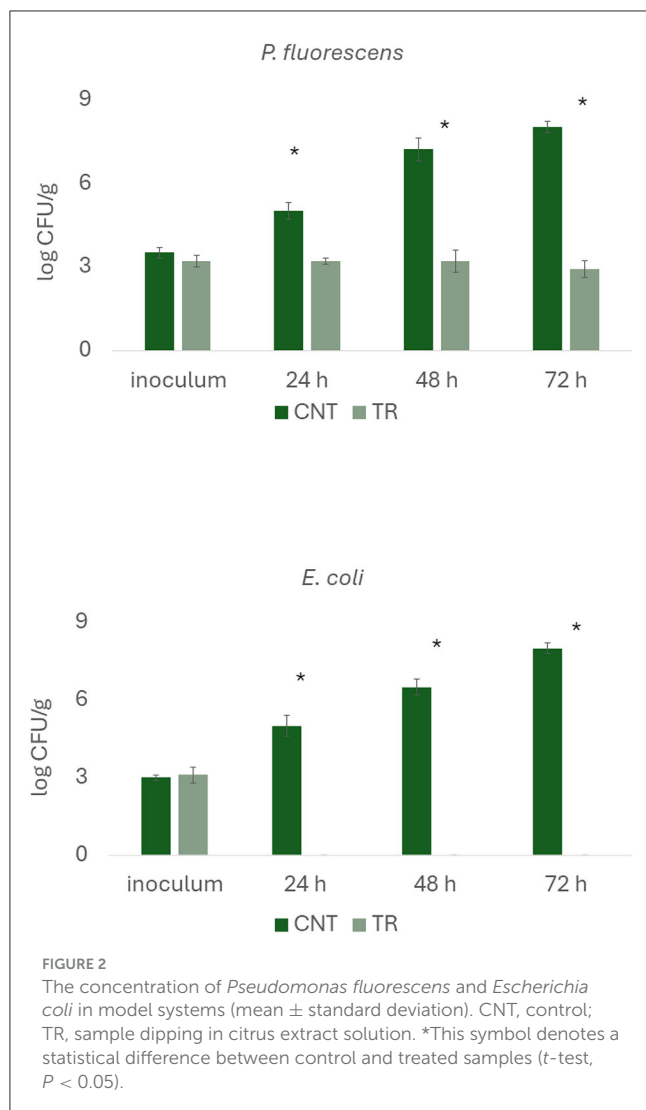
200 mg/L was chosen to study the antimicrobial efficacy on the development kinetics of the two target microorganisms. The test was conducted in a model system at this stage on two representative microorganisms of spoiling (*P. fluorescens*) and pathogenic (*E. coli*) microbiota. In the citrus extract sample, the concentration of *P. fluorescens* was about 3 log CFU/g throughout time, while in the control, the concentration increased from 3.5 to 8.0 log CFU/g after 72 h. As for *E. coli*, the pathogen was already below the detection threshold after 24 h, while the cellular concentration of the microbial target in the control sample was 8.1 log CFU/g after 72 h (Figure 2). These results suggest a possible bacteriostatic effect of citrus extract against *Pseudomonas* spp. and a bactericidal effect against *E. coli*.

The difference between the two test strains, at least for the action on the growth/death kinetic, confirms the possibility that an EO could act differently, depending on various conditions, but mainly due to the characteristics of the external layers. In the case of *E. coli*, several authors postulated different modes of action. For example, Álvarez-Ordóñez et al. (40) found that a

TABLE 5 Inhibition effects of natural compounds tested against *Pseudomonas fluorescens*, *Staphylococcus* spp., and *Escherichia coli*.

Natural compound	Target strain	Diameter of the zones of inhibition (mm)			
		200 mg/L	300 mg/L	400 mg/L	500 mg/L
Thymol	<i>Pseudomonas fluorescens</i>	0.87 ± 0.12	0.93 ± 0.06	1.17 ± 0.06	1.40 ± 0.17
	<i>Staphylococcus</i> spp.	-	-	-	-
	<i>Escherichia coli</i>	0.63 ± 0.06	0.73 ± 0.06	1.10 ± 0.20	1.13 ± 0.15
Citrus extract	<i>Pseudomonas fluorescens</i>	1.30 ± 0.40	1.60 ± 0.12	2.00 ± 0.00	2.20 ± 0.20
	<i>Staphylococcus</i> spp.	2.30 ± 0.17	2.20 ± 0.17	2.20 ± 0.20	2.13 ± 0.15
	<i>Escherichia coli</i>	2.90 ± 0.10	1.80 ± 0.12	2.00 ± 0.00	2.03 ± 0.06
Lemon extract	<i>Pseudomonas fluorescens</i>	1.60 ± 0.00	1.77 ± 0.25	1.93 ± 0.12	2.13 ± 0.12
	<i>Staphylococcus</i> spp.	2.50 ± 0.00	2.43 ± 0.12	2.23 ± 0.25	2.67 ± 0.29
	<i>Escherichia coli</i>	2.00 ± 0.00	2.00 ± 0.00	2.07 ± 0.12	2.00 ± 0.00

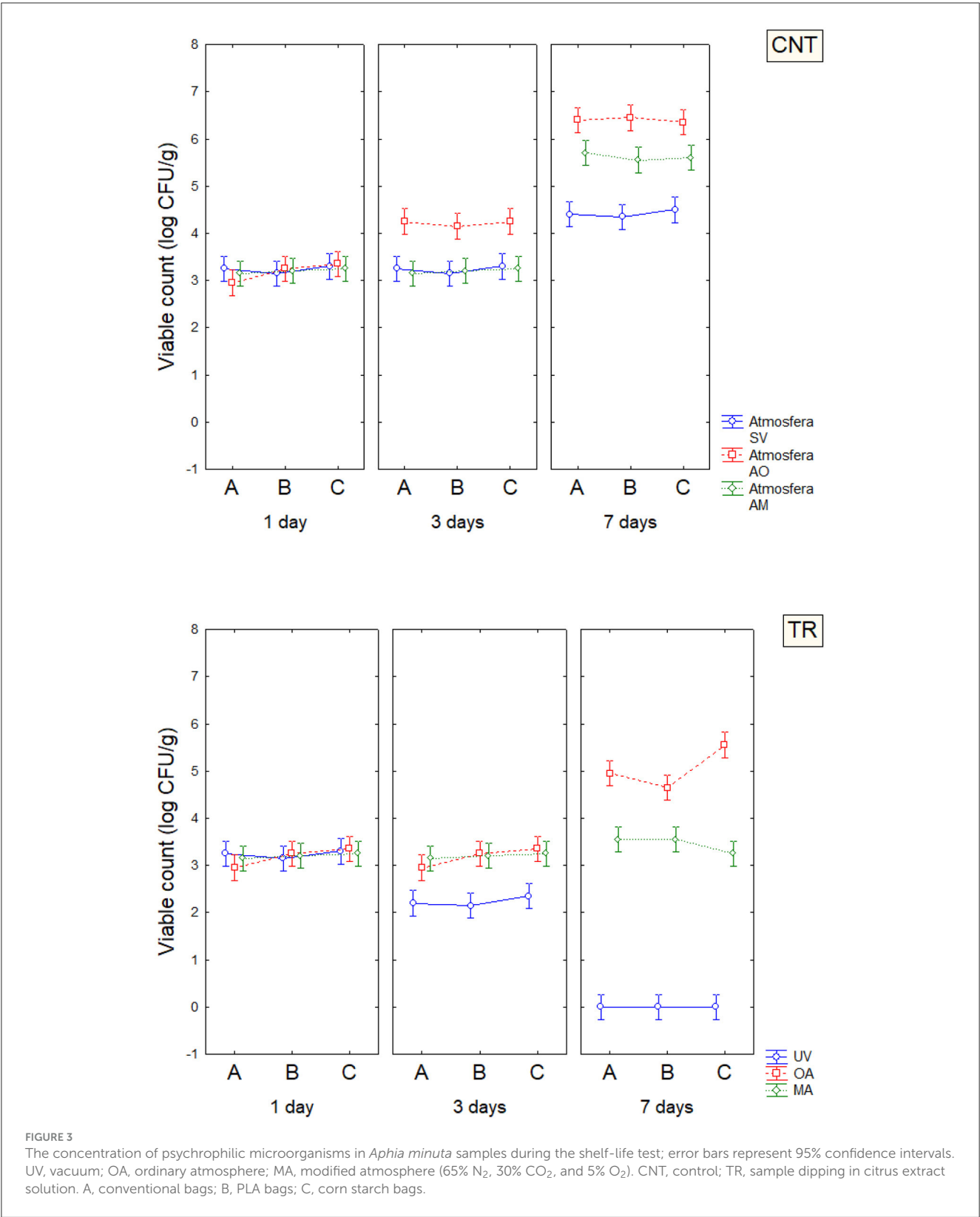
The mean values ± standard deviation.



commercial citrus extract determined the formation of pores with the leakage of cellular components due to the interaction with the carboxylic groups of the fatty acids of the membrane. On the

other hand, the same extract used in this study was tested by de Nova et al. (41), who also found a morphological alternation of the cell envelope. These changes, along with possible changes in the hydrophobicity of the cell surface (38), would have been responsible for the bactericidal effect on *E. coli*. In the case of *Pseudomonas* spp., different mechanisms have been postulated, but the most important ones are the reduction of cell motility and the disturbance of cell-to-cell communication, which could determine a delay rather than inactivation (42).

Based on the results obtained in the model system, a shelf-life test was carried out. Enterobacteriaceae, staphylococci, and SSO contamination were random and variable, neither affected by treatment conditions nor packaging, as many samples were below the detection limit. On the other hand, psychrophilic microorganisms showed consistent developmental kinetics that were responsive to the input variables and allowed accurate assessment of the microbiological quality of the product; this result is of concern, as it is well-known that psychrophilic microorganisms are limiting for the quality and the shelf life of fish (43–45). Data on the cellular concentration of psychrophilic microorganisms in *Aphia minuta* samples during the shelf-life test are shown in Figure 3. In the control samples, there was an increase in the concentration of psychrophilic microorganisms over time (4–6 log CFU/g), which was mainly dependent on the type of storage atmosphere, as after 7 days the samples UV-packed showed a significantly lower viable count (4.2–4.5 vs. 6.2–6.5 log CFU/g in AO samples); these results are probably because pseudomonads represent a significant proportion of psychrophilic microbiota in fish (46), and the removal of oxygen could exert a detrimental effect as they are aerobic. Under vacuum, the citrus extract exerted a biocidal effect, as the target microbes were below the detection threshold after 7 days, due probably to the combination of oxygen removal and the antimicrobial effect of EO. To better understand the effects of the variables, MANOVA modeled the data; the table of standardized effects shows that all predictors were significant as single terms but with different statistical weights (Table 6). The most significant predictor variable was the dipping treatment (*F*-test, 926.44), followed by the storage atmosphere (*F*-test, 569.86), storage time (*F*-test, 301.25), and packaging type (*F*-test, 4.39). In addition,



statistical analysis showed the significance of some interactive terms (in order of statistical weight: dipping treatment*storage time, storage atmosphere*storage time, storage atmosphere*dipping treatment, storage atmosphere*dipping treatment*storage time). Estimating the quantitative effects of predictors is possible by decomposing the statistical hypothesis, which does not show real

trends but the mathematical correlation of each predictor vs. the dependent variable. Figures 4, 5 show the decomposition of the statistical hypothesis for the individual effects of predictors (storage atmosphere, treatment). As expected, the most effective storage atmosphere was UV (2.7 log CFU/g), followed by MA (3.6 log CFU/g), and finally, AO (4.3 log CFU/g; Figure 4). Regarding the effect of the treatment (Figure 5), the cell concentration of

psychrophilic microorganisms was 4.1 log CFU/g in the control and 3.1 log CFU/g in the treated sample, indicating a very strong quantitative effect.

4 Conclusion

This study provides valuable insights into the nutritional values, fatty acid and amino acid profiles, and the shelf life of *Aphia minuta* collected from the Adriatic Sea.

Aphia minuta is a rich source of n-3 fatty acids and amino acids. It has the highest content of n-3 fatty acids and essential amino acids during spring and summer. Additionally, it maintains a very high content of eicosapentaenoic and docosahexaenoic fatty acids throughout the year. These acids are essential for human development and offer various beneficial effects on human health.

Concerning the microbiological quality, psychrophilic microbiota could present an issue. However, combining natural antimicrobial compounds and packaging could be a valuable strategy to prolong the shelf life. Experiments conducted in the model system suggest that the effect of the citrus extract could be either bacteriostatic or bactericidal, depending on the target microorganisms. Nevertheless, this is a promising strategy. Specifically, the combination of UV packaging and dipping in a citrus extract solution at 100 mg/L inhibited the growth of psychrophilic microorganisms, reducing their viable count below the detection limit after 7 days. However, the packaging material did not exert a significant effect under the conditions used in this research.

TABLE 6 Standardized effects of packaging, dipping in citrus extract solution (treatment), storage time, and atmosphere.

Variable	Fisher test
{1} Packaging	4.39
{2} Storage atmosphere	560.86
{3} Treatment	926.44
{4} Storage time	301.25
Packaging-Storage atmosphere	-
Packaging-Treatment	-
Storage atmosphere-Treatment	92.38
Packaging-Storage time	-
Storage atmosphere-Storage time	295.91
Treatment-Storage time	475.10
Packaging-Storage atmosphere-Treatment	-
Packaging-Storage atmosphere-Storage time	-
Packaging-Treatment-Storage time	-
Storage atmosphere-Treatment-Storage time	74.14
1-2-3-4	-

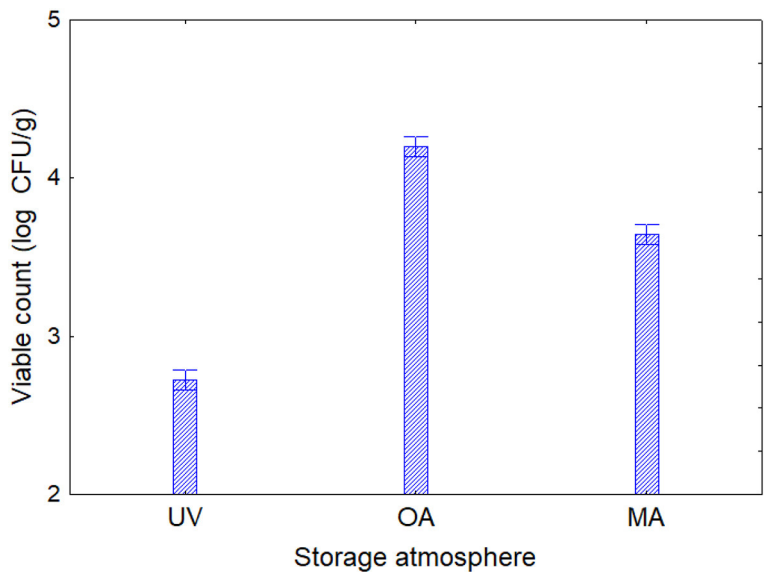


FIGURE 4
Decomposition of the statistical hypothesis for the effect of the storage atmosphere on the concentration of psychrophilic microorganisms during the shelf-life test. Error bars represent the 95% confidence interval. UV, vacuum; OA, ordinary atmosphere; MA, modified atmosphere (65% N₂, 30% CO₂, and 5% O₂).

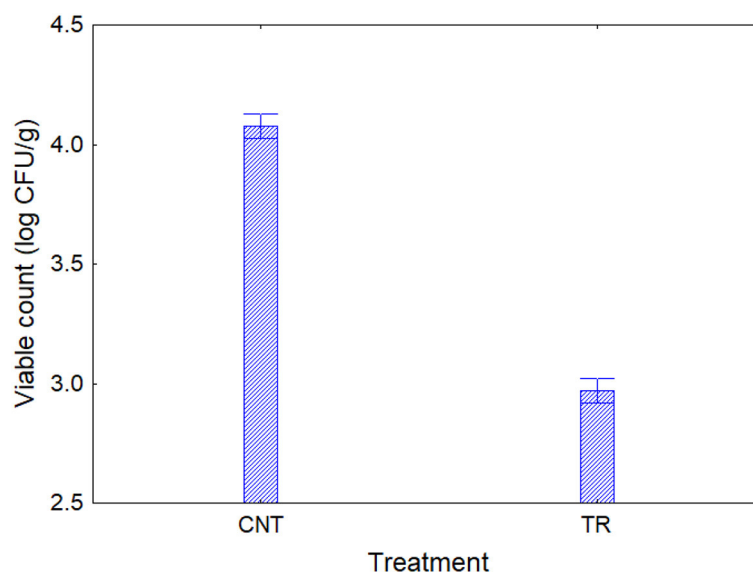


FIGURE 5

Decomposition of the statistical hypothesis for the treatment on the concentration of psychrophilic microorganisms during the shelf-life test. Error bars represent the 95% confidence interval. CNT, control sample; TR, sample dipping in the citrus extract solution.

In conclusion, the information and results reported in this study could be very useful for exploiting and expanding the market of the *Aphia minuta* and paving the way for new valorization strategies.

Investigation, Methodology, Project administration, Writing – review & editing.

Data availability statement

The data analyzed in this study is subject to the following licenses/restrictions. The datasets for this study are available upon request to interested researchers. Requests to access these datasets should be directed to RM, rosaria.marino@unifg.it.

Ethics statement

The animal study was approved by Institutional Animal Care and Use Committee of University of Foggia (protocol number: 006-2022). The study was conducted in accordance with the local legislation and institutional requirements.

Author contributions

RM: Conceptualization, Funding acquisition, Investigation, Methodology, Project administration, Writing – original draft, Writing – review & editing. MA: Supervision, Validation, Visualization, Writing – review & editing. AM: Formal analysis, Software, Writing – review & editing. AR: Formal analysis, Software, Writing – original draft. BS: Validation, Visualization, Writing – review & editing. AB: Conceptualization,

Funding

The author(s) declare financial support was received for the research, authorship, and/or publication of this article. This study was supported by Biologia ed ecologia del rossetto, *Aphia minuta* (pelagic goby, transparent goby) nel golfo di Manfredonia ed aspetti socio economici finanziato dalla Regione Puglia-bando PO FEAMP 2014/2020-Misura 1.26 | delibera n. 2018 del 25/11/2019.

Conflict of interest

The authors declare that the research was conducted in the absence of any commercial or financial relationships that could be construed as a potential conflict of interest.

The author(s) declared that they were an editorial board member of Frontiers, at the time of submission. This had no impact on the peer review process and the final decision.

Publisher's note

All claims expressed in this article are solely those of the authors and do not necessarily represent those of their affiliated organizations, or those of the publisher, the editors and the reviewers. Any product that may be evaluated in this article, or claim that may be made by its manufacturer, is not guaranteed or endorsed by the publisher.

References

- Risso A. *Ichthyologie de Nice, ou histoire naturelle des poissons du département des Alpes Maritimes, Paris* (1810). p. 388. doi: 10.5962/bhl.title.7052
- Miller PJ. In: Gobiidae PJP, Whitehead ML, Bauchot JC, Hureau J, Nielsen E, Tortonese A, editors. *Fishes of the North-Eastern Atlantic and the Mediterranean, Vol. III*. Paris: UNESCO (2021). p. 1019–85.
- Relini G, Palandri M, Relini F, Garibaldi G, Torchia C, Cima B, et al. Pesca sperimentale del rossetto in Liguria. *Biol Mar Medit*. (1998) 5:487–502.
- Auteri R, Baino A, Abella A. Biology and population dynamic of the transparent goby: a locally important resource of artisanal fisheries. *Biol Mar Medit*. (2000) 7:144–57.
- Ungaro N, Casavola N, Marano G, Rizzi E. Bianchetto and rossetto fry fisheries in the Manfredonia Gulf: effort exerted and catch composition. *Oebalia*. (1994) 20:99–106.
- Frogia C, La Mesa M, Arneri E, Gramitto ME. La pesca del rossetto nel compartimento marittimo di Pescara (Medio Adriatico). *Biol Mar Medit*. (1998) 5:503–12.
- Sanfilippo M, Pulicano G, Costa F, Manganaro A. Juvenile fish populations in two areas of the Sicilian coast. *Nat Rerum*. (2011) 1:43–50.
- La Mesa M, Arneri E, Caputo V, Iglesias M. The transparent goby, *Aphia minuta*: review of biology and fisheries of a paedomorphic European fish. *Rev Fish Biol Fish*. (2005) 15:89–109. doi: 10.1007/s11160-005-1613-4
- Ahern M, Thilsted SH, Oenema S, Barange M, Cartmill MK, Brandstrup SC, et al. *The Role of Aquatic Foods in Sustainable Healthy Diets*. UN Nutrition (2021). Available at: <https://www.unnnutrition.org>
- La Mesa M. Age and growth of *Aphia minuta* (Pisces, Gobiidae) from the central Adriatic Sea. *Sci Mar*. (1999) 63:147–55. doi: 10.3989/scimar.1999.63n2147
- Saleh EA, Al-Hawary II, Elnajar MM. Antibacterial and anti-oxidant activities of laurel oil against *Staphylococcus aureus* and *Pseudomonas fluorescens* in oreochromis niloticus fillets. *Slov Vet Res*. (2019) 55:313–9. doi: 10.26873/SVR-770-2019
- Calo JR, Crandall PG, O'Bryan CA, Ricke SC. Essential oils as antimicrobials in food systems—a review. *Food Control*. (2015) 54:111–9. doi: 10.1016/j.foodcont.2014.12.040
- Mei J, Ma X, Xie J. Review on natural preservatives for extending fish shelf life. *Foods*. (2019) 8:490. doi: 10.3390/foods8100490
- Navarro-Segura L, Ros-Chumillas M, Martinez-Hernandez GB, Lopez-Gomez A. A new advanced packaging system for extending the shelf life of refrigerated farmed fish fillets. *J Sci Food Agric*. (2020) 100:4601–11. doi: 10.1002/jsfa.10520
- Association of Official Analytical Chemists. *Official Methods of Analysis, Volume 2*. 16th ed. Arlington, VA: AOAC (1995).
- O'Fallon JV, Busboom JR, Nelson ML, Gaskins CT. A direct method for fatty acid methyl ester synthesis: application to wet meat tissues, oils, and feedstuffs. *J Anim Sci*. (2007) 85:1511–21. doi: 10.2527/jas.2006-491
- Marino R, della Malva A, De Palo P, Maggolino A, d'Angelo F, Lorenzo JM, et al. Nutritional profile of donkey and horse meat: effect of muscle and aging time. *Animals*. (2022) 12:746. doi: 10.3390/ani12060746
- Marino R, Caroprese M, della Malva A, Santillo A, Sevi A, Albenzio M. Role of whole linseed and sunflower seed on the nutritional and organoleptic properties of Podolian x Limousine meat. *Ital J Anim Sci*. (2024) 23:868–79. doi: 10.1080/1828051X.2024.2359588
- Marino R, Albenzio M, della Malva A, Muscio A, Sevi A. Nutritional properties and consumer preference of donkey bresaola and salami: comparison with conventional products. *Meat Sci*. (2015) 101:19–24. doi: 10.1016/j.meatsci.2014.11.001
- SAS Institute SAS Enterprise Guide: Statistics; Version 9.4. Cary, NC: SAS Institute Inc. (2013).
- Gokçe MA, Tasbozan O, Çelik M, Tabakoglu S. Seasonal variations in proximate and fatty acid compositions of female common sole (*Solea solea*). *Food Chem*. (2004) 88:419–23. doi: 10.1016/j.foodchem.2004.01.051
- Šimat V, Hamed I, Petricević S, Bogdanović T. Seasonal changes in free amino acid and fatty acid compositions of sardines, *Sardina pilchardus* (Walbaum, 1792): implications for nutrition. *Foods*. (2020) 9:867. doi: 10.3390/foods9070867
- Soldo B, Šimat V, Vlahović J, Skroza D, Ljubenkov I, Generalić Mekinić I. High quality oil extracted from sardine by-products as an alternative to whole sardines: production and refining. *Eur J Lipid Sci Technol*. (2019) 121:1800513. doi: 10.1002/ejlt.201800513
- Zlatanos S, Laskaridis K. Seasonal variation in the fatty acid composition of three Mediterranean fish-sardine (*Sardina pilchardus*), anchovy (*Engraulis encrasicolus*), and picarel (*Spicara smaris*). *Food Chem*. (2020) 10:725–8. doi: 10.1016/j.foodchem.2006.09.013
- Sarojinalini C, Hei A. *Fish as an Important Functional Food for Quality Life*. (2020). Available at: <https://www.intechopen.com/books/functional-foods> (accessed May 2, 2020).
- European Food Safety Authority. Panel on dietetic products, nutrition, and fatty acids, polyunsaturated fatty acids, monounsaturated fatty acids, trans fatty acids, and cholesterol. *EFSA J*. (2010) 8:1461. doi: 10.2903/j.efsa.2010.1461
- Dal Bosco A, Cartoni Mancinelli A, Vaudo G, Cavallo M, Castellini C, Mattioli S. Indexing of fatty acids in poultry meat for its characterization in healthy human nutrition: a comprehensive application of the scientific literature and new proposals. *Nutrients*. (2022) 4:3110. doi: 10.3390/nu14153110
- Simopoulos AP. The importance of the ratio of omega-6/omega-3 essential fatty acids. *Biomed. Pharmacother*. (2002) 56:365–79. doi: 10.1016/S0753-3322(02)00253-6
- Bandarra NM, Marçalo A, Cordeiro AR, Pousão-Ferreira P. Sardine (*Sardina pilchardus*) lipid composition: does it change after one year in captivity? *Food Chem*. (2018) 244:408–13. doi: 10.1016/j.foodchem.2017.09.147
- Dale HF, Madsen L, Lied GA. Fish-derived proteins and their potential to improve human health. *Nutr Rev*. (2019) 77:572–83. doi: 10.1093/nutrit/nuz016
- Mohanty B, Mahanty A, Ganguly S, Mitra T, Karunakaran D, Anandan R. Nutritional composition of food fishes and their importance in providing food and nutritional security. *Food Chem*. (2019) 30:561–70. doi: 10.1016/j.foodchem.2017.11.039
- Beaumier L, Castillo L, Yu YM, Ajami AM, Young VR. Arginine: new and exciting developments for an “old” amino acid. *Biomed Environ Sci*. (1996) 9:296–315.
- Zhang Y, Wang Y, Zhu X, Cao P, Wei S, Lu Y. Antibacterial and antibiofilm activities of eugenol from essential oil of *Syzygium aromaticum* (L.) Merr. & L. M. Perry (clove) leaf against periodontal pathogen *Porphyromonas gingivalis*. *Microb. Pathog*. (2017) 113:396–402. doi: 10.1016/j.micpath.2017.10.054
- Semeniuc CA, Pop CR, Rotar AM. Antibacterial activity and interactions of plant essential oil combinations against Gram-positive and Gram-negative bacteria. *J Food Drug Anal*. (2017) 25:403–38. doi: 10.1016/j.jfda.2016.06.002
- Nazzaro F, Fratianni F, De Martino L, Coppola R, De Feo V. Effect of essential oils on pathogenic bacteria. *Pharmaceuticals*. (2013) 6:1451–74. doi: 10.3390/ph6121451
- Speranza B, Bevilacqua A, Campaniello D, Altieri C, Corbo MR, Sinigaglia M. Minimal inhibitory concentrations of thymol and carvacrol: towards a unified statistical approach to find common trends. *Microorganisms*. (2023) 11:1174. doi: 10.3390/microorganisms11071774
- Luciardi MC, Amparo Blázquez M, Alberto MR, Cartagena E, Arena ME. Grapefruit essential oils inhibit quorum sensing of *Pseudomonas aeruginosa*. *Food Sci Technol Int*. (2020) 26:231–41. doi: 10.1177/1082013219883465
- Tang W, Zhang Z, Nie D, Liu S, Li Y, Liu M, et al. Selective antibacterial activity of Citrus medica limonum essential oil against *Escherichia coli* K99 and *Lactobacillus acidophilus* and its antibacterial mechanism. *LWT Food Sci Technol*. (2023) 186:115215. doi: 10.1016/j.lwt.2023.115215
- D'Almeida RE, Sued N, Arena ME. *Citrus paradisi* and *Citrus reticulata* essential oils interfere with *Pseudomonas aeruginosa* quorum sensing in vivo on *Caenorhabditis elegans*. *Phytomed Plus*. (2022) 2:100160. doi: 10.1016/j.phyplu.2021.100160
- Álvarez-Ordóñez A, Carvajal A, Arguello H, Martínez-Lobo FJ, Naharro G, Rubio P. Antibacterial activity and mode of action of a commercial citrus extract. *J Appl Microbiol*. (2013) 115:50–60. doi: 10.1111/jam.12216
- de Nova PJG, Carvajal A, Prieto M, Rubio P. In vitro susceptibility and evaluation of techniques for understanding the mode of action of a promising non-antibiotic citrus fruit extract against several pathogens. *Front Microbiol*. (2019) 10:884. doi: 10.3389/fmicb.2019.00884
- Luciardi MC, Blázquez MA, Alberto MR, Cartagena E, Arena ME. Lemon oils attenuate the pathogenicity of *Pseudomonas aeruginosa* by quorum sensing inhibition. *Molecules*. (2021) 26:2863. doi: 10.3390/molecules26102863
- Mol S, Erkan N, Üçok D, Tosun SY. Effect of psychrophilic bacteria to estimate fish quality. *J Muscle Foods*. (2007) 18:120–7. doi: 10.1111/j.1745-4573.2007.00071.x
- Pyz-Łukasik R, Paszkiewicz W. Microbiological quality of farmed grass carp, bighead carp, Siberian sturgeon, and wels catfish from Eastern Poland. *J Vet Res*. (2018) 62:145–9. doi: 10.2478/jvetres-2018-0023
- Jawa C, Joshi R, Dhuria D, Sain M, Sharma R. Evaluation of microbial quality of raw fish meat sold at fish meat outlets of Bikaner. *Pharma Innov J*. 10:67–70.
- Kumar H, Franzetti L, Kumar D. *Pseudomonas fluorescens*: a potential food spoiler and challenges and advances in its detection. *Ann Microbiol*. (2019) 69:873–83. doi: 10.1007/s13213-019-01501-7

Frontiers in Nutrition

Explores what and how we eat in the context of health, sustainability and 21st century food science

A multidisciplinary journal that integrates research on dietary behavior, agronomy and 21st century food science with a focus on human health.

Discover the latest Research Topics

[See more →](#)

Frontiers

Avenue du Tribunal-Fédéral 34
1005 Lausanne, Switzerland
frontiersin.org

Contact us

+41 (0)21 510 17 00
frontiersin.org/about/contact

